Deciphering the physiology of drug tolerant and resistant *Mycobacterium tuberculosis*

By

Caroline Pule

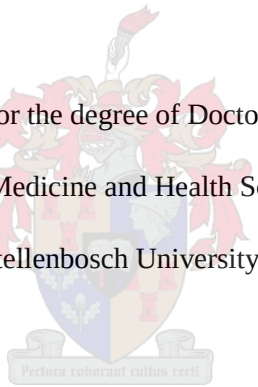

Dissertation presented for the degree of Doctor of Philosophy in the

Faculty of Medicine and Health Sciences at

Stellenbosch University

Supervisor: Prof Samantha Leigh Sampson

Co-supervisors: Dr Gail Erika Louw, Prof Robin Mark Warren and Dr Jacoba Martina Mouton

March 2021

Declaration

By submitting this dissertation electronically, I declare that the entirety of the work contained therein is my own, original work, that I am the sole author thereof (save to the extent explicitly otherwise stated), that reproduction and publication thereof by Stellenbosch University will not infringe any third-party rights and that I have not previously in its entirety or in part submitted it for obtaining any qualification.

February 2021

Abstract

Poor adherence to treatment for tuberculosis (TB) disease and the rising incidents of drug resistant *Mycobacterium tuberculosis* strains are factors that negatively influence TB control. The current study was designed to explore some of the key knowledge gaps concerning *M. tuberculosis* physiology; looking at the effect of the diverse *M. tuberculosis* genetic backgrounds and the presence of *ropB* mutation on the transcriptome, looking at *M. tuberculosis* host response and the likelihood as to whether induced mycobacterial tolerance can provide a reservoir from which genetic resistance can arise. Exploring some of these key knowledge gaps was imperative, given the fact that, lengthy anti-TB drug treatment could be required to entirely eradicate some of *M. tuberculosis* strains, and non-compliance with completing treatment might lead to the emergence of multidrug (MDR)-TB.

Firstly, we investigated the effect of *M. tuberculosis* strains with different genetic backgrounds on their total transcriptomic profiles (as a proxy for the physiological state). Secondly, we examined the influence of *rpoB* Ser531Leu mutation and the effect of isoniazid (INH) treatment (24h) at sub-lethal concentrations on the transcriptomic profiles of rifampicin (RIF)-resistant ($K636^{RIF}$) and susceptible ($K636^{WT}$ and $H37RV^{WT}$) *M. tuberculosis* strains, using RNA-sequencing (RNA-Seq) and Real-Time quantitative polymerase chain reaction (RT-qPCR) techniques. RNA-Seq analysis identified significantly differentially expressed genes in the transcriptomes of $K636^{WT}$, $H37RV^{WT}$ and $K636^{RIF}$ *M. tuberculosis* strains. Our comparative transcriptomic data of $K636^{WT}$ relative to $H37Rv^{WT}$ *M. tuberculosis* strains demonstrated that different genetic backgrounds influenced the total transcriptome. We demonstrated that *rpoB* Ser531Leu mutation has an impact on the transcriptional responses of $K636^{WT}$ relative to $K636^{RIF}$ *M. tuberculosis* strains. Our data did not demonstrate an effect of INH treatment on the transcriptomes of *M. tuberculosis* strains from different genetic backgrounds, making this one of our limitations.

We then assessed the host immune response after infection with RIF-resistant ($K636^{RIF}$ and $H37Rv^{RIF}$) and susceptible ($K636^{WT}$ and $H37RV^{WT}$) *M. tuberculosis* strains using the luminex x multi-analyte profiling (xMAP) technology and enzyme-linked immunosorbent assay (ELISA). Our host response data (Chapter 4) revealed no differences in host response to $K636^{WT}$ and $H37Rv^{WT}$ *M. tuberculosis* strains from different genetic backgrounds. In contrast, there were differences in host response to $K636^{WT}$ and $K636^{RIF}$ *M. tuberculosis* strains in a RAW264.7 macrophage model of infection. This was confirmed by the observed

varying secretion levels of cytokines and chemokines (IL-6, IL-12p40 and RANTES) required to mediate *M. tuberculosis* growth and survival after 24 - 48h of infection.

We further investigated whether viable but non-replicating (VBNR) persisters *Mycobacterium smegmatis* sub-populations, when exposed to high INH concentrations, may provide a pool from which genetic resistant mutants can arise. We used a combination of a fluorescence dilution (FD) reporter system, flow cytometry and fluorescence-activated cell sorting (FACS) to detect, quantify and separate VBNR and actively replicating (AR) *M. smegmatis* bacterial populations following INH treatment. Subsequently, we performed PCR to amplify the *katG* and *inhA* promoter and Sanger sequencing to identify mutations in these genes that are commonly associated with INH resistance. Our flow cytometry results showed successful detection of VBNR and AR bacterial populations in *M. smegmatis*::pTiGc following INH pre-treatment at high concentration (30x MIC) for 72h. Mutation frequencies of different sorted populations were determined as 3.51% for *M. smegmatis*^{VBNR}, 5.20% for *M. smegmatis*^{AR} and 0.02% for *M. smegmatis* UNT. Sanger sequencing data demonstrated a high percentage of mutations in the *inhA* promoter (C-15T) (76% in VBNR; 64% in AR) compared to mutations in the *katG* gene (48% in VBNR; 44% in AR). However, the difference was not statistically significant ($p > 0.1$).

This study addressed the following knowledge gaps: it advanced our understanding about the *M. tuberculosis* physiology. It confirmed that strain genetic background and the presence of *rpoB* Ser531Leu mutation may play a role in the physiological state of *M. tuberculosis* strains as reflected in their transcriptomes. It confirmed that host response *in vitro* is influenced by *M. tuberculosis* strain genotype and that infection with K636^{WT}, H37Rv^{WT} and H37Rv^{RIF} *M. tuberculosis* strains will result in the secretion of pro-inflammatory cytokines and chemokines while infection with K636^{RIF} *M. tuberculosis* strain (with *rpoB* Ser531Leu mutation) might induce secretion of anti-inflammatory cytokines (second line of host defense). This study was the first to successfully use a FACS analysis in combination with the FD reporter system to detect, isolate and quantify VBNR from AR *M. smegmatis*, following INH pre-treatment at high concentrations. We speculate that our results showed that the VBNR persisters' sub-population is likely to provide a reservoir from which genetic resistant mutants can arise, when treated with high INH concentrations as made evident by the observed INH resistant mutants in VBNR *M. smegmatis*. This work contributed further

knowledge to finding better strategies to prevent the spread of emerging MDR, as well as extensively drug resistant *M. tuberculosis.*

Opsomming

Verkeerdelike gebruik van behandeling van tuberkulose (TB) en die toename in die voorkoms van middel weerstandige *Mycobacterium tuberculosis* is faktore wat die beheer van TB negatief beinvloed. Die huidige studie is ontwerp om van die belangrikste gapings in die kennis rondom die fisiologie van *M. tuberculosis* te oorbrug. Die studie het gekyk na die effek van diverse *M. tuberculosis* genetiese agtergronde en die voorkoms van die *rpoB* mutasie op die transkriptoom van *M. tuberculosis*, die response van die gasheer op *M. tuberculosis* en die waarskynlikheid dat mikobakteriële toleransie ‘n poel verskaf waarvan genetiese weerstandigheid kan ontstaan. Die verkenning van verskeie van hierdie belangrike gapings in kennis was noodsaaklik gegewe die feit that langdurige anti-TB behandeling benodig kan word om totaal onstlae te raak van sekere *M. tuberculosis* stamme. Verkeerdelike gebruik en voltooing van behandeling mag lei tot die onstaan van multiweerstandige (MDR)-TB.

Eerstens het ons die effek van die *M. tuberculosis* stamme met verskillende genetiese agtergronde op die totale transkriptoom ondersoek (as indikasie van die fisiologiese toestand). Tweedens het ons die invloed van die *rpoB* Ser531Leu mutasie en die effek van isoniazid (INH) behandeling (24 uur) teen sub-dodelike konsentrasies op die transkriptoom van rifampisien (RIF) weerstandige ($K636^{RIF}$) en die sensitiewe ($K636^{WT}$ en $H37RV^{WT}$) *M. tuberculosis* stamme ondersoek deur gebruik te maak van RNA-volgordebepaling (RNAseq) en werklike tyd, kwantitatiewe polimerase ketting reaksie (RT-qPCR). RNAseq analise het beduidende verskille in die uitdrukking van gene in die transkriptoom van $K636^{WT}$, $H37RV^{WT}$ en $K636^{RIF}$ *M. tuberculosis* stamme getoon. Ons vergelykende transkriptoom data van $K636^{WT}$ en $H37RV^{WT}$ *M. tuberculosis* stamme het gedui dat verskillede genetiese agtergronde die totale transkriptoom beinvloed. Ons het gedemonstreer dat die *rpoB* Ser53Leu mutasie ‘n impak op die transkripsionele respons van $K636^{WT}$ het, relatief tot $K636^{RIF}$ *M. tuberculosis* stamme. ‘n Beperking van die studie was dat ons data nie die effek van INH behandeling op die transkriptoom van *M. tuberculosis* stamme van verskillende genetiese agtergronde gedemonstreer het nie.

Met die assessering van die gasheer se immuun reaksie na infeksie met die RIF-weerstanding ($K636^{RIF}$ en $H37RV^{RIF}$) en die sensitiewe ($K636^{WT}$en $H37RV^{WT}$) *M. tuberculosis* stamme deur die gebruik van luminex x multi-analiet profiel (xMAP) tegnologie en ensiem geassosieerde immunosorbens analises (ELISA) analises. Ons gasheer respons data

(Hoofstuk 4) het geen verskille in gasheer reaksies tot K636^{WT} en H37Rv^{WT} *M. tuberculosis* stamme van verskillende genetiese agtergronde getoon nie. In teenstelling, daar was verskillle in die gasheer respons tot K636^{WT} en K636^{RIF} *M. tuberculosis* stamme in a RAW264.7 makrofaag infeksie model. Dit is bevestig deur die waarneming van variërende sekresie vlakke van sitokienes en chemokiene (IL-6, IL-12p40 en RANTES) wat benodig word om *M. tuberculosis* groei en oorlewing te bemiddel 24 – 48 ure na infeksie.

Ons het verder ondersoek ingestel of lewendige nie-repliserende (VBNR) persister *Mycobacterium smegmatis* sub-populasies, wanneer blootgestel aan hoë dosisse INH konsenstrasies, ‘n poel kan verskaf waarvan geneties weerstandige mutasies kan ontstaan. Ons het ‘n kombinasie van ‘n fluoresensie verdunning (FD) sisteem, vloeisitometrie en fluoreserensie-geaktiveerde sel sortering (FACS) gebruik om VBNR en aktief repliserende (AR) *M. smegmatis* populasies in respons tot INH behandeling te identifiseer, kwatifiseer en isoleer. Gevolglik het ons PKR gebruik om die *katG* en *inhA* promoter te amplifiseer en Sanger volgorde bepaling is gebruik om mutasies in hierdie gene te identifiseer, wat algemeen geassosieer is met INH weerstandigheid. Ons vloesitometrie resultate het gewys dat die identifisering van VBNR en AR bakeriële populasies in *M. tuberculosis*::pTiGc na voorafbehandeling met hoë konsentrasies INH (30x MIC) vir 72 uur. Mutasie frekwensies van verskillende gesorteerde populasies is bepaal as 3.51% vir *M. smegmatis* VBNR, 5.20% vir *M. smegmatis* AR en 0.02% vir *M. smegmatis* UNT. Sanger volgordebepaling het gedemonstreer dat ‘n hoë persentasie van die mutasies in die *inhA* protomoter (C-15T) (76% in VBNR; 64% in AR) geleë is, in vergelyking met mutasies in die *katG* geen (48% in VBNR, 44% in AR), maar die verskille was nie statisties beduidend nie ($p>0.1$).

Hierdie studie adresseer die volgende gapings in kennis: dit bevorder ons begrip van *M. tuberculosis* fisiologie. Dit bevestig dat genetiese agtergrond van stamme en die voorkoms van die *rpoB* Ser153Leu mutasie ‘n rol mag speel in die fisiologiese toestand van *M. tuberculosis* stamme soos gereflekteer in hul transkriptoom. Dit bevestig dat die gasheer respons *in vitro* beinvloed word deur *M. tuberculosis* stam genotipes en dat die infeksie met K636^{WT}, H37RV^{WT} en H37RV^{RIF} *M. tuberculosis* stamme sal lei to die sekresie van pro-inflammatoriese sitokienes en chemokiene, terwyl infeksie met K636^{RIF} *M. tuberculosis* stamme (met die *rpoB* Ser531Leu mutasie) sekresie van anti-inflammatoriese sitokiene (2e linie gasheer beskerming) kan induseer. Hierdie is die eerste studie wat FACS analises in kominasie met die FD sisteem suskesvol gebruik om VBNR van AR *M. smegmatis* na die

vooraf toediening van hoë konsentrasies INH te identifiseer, kwantifiseer en isoleer. Ons spekuleer dat ons resultate toon dat die VBNR persister sub-populasie waarskynlik ‘n poel verskaf waarvan geneties weerstandige mutasies kan ontstaan wanneer dit met hoë konsenstrasies INH behandel word, soos bewys deur die waarneming van die INH weerstandige mutasies in die VBNR *M. smegmatis* populasie. Hierdie werk dra by tot verdere kennis om verbeterede strategieë te identifiseer vir die verkoming van die verspreiding van MDR-TB en uitgebreide middel weerstandige *M. tuberculosis*.

Acknowledgements

I would like to send gratitude to the following people who made this work possible and successful, by supporting me with words of encouragement, wisdom and prayers:

- God, for being my strength, hope and guide. Without my faith in God throughout the years, I don't know if we would have made it. I thank and love you, my God.
- Prof Samantha Sampson (promoter), Dr Gail Louw (co-promoter), Prof Rob Warren (co-promoter) and Dr Jomien Mouton (co-promoter) for their patience, guidance, advice, excellent discussions and suggestions.
- Julia Maruping (grandmother) and Lucia Pule (Mother) for teaching me the power of faith, hard work, forgiveness and the grace of God!
- Dr Thabi Maitin for her remarkable support, prayers and always believing in me.
- My close friend Lauren Catherine Bates for proofreading this thesis.
- My family, friends and church for their love and support always.
- All my colleagues and friends at the department and Task Applied Science team.
- The South African Medical Research Council, Department of Health and the Department of Biomedical Sciences for financial support.
- Dr Stuart Meier for assisting me with my RNA sequencing data analysis.
- Dr Anzaan Dippenaar, Dr Melanie Grobbelaar and Ruzayda Palma for their assistance with my WGS work.
- DST/NRF Centre of Excellence for Biomedical Tuberculosis Research, SAMRC Centre for Tuberculosis Research, for their tools, Biosafety level III facilities and financial support.

Jesus Christ my Lord, saviour and Holy Spirit my helper.

Psalm 119

List of Abbreviations

AR	Actively replicating
ARC	Agricultural Research Council
ATCC	American Type Culture Collection
°C	Degrees Celsius
µl	Microlitres
µg	Micrograms
µm	Micrometers
BCG	Bacillus Calmette–Guérin
BD	Becton Dickinson
bp	Base pairs
BWA	Burrows-Wheeler Alignment Tool
CAF	Central Analytic Facility
CCL2	Chemokine (C-C motif) ligand 2
CCL5	Chemokine (C-C motif) ligand 5
CFU	Colony forming unit
DE	Dispersion estimates
DNA	Deoxyribonucleic acid
DMEM	Dulbecco's modified eagle medium
DST	Drug susceptibility testing
dNTP	Deoxyribonucleoside triphosphate
ELISA	Enzyme-linked immunosorbent assay
EMB	Ethambutol
ETH	Ethionamide
EtOH	Ethanol
FACS	Fluorescence-activated cell sorting
FBS	Fetal bovine serum
FD	Fluorescence dilution
FCS	Forward scatter

FDR	False discovery rate
FQ	Fluoroquinolone
g	Grams
GATK	Genome Analysis Tool Kit
GC	Growth control
GFP	Green fluorescent protein
GLM	Generalized linear model
GM-CSF	Granulocyte-macrophage colony-stimulating factor
GO	Gene ontology
GOEAST	Gene ontology enrichment analysis software toolkit
GU	Growth unit
HIV	Human immuno deficiency virus
INH	Isoniazid
IL-1β	Interleukin 1 beta
IL-4	Interleukin 4
IL-6	Interleukin 6
IL-10	Interleukin 10
IFN-γ	Interferon gamma
IL-12p40	Interleukin -12 subunit p40
LB	Luria-Bertani
MDM	Monocyte-derived macrophages
MDR	Multi Drug Resistant
MIC	Minimum Inhibitory Concentration
MGIT	Middlebrook Growth Indicator Tube
MCP-1	Monocyte chemoattractant protein-1
ml	Millilitres
mM	MilliMolar
mRNA	Messenger RNA
NaCl	Sodium chloride

NaOH	Sodium hydroxide
OADC	Oleic Acid Dextrose Catalase
PBS	Phosphate buffered saline
PBMC	Peripheral blood mononuclear cell
PCR	Polymerase chain reaction
RANTES	Regulated on activation, normal T cell expressed and Secreted
RT-qPCR	Quantitative Real Time PCR
RIF	Rifampicin
RIN	RNA integrity number
RNA	Ribonucleic acid
RRDR	RIF Resistance Determining Region
rRNA	Ribosomal RNA
SA	South Africa
SCC	Side Scatter
SANBI	South African National Bioinformatics Institute
SLID	Second-line injectable drugs
SNP	Single nucleotide polymorphism
TB	Tuberculosis
TC	Tissue Culture
TBE	Tris/Borate/EDTA
TE	Tris/EDTA
TNF-α	Tumor necrosis factor alpha
Tm	Melting temperature
TMM	Trimmed mean of M-values
Tris	Tris (hydroxymethyl) aminomethane
U	Units
V	Volt
VBNR	Viable but non-replicating

WGS	Whole genome sequencing
WHO	World Health Organisation
XDR	Extensively drug resistant
ZN	Ziehl-Neelsen

Table of contents

List of Figures

List of Tables

CHAPTER 1

General Introduction

1.1 The global burden of tuberculosis

Tuberculosis (TB) is a harmful infectious disease caused by the pathogen *Mycobacterium tuberculosis* (1). Despite the availability of anti-TB drugs, it is the ninth leading cause of death worldwide and remains a global health priority (2). The World Health Organization (WHO) estimated a global incidence of 10 million new cases of TB in 2018 (ranging from 9.0–11.1 million (2). The WHO South-East Asia region contributed 44% of the global incidence rate in 2018 (2). This was followed by the WHO African region (24%), the WHO Western Pacific region (18%) and smaller proportions of cases occurring in the WHO Eastern Mediterranean region (8%), the WHO American region (3%) and the WHO European region (3%) (2). An estimated 8.6% TB cases were reported to be co-infected with the human immuno deficiency virus (HIV) (2). The proportion of TB cases co-infected with HIV was highest in men (57%) (aged ≥ 15 years) compared to women (32%) and children (aged ≤ 15 years) with about 11% in 2018 (2). The WHO reported an estimated 251 000 (ranging from 223 000–281 000) deaths from TB disease among HIV-positive people and an additional 1.2 million (ranging from 1.1–1.3 million) deaths from TB disease among HIV-negative people in 2018 (2). Early TB diagnosis and the administration of appropriate treatment for TB disease resulted in an increased global treatment success rate of 85% in 2017 compared to 81% in 2016 (2).

The WHO reported an estimated 558 000 new TB cases in 2018 with resistance to the most potent first-line drug, rifampicin (RIF) (2). Approximately 82% of these cases were infected with a *M. tuberculosis* strain resistant to isoniazid (INH) and were classified as multidrug-resistant TB (MDR-TB) cases (2–4). The WHO recommends multi-drug combination therapy for at least six months for the treatment of drug susceptible TB and up to 2 years (total treatment duration of 18–20 months) for MDR-TB and extensively drug resistant tuberculosis (XDR-TB) (1,4–6). A shorter MDR-TB regimen of 9–12 months is recommended for patients with less than a month of second-line anti-TB drugs (fluoroquinolone (FQ) and second-line injectable drugs (SLID) treatment history (6). XDR-TB is classified as MDR-TB with additional resistance to a FQ and one of the injectables i.e. amikacin, kanamycin or capreomycin (7). Often the lengthy treatment periods lead to poor treatment adherence, which subsequently result in high treatment failure rates, unfavourable treatment outcomes, transmission and the emergence and transmission of drug resistant *M. tuberculosis* strains (8–

10). This highlights the need for the development of new anti-TB drugs with enhanced modes of action that could shorten treatment periods and improve treatment outcomes.

1.2 The prevalence of INH and RIF resistance-conferring mutations in *M. tuberculosis*

Approximately 95% of RIF resistant *M. tuberculosis* isolates harbour mutations in the 81bp RIF Resistance Determining Region (RRDR) of the *rpoB* gene (11–13). Reports indicate that the most frequent mutations in *rpoB* that confer resistance to RIF are located at codon 531 and 526 (14,15). The single-nucleotide polymorphism (SNP) at codon 531 results in a Ser531Leu amino acid change, whereas the SNP at codon 526 results in a His526Arg amino acid change (Table 1.1) (14–17). For INH resistance, the most frequent mutations are located at *katG* codon 315 (Ser315Thr) and in the *inhA* promoter region (C-15T, C-17T and T-8G/A) in *M. tuberculosis* (18–22). These mutations are associated with high (MIC $\geq$ 0.4 µg/ml) and low (MIC $\geq$ 0.1 µg/ml) level INH resistance in clinical *M. tuberculosis* strains, respectively (23).

Approximately 20-30% of INH resistant clinical *M. tuberculosis* isolates do not harbour mutations in known target genes (20,24), while approximately 5% of RIF resistant clinical *M. tuberculosis* isolates do not harbour mutations in the RRDR of *rpoB* (25,26). These observations suggest that alternative and/or additional mechanisms such as active efflux and drug modifying enzymes could be conferring INH and RIF resistance phenotypes. This suggests that drug resistance in *M. tuberculosis* is more complex than was previously assumed. Although mutations in target genes are selected under drug pressure, the impact of these mutations on the mycobacterial physiology is largely unknown. There are limited reports that have studied the impact of mutations on the mycobacterial physiology (27–29). Merker *et al.* explored mutations in 92 genes implicated in resistance to 21 anti-TB drugs using the genomes of 405 phylogenetically diverse *M. tuberculosis* complex (MTBC) strains. They revealed that different loss-of-function mutations affecting MmpL5 (drug efflux subunit), enhance the susceptibility of some MTBC subgroups to bedaquiline and clofazimine (27). Therefore, further understanding the impact of resistance-conferring genetic mutations on mycobacterial physiology will aid in the identification of pathways which allow this pathogen to adapt under selective drug pressure. This may guide future studies in the design of new drugs to eradicate drug resistant TB.

Table 1.1 Characteristics of the first-line anti-TB drugs relevant to the current study and most frequently mutated codons associated with clinical resistance to INH and RIF

Drug name	Mechanism of action	Gene target	Most frequently mutated codons	References
RIF	Inhibits RNA synthesis	*rpoB*	Ser531Leu, His526Arg	(15,17–22)
INH	Inhibits cell wall synthesis	*katG*	Ser315Thr	(18–22,30)
	Disrupts cell wall biosynthesis	*inhA*	C-15T, C-17T and T-8G/A	(18–22,30)

1.3 Transcriptomic profiling of *M. tuberculosis*

Previous studies have used microarray to investigate the global gene expression profiles of *M. tuberculosis* and *M. smegmatis* after exposure to specific stressors, including drugs (31–34). However, limited data exists on the effect of drug exposure in clinical *M. tuberculosis* using RNA sequencing (RNA-Seq). Thus investigating the transcriptomes of susceptible and resistant strains could provide new insight into how resistance influences bacterial physiology. Next generation RNA-Seq technology is rapidly changing the field of gene expression studies (35–38). RNA-Seq generates short reads which are mapped to a reference genome, with the number of mapped reads in a gene referred to as counts, thereby giving quantitative measures of the expression genes (39). These quantitative counts are normalized to a specific reference gene to determine the exact expression levels between samples. Thus, RNA-Seq yields a high-resolution transcriptomic map of an organism by quantifying genes which govern a phenotype through differential gene expression. In the current study we demonstrate the comparison of transcriptomic profiles between a susceptible and resistant *M. tuberculosis* strain.

In this study (chapter 3), we investigate the transcriptional profiles of *M. tuberculosis* strain with different genetic backgrounds or the presence and absence of an *rpoB* Ser531Leu mutation in order to understand how these genomic differences influence the transcriptome. We also investigate the effect of INH exposure (24h) on gene expression in these different *M. tuberculosis* strains. We further validate 5 genes that were significantly differentially

expressed between (i) *M. tuberculosis* strains from different genetic backgrounds and (ii) between the susceptible and resistant (with *rpoB* Ser531Leu mutation) *M. tuberculosis* strains by quantitative Real Time PCR (RT-qPCR).

1.4 The immune response of host macrophages to infection with *M. tuberculosis*

Following the demonstration that *M. tuberculosis* strains with different genetic backgrounds exhibit different transcriptional profiles, we went on to assess the influence of infection with these strains on macrophage secretion of cytokines and chemokines. Macrophages are the first host cells that *M. tuberculosis* encounter in the lung and serve as the first line of defence against *M. tuberculosis* (40,41). The uptake of mycobacteria by macrophages typically induces the release of pro-inflammatory cytokines and chemokines, which eventually leads to the induction of an adaptive immune response (42). The hypervirulent Beijing and HN878 *M. tuberculosis* strains have been extensively studied to understand the effect of genomic variation on the interaction between the pathogen and the host (42). Previous infection studies using the THP-1 monocytic cell line (43,44) and human peripheral blood monocyte-derived macrophages (45) showed a wide variation in the induction of pro-inflammatory and Th_1 type cytokines to infection with Beijing strains compared to non-Beijing strains, and the standard laboratory strain H37Rv (43–45). The host's response to infection with different clinical *M. tuberculosis* strains is partially understood.

This study (chapter 4) is one of the few studies to compare the response of host (murine) macrophages to susceptible and RIF resistant (with *rpoB* Ser531Leu mutation) *M. tuberculosis* strains. This was done by assessing the profiles of secreted cytokines and chemokines at different time points of infections. RAW264.7 macrophages were infected with different *M. tuberculosis* strains and the secreted cytokine and chemokine profiles were assessed at 24h and 48h post infection. The RAW264.7 macrophage cell line was selected for infection since they are an immortalized murine cell line that provides less experimental variability than primary cells. Multiplex (Luminex array) assay technology and enzyme-linked immunosorbent assay (ELISA) (for validation of selected secreted cytokines and chemokines) were used for the analysis of mouse cytokine and chemokine secretion. Results from these analyses will inform us about significant cytokines and chemokines that are released by RAW264.7 macrophages in response to the different *M. tuberculosis* strains. The results of these studies will identify genetic differences that contribute to the differential

secretion of cytokines and chemokines which in turn may guide the identification of bacterial biomarkers that are important for immune protection.

1.5 The effect of drug tolerance and its association with genetic resistance in *M. tuberculosis* physiology

M. tuberculosis has an extraordinary ability to adapt to various environmental conditions inside the host throughout the course of infection (46). The physiological changes that occur in *M. tuberculosis* exposed to different environments are complex and can modulate tolerance to anti-TB drugs which in turn drive the need for prolonged anti-TB treatment. One physiological adaptation involves the formation of persister bacteria. These are viable but non-replicating (VBNR) bacteria that typically exhibit a drug tolerant phenotype (47). Persisters are subpopulations of cells that can survive increased concentrations of drugs, in the absence of the emergence of genetic resistance (48–50). However, the physiology of persister cells remains poorly understood. It is likely that this key knowledge gap negatively influences progress in reducing the duration of anti-TB treatment, which hinders TB control globally (48). A recent study showed that the formation of persister phenotype as a result of continuous exposure of *M. tuberculosis* H37Ra cells to 2 μg/ml RIF or 1 μg/ml moxifloxacin resulted in the accumulation of hydroxyl ions, which subsequently resulted in chromosomal mutation and the emergence of *rpoB* and *gryA* mutations (51). This suggests that the formation of persister cells can lead to the emergence of genetic drug resistance *M. tuberculosis* strains *in vitro,* increasing the level of phenotypic resistance (as defined by the minimum inhibitory concentration).

Certain *in vitro* conditions which include low pH, nitrosative and oxidative stress, hypoxia and nutrient limitation are thought to induce a drug tolerant state (52,53). Additionally, exposing *M. tuberculosis* bacterial population to high drug concentrations enriches for drug tolerant persisters *in vitro* (47,54). Knowledge on the physiology of persistent *M. tuberculosis* has been restricted by the lack of tools to identify, isolate and characterize persistent populations. A recently developed fluorescence dilution (FD) reporter system demonstrated the replication dynamics of a persistent *Salmonella enterica* serovar Typhimurium population in murine macrophages (55). Subsequently, this approach has been adapted for use in *M. tuberculosis* (47). Briefly, the FD reporter exploits two fluorescent reporters: a constitutive green fluorescent reporter that allows the tracking of viable bacteria, and an inducible red

fluorescent reporter which enables the measurement of bacterial replication (Figure 1.1) (47). In this study, FD was exploited to isolate and characterise INH drug-tolerant persisters in *M. smegmatis* populations. In this study (chapter 5), we investigate how a sub-population of VBNR (drug-tolerant) persisters may provide a pool of INH resistance when exposed to high lethal INH concentrations in *M. smegmatis*.

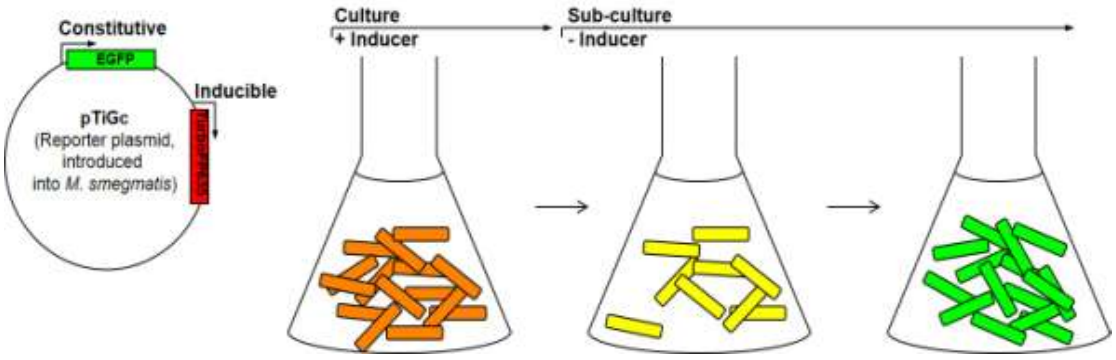

Figure 1.1 Principle of the FD reporter system to explore the replication dynamics of *M. smegmatis*. The figure depicts the FD reporter system where the green fluorescent protein (GFP) (green) reporter serves as a marker for viability and the TurboFP635 (red) reporter is under regulation of an inducible promoter and allows tracking of bacterial replication (47). In the presence of the inducer (Theophylline), GFP and TurboFP635 are maximally expressed. Upon removal of the inducer, the TurboFP635 signal is diluted in an actively growing culture.

1.6 Rationale, overall aim and specific objectives of this study

1.6.1 Problem statement

M. tuberculosis is a highly specialized slow-growing pathogen that employs survival strategies to tolerate a wide variety of challenging environments such as nutrient deprivation, hypoxia and stress conditions, including those caused by antibiotic treatment in a host. A drug treatment regimen of at least six months, assumed to diminish the sensitive and tolerant population, is recommended (4). Ensuring treatment adherence is labour-intensive and costly, while poor adherence leads to treatment failure and an increased risk of acquired resistance (56). This negatively influences TB control resulting in the need for prolonged TB treatment and incidence of MDR-TB cases (4,57). Although drug resistance in *M. tuberculo*sis strains has been extensively studied, the influence of genetic diversity, the presence of the most frequent resistant mutations in these strains and effect of anti-TB drugs on mycobacterial

physiology has not been thoroughly investigated. More knowledge about underlying mechanisms used by *M. tuberculosis* to adapt to and survive anti-TB treatment in enhancing the emergence of genetic resistance, will help provide the in-depth understanding of the physiology of drug resistant *M. tuberculosis* strains. Furthermore, understanding the influence of genetic diversity in *M. tuberculosis* strains will provide information about the transcriptional changes within these strains, which will help in understanding the expression of genes that play a role in driving the continuous evolution of resistance and prolonged TB treatment.

1.6.2 Hypothesis

We hypothesise that RIF-resistant and susceptible *M. tuberculosis* strains will exhibit a differential transcriptomic profile. We further hypothesize that the resistance-conferring mutation (*rpoB* Ser531Leu mutation) in combination with INH treatment will result in adaptive physiological changes that will be reflected in the total transcriptome. We anticipate that the infection of RAW264.7 macrophages with RIF-resistant and susceptible *M. tuberculosis* strains will induce different host responses reflected by the secretion of cytokines and chemokines. We further hypothesize that VBNR (drug tolerant) persister populations may provide a reservoir from which resistant mutants can arise in *M. smegmatis*.

1.6.3 Overall Aims

1. To decipher the effect of *M. tuberculosis* strains with different genetic backgrounds on their total transcriptomic profiles (as a proxy for the physiological state). Following from this, the influence of *rpoB* Ser531Leu mutation on the transcriptomic profiles of RIF-resistant ($K636^{RIF}$) and susceptible ($K636^{WT}$ and $H37RV^{WT}$) *M. tuberculosis* strains. Lastly, the effect of INH treatment (24h) at sub-lethal concentrations on the transcriptomic profiles of *M. tuberculosis* strains.

2. To assess the host immune response after infection with RIF-resistant ($K636^{RIF}$ and $H37Rv^{RIF}$) and susceptible ($K636^{WT}$ and $H37RV^{WT}$) *M. tuberculosis* strains.

3. To investigate whether VBNR (persisters) *M. smegmatis* sub-populations, when exposed to high INH concentrations, may provide a reservoir of INH resistance from which genetic resistant mutants can emerge.

1.6.4 Objectives

1. To characterize the physiology of *in vitro* generated RIF-resistant mutants and susceptible *M. tuberculosis* strains.

a. To establish an optimal sub-lethal concentration of INH that allows growth of $K636^{WT}$ (drug susceptible clinical strain), $K636^{RIF}$ (drug-resistant clinical strain) and $H37Rv^{WT}$ (susceptible laboratory strain) *M. tuberculosis* strains during treatment.

b. To characterize the transcriptional profiles of $K636^{WT}$ (drug susceptible clinical strain), $K636^{RIF}$ (drug-resistant clinical strain) and $H37Rv^{WT}$ (susceptible laboratory strain) *M. tuberculosis* strains, both treated and untreated with a sub-lethal INH concentration, using RNA-Seq and RT-qPCR.

2. To evaluate the host immune response to infection with RIF-resistant and susceptible *M. tuberculosis* strains with different genetic backgrounds in a RAW264.7 macrophage model.

To determine the secretion of the cytokines (tumor necrosis factor alpha (TNF-α), interleukin 1 beta (IL-1β), interleukin 10 (IL-10), interferon gamma (IFN-γ), interleukin 4 (IL-4), interleukin 6 (IL-6) and interleukin-12 subunit p40 (IL-12p40) and chemokines [(granulocyte-macrophage colony-stimulating factor (GM-CSF), chemokine (C-C motif) ligand 5 (RANTES/CCL5) and chemokine (C-C motif) ligand 2 (MCP-1)] in the harvested cell culture supernatants using the multiplex cytokine (luminex array) assay and ELISA technology; supernatants harvested during 24h and 48h of RAW264.7 macrophage infection with $K636^{WT}$ (drug susceptible clinical strain), $K636^{RIF}$ (drug-resistant clinical strain), $H37Rv^{WT}$ (drug susceptible laboratory strain) and $H37Rv^{RIF}$ (drug resistant laboratory strain) *M. tuberculosis* strains.

3. To investigate whether a VBNR *M. smegmatis* sub-population is more likely to provide a reservoir of INH resistance from which genetic resistant mutants can emerge

a. To detect and quantify VBNR and actively replicating (AR) *M. smegmatis* bacterial populations following INH treatment at high concentrations using a combination of FD and flow cytometry.

b. To isolate *M. smegmatis* VBNR from AR populations using fluorescence-activated cell sorting (FACS), following INH treatment at high concentrations (30x MIC) for 72h.

c. To identify the proportion of genetic INH resistant *M. smegmatis* that can emerge from a VNBR subpopulation that was exposed to 30x MIC INH, by amplification of *katG* and *inhA* promoter and identification of mutations in these genes that are predominantly associated with INH resistance.

1.6.5 Experimental approach

RNA-Seq, followed by RT-qPCR, was applied to characterize the physiology of RIF-resistant ($K636^{RIF}$) and susceptible ($K636^{WT}$ and $H37RV^{WT}$) *M. tuberculosis* strains in the absence or presence of INH (0.05 µg/ml) under *in vitro* conditions (Figure 1.2). The RAW264.7 macrophage infection model, multiplex cytokine (Luminex array) assay technology and ELISA were used to evaluate the host immune response to infection with RIF-resistant (with *rpoB* Ser531Leu mutation) ($K636^{RIF}$ and $H37Rv^{RIF}$) and susceptible ($K636^{WT}$ and $H37RV^{WT}$) *M. tuberculosis* strains (Figure 1.2). A combination of FD, flow cytometry and FACS analyses were exploited to isolate and characterise persister/drug-tolerant *M. tuberculosis* populations in the current study (Figure 1.2). Additionally, Sanger sequencing (of *katG* and *inh*A promoter genes) was explored to determine whether the INH-induced VBNR *M. smegmatis* sub-population provides a pool from which genetic resistant mutants can emerge.

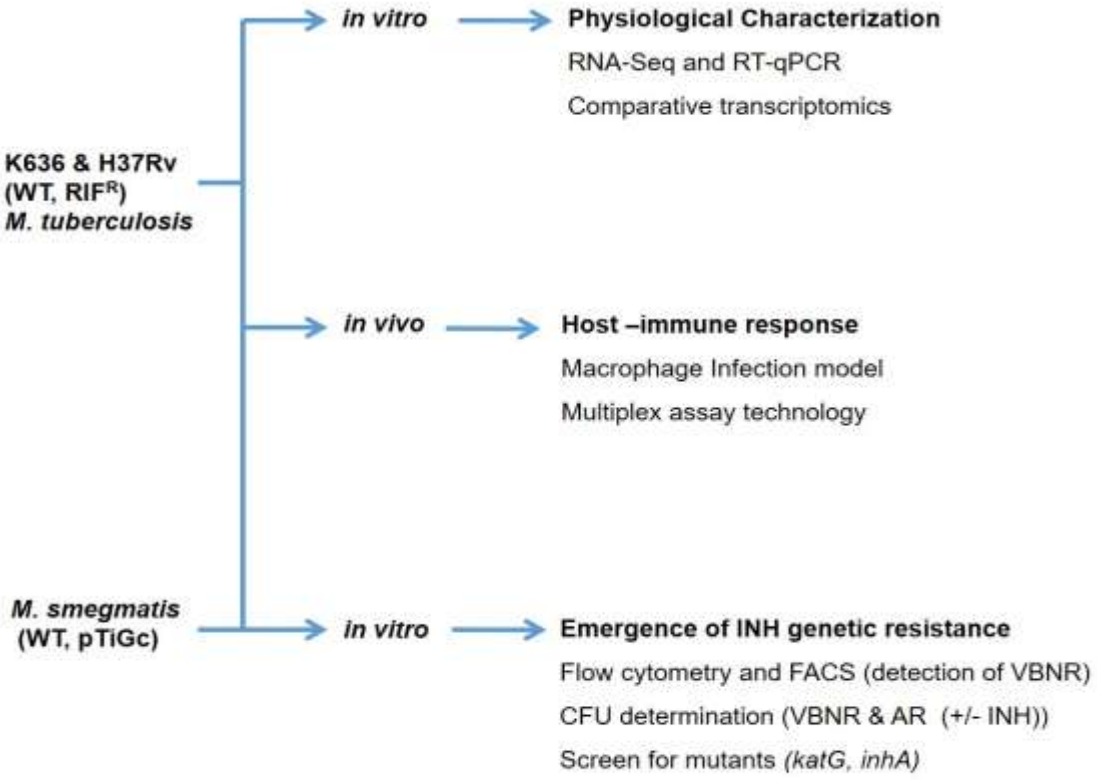

Figure 1.2 Schematic illustration of the different technologies applied in the experimental approach of the current study.

1.7 Thesis structure

1.7.1 Chapter 1. Introduction

This chapter introduces the study. The chapter covers the global concerns regarding the emergence and spread of MDR-TB and highlights the need for new anti-TB drug development. It emphasizes the limited knowledge available on the physiological changes of *M. tuberculosis* strains both *in vivo* and *in vitro*, during anti-TB treatment. Therefore, assessing the influence of genetic background of RIF-resistant and susceptible *M. tuberculosis* clinical strains and exposure to INH treatment on the transcriptional profile of these strains, in order to investigate mycobacterial physiology, using RNA-Seq will help address this knowledge gap. This chapter further emphasizes the importance of studying the host response reflected by the secretion of various cytokines and chemokines by RAW264.7 macrophages upon infection with susceptible and resistant *M. tuberculosis* strains. Moreover, the chapter emphasises the importance of understanding the drug tolerance mechanisms

linked to continuous emergence of generic resistance; by looking at the likelihood of VBNR *M. smegmatis* sub-population providing a reservior from which genetic resistant mutants can emerge, when exposed to high concentrations of INH. The knowledge could ultimately lead to the identification of novel drug targets to combat the spread of drug-resistant TB and emergence of drug tolerant sub-populations.

1.7.2 Chapter 2. The impact of INH resistance on *M. tuberculosis*

This chapter presents a literature review highlighting the fundamentals of INH drug resistance in mycobacteria. It focuses on the epidemiological significance of the emergence of INH drug resistance, the molecular mechanisms of INH resistance in mycobacteria and the impact of INH resistance on mycobacterial physiology. It highlights currently available evidence and information on the emergence of INH drug-resistant *M. tuberculosis* strains and the mechanisms they adapt in order to continuously spread.

1.7.3 Chapter 3. The transcriptomic profiling of resistant and susceptible *M. tuberculosis* strains

This chapter provides evidence on the impact of genetic strain diversity and *rpoB* Ser531Leu mutation on the *M. tuberculosis* transcriptome. It focusses on assessing global gene expression and characterization of the transcriptional profiles of $K636^{WT}$, $H37RV^{WT}$ and $K636^{RIF}$ *M. tuberculosis* strains, from different genetic backgrounds. In addition, it assesses the effect of INH treatment on the *M. tuberculosis* physiology of $K636^{WT}$ (treated vs untreated) and $K636^{RIF}$ (treated vs untreated) as a measure of the global transcriptome, using RNA-Seq and validation by RT-qPCR.

1.7.4 Chapter 4. Evaluation of host immune response to genetically resistant and susceptible *Mycobacterium tuberculosis* strains in a macrophage model

This chapter details the host immune responses to RIF susceptible and resistant *M. tuberculosis* strains from different genetic backgrounds by infecting RAW264.7 macrophages and assessing the secreted chemokines and cytokines at 24h and 48h after infection using the multiplex cytokine (Luminex array) assay and ELISA technology.

1.7.5 Chapter 5. The determination of the likelihood of VBNR *M. smegmatis* sub-population to provide a reservoir of INH resistance from which genetic resistant mutants can emerge

This chapter details the detection and quantification of VBNR and AR *M. smegmatis* sub-populations following INH treatments (72h) at high concentrations. It further separates the VBNR bacterial population from the AR population using FACS and examines the likelihood of VBNR *M. smegmatis* sub-population to provide a reservoir from which genetic resistant mutants can emerge. It further confirms the anticipated genetic resistant mutant using the PCR amplification and DNA Sanger sequencing (of *katG* gene and *inhA* promoter).

1.7.6 Chapter 6. General conclusion

The general conclusion summarizes and synthesises essential findings of all chapters. It further explains the limitations of the study and proposes future work to address the limitations.

1.8 References

1. **Dye C, Scheele S, Dolin P, Pathania V, Raviglione MC.** 1999. Consensus statement. Global burden of tuberculosis: estimated incidence, prevalence, and mortality by country. WHO global surveillance and monitoring project. JAMA J Am Med Assoc. **282**:677–86.

2. **WHO**. Global tuberculosis report 2020. WHO. World Health Organization

3. **Fischbach MA, Walsh CT**. 2009. Antibiotics for emerging pathogens. Science. **325**:1089–93.

4. **Yew WW, Lange C, Leung CC**. Treatment of tuberculosis: update 2010. Eur Respir J. **37**:441–62.

5. **B, Pike USNL of M 8600 R, MD B,** USA 20894. 2014. Treatment strategies for MDR-TB and XDR-TB. World Health Organization.

6. **WHO.** 2019. WHO consolidated guidelines on drug-resistant tuberculosis treatment.

7. **Holtz TH.** XDR-TB in South Africa: revised definition. 2007. PLoS Med. **4**:161.

8. **Ragonnet R, Trauer JM, Denholm JT, Marais BJ, McBryde ES**. 2017. High rates of multidrug-resistant and rifampicin-resistant tuberculosis among re-treatment cases: where do they come from? BMC Infect Dis.**17**:36.

9. **Zelner JL, Murray MB, Becerra MC, Galea J, Lecca L, Calderon R**, *et al*. 2016. Identifying hotspots of multidrug-resistant tuberculosis transmission using spatial and molecular genetic data. J Infect Dis. **213**:287–94.

10. **Kendall EA, Fofana MO, Dowdy DW.** 2015. Burden of transmitted multidrug resistance in epidemics of tuberculosis: a transmission modelling analysis. Lancet Respir Med. **3**:963–72.

11. **Tan Y, Hu Z, Zhao Y, Cai X, Luo C, Zou C,** *et al*. 2012. The beginning of the *rpoB* gene in addition to the rifampin resistance determination region might be needed for identifying rifampin/rifabutin cross-resistance in multidrug-resistant *Mycobacterium tuberculosis* isolates from southern china. J Clin Microbiol. **50**:81–5.

12. **Campbell EA, Korzheva N, Mustaev A, Murakami K, Nair S, Goldfarb A,** *et al*. 2001. Structural mechanism for rifampicin inhibition of bacterial RNA polymerase. Cell. **104**:901–12.

13. **Aristoff PA, Garcia GA, Kirchhoff PD, Hollis Showalter HD**. 2010. Rifamycins – obstacles and opportunities. Tuberculosis. 90:94–118.

14. **Morlock GP, Plikaytis BB, Crawford JT**. 2000. Characterization of spontaneous, *in vitro*-selected, rifampin-resistant mutants of *Mycobacterium tuberculosis* strain H37Rv. Antimicrob Agents Chemother. **44**:3298–301.

15. **Pang Y, Lu J, Wang Y, Song Y, Wang S, Zhao Y**. 2013. Study of the rifampin monoresistance mechanism in *Mycobacterium tuberculosis*. Antimicrob Agents Chemother **57**:893–900.

16. **Billington OJ, McHugh TD, Gillespie SH.** 1999. Physiological cost of rifampin resistance induced *in vitro* in *Mycobacterium tuberculosis*. Antimicrob Agents Chemother. **43**:1866–9.

17. **Bahrmand AR, Titov LP, Tasbiti AH, Yari S, Graviss EA.** 2009. High-level rifampin resistance correlates with multiple mutations in the *rpoB* gene of pulmonary tuberculosis isolates from the Afghanistan border of Iran. J Clin Microbiol. **47**:2744–50.

18. **Ballif M, Harino P, Ley S, Coscolla M, Niemann S, Carter R,** *et al*. 2012. Drug resistance-conferring mutations in *Mycobacterium tuberculosis* from Madang, Papua New Guinea. BMC Microbiol. **12**:191.

19. **Chopra I, Brennan P**. Molecular action of anti-mycobacterial agents. 1998. Tuber Lung Dis. **78**:89–98.

20. **Ramaswamy S, Musser JM**. 1998. Molecular genetic basis of antimicrobial agent resistance in *Mycobacterium tuberculosis*: 1998 update. Tuber Lung Dis Off J Int Union Tuberc Lung Dis. **79**:3–29.

21. **Silva PEAD, Palomino JC**. 2011. Molecular basis and mechanisms of drug resistance in *Mycobacterium tuberculosis*: classical and new drugs. J Antimicrob Chemother.

22. **S. A, C. P**. 2012. Old and new TB drugs: Mechanisms of action and resistance. In: Cardona P-J, editor. Understanding tuberculosis - New approaches to fighting against drug resistance. **9**:376

23. **Vijdea R, Stegger M, Sosnovskaja A, Andersen AB, Thomsen VØ, Bang D**. 2008. Multidrug-resistant tuberculosis: rapid detection of resistance to rifampin and high or low levels of isoniazid in clinical specimens and isolates. Eur J Clin Microbiol Infect Dis Publ Eur Soc Clin Microbiol. **27**:1079–86.

24. **Ramaswamy SV, Reich R, Dou S-J, Jasperse L, Pan X, Wanger A**, *et al*. 2003. Single nucleotide polymorphisms in genes associated with isoniazid resistance in *Mycobacterium tuberculosis*. Antimicrob Agents Chemother. **47**:1241–50.

25. **Telenti A, Imboden P, Marchesi F, Lowrie D, Cole S, Colston MJ**, *et al*. 1993 Detection of rifampicin-resistance mutations in *Mycobacterium tuberculosis*. Lancet. **341**:647–50.

26. **Louw GE**. 2009. Resistance to first line anti-TB drugs by gene mutation and gene modulation. Thesis. University of Stellenbosch.

27. **Merker M, Kohl TA, Barilar I, Andres S, Fowler PW, Chryssanthou E,** *et al*. 2000. Phylogenetically informative mutations in genes implicated in antibiotic resistance in *Mycobacterium tuberculosis* complex. Genome Med. **12**:27.

28. **Koch A, Mizrahi V, Warner DF**. 2014. The impact of drug resistance on *Mycobacterium tuberculosis* physiology: what can we learn from rifampicin? Emerg Microbes Infect. **3**:17.

29. **Gomez-Gonzalez PJ, Andreu N, Phelan JE, de Sessions PF, Glynn JR, Crampin AC**, *et al*. 2019. An integrated whole genome analysis of *Mycobacterium tuberculosis* reveals insights into relationship between its genome, transcriptome and methylome. **9**:5204.

30. **Aslan G, Tezcan S, Serin MS, Emekdas G**. 2008. Genotypic analysis of isoniazid and rifampin resistance in drug-resistant clinical *Mycobacterium tuberculosis* complex isolates in southern Turkey. Jpn J Infect Dis. **61**:255–60.

31. **Wilson M, DeRisi J, Kristensen H-H, Imboden P, Rane S, Brown PO,** *et al*. 1999. Exploring drug-induced alterations in gene expression in *Mycobacterium tuberculosis* by microarray hybridization. Proc Natl Acad Sci U S A. **96**:12833–8.

32. **Waddell SJ, Stabler RA, Laing K, Kremer L, Reynolds RC, Besra GS**. 2004. The use of microarray analysis to determine the gene expression profiles of *Mycobacterium tuberculosis* in response to anti-bacterial compounds. Tuberculosis. **84**:263–74.

33. **Niki M, Niki M, Tateishi Y, Ozeki Y, Kirikae T, Lewin A,** *et al*. 2012. A novel mechanism of growth phase-dependent tolerance to isoniazid in mycobacteria. J Biol Chem. **287**:27743–52.

34. **Betts JC, McLaren A, Lennon MG, Kelly FM, Lukey PT, Blakemore SJ,** *et al*. 2003. Signature gene expression profiles discriminate between isoniazid-, thiolactomycin-, and triclosan-treated *Mycobacterium tuberculosis*. Antimicrob Agents Chemother.**47**:2903–13.

35. **Nagalakshmi U, Wang Z, Waern K, Shou C, Raha D, Gerstein M**, *et al*. 2008. The transcriptional landscape of the yeast genome defined by RNA sequencing. Science. **320**:1344–9.

36. **Lowe R, Shirley N, Bleackley M, Dolan S, Shafee T.** 2017. Transcriptomics technologies. PLoS Comput Biol. **13**(5):e1005457.

37. **Nalpas NC, Magee DA, Conlon KM, Browne JA, Healy C, McLoughlin KE,** *et al*. 2015. RNA sequencing provides exquisite insight into the manipulation of the alveolar macrophage by tubercle bacilli. Sci Rep. **5**:13629.

38. **Wang Z, Gerstein M, Snyder M.** 2009. RNA-Seq: a revolutionary tool for transcriptomics. Nat Rev Genet. 10:57–63.

39. **Finotello F, Di Camillo B.** 2015. Measuring differential gene expression with RNA-seq: challenges and strategies for data analysis. Brief Funct Genomics. **14**:130–42.

40. **Cooper AM, Khader SA**. 2008. The role of cytokines in the initiation, expansion, and control of cellular immunity to tuberculosis. Immunol Rev. **226**:191–204.

41. **Russell DG**. 2007. Who puts the tubercle in tuberculosis? Nat Rev Microbiol. **5**:39–47.

42. **Sharma M, Bose M, Abhimanyu, Sharma L, Diwakar A, Kumar S,** *et al*. 2012. Intracellular survival of *Mycobacterium tuberculosis* in macrophages is modulated by phenotype of the pathogen and immune status of the host. Int J Mycobacteriology. **1**:65–74.

43. **Tanveer M, Hasan Z, Kanji A, Hussain R, Hasan R**. 2009. Reduced TNF-alpha and IFN-gamma responses to Central Asian strain 1 and Beijing isolates of *Mycobacterium tuberculosis* in comparison with H37Rv strain. Trans R Soc Trop Med Hyg. **103**:581–7.

44. **Chakraborty P, Kulkarni S, Rajan R, Sainis K.** 2013. Drug resistant clinical isolates of *Mycobacterium tuberculosis* from different genotypes exhibit differential host responses in THP-1 cells. PLoS ONE. **8**(5):e62966.

45. **Portevin D, Gagneux S, Comas I, Young D**. 2011. Human macrophage responses to clinical isolates from the *Mycobacterium tuberculosis* complex discriminate between ancient and modern lineages. PLOS Pathog. **7**:1001307.

46. **Cook GM, Berney M, Gebhard S, Heinemann M, Cox RA, Danilchanka O**, *et al*. 2009. Physiology of mycobacteria. Adv Microb Physiol. **55**:81–319.

47. **Mouton JM, Helaine S, Holden DW, Sampson SL.** 2016. Elucidating population-wide mycobacterial replication dynamics at the single-cell level. Microbiology. **162**(6):966-978.

48. **Brauner A, Fridman O, Gefen O, Balaban NQ.** 2016. Distinguishing between resistance, tolerance and persistence to antibiotic treatment. Nat Rev Microbiol. **14**:320–30.

49. **Gefen O, Balaban NQ.** 2009. The importance of being persistent: heterogeneity of bacterial populations under antibiotic stress. FEMS Microbiol Rev. **33**:704–17.

50. **Balaban NQ, Helaine S, Lewis K, Ackermann M, Aldridge B, Andersson DI,** *et al.* Definitions and guidelines for research on antibiotic persistence. Nat Rev Microbiol. **17**:441–8.

51. **Sebastian J, Swaminath S, Nair RR, Jakkala K, Pradhan A, Ajitkumar P.** 2017. *De novo* emergence of genetically resistant mutants of *Mycobacterium tuberculosis* from the

persistence phase cells formed against antituberculosis drugs *in vitro*. Antimicrob Agents Chemother. **61**:01343-16.

52. **Höner zu Bentrup K, Russell DG**. 2001. Mycobacterial persistence: adaptation to a changing environment. Trends Microbiol. **9**:597–605.

53. **Cumming BM, Lamprecht DA, Wells RM, Saini V, Mazorodze JH, Steyn AJC**. 2014. The physiology and genetics of oxidative stress in mycobacteria. Microbiol Spectr. **2**(3).

54. **Keren I, Minami S, Rubin E, Lewis K.** 2011.Characterization and transcriptome analysis of *Mycobacterium tuberculosis* persisters. mBio. 2:00100-11.

55. **Helaine S, Thompson JA, Watson KG, Liu M, Boyle C, Holden DW**. 2010. Dynamics of intracellular bacterial replication at the single cell level. Proc Natl Acad Sci. **107**(8):3746-51.

56. **WHO.** 2018. TB/HIV: A clinical manual. **2**:212.

57. **Becerra MC, Freeman J, Bayona J, Shin SS, Kim JY, Furin JJ,** *et al.* 2000. Using treatment failure under effective directly observed short-course chemotherapy programs to identify patients with multidrug-resistant tuberculosis. Int J Tuberc Lung Dis Off J Int Union Tuberc Lung Dis. **4**:108–14.

CHAPTER 2

The impact of isoniazid resistance on *Mycobacterium tuberculosis*

My contribution: Literature search

Writing and editing of the review

2.1 Introduction

Tuberculosis (TB) still remains a major health problem globally with more than 10 million cases of active TB per year despite the availability of anti-TB drugs to treat the disease (1,2). In addition, TB disease is one of the top ten causes of death worldwide (2). TB is caused by a slow-growing pathogen, *Mycobacterium tuberculosis* (*M. tuberculosis*) (3). The World Health Organization (WHO) estimated a global incidence of 10 million new cases of TB in 2018 (ranging from 9.0–11.1 million) (2). Interestingly, an estimated 8.6% of the TB cases in 2018 were individuals co-infected with the human immuno deficiency virus (HIV) (2). The proportion of TB cases co-infected with HIV was highest in men compared to women (32%) and children (11%) in 2018 (2). An estimated 251 000 (ranging from 223 000–281 000) deaths from TB disease among HIV-positive individuals and an additional 1.2 million (ranging from 1.1–1.3 million) deaths from TB disease among HIV-negative people in 2018, was also reported (2). The WHO recommended the use of isoniazid (INH) preventive therapy for HIV-positive patients, who are latently infected with TB, in order to reduce their risk of developing active TB disease (4). One of the greatest challenges in eradicating TB is the emergence and transmission of drug resistance. Factors that fuel the emergence of TB drug resistance include inappropriate treatment administration by health care facilities and poor treatment compliance (5).

The WHO recommends a drug treatment regimen of at least six months, that is assumed to decrease the population of drug susceptible actively replicating bacteria (6). However, the lengthy treatment period leads to poor adherence that subsequently results in high treatment failure rates and continuous emergence and amplification of drug resistance (6). The WHO reported an estimated 558 000 new TB cases with resistance to the most potent first-line drug, rifampicin (RIF) (2). Approximately 82% of these cases were infected with a *M. tuberculosis* strain resistant to isoniazid (INH) and were classified as multidrug-resistant TB (MDR-TB) cases (2,5,6). MDR-TB is defined as *M. tuberculosis* strains resistant to the first-line anti-TB drugs, INH and RIF (7–9). This high prevalence of MDR-TB increasingly exerts pressure on TB control programmes and thus negatively influences TB infection control (2,5). Early TB diagnosis and the administration of appropriate treatment for TB disease resulted in an increased global treatment success rate of 85% in 2017 compared to 81% in 2016 (2,10).

RIF resistance is suggested to be a surrogate marker for MDR-TB (11). Reports indicate that RIF resistance in approximately 95% of *M. tuberculosis* clinical isolates is attributed to mutations in the *rpoB* gene which encodes the beta-subunit of RNA polymerase (12). These mutations are clustered within the rifampicin resistance determining region (RRDR) of the *rpoB* gene (12). Mutations in *katG, inhA, kasA, oxyR* and *ahpC* genes have been shown to cause INH resistance in clinical *M. tuberculosis* strains, with 60-90% of mutations occurring at codon 315 of *katG* and in the promoter region of *inhA* (13,14). Commercial assays have been developed that detect mutations in *rpoB*, *katG* and the *inhA* promoter to rapidly identify RIF and INH resistance (14,15). These include the line-probe assay (GenoType® MTBDR*plus*), which was endorsed by the WHO in 2008 and previously assessed in South Africa and Europe (16–18). The introduction of the GeneXpert assay resulted in a breakthrough of ehancing the point-of-care TB diagnostics, with an increased number of TB suspects being screened (19). The implementation of the GeneXpert assay rapidly detects TB disease and RIF resistant *M. tuberculosis* infection in symptomatic patients (20). Rapid diagnosis limits diagnostic delay and allows fast and effective treatment administration, which subsequently limit disease transmission.

It has been shown that *M. tuberculosis* resistant to RIF is more likely to be associated with resistance to INH (11). INH is a hydrophilic pro-drug that has been used to treat TB disease since 1952 (21). The mode of action of INH is complex and not fully understood, despite its simple chemical structure (Figure 2.1). INH is proposed to enter the mycobacterial cell by passively diffusing through porin proteins (22). It is subsequently activated by the bacterial catalase-peroxidase enzyme (KatG) (21,22). The active form of INH targets one of the components of the mycobacterial cell wall i.e. mycolic acids, which is essential for the survival of *M. tuberculosis* (23–25). The isoenzyme NADH-specific enoyl-acyl carrier protein reductase (InhA), encoded by *inhA,* is instrumental in mycolic acid biosynthesis and is reported to be the intracellular target of INH (23,24,26). Understanding the mechanisms by which INH is activated and binds to its target to subsequently inhibit mycolic acid biosynthesis and the mechanism of compensation for the loss of KatG function will aid in understanding the molecular mechanisms of INH resistance.

This review aims to highlight the fundamentals of INH drug resistance and its impact on *M. tuberculosis*. It focuses on the significance of the mechanism of action of INH, the molecular

mechanisms of INH resistance and the influence of INH resistance on continuous evolution of drug resistance and MDR-TB incidences in *M. tuberculosis*. It further provides information on consequences of the molecular epidemiology of INH resistance, INH drug tolerance and the pathogenesis, fitness and transmissibility of INH resistant strains in *M. tuberculosis.*

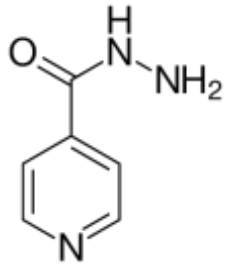

Figure 2.1 2D structure of INH (Structure was obtained from PubChem; http://www.ncbi.nlm.nih.gov/pccompound)

2.2 INH mechanism of action and mycobacterial cell wall

INH selectively kills actively replicating mycobacterial cells and has a minimum inhibitory concentration (MIC) *in vitro* ranging from 0.15 to 0.44 µM in *M. tuberculosis* (21,27). It employs a bactericidal effect during initial 24h exposure of *M. tuberculosis* to INH, after which its action becomes bacteriostatic (21,27). However, a 3 to 4 log decrease in colony-forming units (CFU) is frequently observed in *M. tuberculosis* cells after 4 days of treatment at low (0.2 µg/ml) or high (1.0 µg/ml) concentrations of INH (21).

INH targets the mycobacterial cell wall (21,27). The structure of the mycobacterial cell wall influences the pathogenic ability of *M. tuberculosis* and is essential in mycobacterial viability and virulence (28,29). The mycobacterial cell wall is composed of peptidoglycan, arabinogalactan and mycolic acids, assembled by glycosyltransferases working in sequence through metabolic pathways (30,31). This multi-layered structure protects *M. tuberculosis* from the immune system of the host (28). In addition, it functions as a permeability barrier to limit the influx of anti-TB drugs into the bacterial cell (28,31). *M. tuberculosis* is able to exploit the complexity of the cell wall to adapt and survive anti-TB drug treatment (32). INH

has been shown to specifically target mycolic acid synthesis, which is an essential component of the mycobacterial cell wall (30,31,33,34).

Mycolic acids are long-chain α-alkyl β-hydroxy fatty acids (C70 – C90 carbons in length) and essential components of the cell wall (28,35,36). The long meromycolate and short α-chains complete the attachments of the mycolic acids to both peptidoglycan and arabinogalactan covalently (28,36). Literature shows that the disruption of the cell wall results in the dispersion of free lipids, proteins, lipoarabinomannan and mannosides except for mycolic acid-arabinogalactan-peptidoglycan complex (28,36). However, the cell wall remains intact, indicating that these components are conserved and help maintain the mycobacterial cellular structure (28,36).

INH enters the mycobacterial cell through passive diffusion and is activated intracellularly by the catalase-peroxidase, KatG (Figure 2.2) (36). This protein is a hemoprotein that functions both as a peroxynitritase and nicotinamide adenine dinucleotide hydrogenase (NADH) oxidase (37–39). After its activation, it binds to enoyl-ACP reductase (InhA) and forms an InhA-NAD (nicotinamide adenine dinucleotide) adduct complex (40). InhA forms part of the fatty acid synthase type II (FASII) system (Figure 2.2), that is responsible for the synthesis of mycolic acids (33,41,42). Therefore, the inhibition of InhA prevents fatty acid elongation that subsequently results in the accumulation of long-chain fatty acids (Figure 2.2) (43). The disruption of mycolic acid biosynthesis ultimately results in mycobacterial cell death (Figure 2.2) (36,40).

Another gene involved in mycolic acid biosynthesis is *mabA* (Figure 2.2) (33,44). *MabA* is found upstream of *inhA* and is a potential target of INH and ethionamide (ETH) in *M. tuberculosis* (24,45). Studies suggests that the overexpression of MabA, which results in mycolic acid synthesis, may contribute to INH resistance (24,45). A previous study indicated that a silent *mabA* (G609A) mutation results in the upregulation of *inhA*, converting the region adjacent to the mutation into an alternative promoter for *inhA* (46). This results in a novel mechanism of INH resistance in *M. tuberculosis* clinical strains in the absence of other known INH resistance conferring mutations (46). Shutting down of the mycolic acid biosynthetic pathway is essential, as it acts as the core of the mycobacterial cell wall that *M.*

tuberculosis use to adapt to and survive stressful environments (28,40). This emphasizes the importance of the mycobacterial cell wall components for *M. tuberculosis* survival.

The β-ketoacyl-ACP synthase (KasA), encoded by the *kasA* gene, is also involved in the synthesis of mycolic acids (47) (Figure 2.2). Larsen *et al*. (2002) showed that the overexpression of *inhA*, but not *kasA*, confers resistance to INH and ETH in *M. smegmatis*, *M. bovis* Bacillus Calmette–Guérin (BCG) and *M. tuberculosis* (48). In support, Kremer *et al.* (2003) further revealed that INH targets *inhA* and not *kasA* and that the inhibition of *inhA* activity, but not *kasA* activity, induces formation of a *kasA*-containing complex in mycobacteria (49). Reports showed that *kasA* is associated with the upregulation of a saturated hexacosanoic acid (AcpM) in response to INH treatment (47). Nevertheless, the mechanism by which KasA switches off mycolic acids synthesis is yet to be discovered.

Interestingly, INH activation also has a physiological role. It results in the formation of numerous free radical species that can disable many cellular processes in *M. tuberculosis* (50). These include some pathways involved in macromolecular synthesis, such as lipid synthesis and carbohydrate synthesis (51), nucleic acid synthesis (52) and protein synthesis (53). However, KatG protects *M. tuberculosis* during oxidative stress as it detoxifies reactive oxygen species (54). A previous study employing a quantitative proteomic analysis showed that overexpression of *fbpC* in *M. bovis* BCG increases the susceptibility to INH by upregulating the expression of *katG* (55,56). *FbpC* maintains the integrity of the cell wall by catalyzing the transfer of mycolic acids to cell wall arabinogalactan through the synthesis of alpha, alpha-trehalose dimycolate (57). It is suggested that the increase in *katG* expression, which is induced by the overexpression of *fbpC* in *M. bovis* BCG, lead to an increased rate of INH activation in *M. tuberculosis*, thereby resulting in phenotypic susceptibility to INH (58).

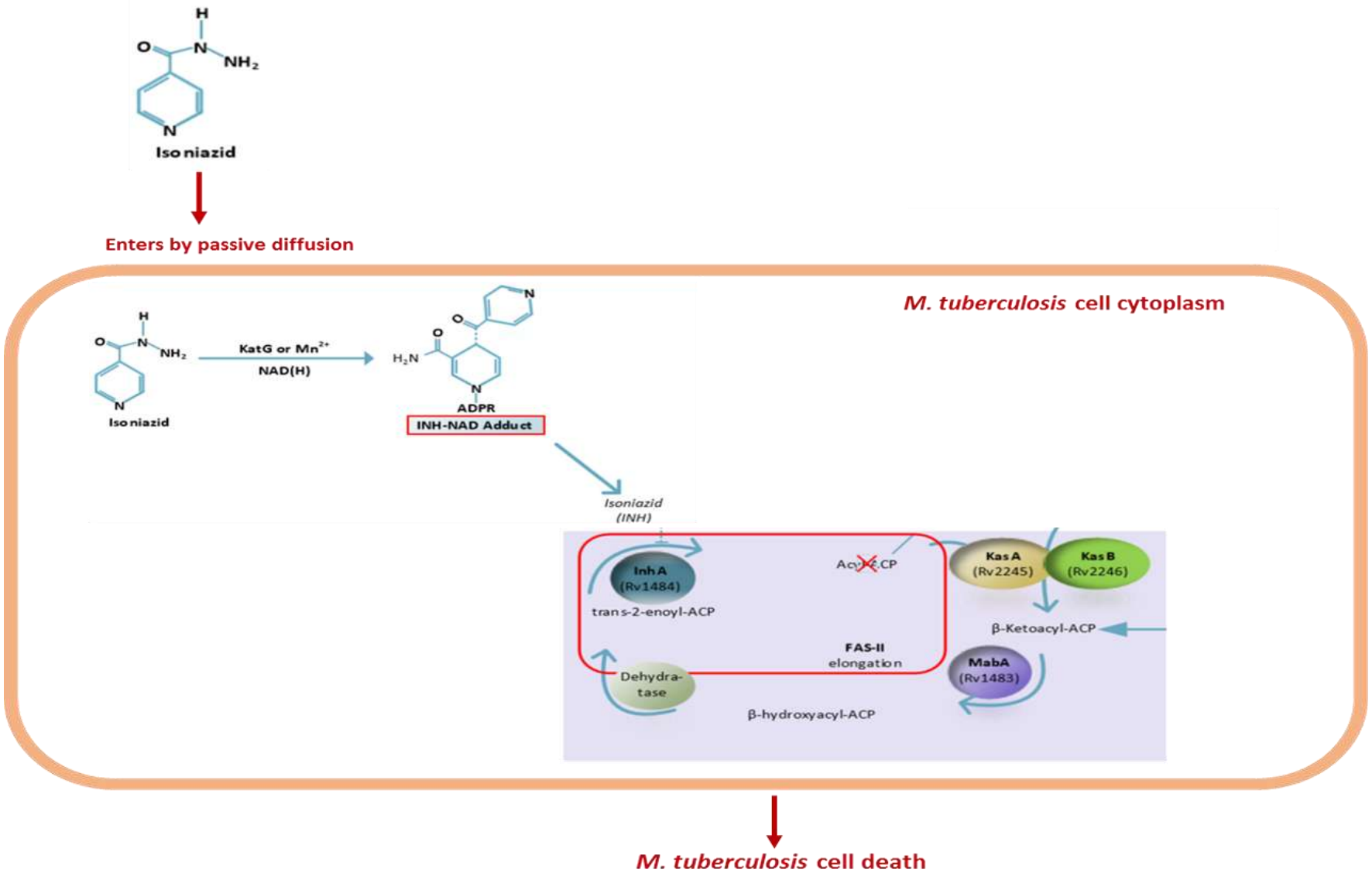

Figure 2.2 INH mechanism of action in the context of the mycolic acid synthesis pathway. INH enters the mycobacterial cell cytoplasm by passive diffusion and is activated by KatG. The formed INH-NAD adduct subsequently inhibits enoyl-ACP reductase (InhA), beta-ketoacyl ACP synthesase (KasA/KasB) and β-hydroxyacyl-ACP (MabA) of the FASII. This inhibition results in the disruption of mycolic acids biosynthesis and ultimately causes cell death. The figure was reproduced from (59).

2.3 Mechanisms of INH resistance

2.3.1 INH resistance-conferring mutations in *M. tuberculosis*

The mutation frequency in response to INH in *M. tuberculosis* is 1 in 10^{-7} to 10^{-8} bacilli (60). INH resistance in *M. tuberculosis* clinical strains is primarily attributed to mutations in *katG*, with Ser315Thr reported as the most clinically prevalent mutation (61–65). Several mutations in *katG* result in the loss of catalase activity (61–65), which subsequently influences the rate of INH activation and confers high-level resistance to INH (> 0.4 µg/ml) (Table 2.1) (37,66–68). Sequence analysis done on INH resistant *M. tuberculosis* strains identified the *katG* Ser315thr mutations in 76% of these strains. In addition, the C-15T variant in *inhA* promoter was identified in 8% of the residual INH resistant *M. tuberculosis* strains (69). This indicates that mutations in *katG* and *inhA* promoter are the primary cause of INH resistance in *M. tuberculosis.*

DNA sequencing analysis of INH resistant and ETH resistant *M. smegmatis* and *M. bovis* BCG isolates identified a Ser94Ala mutation in *inhA* that was further shown to result in the conformational change in the InhA protein, suggesting ineffective binding of INH to NAD (24,70). Subsequent reports indicated that the overexpression of *inhA* in *M. smegmatis* resulted in high-level resistance to INH with an MIC > 0.2 µg/ml (71,72), suggesting that *inhA* overexpression contributes to intrinsic resistance to INH in *M. smegmatis*. Previous studies reported that other mutations in the *inhA* promoter (T-8G/A, C-15T and A-16G) lead to overexpression of the InhA protein and subsequent low-level resistance to INH in *M. tuberculosis* (48,63) (Table 2.1). Interestingly, 15-25% of INH resistant clinical isolates do not harbour mutations in the *inhA* promoter or the hot spot of the *katG* gene in *M. tuberculosis* (71,72). This suggests that other rare mutations may be responsible or may contribute to INH resistance in mycobacteria. Alternative mutations in *inhA* (Ile16Thr, Ile21Val, Ile95Pro and Ile47Thr) have also been reported to confer clinical resistance to INH (73–77).

Table 2.1 Genetic mutations that confer INH resistance in mycobacteria

Gene/intergenic region	Mutation	Mycobacterial strain	Reference
katG	Ser315Thr	*M. tuberculosis*	(37,66–68)
inhA	Ile16Thr Ile21Val Ile95Pro	*M. tuberculosis*	(73–77)
inhA	Ser94Ala Ile47Thr	*M. smegmatis, M. bovis* BCG	(24,70)
inhA prom	C-15T	*M. tuberculosis*	(73–77)
kasA	Asp66Asn Gly269Ser Gly312Ser	*M. tuberculosis*	(34,47,58,78)
ahpC	G-48A G-51A C-54T G-74A C-81T	*M. tuberculosis*	(34)
furA	Ser5Pro	*M. tuberculosis*	(79)
Rv1772	Thr4Ala	*M. tuberculosis*	(80)
efpA	Glu520Val	*M. tuberculosis*	(81)

2.3.2 Rare mutations which confer INH resistance in mycobacteria

Some INH resistance causing mutations result in fitness costs in *M. tuberculosis* (82,83), leading to the evolution of a mycobacterial population that harbour compensatory mutations (82–84). For example, the overexpression *ahpC* gene compensates for the loss of *katG* function (due to the presence of the Ser315Thr mutation in *katG*) in INH resistant *M. tuberculosis* clinical isolates (85,86). The AhpC (alkyl hydro peroxidase) protein is encoded by *ahpC* and activates the reduction of substrate peroxides (85). A subsequent study identified 5 mutations in the *ahpC* promoter (G−48A, G−51A, C−54T, G−74A and C−81T) that lead to the overexpression of AhpC in INH resistant isolates (Table 2.1) (34). These mutations are thought to be rare but are mostly linked to *katG* mutations (in addition to Ser315Thr) responsible for the complete loss of KatG activity (34). Studies in *M. smegmatis* suggest that the overexpression of *ahpC* results in resistance to INH, conversely, the inactivation of *ahpC* results in INH susceptibility (87,88). These studies were performed *in vitro*, and limited information on the mechanisms of INH resistance *in vivo* is available. A study by Bergval *et al.* (2009) showed that an *in vivo* mechanism of INH resistance does not correlate with findings from *in vitro* studies (89). This was confirmed by characterizing spontaneous INH resistant mutants, which revealed the presence of clinically relevant INH resistance mutations in less than 0.8% of *M. tuberculosis* INH resistant strains selected *in vitro* (89).

Interestingly, the expression of both KatG and AhpC are regulated in response to oxidative stress by OxyR (34,90,91). OxyR is a transcription factor that is sensitive to peroxide-induced stress in Gram-negative bacteria (34,90,91) and is activated by exposure to low dosages of hydrogen peroxide (91). The *ahpC* gene forms part of the *oxyR*-dependent peroxide-inducible branch and it uses the basal levels of peroxides generated during aerobic growth via AhpC expression, to regulate KatG levels (34). Literature shows that *oxyR* activates 9 proteins that protect the cell against oxidative stress conditions (92,93). However, the presence of deletions in these proteins, results in the inactivation of *oxyR* in *M. tuberculosis*, exposing the cell wall to oxidative stress (92,93). Previously, high level INH resistance was reported in *M. tuberculosis* H37Rv transformed with the *oxyR-ahpC* region of *M. leprae* (87,93–95). This suggests that other *oxyR* mutations are associated with INH resistance in *M. tuberculosis* (88,96).

Other known compensatory mutations include mutations in *kasA*, leading to low-level INH resistance (84). Treating INH resistant *M. tuberculosis* clinical isolates with INH, results in the upregulation of *kasA* (84), which results in increased synthesis of mycolic acids (47). Sequence analysis of INH-resistant *M. tuberculosis* clinical isolates identified 4 mutations (Asp66Asn, Gly269Ser, Gly312Ser and Phe413Lys) in the *kasA* gene (Table 2.1) (47,78). The Phe413Lys mutation is positioned at the carboxyl terminus of the KasA protein and is shown to modify protein-protein interactions (78). DNA microarrays and mRNA analysis of INH treated *M. tuberculosis* implicated hyper-expression of *kasA* in INH resistance (34,58).

Reports indicate that mutations in *furA*, *Rv1592c* and *Rv1772* are also associated with INH resistance (80,81,98–100). The *furA* gene, encodes a homolog of Fur (ferric uptake regular) (79). Three mutations at position 5, 205 and 291 in the *furA* coding region were identified in INH resistant *M. tuberculosis* that also harboured *katG* mutations (Table 2.1) (79). These findings are important because FurA is a regulatory factor thought to respond to fluctuations in the formulation of transition metals, including iron, which is important for growth in *M. tuberculosis* (79). Limited data exists on the roles of *Rv1592c* and *Rv1772* in *M. tuberculosis* in INH resistance (80,98). A study by Ali *et al*. (2015) identified the Gly9Asp mutation in *Rv1592c* by whole genome sequencing that was present only in INH resistant strains that harboured the *katG* Ser315Thr mutation (80,98). Additionally, one of the INH resistant isolates harboured a Thr4Ala substitution in *Rv1772*, absent in INH susceptible isolates (Table 2.1) (80,98). DNA sequencing analysis revealed an Asp355Glu mutation in the *Rv1592c* gene in INH-susceptible *M. tuberculosis* strain (80). Furthermore, it also revealed substitutions at codon 221 (synonymous) and 322 (non- synonymous), in the *Rv1259c* gene in *M. tuberculosis* (80). However, the latter mutations do not directly confer INH resistance.

2.3.3 Metabolic pathways affected by INH resistance in *M. tuberculosis*

A study exploring an omics approach to compare the metabolomes of INH resistant *M. tuberculosis* clinical strains harbouring *katG* mutations (Ser315Leu and mutation at codon 321 of the *katG* gene) and a sensitive *M. tuberculosis* clinical strain, reported increased synthesis and uptake of alkanes and fatty acids in the INH resistant strain (92). This report supports the previous findings of Rojo *et al*. (2009) that fatty acids are the final product of the degradation pathway of alkanes and can be used as an

energy source or for cell wall synthesis (92,101). This suggests that INH resistant *M. tuberculosis* strains use the degradation pathway of alkanes when under oxidative stress and unfavourable conditions to yield needed energy.

2.3.4 Efflux and INH resistance

The *iniABC* genes encode efflux proteins that have a similar function to MDR-pumps (102). Previously it was shown in *M. tuberculosis* that the expression of *iniA, iniB and iniC* were induced upon INH and ethambutol (EMB) treatment *in vitro* (99,100). The overexpression of *M. tuberculosis iniA* (induced along with *iniB* and *iniC*) in *M. bovis* BCG conferred resistance to EMB (100,102). This suggests that the *iniA* efflux mechanism reduced the intracellular accumulation of EMB within the mycobacterial cell, resulting in the increase in the level of EMB resistance. The addition of the efflux pump inhibitor reserpine, (which inhibit the ability of the transport to export drugs out of the cell) resulted in the increased intracellular EMB accumulation within the mycobacterial cell (100,102). This decreased the EMB level of resistance and enhanced its susceptibility and therefore, indicating that efflux mechanism might contribute to EMB resistance in *M. bovis* BCG. Furthermore, several mutations that result in amino acid substitutions in *iniA* (5-bp deletion at position 94), in *iniB* (substitution at position 83) and a frameshift in *iniC* (12-bp deletion at position 222) were identified. These mutations were identified in the presence of other INH resistance associated mutants (*katG* Ser315Thr and *iniA* Arg537His) in the INH resistant *M. tuberculosis* isolates (80). Previous studies showed that treatment of INH resistant *M. tuberculosis* strains with INH results in the upregulation of *efpA* (encoding an efflux protein) and identification of Glu520Val mutation in this *efpA* gene (Table 2.1) (58,81,103,104). This was observed in the absence of other INH resistance associated mutants and therefore, suggesting that *efpA* could play a minor role in low-level INH resistance in *M. tuberculosis*.

2.4 Molecular epidemiology of INH resistance

Previous studies have provided evidence of the transmission of INH resistant *M. tuberculosis* and its contribution to the MDR-TB epidemic (105,106). A recent study showed that patients infected with INH-monoresistant *M. tuberculosis* strains were less likely to have a favourable treatment outcome (odds ratio (OR) = 0.63, 95% confidence interval (CI) 0.49–0.80, p= 0.001) compared to patients infected with a drug-sensitive *M. tuberculosis* strain (107). The WHO TB treatment guidelines

recommends a longer therapy for patients infected with INH-monoresistant *M. tuberculosis* strains and the longer treatment duration could increase the risk of treatment non-compliance (Figure 2.3) (108,109). There are many aspects that contribute to the acquisition of INH resistance; below we propose a theoretical model showing the different stages in TB infection whereby *M. tuberculosis* may acquire INH resistance (Figure 2.3) (108,109).

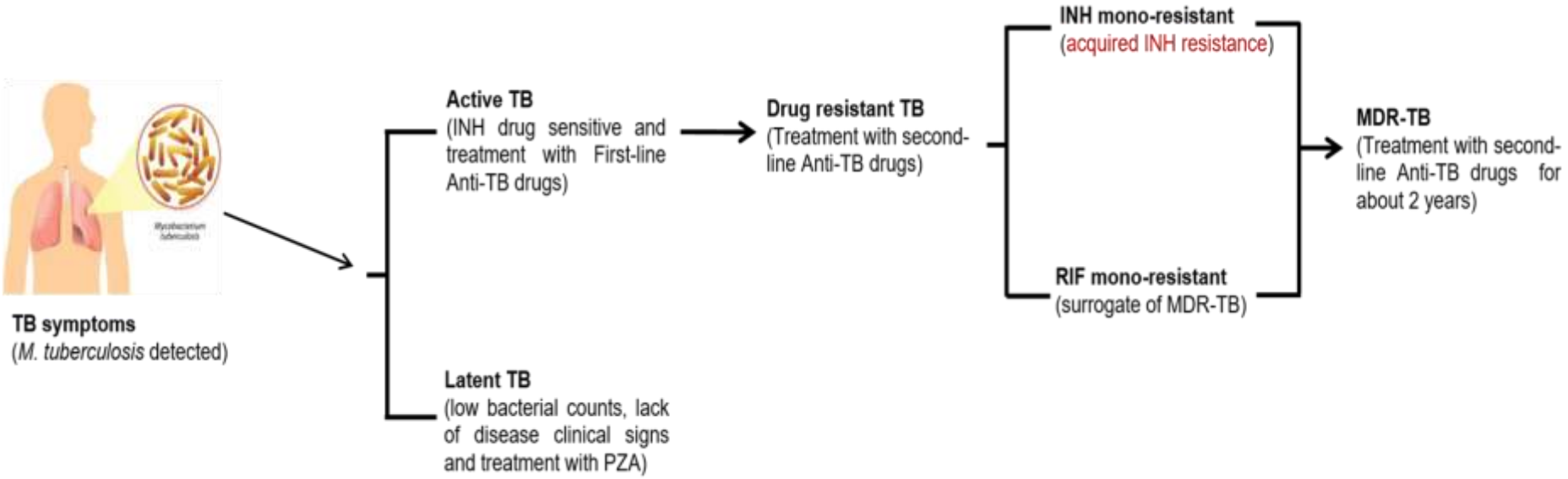

Figure 2.3 Proposed theoretical model showing the different stages in TB infection whereby *M. tuberculosis* may acquire INH resistance. This model is based on the assumption that the patient is infected with INH sensitive *M. tuberculosis* strain initially (primary infection). It depicts briefly that, (a) TB diseased patient; with a positive smear microscopy culture has active TB disease, which is sensitive to INH and other first-line anti-TB drugs. (b) Latently infected TB patients (based on positive TB skin-test result) are treated with INH for 9 months or PZA (under recommendation). (c) Due to prolonged anti-TB drug treatment many complications might occur and lead to anti-TB drug treatment non-compliance or relapse that results in the sensitive TB progressing to INH or RIF drug resistant TB (treated with addition of second-line anti-TB drugs). (d) DST will be done and if it confirms INH mono- resistance, other alternative anti-TB drugs would be considered for treatment. (e) However, if the DST confirms resistance to both INH and RIF it means they would have acquired MDR-TB with the possibility for 2 years anti-TB drug treatment duration (108,109).

Several epidemiological studies have shown the correlation between the prevalence of INH-monoresistance and MDR-TB transmission (105,110,111). A study conducted in China showed a prevalence of 41.2% and 8.3% of INH-monoresistant and MDR-TB, respectively, compared to the global estimates of 13.3% for INH-monoresistance and 4.8% for MDR-TB (Table 2.2) (105). An INH-monoresistant TB outbreak (1995 - 2014) was also reported in England and Wales with a prevalence of 39% and 7%, respectively (111). Recently, a Vietnamese study reported that 90.4% of the INH-monoresistant strains harboured mutations in INH resistance-conferring genes, of which 75.3% occurred in *katG* and 24.7% occurred in the *inhA* promoter region (Table 2.2) (112). In this study, the overall proportion of INH-monoresistant isolates was 5.7% of which 12.6% were identified amongst previously treated TB patients and 5% in new TB patients. Since some studies suggest that INH-monoresistance is a precursor to MDR-TB (113), more knowledge about the prevalence of INH-monoresistance could provide insight on the continuous spread of drug-resistant TB and the evolution of MDR-TB. Additionally, understanding this can aid in development of MDR-TB infection preventative strategies. Denkinger *et al*. demonstrated that adding the detection of INH-resistance marker to a rapid test for TB plus RIF-resistance results in the decrease of the prevalence of MDR-TB from 3.8% to 3.6% and of INH mono-resistance from 15.8% to 15.1% compared to that without the markers (114). Therefore, this suggests that the addition of INH resistance markers had minimal impact on the transmission of drug susceptible, INH-monoresistant and MDR-TB.

An epidemiological study conducted in San Francisco confirmed 152 (85.9%) out of 177 studied *M. tuberculosis* strains to be INH resistant. From the 152 INH resistant *M. tuberculosis* strains confirmed, transmission dynamics were for the 143 strains and it showed that 89.9% of these strains had at least 1 mutation in either *katG* Ser315Thr or the *inhA* promoter (C-15T) (Table 2.2) (115). This suggests that *M. tuberculosis* strains harbouring a *katG* Ser315Thr or *inhA* promoter mutation are more likely to spread than *M. tuberculosis* strains with mutations in other genes associated with INH-resistance (115). An epidemiological study conducted in Western Sweden showed 10% of TB patients were infected with INH-monoresistant *M. tuberculosis* strains (116). Further analysis of strain types, demonstrated that 23.2% of these INH-resistant isolates belonged to the Haarlem and 9.8% to the Beijing families (116).

Interestingly, genetic analysis revealed that 44.0% of *M. tuberculosis* isolates in patients from South Ukraine harboured mutations that conferred resistance to INH (117). The *katG* Ser315Thr mutation was identified in 71.4% of strains that belonged to the Beijing family (Table 2.2) (117). These observations support previous reports that strain genetic background influences the transmission of INH resistance in different geographical settings.

2.5 Pathogenesis, fitness and transmissibility of INH resistant strains

Bacterial fitness plays a role in the emergence of drug-resistant bacteria (118,119), based on the dogma that drug-resistant strains are less fit than their drug-susceptible counterparts (120,121). Factors that are known to affect the fitness of circulating strains include drug pressure, environmental changes, the genotype of the strain and the stress induced by the competing strains (122). The resistance conferring mutations that occur in essential genes have a negative influence on the key physiological functions in *M. tuberculosis* (118,120). Reports indicate that drug resistant *M. tuberculosis* strains exhibit reduced "fitness", which results in these strains being less transmissible and therefore less likely to spread successfully in immunocompetent human populations (121). It was previously shown that infecting guinea pigs with INH-resistant tubercle bacilli resulted in reduced pathogenicity compared to infection with INH-sensitive *M. tuberculosis* bacilli (123). It was previously demonstrated that not all INH resistance-causing mutations in genes including *katG, inhA,* and *ahpC* achieve equal levels of fitness-cost in the absence of INH (124). Some studies report that various INH resistant *M. tuberculosis* strains transmission might be driven by the specific INH resistant mutations that are associated with low fitness cost (120,125–129). For example, INH resistant *M. tuberculosis* strains with *katG* (Ser315Thr) mutation is assumed to confer only a very small fitness deficit and higher ''baseline fitness'' compared to *in vitro* INH-mutants with low ''baseline fitness''(130–135).

Strains with mutations that confer little fitness costs are not in need of restoration of fitness and this suggests that these strains are not likely to acquire adaptive or compensatory mutations (136). Previously, it was reported that *inhA* promoter (C-15T) and *katG* (Ser315Thr) mutations are the most frequently circulating mutations associated with INH resistance within communities in different settings with a high prevalence of MDR *M. tuberculosis* clinical strains (137–139). These include INH resistant strains that harbour *katG* (Ser315Thr) and *inh*A prom (C-15T) mutations,

found to be circulating within China and San Francisco (refer to Table 2.2) (105,130). Moreover, INH resistant strains that harbour *katG* (Ser315Thr) and *inh*A prom (C-15T) mutations, were found to be circulating within Taiwan, South Africa and The Philippines, and within Vietnam and South Ukraine, respectively (refer to Table 2.2) (19,66,112,117).

Table 2.2 Frequency of most common mutations in *katG* and *inh*A promoter that confer resistance to INH in clinical *M. tuberculosis* strains

Country Setting	***M. tuberculosis* clinical strains resistance profile**	**Frequency of *katG* (Ser315Thr) mutation**	**Frequency of *inhAprom* (C-15T) mutation**	**References**
China	MDR	41.2%	8.3%	(105)
Taiwan	INH mono-resistant	29%	2.44%	(66)
Vietnam	INH mono-resistant	75.3%	24.7%	(112)
South Africa and The Philippines	INH mono-resistant	82%	10%	(19)
South Ukraine	INH mono-resistant	71.4%	45.7%	(117)
San Francisco	MDR	57.7%	32.2%	(115)

2.6 *In vitro* assessment of fitness

In vitro growth assays are used to assess fitness of INH and RIF resistant *M. tuberculosis* strains (140). A competitive relative fitness assay of *M. tuberculosis* resistant strains from different lineages (Beijing, CAS and MANU) showed reduced fitness when compared to susceptible strains from different lineages from a TB endemic region of Mumbai, India (141). Another study also reported that the *katG* Gly158Ser mutations in *M. tuberculosis* resistant strains confer no fitness cost compared to susceptible strains when measured by *in vitro* growth assays (142). It can be suggested that *M. tuberculosis* resistant strains that harbour INH resistance-conferring mutations exhibit different levels of fitness cost in the presence/absence of INH treatment (142).

2.7 Epistasis in INH resistance

Epistasis is defined as the effect of the interaction between two or more mutations (drug resistance-conferring mutation and a compensatory mutation) on an organism's phenotype (143–145). Studies in drug-resistant bacteria have shown that epistasis manifests when a certain drug resistance-conferring mutation has a fitness cost that is dependent on its genetic background (125,146,147). The effect could either be (i) positive epistasis, which results when the combined cost of the multiple resistance mutations is less than what is expected if the mutations had independent and simple effects of fitness or (ii) negative epistasis, which is known to influence the evolution of MDR by aggravating its cost (143,145). Interestingly, *in vitro* evidence suggests that the nature of pre-existing INH resistant alleles can have an impact on the spectrum of subsequent *rpoB* mutations, which causes resistance to RIF (148). Additionally, analyses of drug resistant clinical *M. tuberculosis* strains revealed that specific INH resistant alleles are more frequently associated with resistance to other drugs (86,149). This suggests that epistatic interactions between INH resistance alleles and RIF resistance-conferring mutations reported in *M. tuberculosis* might play a significant role in continuous transmission of INH resistant *M. tuberculosis* strains. This has important clinical implications for the success of MDR-TB strains. The epistatic interactions between mutations in MDR and XDR *M. tuberculosis* strains, might be a consequence of their continuous increase in the clinical setting (150).

2.8 Regulators of INH resistance in mycobacteria

Transcriptional regulation plays a significant role in the mycobacterial response to environmental stresses (151). Drug exposure is a common stress to the bacteria that alters transcriptional regulation and in turn, increases bacterial drug resistance. Information regarding transcription factors that regulate INH resistance in *M. tuberculosis* is limited. It was suggested that transcriptional regulators such as the GntR family transcription factor, organic hydroperoxide stress resistance regulator (OhrR) and inbR, a Tet repressor proteins (TetR) family regulator, could play a role in INH resistance in mycobacteria upon drug exposure (151–153).

2.8.1 GntR family transcription factors

GntR family transcription factors are widely distributed among bacteria and contain a conserved N-terminal helix-turn-helix (HTH) domain for DNA-binding and diverse C-terminal domains (151,154). GntR family members are mostly known to function as transcriptional repressors, although some of them are transcriptional activators (151). The *M. smegmatis* GntR family transcription factor, encoded by *Ms0535,* binds to its own promoter by recognizing a 26-bp palindromic sequence motif that is separated by four nucleotides (151). Ms0535 also functions as a transcriptional activator that regulates the expression of the major facilitator superfamily (MFS) permease gene *Ms0534*, which is located in the same operon (151,154). Hu *et al.* showed that over-expression of *Ms0535 and Ms0534* in *M. smegmatis* resulted in a significant 4-fold increase in the level of INH resistance (151). In addition, *Ms0534* and *Ms0535* deletion mutants were found to be more sensitive to INH than the wild-type strain (151). This suggests that these transcriptional repressors regulate the level of INH resistance in mycobacteria.

2.8.2 Organic Hydroperoxide Stress Resistance Regulator (OhrR)

Organic Hydroperoxide Stress Resistance Regulator (OhrR) is a MarR type transcriptional regulator that primarily regulates the expression of organic hydroperoxide reductase (Ohr) in bacteria (153,155,156). In the absence of stress, OhrR represses *ohr* expression by binding tightly to its promoter region, through autoregulation (153). In this study, Saikolappan *et al*. constructed *M. smegmatis* mutant strains lacking the reductase (MSΔohr), its regulator (MSΔohrR), as well as the complemented strain (MSΔohrR/c) where the regulator was reintroduced. INH sensitivity testing in these strains showed that sensitivity to INH at MIC was restored

to wild type levels in the complemented strain (MSΔohrR/c), suggesting that the constitutive expression of the MSΔohrR mutant had a significant effect on the sensitivity (153). Similarly to MSΔohr, an increased level of INH resistance was observed in the MSΔohrR mutant compared to the level of resistance of the sensitive progenitor. It was suggested that the deletion of *ohr* and *ohrR* may possibly alter the expression of catalase-peroxidase in these strains, which in return may reduce the sensitivity of INH in *M. tuberculosis* (153).

2.8.3 InbR transcription factor

The TetR family is a large family of transcriptional regulators that contain a conserved helix-turn-helix DNA binding domain and a C-terminal ligand domain (152). InbR transcription factor is a TetR family regulator (Rv0275c) that is directly responsive to INH by directly binding (152). This family of regulators has been shown to be involved in the regulation of drug transporters and efflux pumps involved in drug resistance e.g. *iniBAC*, in other bacteria (152,157). Moreover, the genomes of both *M. tuberculosis* and *M. bovis* BCG encode a large group of TetR family regulators (152). Recently, it was reported that disruption of *inbR* leads to INH hypersensitivity (from 0.04 µg/ml to 0.01 µg/ml), while its overexpression decreased INH susceptibility (from 0.04 µg/ml to 0.16 µg/ml) in *M. bovis* BCG (152). This suggests that InbR is potentially involved in the regulation of INH resistance in *M. bovis* BCG.

2.8.4 Other transcription regulators/factors

A previous study showed that the *ΔsigI* mutant exhibited resistance to INH (MIC_{90} = 0.18 µg/ml) compared to the wild-type strain (MIC_{90}= 0.04 µg/ml in *M. tuberculosis*, suggesting that SigI-mediated expression of *katG* affects *M. tuberculosis* resistance to INH (158). This finding further suggests that the transcriptional responses of INH resistant *M. tuberculosis* might provide essential information about the physiological state of the bacterium that is essential for identifying new drug targets. Interestingly, microarray analysis studies demonstrated that *M. tuberculosis* gene expression in response to INH induces several genes that encode proteins physiologically relevant to the drug's mode of action (58,159); namely, Rv2243 (*fabD*), Rv2244 (*acpM*), Rv2245 (*kasA*), Rv2246 (*kasB*) and Rv2247(*accD6*) forming operonic cluster of five genes encoding type II fatty acid synthase enzymes (160) and *fbpC* that encodes trehalose dimycolyl transferase (58,159).

2.9 INH drug tolerance and persistence

Bacterial persistence results when subpopulation of a clonal bacterial population survives an exposure to high concentrations of antibiotic treatments and this population may persist for longer time periods (161–163). Bacterial persisters, are classified as the surviving bacterial cells (subpopulations) (161–163). It is suggested that bacterial persisters might increase the chances of high-level INH resistance mutations acquisition, by persisting over the average lifetime of bacterial exposure to INH drug (164). Bacteria that are in a stationary phase are not completely eradicated by INH due to the presence of non-replicating persisters which exhibit a drug-tolerant phenotype (164). A time-dependent experiment in *E. coli* demonstrated a distinctive biphasic killing with a fraction of bacterial persisters in mid-exponential phase after 3h treatment with ampicillin (100 μg/ml) (165). It was suggested, this might be due to the heterogeneous response of persistent and non-persistent subpopulations (165). A previous study reported mutations that either impair or enhance persistence in mice that were infected with 200 CFUs of *M. tuberculosis* and treated INH (25 mg/kg/day) (166). This observation was suggested to be a consequence of the disruption of *cydC* gene which accelerated the mycobacterial clearance in the INH-treated mice without affecting growth or survival of the untreated mice (166). The *cydC* is the last ORF in an annotated four-gene cluster (*cydABDC*) that encodes a putative ATP-binding cassette transporter subunit and plays a role in INH drug tolerance (166).

2.10 Concluding remarks

The current review provided comprehensive information about the current state of INH resistance in *M. tuberculosis*, globally. It highlighted key factors that influence continuous spread of INH resistance. That is, the epidemiology and success of INH resistant *M. tuberculosis* strains and the specific role they play in driving MDR-TB epidemic and transmission. INH is one of the key components of global TB control programmes and thus essential to understand its role in TB drug resistance contribution to improved knowledge related to INH resistance's role towards the need for prolonged TB treatment. After many decades, there are still drug-resistant TB cases linked to INH mono-resistance and the association between INH resistant genotype and phenotype is still not fully understood. The continuous evolution of INH resistance makes it challenging to use the current rapid sequencing techniques as part of the diagnostic process for the determination of the most suitable anti-TB

treatment regimen for infected patients and there is a need for better TB diagnostic tools, as highlighted in the review. INH resistance is also driven by the prevalent INH resistant conferring mutations globally that contributes to resistance in different populations. These INH resistant mutations include *katG* Ser315Thr mutation, which occurs in the *katG* gene encoding the KatG protein, and is essential for the optimal functionality of the INH. The review also highlighted the significance of INH drug tolerance and persistence in contributing to INH resistance. This knowledge is essential for the design of new anti-TB drug targets.

2.11 References

1. **Dye C, Scheele S, Dolin P, Pathania V, Raviglione MC**. 1999. Consensus statement. Global burden of tuberculosis: estimated incidence, prevalence, and mortality by country. WHO global surveillance and monitoring project. JAMA J Am Med Assoc. **282**:677–86.

2. **WHO.** 2020. Global tuberculosis report 2019. World Health Organization.

3. **Koch R.** 1933. The Aetiology of Tuberculosis. Arch Intern Med. **51**:818–818.

4. **WHO**. 2017. New WHO guidelines: TB prevention for people with HIV. WHO

5. **Fischbach MA, Walsh CT.** 2009. Antibiotics for emerging pathogens. Science. **325**:1089–93.

6. **Yew WW, Lange C, Leung CC.** 2011. Treatment of tuberculosis: update 2010. Eur Respir J. **37**:441–62.

7. **WHO.** 2019. TB drug resistance types.

8. **Prasad R, Gupta N, Banka A.** 2018. Multidrug-resistant tuberculosis/rifampicin-resistant tuberculosis: Principles of management. Lung India Off Organ Indian Chest Soc. **35**:78–81.

9. **Holtz TH.** 2007. XDR-TB in South Africa: revised definition. PLoS Med. **4**:161.

10. **WHO.** 2018. Global tuberculosis report.

11. **Somoskovi A, Parsons LM, Salfinger M**. 2001. The molecular basis of resistance to isoniazid, rifampin, and pyrazinamide in *Mycobacterium tuberculosis*. Respir Res. **2**:164.

12. **Ali A, Hasan Z, Moatter T, Tanveer M, Hasan R. M.** 2009. Tuberculosis central Asian strain 1 MDR isolates have more mutations in *rpoB* and *katG* genes compared with other genotypes. Scand J Infect Dis. **41**:37–44.

13. **Ling DI, Zwerling AA, Pai M**. 2008. GenoType MTBDR assays for the diagnosis of multidrug-resistant tuberculosis: a meta-analysis. Eur Respir J. **32**:1165–74.

14. **Farooqi JQ, Khan E, Alam SMZ, Ali A, Hasan Z, Hasan R**. 2012. Line probe assay for detection of rifampicin and isoniazid resistant tuberculosis in Pakistan. JPMA J Pak Med Assoc. **62**:767–72.

15. **Brossier F, Veziris N, Truffot-Pernot C, Jarlier V, Sougakoff W**. 2006. Performance of the genotype MTBDR line probe assay for detection of resistance to rifampin and isoniazid in strains of *Mycobacterium tuberculosis* with low- and high-level Resistance. J Clin Microbiol. **44**:3659–64.

16. **Organization WH.** 2016. The use of molecular line probe assay for the detection of resistance to isoniazid and rifampicin: policy update. World Health Organization.

17. **Barnard M, Albert H, Coetzee G, O'Brien R, Bosman ME.** 2008. Rapid molecular screening for multidrug-resistant tuberculosis in a high-volume public health laboratory in South Africa. Am J Respir Crit Care Med. **177**:787–92.

18. **Miotto P, Piana F, Penati V, Canducci F, Migliori GB, Cirillo DM**. 2006. Use of genotype MTBDR assay for molecular detection of rifampin and isoniazid resistance in *Mycobacterium tuberculosis* clinical strains isolated in italy. J Clin Microbiol. **44**:2485–91.

19. **Torres JN, Paul LV, Rodwell TC, Victor TC, Amallraja AM, Elghraoui A, *et al***. 2015. Novel *katG* mutations causing isoniazid resistance in clinical *M. tuberculosis* isolates. Emerg Microbes Infect. **4**:42.

20. **WHO**. 2017. Global tuberculosis report 2017.

21. **Pansy F, Stander H, Donovick R**. 1952. *In vitro* studies on isonicotinic acid hydrazide. Am Rev Tuberc. **65**:761–4.

22. **Bardou F, Raynaud C, Ramos C, Lanéelle MA, Lanéelle G**. 1998. Mechanism of isoniazid uptake in *Mycobacterium tuberculosis*. Microbiol Read Engl. **144**:2539–44.

23. **Dessen A, Quémard A, Blanchard JS, Jacobs WR, Sacchettini JC.** 1995. Crystal structure and function of the isoniazid target of *Mycobacterium tuberculosis*. Science. **267**:1638–41.

24. **Banerjee A, Dubnau E, Quemard A, Balasubramanian V, Um KS, Wilson T, *et al*.** 1994. *inhA*, a gene encoding a target for isoniazid and ethionamide in *Mycobacterium tuberculosis.* Science. **263**:227–30.

25. **Barry CE, Lee RE, Mdluli K, Sampson AE, Schroeder BG, Slayden RA, *et al*.** 1998. Mycolic acids: structure, biosynthesis and physiological functions. Prog Lipid Res. **37**:143–79.

26. **Rozwarski DA, Grant GA, Barton DH, Jacobs WR, Sacchettini JC.** 1998. Modification of the NADH of the isoniazid target (InhA) from *Mycobacterium tuberculosis*. Science. **279**:98–102.

27. **Ramaswamy S, Musser JM**. 1998. Molecular genetic basis of antimicrobial agent resistance in *Mycobacterium tuberculosis*: 1998 update. Tuber Lung Dis Off J Int Union Tuberc Lung Dis. **79**:3–29.

28. **Brennan PJ.** 2003. Structure, function, and biogenesis of the cell wall of *Mycobacterium tuberculosis*. Tuberc Edinb Scotl. **83**:91–7.

29. **Wolfe LM, Mahaffey SB, Kruh NA, Dobos KM**. 2010. Proteomic definition of the cell wall of *Mycobacterium tuberculosis*. J Proteome Res. **29**:5816–26.

30. **Chatterjee D.** 1997. The mycobacterial cell wall: structure, biosynthesis and sites of drug action. Curr Opin Chem Biol. **1**(4):579–88.

31. **Tam P-H, Lowary TL.** 2009. Recent advances in mycobacterial cell wall glycan biosynthesis. Curr Opin Chem Biol. **13**:618–25.

32. **Campanerut-Sá PA, Ghiraldi-Lopes LD, Meneguello JE, Fiorini A, Evaristo GP, Siqueira VL, *et al*.** 2016. Proteomic and morphological changes produced by subinhibitory concentration of isoniazid in *Mycobacterium tuberculosis.* Future Microbiol. **11**:1123–32.

33. **Quémard A, Sacchettini JC, Dessen A, Vilcheze C, Bittman R, Jacobs WR, *et al.*** 1995. Enzymatic characterization of the target for isoniazid in *Mycobacterium tuberculosis*. Biochemistry. **34**:8235–41.

34. **Slayden RA, Barry CE**. 2000. The genetics and biochemistry of isoniazid resistance in *Mycobacterium tuberculosis.* Microbes Infect Inst Pasteur. **2**:659–69.

35. **Winder FG, Collins PB.** 1970. Inhibition by isoniazid of synthesis of mycolic acids in *Mycobacterium tuberculosis*. J Gen Microbiol. **63**:41–8.

36. **Vilchèze C, Jacobs WR.** 2007. The mechanism of isoniazid killing: clarity through the scope of genetics. Annu Rev Microbiol. **61**:35–50.

37. **Zhang Y, Heym B, Allen B, Young D, Cole S**. 1992. The catalase-peroxidase gene and isoniazid resistance of *Mycobacterium tuberculosis*. Nature. **358**:591–3.

38. W**engenack NL, Jensen MP, Rusnak F, Stern MK.** 1999. *Mycobacterium tuberculosis* KatG is a peroxynitritase. Biochem Biophys Res Commun. **256**:485–7.

39. **Singh R, Wiseman B, Deemagarn T, Donald LJ, Duckworth HW, Carpena X, *et al*.** 2004. Catalase-peroxidases (KatG) exhibit NADH oxidase activity. J Biol Chem. **279**:43098–106.

40. **Rawat R, Whitty A, Tonge PJ.** 2003. The isoniazid-NAD adduct is a slow, tight-binding inhibitor of InhA, the *Mycobacterium tuberculosis* enoyl reductase: adduct affinity and drug resistance. Proc Natl Acad Sci USA. **100**:13881–6.

41. **Minnikin DE, Kremer L, Dover LG, Besra GS**. 2002. The methyl-branched fortifications of *Mycobacterium tuberculosis*. Chem Biol. **9**:545–53.

42. **Schaeffer ML, Agnihotri G, Volker C, Kallender H, Brennan PJ, Lonsdale JT.** 2001. Purification and biochemical characterization of the *Mycobacterium tuberculosis* beta-ketoacyl-acyl carrier protein synthases KasA and KasB. J Biol Chem. **276**:47029–37.

43. **Takayama K, Wang L, David HL.** 1972. Effect of isoniazid on the in vivo mycolic acid synthesis, cell growth, and viability of *Mycobacterium tuberculosis*. Antimicrob Agents Chemother. **2**:29–35.

44. **Kuchi S, Takeuchi T, Yasui M, Kusaka T, Kolattukudy PE.** 1989. A very long-chain fatty acid elongation system in *Mycobacterium avium* and a possible mode of action of isoniazid on the system. Agric Biol Chem. **53**:1689–98.

45. **Banerjee A, Sugantino M, Sacchettini JC, Jacobs WR.** 1998. The *mabA* gene from the *inhA* operon of *Mycobacterium tuberculosis* encodes a 3-ketoacyl reductase that fails to confer isoniazid resistance. Microbiol Read Engl. **144**:2697–704.

46. **Ando H, Miyoshi-Akiyama T, Watanabe S, Kirikae T.** 2014. A silent mutation in *mabA* confers isoniazid resistance on *Mycobacterium tuberculosis*. Mol Microbiol. **91**:538–47.

47. **Mdluli K, Slayden RA, Zhu Y, Ramaswamy S, Pan X, Mead D, *et al*.** 1998. Inhibition of a *Mycobacterium tuberculosis* beta-ketoacyl ACP synthase by isoniazid. Science. **280**:1607–10.

48. **Larsen MH, Vilchèze C, Kremer L, Besra GS, Parsons L, Salfinger M, *et al.*** 2002. Overexpression of *inhA*, but not *kasA*, confers resistance to isoniazid and ethionamide in *Mycobacterium smegmatis*, *M. bovis* BCG and *M. tuberculosis*. Mol Microbiol. **46**:453–66.

49. **Kremer L, Dover LG, Morbidoni HR, Vilchèze C, Maughan WN, Baulard A, *et al.*** 2003. Inhibition of InhA activity, but not KasA activity, induces formation of a KasA-containing complex in mycobacteria. J Biol Chem. **278**:20547–54.

50. **Lei B, Wei CJ, Tu SC.** 2000. Action mechanism of antitubercular isoniazid. Activation by *Mycobacterium tuberculosis* KatG, isolation, and characterization of inha inhibitor. J Biol Chem. **275**:2520–6.

51. **Winder FG, Rooney SA**. 1970. The effects of isoniazid on the carbohydrates of *Mycobacterium tuberculosis* BCG. Biochem J. **117**:355–68.

52. **Ito K, Yamamoto K, Kawanishi S.** 1992. Manganese-mediated oxidative damage of cellular and isolated DNA by isoniazid and related hydrazines: non-Fenton-type hydroxyl radical formation. Biochemistry. **31**:11606–13.

53. **Tsukamura M, Tsukamura S.** 1964. Effect of isoniazid on protein synthesis of mycobacteria. Am Rev Respir Dis. **89**:572–4.

54. **Ng VH, Cox JS, Sousa AO, MacMicking JD, McKinney JD**. 2004. Role of KatG catalase-peroxidase in mycobacterial pathogenesis: countering the phagocyte oxidative burst. Mol Microbiol. **52**:1291–302.

55. **Hu X, Li X, Huang L, Chan J, Chen Y, Deng H, *et al*.** 2015. Quantitative proteomics reveals novel insights into isoniazid susceptibility in mycobacteria mediated by a universal stress protein. J Proteome Res. **14**:1445–54.

56. **McClatchy JK.** 1971. Mechanism of action of isoniazid on *Mycobacterium bovis* strain BCG. Infect Immun. **3**(4):530–4.

57. **Banerjee DI, Gohil TP.** 2016. Interaction of antimicrobial peptide with mycolyl transferase in *Mycobacterium tuberculosis*. Int J Mycobacteriology. **5**:83–8.

58. **Wilson M, DeRisi J, Kristensen HH, Imboden P, Rane S, Brown PO, *et al*.** 1999. Exploring drug-induced alterations in gene expression in *Mycobacterium tuberculosis* by microarray hybridization. Proc Natl Acad Sci USA. **96**:12833–8.

59. **Crellin PK, Luo C-Y, Morita YS.** 2013. Metabolism of plasma membrane lipids in mycobacteria and corynebacteria. **6**:3986

60. **Ford CB, Shah RR, Maeda MK, Gagneux S, Murray MB, Cohen T, *et al.*** 2013. *Mycobacterium tuberculosis* mutation rate estimates from different lineages predict substantial differences in the emergence of drug-resistant tuberculosis. Nat Genet. **45**:784–90.

61. **Abate G, Hoffner SE, Thomsen VO, Miörner H.** 2001. Characterization of isoniazid-resistant strains of *Mycobacterium tuberculosis* on the basis of phenotypic properties and mutations in *katG*. Eur J Clin Microbiol Infect Dis Off Publ Eur Soc Clin Microbiol. **20**:329–33.

62. **Marttila HJ, Soini H, Eerola E, Vyshnevskaya E, Vyshnevskiy BI, Otten TF, *et al.*** 1998. A Ser315Thr substitution in KatG is predominant in genetically heterogeneous multidrug-resistant *Mycobacterium tuberculosis* isolates originating from the St. Petersburg area in Russia. Antimicrob Agents Chemother. **42**:2443–5.

63. **Musser JM, Kapur V, Williams DL, Kreiswirth BN, van Soolingen D, van Embden JD.** 1996. Characterization of the catalase-peroxidase gene (*katG*) and *inhA* locus in isoniazid-resistant and -susceptible strains of *Mycobacterium tuberculosis* by automated DNA sequencing: restricted array of mutations associated with drug resistance. J Infect Dis. **173**:196–202.

64. **Dobner P, Rüsch-Gerdes S, Bretzel G, Feldmann K, Rifai M, Löscher T, *et al.*** 1997. Usefulness of *Mycobacterium tuberculosis* genomic mutations in the genes *katG* and *inhA* for the prediction of isoniazid resistance. Int J Tuberc Lung Dis Off J Int Union Tuberc Lung Dis. **4**:365–9.

65. **Telenti A, Honoré N, Bernasconi C, March J, Ortega A, Heym B, *et al.*** 1997. Genotypic assessment of isoniazid and rifampin resistance in *Mycobacterium tuberculosis*: a blind study at reference laboratory level. J Clin Microbiol. **35**:719–23.

66. **Tseng S-T, Tai C-H, Li C-R, Lin C-F, Shi Z-Y.** 2015. The mutations of *katG* and *inhA* genes of isoniazid-resistant *Mycobacterium tuberculosis* isolates in Taiwan. J Microbiol Immunol Infect Wei Mian Yu Gan Ran Za Zhi. **48**:249–55.

67. **Heym B, Alzari PM, Honoré N, Cole ST.** 1995. Missense mutations in the catalase-peroxidase gene, katG, are associated with isoniazid resistance in *Mycobacterium tuberculosis*. Mol Microbiol. **15**:235–45.

68. **Dantes R, Metcalfe J, Kim E, Kato-Maeda M, Hopewell PC, Kawamura M, *et al.*** 2012. Impact of isoniazid resistance-conferring mutations on the clinical presentation of isoniazid monoresistant tuberculosis. PLoS ONE. **7**:37956.

69. **Kigozi E, Kasule GW, Musisi K, Lukoye D, Kyobe S, Katabazi FA, *et al.*** 2018. Prevalence and patterns of rifampicin and isoniazid resistance conferring mutations in *Mycobacterium tuberculosis* isolates from Uganda. PLoS ONE. **13**:0198091.

70. **Vilchèze C, Wang F, Arai M, Hazbón MH, Colangeli R, Kremer L, *et al*.** 2006. Transfer of a point mutation in *Mycobacterium tuberculosis inhA* resolves the target of isoniazid. Nat Med. **12**:1027–9.

71. **Ramaswamy S, Musser JM.** 1998. Molecular genetic basis of antimicrobial agent resistance in *Mycobacterium tuberculosis*: 1998 update. Tuber Lung Dis Off J Int Union Tuberc Lung Dis. **79**:3–29.

72. **Mdluli K, Sherman DR, Hickey MJ, Kreiswirth BN, Morris S, Stover CK, *et al*.** 1996. Biochemical and genetic data suggest that InhA is not the primary target for activated isoniazid in *Mycobacterium tuberculosis*. J Infect Dis. **174**:1085–90.

73. **Sepkowitz KA, Telzak EE, Recalde S, Armstrong D.** 1994. Trends in the susceptibility of tuberculosis in New York City, 1987-1991. New York city area tuberculosis working group. Clin Infect Dis Off Publ Infect Dis Soc Am. **18**:755–9.

74. **Inderlied CB.** 1994. Antimycobacterial susceptibility testing: present practices and future trends. Eur J Clin Microbiol Infect Dis Off Publ Eur Soc Clin Microbiol. **13**:980–93.

75. **Mahmoudi A, Iseman MD.** 1993. Pitfalls in the care of patients with tuberculosis. Common errors and their association with the acquisition of drug resistance. JAMA. 270:65–8.

76. **Altamirano M, Marostenmaki J, Wong A, FitzGerald M, Black WA, Smith JA.** 1994. Mutations in the catalase-peroxidase gene from isoniazid-resistant *Mycobacterium tuberculosis* isolates. J Infect Dis. **169**:1162–5.

77. **Morlock GP, Metchock B, Sikes D, Crawford JT, Cooksey RC.** 2003. *ethA*, *inhA*, and *katG* loci of ethionamide-resistant clinical *Mycobacterium tuberculosis* isolates. Antimicrob Agents Chemother. **47**:3799–805.

78. **Lee AS, Lim IH, Tang LL, Telenti A, Wong SY**. 1999. Contribution of *kasA* analysis to detection of isoniazid-resistant *Mycobacterium tuberculosis* in Singapore. Antimicrob Agents Chemother. **43**:2087–9.

79. **Pym AS, Domenech P, Honoré N, Song J, Deretic V, Cole ST**. 2001. Regulation of catalase-peroxidase (KatG) expression, isoniazid sensitivity and virulence by *furA* of *Mycobacterium tuberculosis*. Mol Microbiol. **40**:879–89.

80. **Ramaswamy SV, Reich R, Dou S-J, Jasperse L, Pan X, Wanger A, *et al.*** 2003. Single nucleotide polymorphisms in genes associated with isoniazid resistance in *Mycobacterium tuberculosis*. Antimicrob Agents Chemother. **47**:1241–50.

81. **Zhang M, Yue J, Yang Y-P, Zhang H-M, Lei J-Q, Jin R-L, *et al.*** 2005. Detection of mutations associated with isoniazid resistance in *Mycobacterium tuberculosis* isolates from China. J Clin Microbiol. **43**:5477–82.

82. **Levin BR, Perrot V, Walker N.** 2000. Compensatory mutations, antibiotic resistance and the population genetics of adaptive evolution in bacteria. Genetics. **154**:985–97.

83. **Strauss OJ, Warren RM, Jordaan A, Streicher EM, Hanekom M, Falmer AA, *et al.*** 2008. Spread of a Low-Fitness Drug-Resistant *Mycobacterium tuberculosis*

strain in a setting of high human immunodeficiency virus prevalence. J Clin Microbiol. **46**:1514–6.

84. **Andersson DI, Hughes D.** 2010. Antibiotic resistance and its cost: is it possible to reverse resistance? Nat Rev Microbiol. **8**:260–71.

85. **Sherman DR, Mdluli K, Hickey MJ, Arain TM, Morris SL, Barry CE, *et al.*** 1996. Compensatory *ahpC* gene expression in isoniazid-resistant *Mycobacterium tuberculosis.* Science. **272**:1641–3.

86. **Hazbón MH, Brimacombe M, Bobadilla del Valle M, Cavatore M, Guerrero MI, Varma-Basil M, *et al.*** 2006. Population genetics study of isoniazid resistance mutations and evolution of multidrug-resistant *Mycobacterium tuberculosis.* Antimicrob Agents Chemother. **50**:2640–9.

87. **Dhandayuthapani S, Zhang Y, Mudd MH, Deretic V.** 1996. Oxidative stress response and its role in sensitivity to isoniazid in mycobacteria: characterization and inducibility of *ahpC* by peroxides in *Mycobacterium smegmatis* and lack of expression in *M. aurum* and *M. tuberculosis*. J Bacteriol. **178**:3641–9.

88. **Zhang Y, Dhandayuthapani S, Deretic V.** 1996. Molecular basis for the exquisite sensitivity of *Mycobacterium tuberculosis* to isoniazid. Proc Natl Acad Sci USA. **93**:13212–6.

89. **Bergval IL, Schuitema ARJ, Klatser PR, Anthony RM.** 2009. Resistant mutants of *Mycobacterium tuberculosis* selected *in vitro* do not reflect the *in vivo* mechanism of isoniazid resistance. J Antimicrob Chemother. **64**:515–23.

90. **Toledano MB, Kullik I, Trinh F, Baird PT, Schneider TD, Storz G.** 1994. Redox-dependent shift of OxyR-DNA contacts along an extended DNA-binding site: a mechanism for differential promoter selection. Cell. **78**:897–909.

91. **Storz G, Imlayt JA.** 1998. Oxidative stress. Curr Opin Microbiol. **2**:188–94.

92. **Loots DT.** 2014. An altered *Mycobacterium tuberculosis* metabolome induced by *katG* mutations resulting in isoniazid resistance. Antimicrob Agents Chemother. **58**:2144–9.

93. **Sherman DR, Sabo PJ, Hickey MJ, Arain TM, Mahairas GG, Yuan Y, *et al.*** 1995. Disparate responses to oxidative stress in saprophytic and pathogenic mycobacteria. Proc Natl Acad Sci USA. **92**:6625–9.

94. **Deretic V, Philipp W, Dhandayuthapani S, Mudd MH, Curcic R, Garbe T**, ***et al***. 1995. *Mycobacterium tuberculosis* is a natural mutant with an inactivated oxidative-stress regulatory gene: implications for sensitivity to isoniazid. Mol Microbiol. **17**:889–900.

95. **Dhandayuthapani S, Mudd M, Deretic V.** 1997. Interactions of OxyR with the promoter region of the *oxyR* and *ahpC* genes from *Mycobacterium leprae* and *Mycobacterium tuberculosis*. J Bacteriol. **179**:2401–9.

96. **Deretic V, Pagán-Ramos E, Zhang Y, Dhandayuthapani S, Via LE.** 1996. The extreme sensitivity of *Mycobacterium tuberculosis* to the front-line antituberculosis drug isoniazid. Nat Biotechnol. **14**:1557–61.

97. **Mdluli K, Slayden RA, Zhu Y, Ramaswamy S, Pan X, Mead D, *et al***. 1998. Inhibition of a *Mycobacterium tuberculosis* beta-ketoacyl ACP synthase by isoniazid. Science. **280**:1607–10.

98. **Ali A, Hasan Z, McNerney R, Mallard K, Hill-Cawthorne G, Coll F, *et al.* 2015.** Whole genome sequencing based characterization of extensively drug-resistant *Mycobacterium tuberculosis* isolates from Pakistan. PLoS ONE. **10**:0117771.

99. **Alland D, Kramnik I, Weisbrod TR, Otsubo L, Cerny R, Miller LP, *et al.*** 1998. Identification of differentially expressed mRNA in prokaryotic organisms by customized amplification libraries (DECAL): The effect of isoniazid on gene expression in *Mycobacterium tuberculosis*. Proc Natl Acad Sci. **95**:13227–32.

100. **Alland D, Steyn AJ, Weisbrod T, Aldrich K, Jacobs WR.** 2000. Characterization of the *Mycobacterium tuberculosis iniBAC* promoter, a promoter that responds to cell wall biosynthesis inhibition. J Bacteriol. **182**:1802–11.

101. **Rojo F.** 2009. Degradation of alkanes by bacteria. Environ Microbiol. **11**:2477–90.

102. **Colangeli R, Helb D, Sridharan S, Sun J, Varma-Basil M, Hazbón MH, *et al.*** 2005. The *Mycobacterium tuberculosis iniA* gene is essential for activity of an

efflux pump that confers drug tolerance to both isoniazid and ethambutol. Mol Microbiol. **55**:1829–40.

103. **Vilchèze C, Hartman T, Weinrick B, Jain P, Weisbrod TR, Leung LW, *et al.* 2017.** Enhanced respiration prevents drug tolerance and drug resistance in *Mycobacterium tuberculosis.* Proc Natl Acad Sci. **114**:4495–500.

104. **Lee AS, Teo AS, Wong SY.** 2001. Novel mutations in ndh in isoniazid-resistant *Mycobacterium tuberculosis* isolates. Antimicrob Agents Chemother. **245**:2157–9.

105. **Hu Y, Hoffner S, Jiang W, Wang W, Xu B.** 2010. Extensive transmission of isoniazid resistant *M. tuberculosis* and its association with increased multidrug-resistant TB in two rural counties of eastern China: A molecular epidemiological study. BMC Infect Dis. **10**:43.

106. **Eldholm V, Monteserin J, Rieux A, Lopez B, Sobkowiak B, Ritacco V, *et al.*** 2015. Four decades of transmission of a multidrug-resistant *Mycobacterium tuberculosis* outbreak strain. Nat Commun. **6**:8119.

107. **van der Heijden YF, Karim F, Mufamadi G, Zako L, Chinappa T, Shepherd BE, *et al.*** 2017. Isoniazid-monoresistant tuberculosis is associated with poor treatment outcomes in Durban, South Africa. Int J Tuberc Lung Dis Off J Int Union Tuberc Lung Dis. **21**:670–6.

108. **WHO.** 2018. Treatment of drug-resistant TB: Resources.

109. **WHO.** 2018. WHO treatment guidelines for isoniazid-resistant tuberculosis.

110. **Mitchison DA, Nunn AJ.** 1986. Influence of initial drug resistance on the response to short-course chemotherapy of pulmonary tuberculosis. Am Rev Respir Dis. **133**:423–30.

111. **Smith CM, Trienekens SCM, Anderson C, Lalor MK, Brown T, Story A, *et al.*** 2017. Twenty years and counting: epidemiology of an outbreak of isoniazid-resistant tuberculosis in England and Wales, 1995 to 2014. Eurosurveillance.

112. **Huyen MNT, Cobelens FGJ, Buu TN, Lan NTN, Dung NH, Kremer K, *et al.*** 2013. Epidemiology of isoniazid resistance mutations and their effect on tuberculosis treatment outcomes. Antimicrob Agents Chemother. **57**:3620–7.

113. **O'Donnell M.** 2018. Isoniazid monoresistance: a precursor to multidrug-resistant tuberculosis? Ann Am Thorac Soc. **15**:306–7.

114. **Denkinger CM, Pai M, Dowdy DW.** 2014. Do we need to detect isoniazid resistance in addition to rifampicin resistance in diagnostic tests for tuberculosis? PLoS ONE. **9**(1):e84197

115. **Gagneux S, Burgos MV, DeRiemer K, Enciso A, Muñoz S, Hopewell PC, *et al.*** 2006. Impact of bacterial genetics on the transmission of isoniazid-resistant *Mycobacterium tuberculosis.* PLoS Pathog. **2**(6):e61

116. **Brudey K, Gordon M, Moström P, Svensson L, Jonsson B, Sola C, *et al.* 2004.** Molecular epidemiology of *Mycobacterium tuberculosis* in Western Sweden. J Clin Microbiol. **42**:3046–51.

117. **Nikolayevskyy VV, Brown TJ, Bazhora YI, Asmolov AA, Balabanova YM, Drobniewski FA.** 2007. Molecular epidemiology and prevalence of mutations conferring rifampicin and isoniazid resistance in *Mycobacterium tuberculosis* strains from the southern Ukraine. Clin Microbiol Infect Off Publ Eur Soc Clin Microbiol Infect Dis. **13**:129–38.

118. **Levin BR, Lipsitch M, Perrot V, Schrag S, Antia R, Simonsen L, *et al.*** 1997. The population genetics of antibiotic resistance. Clin Infect Dis Off Publ Infect Dis Soc Am. **1**:9-16.

119. **MacLean RC, Hall AR, Perron GG, Buckling A.** 2010. The population genetics of antibiotic resistance: integrating molecular mechanisms and treatment contexts. Nat Rev Genet. **11**:405–14.

120. **Sander P, Springer B, Prammananan T, Sturmfels A, Kappler M, Pletschette M, *et al.*** 2002. Fitness cost of chromosomal drug resistance-conferring mutations. Antimicrob Agents Chemother. **46**:1204–11.

121. **Keshavjee S, Farmer PE.** 2012. Tuberculosis, drug resistance, and the history of modern medicine. N Engl J Med. **367**:931–6.

122. **Dhar N, McKinney JD.** 2007. Microbial phenotypic heterogeneity and antibiotic tolerance. Curr Opin Microbiol. **10**:30–8.

123. **Barnett M, Bushby SRM, Mitchison DA.** 1953. Tubercle bacilli resistant to isoniazid: virulence and response to treatment with isoniazid in guinea pigs and mice. Br J Exp Pathol. **34**:568–81.

124. **Dalla Costa ER, Ribeiro MO, Silva MSN, Arnold LS, Rostirolla DC, Cafrune PI, *et al***. 2009. Correlations of mutations in *katG*, *oxyR-ahpC* and *inhA* genes and in vitro susceptibility in *Mycobacterium tuberculosis* clinical strains segregated by spoligotype families from tuberculosis prevalent countries in South America. BMC Microbiol. **9**:39.

125. **Gagneux S, Long CD, Small PM, Van T, Schoolnik GK, Bohannan BJM**. 2006. The competitive cost of antibiotic resistance in *Mycobacterium tuberculosis*. Science. **312**:1944–6.

126. **Billington OJ, McHugh TD, Gillespie SH.** 1999. Physiological cost of rifampin resistance induced in vitro in *Mycobacterium tuberculosis*. Antimicrob Agents Chemother. **43**:1866–9.

127. **Davies AP, Billington OJ, Bannister BA, Weir WR, McHugh TD, Gillespie SH.** 2000. Comparison of fitness of two isolates of *Mycobacterium tuberculosis*, one of which had developed multi-drug resistance during the course of treatment. J Infect. **41**:184–7.

128. **Pym AS, Saint-Joanis B, Cole ST.** 2002. Effect of katG mutations on the virulence of *Mycobacterium tuberculosis* and the implication for transmission in humans. Infect Immun. **70**:4955–60.

129. **Böttger EC, Springer B, Pletschette M, Sander P.** 1998. Fitness of antibiotic-resistant microorganisms and compensatory mutations. Nat Med. **4**:1343–4.

130. **Gagneux S, Burgos MV, DeRiemer K, Enciso A, Muñoz S, Hopewell PC, *et al.*** 2006. Impact of bacterial genetics on the transmission of isoniazid-resistant *Mycobacterium tuberculosis*. PLoS Pathog. **2**(6):e61

131. **Pym AS, Saint-Joanis B, Cole ST.** Effect of *katG* mutations on the virulence of *Mycobacterium tuberculosis* and the implication for transmission in humans. Infect Immun. **70**:4955–60.

132. **O'Sullivan DM, McHugh TD, Gillespie SH.** 2010. Mapping the fitness of *Mycobacterium tuberculosis* strains: a complex picture. J Med Microbiol. **59**:1533–5.

133. **Li Z, Kelley C, Collins F, Rouse D, Morris S.** 1998. Expression of *katG* in *Mycobacterium tuberculosis* is associated with its growth and persistence in mice and guinea pigs. J Infect Dis. **177**:1030–5.

134. **van Soolingen D, de Haas PE, van Doorn HR, Kuijper E, Rinder H, Borgdorff MW.** 2000. Mutations at amino acid position 315 of the *katG* gene are associated with high-level resistance to isoniazid, other drug resistance, and successful transmission of *Mycobacterium tuberculosis* in the Netherlands. J Infect Dis. **182**:1788–90.

135. **Bergval I, Kwok B, Schuitema A, Kremer K, van Soolingen D, Klatser P, *et al.*** 2012. Pre-existing isoniazid resistance, but not the genotype of *Mycobacterium tuberculosis* drives rifampicin resistance codon preference *in vitro*. PLoS ONE. **7**:29108.

136. **Sander P, Springer B, Prammananan T, Sturmfels A, Kappler M, Pletschette M, *et al.*** 2002. Fitness cost of chromosomal drug resistance-conferring mutations. Antimicrob Agents Chemother. **46**:1204–11.

137. **Vilchèze C, Jacobs WR.** 2014. Resistance to isoniazid and ethionamide in *Mycobacterium tuberculosis:* genes, mutations, and causalities. Microbiol Spectr. **2**:2-0014–2013.

138. **Böttger EC.** 2011. The ins and outs of *Mycobacterium tuberculosis* drug susceptibility testing. Clin Microbiol Infect Off Publ Eur Soc Clin Microbiol Infect Dis. **17**:1128–34.

139. **Lempens P, Meehan CJ, Vandelannoote K, Fissette K, Rijk P de, Deun AV, *et al*.** 2018. Isoniazid resistance levels of *Mycobacterium tuberculosis* can largely be predicted by high-confidence resistance-conferring mutations. Sci Rep. **8**:3246.

140. **Mariam DH, Mengistu Y, Hoffner SE, Andersson DI.** 2004. Effect of *rpoB* mutations conferring rifampin resistance on fitness of *Mycobacterium tuberculosis.* Antimicrob Agents Chemother. **48**:1289–94.

141. **Bhatter P, Chatterjee A, D'souza D, Tolani M, Mistry N.** 2012. Estimating fitness by competition assays between drug susceptible and resistant *Mycobacterium tuberculosis* of predominant lineages in Mumbai, India. PLoS ONE.**10**:1371.

142. **Pym AS, Saint-Joanis B, Cole ST.** 2002. Effect of *katG* mutations on the virulence of *Mycobacterium tuberculosis* and the implication for transmission in humans. Infect Immun. **70**:4955–60.

143. **Borrell S, Gagneux S.** 2011. Strain diversity, epistasis and the evolution of drug resistance in *Mycobacterium tuberculosis*. Clin Microbiol Infect Off Publ Eur Soc Clin Microbiol Infect Dis. **17**:815–20.

144. **Cordell HJ.** 2002. Epistasis: what it means, what it doesn't mean, and statistical methods to detect it in humans. Hum Mol Genet. **11**:2463–8.

145. **Trindade S, Sousa A, Xavier KB, Dionisio F, Ferreira MG, Gordo I.** 2009. Positive epistasis drives the acquisition of multidrug resistance. PLOS Genet. **5**:1000578.

146. **Cohan FM, King EC, Zawadzki P.** 1994. Amelioration of the deleterious pleiotropic effects of an adaptive mutation in *Bacillus subtilis*. Evolution. **48**:81–95.

147. **Luo N, Pereira S, Sahin O, Lin J, Huang S, Michel L, *et al.*** 2005. Enhanced *in vivo* fitness of fluoroquinolone-resistant *Campylobacter jejuni* in the absence of antibiotic selection pressure. Proc Natl Acad Sci USA. **102**:541–6.

148. **Bergval I, Kwok B, Schuitema A, Kremer K, van Soolingen D, Klatser P, *et al.*** 2012. Pre-existing isoniazid resistance, but not the genotype of *Mycobacterium tuberculosis* drives rifampicin resistance codon preference *in vitro*. PLoS ONE. **7**:29108.

149. **van Soolingen D, de Haas PE, van Doorn HR, Kuijper E, Rinder H, Borgdorff MW.** 2000. Mutations at amino acid position 315 of the *katG* gene are associated with high-level resistance to isoniazid, other drug resistance, and successful transmission of *Mycobacterium tuberculosis* in the Netherlands. J Infect Dis. **182:**1788–90.

150. **Koch A, Mizrahi V, Warner DF.** 2014. The impact of drug resistance on *Mycobacterium tuberculosis* physiology: what can we learn from rifampicin? Emerg Microbes Infect. ;**3**:17.

151. **Hu J, Zhao L, Yang M.** 2015. A GntR family transcription factor positively regulates mycobacterial isoniazid resistance by controlling the expression of a putative permease. BMC Microbiol. **15**:214.

152. **Yang M, Gao C-H, Hu J, Zhao L, Huang Q, He Z-G**. 2015. InbR, a TetR family regulator, binds with isoniazid and influences multidrug resistance in *Mycobacterium bovis* BCG. Sci Rep. **5**:13969.

153. **Saikolappan S, Das K, Dhandayuthapani S.** 2015. Inactivation of the Organic Hydroperoxide Stress Resistance Regulator OhrR Enhances Resistance to Oxidative Stress and Isoniazid in *Mycobacterium smegmatis*. J Bacteriol. **197**:51–62.

154. **Haydon DJ, Guest JR.** 1991. A new family of bacterial regulatory proteins. FEMS Microbiol Lett. **63**:291–5.

155. **Vázquez-Torres A.** 2012. Redox active thiol sensors of oxidative and nitrosative stress. Antioxid Redox Signal. **17**:1201–14.

156. **Mongkolsuk S, Helmann JD.** 2002. Regulation of inducible peroxide stress responses. Mol Microbiol. **45**:9–15.

157. **Hillen W, Berens C.** 1994. Mechanisms underlying expression of Tn10 encoded tetracycline resistance. Annu Rev Microbiol. **48**:345–69.

158. **Lee J-H, Ammerman NC, Nolan S, Geiman DE, Lun S, Guo H, *et al.*** 2012. Isoniazid resistance without a loss of fitness in *Mycobacterium tuberculosis*. Nat Commun. **3**:753.

159. **Karakousis PC, Williams EP, Bishai WR.** 2008. Altered expression of isoniazid-regulated genes in drug-treated dormant *Mycobacterium tuberculosis.* J Antimicrob Chemother. **61**:323–31.

160. **Cole ST, Brosch R, Parkhill J, Garnier T, Churcher C, Harris D, *et al.* 1998.** Deciphering the biology of *Mycobacterium tuberculosis* from the complete genome sequence. Nature. **393**:537–44.

161. **Brauner A, Fridman O, Gefen O, Balaban NQ.** 2016. Distinguishing between resistance, tolerance and persistence to antibiotic treatment. Nat Rev Microbiol. **14**:320–30.

162. **Gefen O, Balaban NQ.** 2009. The importance of being persistent: heterogeneity of bacterial populations under antibiotic stress. FEMS Microbiol Rev. **33**:704–17.

163. **Balaban NQ, Helaine S, Lewis K, Ackermann M, Aldridge B, Andersson DI, *et al.*** 2019. Definitions and guidelines for research on antibiotic persistence. Nat Rev Microbiol. **17**:441–8.

164. **Gold B, Nathan C.** 2017. Targeting phenotypically tolerant *Mycobacterium tuberculosis*. Microbiol Spectr. **5**(1): 1128-10.

165. **Keren I, Kaldalu N, Spoering A, Wang Y, Lewis K.** 2004. Persister cells and tolerance to antimicrobials. FEMS Microbiol Lett. **230**:13–8.

166. **Dhar N, McKinney JD.** 2010. *Mycobacterium tuberculosis* persistence mutants identified by screening in isoniazid-treated mice. Proc Natl Acad Sci USA. **107**:12275–80.

CHAPTER 3

Transcriptomic profiling of resistant and susceptible *Mycobacterium tuberculosis* strains

---

My contribution:

Project planning and design

Genotypic and phenotypic characterization of the strains

RNA extractions and sample preparations

RT-qPCR sample preparations and run in the instruments.

Interpretation of results and raw data with the help of a Bioinformatician

Writing and editing of the chapter

3.1 Introduction

One major challenge in managing Tuberculosis (TB) is the emergence and transmission of multidrug-resistant TB (MDR-TB) strains. MDR-TB is defined as *Mycobacterium tuberculosis* with resistance to the first-line anti-TB drugs (isoniazid (INH) and rifampicin (RIF)) (1). RIF inhibits transcription by binding to the beta subunit of RNA polymerase and INH inhibits mycolic acids synthesis (2). RIF resistance in *M. tuberculosis* is often associated with resistance to INH and is thereby considered as a surrogate marker for MDR-TB (2). Drug resistance in *M. tuberculosis* strains has been extensively studied; however, limited knowledge exists on the physiological changes that occur at the transcriptional level, both *in vivo* and *in vitro*, during INH treatment (2). In addition, the effect of specific mutations in target genes on the *M. tuberculosis* transcriptome is unknown.

Previous studies used microarray to investigate the global gene expression profiles of *M. tuberculosis* and *Mycobacterium smegmatis* after exposure to specific stressors, including drugs (3–6). Waddell *et al.* (2004) assessed the effect of exposing *M. tuberculosis* and *M. smegmatis* strains to different concentrations of INH on global gene expression (4). Results from these studies demonstrated significant upregulation of *efpA acpM, Rv1772, ahpC, iniA, iniB, kasA* and *accD6* in *M. tuberculosis* clinical strains treated with 0.1 and 0.2 µg/ml INH for 24h (4,6,7). These results suggested that INH exposure induced the expression of multiple genes in the fatty acid synthase II (FAS-II) pathway in *M. tuberculosis* (3,7). Based on these findings, genes in the FAS-II pathway were identified as potential novel drug targets for the development of new drugs that are active against drug susceptible, drug tolerant and INH resistant *M. tuberculosis* (3,7,8).

Recent research efforts have been geared towards understanding genetic diversity of pathogenic *M. tuberculosis* clinical strains and the effect of genetic diversity on the emergence and transmission of drug resistance (9,10). Previous studies employing whole genome sequencing technology reported significant genetic diversity amongst clinical *M. tuberculosis* strains (9,10). Reports also demonstrate that *M. tuberculosis* strains from the Beijing lineage are frequently associated with drug resistance and MDR-TB transmission (11–14). These observations also showed that *M. tuberculosis* strains from the Beijing lineage are over-represented and thereby indicate that

transmission of drug resistance may be influenced by the *M. tuberculosis* strain lineage (11–14).

The availability of the complete genome sequence of *M. tuberculosis* H37Rv has aided in the comparative genomics to ascertain genomic differences and towards understanding the fundamental biological differences between *M. tuberculosis* strains (15,16). Recent technological advances, such as RNA sequencing (RNA-Seq), have provided deeper insight into the global gene expression profile of various *M. tuberculosis* strains after the exposure to different stressors (17–19). However, information obtained from these studies is limited to assessing the gene expression of the laboratory H37Rv *M. tuberculosis* and *Mycobacterium bovis* strains (17–19). To date only one study has investigated the transcriptional response to INH in clinical XDR *M. tuberculosis* strains using microarrays (20). Their data revealed a strong association between INH response genes with the differentially expressed genes of resistant strains compared to those of H37Rv *M. tuberculosis* strain (20). This emphasises the limited amount of information that is available on gene expression in clinical *M. tuberculosis* strains.

The ability of RNA-Seq technology to sequence all transcripts present in the bacillus is an advantage over microarray technology which employs a limited number of probes complementary to specific transcripts (21). In addition, RNA-Seq is more sensitive in detecting transcripts with low abundance compared to microarray (22). RNA-Seq generates short reads which are mapped to a reference genome, with the number of mapped reads in a gene referred to as counts, thereby giving quantitative measures of gene expression (21). These quantitative counts are normalized to a specific reference gene to determine the exact expression levels between samples. Thus, RNA-Seq yields a high-resolution transcriptomic map of an organism by identifying genes which govern a phenotype through differential gene expression.

In this study we **hypothesised** that the genetic background of *M. tuberculosis* strains will have an influence on their transcriptional profiles.we further hypothesised that the resistance-conferring mutation (*ropB* Ser531Leu mutation) influences gene expression in RIF-susceptible and RIF-resistant *M. tuberculosis* strains. In addition, we hypothesised that exposure of these isogenic strains to sub-lethal concentrations of

INH will induce adaptive physiological changes that will be reflected in the total transcriptome.

In this study we **aimed** to investigate whether the genetic background of different *M. tuberculosis* strains and RIF-resistant conferring mutations have an effect on the *M. tuberculosis* transcriptome. Additional **objectives** included assessing the growth of *M. tuberculosis* at sub-lethal concentration of INH and determining the effect of INH exposure on the *M. tuberculosis* transcriptome. The findings of the current study provided knowledge on the impact of genetic diversity, drug resistance-conferring mutations and INH exposure on the *M. tuberculosis* transcriptome.

3.2 Materials and methods

Experimental approach

RNA-Seq, followed by RT-qPCR, was applied to characterize the physiology of RIF-susceptible and RIF-resistant *M. tuberculosis* strains in the absence or presence of INH (0.05 µg/ml) under in *vitro* conditions (Figure 3.1). Below is an overview of the experimental approach explored (Figure 3.1).

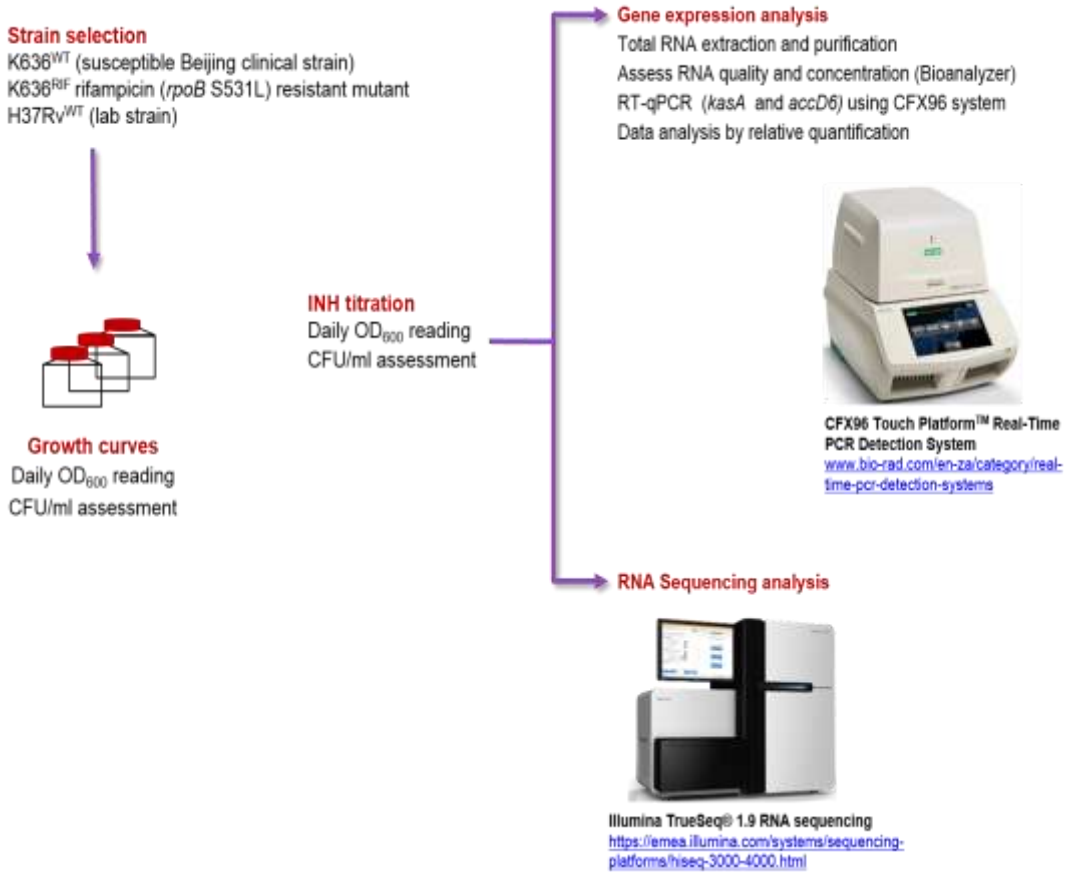

Figure 3.5 Overview of the experimental approach used in the current chapter.

3.2.1 Mycobacterial strains and culture conditions

Three *M. tuberculosis* strains, summarised in Table 3.1, were selected for this study. These included a pan-susceptible clinical *M. tuberculosis* isolate from the Beijing cluster 208 (K636) (denoted as $K636^{WT}$), RIF-resistant mutant [generated by *in vitro* selection (Appendix A)] with *rpoB* Ser531Leu mutation (denoted as $K636^{RIF}$) derived from the pan-susceptible K636 progenitor and susceptible laboratory reference strain H37Rv (ATCC 27294) (denoted as $H37Rv^{WT}$). These strains were selected from an existing sample bank maintained at Stellenbosch University, South Africa (Table 3.1).

M. tuberculosis freezer stocks were prepared and preserved by adding 800 µl of *M. tuberculosis* culture into sterile 2 ml vials Nunc® (Sigma-Aldrich, St Louis, Missouri, USA) containing 7- 8 glass beads (4 mm diameter) and stored at -80°C. *M. tuberculosis* cultures were generated from frozen stocks by inoculating a single glass bead coated with respective *M. tuberculosis* strains into BACTEC™ Mycobacterial Growth Indicator Tubes (MGIT) (BD Biosciences, New Jersey, USA) supplemented with 10% oleic acid-albumin-dextrose-catalase (OADC) (BD Biosciences). Each inoculated MGIT was incubated in the BACTEC^{TM} MGIT 960 instrument at 37^{o}C. Contamination of the *M. tuberculosis* cultures was assessed by Ziehl–Neelsen (ZN) staining and culturing on blood agar plates (Appendix A). MGITs with positive growth unit (GU) ≥100 were incubated at 37^{o}C for an additional 3-5 days to allow for maximum mycobacterial growth. Following this, 1 ml of *M. tuberculosis* MGIT stock culture was used to inoculate a starter culture in 8 ml of filtered 7H9 Middlebrook medium supplemented with 10% OADC, 0.2% (v/v) glycerol (Merck Laboratories, Saarchem, SA) and 0.05% Tween 80 (BD Biosciences) (7H9-OGT). Cultures were then grown horizontally in 25cm² aerated screw cap tissue culture flasks (Greiner Bio-one, Maybachstreet, Germany) without shaking at 37°C until an optical density (OD_{600nm}) of 0.7 - 0.8 was reached. The OD_{600nm} was measured on the spectrophotometer by taking an OD_{600nm} reading of 7H9-OGT for the blank sample and followed by the OD_{600nm} reading of the tested culture sample.

Table 3. 4 Characteristics of *M. tuberculosis* strains in the current study

Name of Strains	**Description**	**Source/Reference**
M. tuberculosis K636 (denoted as K636^{WT})	Susceptible *M. tuberculosis* clinical strain from the Beijing family	In-house strain collection
M. tuberculosis K636 ^{RIF} (denoted as K636^{RIF})	*M. tuberculosis in vitro* mutant with the *rpoB* Ser531Leu mutation derived from the susceptible clinical strain	A kind gift from Dr M. de Vos
M. tuberculosis H37Rv (ATCC 27294) (denoted as H37Rv^{WT})	Susceptible *M. tuberculosis* laboratory strain	In-house strain collection

3.2.2 Genotypic and phenotypic characterization of *M. tuberculosis* strains:

Genotypic and phenotypic characterization of the selected *M. tuberculosis* strains ($K636^{WT}$; $K636^{RIF,}$ and $H37Rv^{WT}$) was performed to rule out contamination, confirm the identity of the strains and to confirm the previously determined MIC_{99} of RIF level of resistance for *M. tuberculosis* strains. ZN staining of the *M. tuberculosis* strains indicated the presence of acid-fast mycobacteria (Appendix C: Figure S3.1).

PCR amplification and mutation detection

A volume of 500 µl aliquots of $H37Rv^{WT}$; $K636^{WT}$ and $K636^{RIF}$ *M. tuberculosis* strains grown in 7H9-OGT were incubated at 100^{o}C for 20 to 30 min to kill the bacilli and release the crude lysate. The lysate containing DNA was stored at 4^{o}C for subsequent analysis. To confirm the presence or absence of the RIF resistance-conferring Ser531Leu mutation in the *rpoB* gene, a 437 bp fragment was amplified using primers obtained from an oligonucleotide primer bank maintained at Stellenbosch University, Western Cape, South Africa (Table 3.2). The master mix for the PCR amplification comprised 5 µl of 10X buffer (Qiagen, Hilden, Germany), 1 µl of $MgCl_2$ (2.5 mM), 10 µl of 1X Q-solution (Qiagen), 4 µl deoxyribonucleotide triphosphates (dNTPs) (Promega, Madison, Wisconsin, USA) (0.2 mM of each dNTP), 0.25 µl of each forward and reverse *rpoB* primers (50 pmol/µl), and 0.15 µl l Hotstart Taq polymerase (5 units/µl) (Qiagen). Subsequently, 2.5 µl of the DNA template (crude lysate) was added to the PCR master mix with water added to a final volume of 50 µl. Template free controls were included in each reaction to assess amplicon contamination.

The PCR reactions were performed using the GeneAmp PCR System 2400 (Applied Biosystems, California, USA) and thermal cycling conditions as follows: an initial denaturing step at 95^{o}C for 15 min, followed by 40 cycles of denaturation at 94^{o}C for 1 min, annealing at the melting temperature (T_m) specific to the specific gene primer pair (Table 3.2) for 1 min, extension at 72^{o}C for 1 min and a final extension step at 72^{o}C for 10 min. To confirm successful PCR amplification of the *rpoB* gene, gel electrophoresis was performed for the obtained PCR products. Briefly, PCR amplicons were visualized in 1.5% agarose containing Tris/Borate/Ethylenediaminetetraacetic acid (EDTA) (TBE) and 2 µl of ethidium bromide (10 mg/mL in H_2O) (Sigma-Aldrich). The PCR products were purified

(according to PCR clean-up standard protocols) (Promega) and Sanger sequencing was performed at the Central Analytic Facility (CAF) at Stellenbosch University. The sequencing was done using the ABI 3730xl DNA Sequencer (Thermo Fisher Scientific, Waltham, Massachusetts, USA). To detect genetic variants, gene sequences obtained from CAF were aligned to the gene sequence of *M. tuberculosis* H37Rv reference strain (http://genolist.pasteur.fr/Tuberculist) using DNA MAN Version 4.1 (Lynnon Biosoft, San Ramon, California, USA).

Table 3.5 Primers used for the amplification of *M. tuberculosis* genes harbouring drug resistance conferring mutations and for the amplification of cDNA for RT-qPCR

	Application	Gene	Primer	Sequence (5'-3')	[a]T_m (^{0}C)	Fragment length ([b]bp)
RIF resistance mutation	**Mutation detection**	*rpoB*	Forward Reverse	TGGTCCGCTTGCACGAGGGTCAGA CTCAGGGGTTTCGATCGGGGCACAT	72	437
Housekeeping genes	**RT-qPCR**	*sigA*	Forward	GTGCACATGGTCGAGGTGAT	61	114
			Reverse	CGGGGTGATGTCCATCTCTT		
		16S rRNA	Forward	CTGGGTTTGACATGCACAGG	61	104
			Reverse	ACCCAACATCTCACGACACG		
Candidate genes		*kasA*	Forward	CCGACCCTGAACTACGAGAC	61	107

			Reverse	AACCCGAACGAGTTGTTGAC		
		accD6	Forward	GGTGTCGACCAGGAGTGG	61	108
			Reverse	GTAGGTCTTTCGGGTGACCA		
		cyp128	Forward	GCCGTTACCCTGTGACTGTT	58	148
			Reverse	TTCGTCGTCTCGACTTTCCC		
		whiB7	Forward	TCACTTTCGAAGAACCGCCA	60	373
			Reverse	CTCAGACGACGATCGCGT		
		Rv3211	Forward	TGAACCGCGACAGAGAAACA	60	200
			Reverse	CCGCACCAAGACCGATATCG		
		pks6	Forward	ATGCGCAAAGCAGTACGGAG	60	400
			Reverse	GTGCCAGGATGTTGGTCTCT		
		Rv0073	Forward	GATTGAAGCGCGTGGTGAC	60	173
			Reverse	CTTGGCCGGAACTAGCCACT		
		Rv1760	Forward	AATGGCACGGTCACCGACAT	60	220
			Reverse	TCAGAACCGGTAGTCGGTGC		

***a**: Tm (melting temperature), **b**: bp (base pairs)*

Whole genome sequencing (WGS) analysis. $K636^{WT}$, $K636^{RIF}$ and $H37Rv^{WT}$ *M. tuberculosis* strains were further characterised by whole genome sequencing (WGS) to identify single nucleotide polymorphism (SNPs). WGS for $K636^{RIF}$ and $H37Rv^{WT}$ *M. tuberculosis* strains were previously done (by Dr M. de Vos from our department, following the same procedure described below for $K636^{WT}$ WGS) and the genomic data for these strains were thus available. Therefore, WGS was only done on $K636^{WT}$ by culturing $K636^{WT}$ on 7H10 agar plates until a dense lawn of growth was observed. Subsequently, genomic DNA of $K636^{WT}$ was extracted according to gDNA extraction standard protocols (23) (Appendix A), with the assistance of the lab technologist (Mrs Ruzayda Palma). The quantity and quality of the extracted DNA was assessed by Nanodrop (Thermo Fischer Scientific, USA) and PCR amplification and WGS was done in collaboration with the South African National Bioinformatics Institute (SANBI), University of the Western Cape. Sequencing library for $K636^{WT}$ was constructed using the standard genomic DNA sample preparation kits from Illumina (Illumina, Inc, San Diego, CA), according to the manufacturer's instructions. The whole genome of the $K636^{WT}$ *M. tuberculosis* strain was sequenced using the Illumina MiSeq platforms. Mapping and variant detection of the sequencing data of $K636^{WT}$, $K636^{RIF}$ and $H37Rv^{WT}$ was performed using an in-house automated pipeline for *M. tuberculosis* next generation sequencing (NGS) (24). Briefly, the quality assessment of the sequencing data (in FASTQ format) was performed using FASTQC (25). The trimming of adapters and low-quality bases was performed using a Phred quality score of less than 20 and filtering for a minimum read length of 36 using Trimmomatic (26,27). Subsequently, the reads were mapped to the *M. tuberculosis* H37Rv genome (Genbank: AL123456) using the Burrows-Wheeler Alignment Tool (BWA) (28) and SMALT (29). The Genome Analysis Tool Kit (GATK) was used to detect SNPs and small insertions and deletions (In/Dels) (30) and annotation was performed using data from Tuberculist (http://genolist.pasteur.fr/Tuberculist) (31). Bioinformatics analysis for $K636^{WT}$, $K636^{RIF}$ and $H37Rv^{WT}$ *M. tuberculosis* strains was done in consultation with bioinformaticians, Dr Anzaan Dippenaar and Dr Melanie Grobbelaar.

Drug Susceptibility testing (DST). The DST was performed to confirm the level of resistance for previously determined RIF minimum inhibitory concentrations (MICs) [0.2 µg/ml ($H37Rv^{WT}$); 0.5 µg/ml ($K636^{WT}$), 150 µg/ml and 200 µg/ml ($K636^{RIF}$)] for

M. tuberculosis strains. This was done by using the BACTEC MGIT 960 instrument according to the manufacturer's instructions; a method adapted and modified from Siddiqi *et al.* (2012) (32). The MIC_{99} was defined as the lowest concentration of RIF required to inhibit 99% of bacterial growth in a culture (32). Sub-cultures were prepared by inoculating 200 µl of previously prepared *M. tuberculosis* glycerol stock-cultures into MGIT tubes. These sub-cultures were then incubated at 37^{o}C in the MGIT 960 instrument until a growth unit (GU) > 400 was obtained, indicating positive bacterial growth. Two days after obtaining positive growth, the growth control tubes were prepared by inoculating 500 µl of the 1:100 diluted sub-cultures into MGIT tubes enriched with 800 µl OADC. Following this, 500 µl of the undiluted positive sub-cultures were inoculated into MGIT tubes enriched with OADC and 100 µl of RIF (Sigma-Aldrich) to final predetermined concentrations of 0.2 µg/ml ($H37Rv^{WT}$); 0.5 µg/ml ($K636^{WT}$), 150 µg/ml and 200 µg/ml ($K636^{RIF}$), respectively. The MGIT tubes were then registered on the EpiCenter TBeXist software (version 5.75A) (BD Biosciences) and placed in a BACTEC MGIT 960 instrument to continuously monitor the growth for 14 consecutive days. The results were read when the growth control reached a growth unit (GU) > 400. When the GU of the tested drug tube was ≥ 100, the *M. tuberculosis* sample was interpreted as being resistant (R). In contrast the *M. tuberculosis* sample was sensitive (S) if the GU of the tested drug was <100 and remained the same after being incubated for 7 more days. The *M. tuberculosis* sample was interpreted as intermediate (I) if the GU of the tested drug tube was >100 during 7 days after the growth control reached > 400 (33).

Growth assessment of *M. tuberculosis* strains. Briefly, 1 ml of *M. tuberculosis* MGIT stock culture was inoculated into 8 ml of 7H9-OGT as an initial starter culture, incubated at 37^{o}C and allowed to grow to an OD_{600nm} of approximately 1.0. The culture was centrifuged (4000 rpm, 10 min) and adjusted to an OD_{600nm} of 1.0. Following this, 5 ml of the culture was inoculated into 45 ml 7H9-OGT to achieve a starting OD of 0.1. Subsequently, the growth for each culture was assessed every second day by measuring the OD_{600nm} over a period of 25 days in order to determine when the culture was in mid-log phase. In parallel, CFU determination was done every second day, by plating 10-fold serial dilutions of *M. tuberculosis* culture on 7H10 solid Middlebrook medium (BD, Bioscience, New Jersey, USA), supplemented

with 10% OADC and 0.2% (v/v) glycerol (Merck Laboratories, Saarchem, SA). The 7H10 agar plates were incubated at 37^{o}C for 25 days before colony counting.

3.2.3 Determination of sub-lethal concentration of INH treatment

INH (Sigma-Aldrich) working stocks were prepared with the final concentration of 1000 µg/ml dissolved in distilled H_2O. The INH titration experiments were performed to determine sub-lethal concentrations of INH that inhibit *M. tuberculosis* growth by < 10% after 24h INH treatment. Starter cultures were prepared of K636^{WT} and H37Rv^{WT} *M. tuberculosis* strains by inoculating 1 ml of the MGIT stock cultures, into 10 ml of 7H9-OGT. Once the cultures reached mid-log phase (OD_{600nm} of 0.7 - 0.8), it was filtered through 40 µm cell strainers (Falcon®, Sigma-Aldrich) to minimize clumping. OD_{600nm} readings of the cultures were taken and cultures then were centrifuged (4000 rpm, 10 min) and resuspended in 7H9-OGT to adjust to an OD_{600nm} of 1.0. Subsequently, 5 mL of each culture was inoculated into separate 50 ml 7H9-OGT in tissue culture (TC) flasks and grown to an OD_{600nm} of 0.5- 0.6. Following this, the 50 ml cultures were filtered and adjusted to an OD_{600nm} of 1.0, then used for inoculation to a final OD_{600nm} of 0.1 in 30 ml 7H9-OGT in 250 ml TC flasks with varying INH concentrations (0.02, 0.03 and 0.05 µg/ml). An INH-free culture was also included as drug-free control. A volume of 1200 µl from each sample was taken every second day; 1000 µl for OD_{600nm} measurement and 200 µl for plating for colony forming unit (CFUs) on 7H10 solid media with serial dilutions ranging from 10^{-3}-10^{-9}. The 7H10 agar plates were incubated at 37^{o}C for 25 days, after which CFUs were recorded.

3.2.4 Culture conditions and RNA extraction

Culture conditions. Starter cultures were prepared by inoculating 1 ml of each of the H37Rv^{WT}; K636^{WT} and K636^{RIF} *M. tuberculosis* MGIT stock cultures; into separate 10 ml of 7H9-OGT (samples per tested strains were prepared in biological triplicates). Once the cultures reached mid-log phase (OD_{600nm} of 0.7 - 0.8), it was filtered through 40 µm cell strainers (Sigma-Aldrich) to minimize clumping. OD_{600nm} readings of the cultures were done and cultures then were centrifuged at 4000 rpm for10 min and resuspended in 7H9-OGT to adjust to an OD_{600nm} of 1.0. Then 5 ml culture of each strain was inoculated into separate 50 ml 7H9-OGT in tissue culture (TC) flasks and grown to an OD_{600nm} of 0.7- 0.8. At mid-log phase, each 50 ml culture was split into 2x

25 ml cultures. The first 25 ml culture was exposed to the sub-lethal concentration of INH (as determined in 3.2.3) for a period of 24h before RNA was extracted. The second 25 ml culture served as an unexposed control and was treated with ddH_2O under the same conditions.

Total RNA extraction and purification. RNA was extracted from $H37Rv^{WT}$; $K636^{WT}$ and $K636^{RIF}$ *M. tuberculosis* strains using the FastRNA® Blue kit (MP Biomedicals, LLC, USA). Briefly, cultures were centrifuged at 4000 rpm for 15 minutes at 4^oC. The pellets were resuspended into 1/10 original culture volume of RNAprotect (Qiagen) and centrifuged again at 4000 rpm for 15 min at 4^oC. Each pellet was resuspended in 2 ml of RNApro solution (MP Biomedicals) and subsequently transferred to three 2 ml blue screw-cap tubes containing Lysing Matrix beads (Qbiogene, Inc., USA).

Culture suspensions were subsequently homogenized in a FastPrep®-24 instrument (MP Biomedicals) by 4 cycles of 25 seconds at a speed of 4.5 W. Samples were cooled on ice for 1 min between each pulse. The homogenates were then centrifuged at 12 000 rpm for 15 min at 4^oC. A volume of 600 to 700 µl of each supernatant was transferred to a fresh 1.5 ml tube and 300 µl of chloroform (Sigma-Aldrich) was added to each tube. Subsequently the samples were vortexed and incubated for 5 min at room temperature. This was followed by centrifugation at 12 000 rpm for 15 min at 4^oC, and each aqueous phase was transferred to a new RNase-free Eppendorf tube containing 500 µl RNase-free absolute ethanol (Sigma-Aldrich) (pre-cooled to -20^oC). The samples were vortexed for 10 seconds and subsequently incubated at -20^oC for 2h to allow for precipitation of the nucleic acids. Following this, nucleic acids were centrifuged at 12 000 rpm for 20 min at 4^oC and then washed with 500 µl RNase free 75% ethanol (Sigma-Aldrich) (pre-cooled to -20^oC). Following the wash steps, the supernatant was discarded and each nucleic acid pellet left to air dry for 10 min. Pellets (three aliquots of RNA for each 25 ml culture) were resuspended in a total volume of 50 µl RNase-free H_2O and stored at -80^oC until further use.

For the next step, 15 µl aliquots from each of the three RNA samples, respectively, were subsequently treated with RNase-free DNase (Promega) to remove residual genomic DNA (gDNA). Briefly, 15 µl RNA was added to 15 µl RNase-free H_2O, 6 µl DNase Buffer (10X reaction buffer) and 6 µl of RQ1 DNase (1 U/µl) (Promega) as

per protocol. The DNase treatment reaction mixture was incubated at 37^{o}C for 30 min before RNase-free H_2O was added to the reaction to a total volume of 200 µl. An equal volume of cooled phenol: chloroform (4:1, v/v) (Sigma-Aldrich) was added and then mixed by vortexing every 2 min and incubation on ice for 10 min. Samples were subsequently centrifuged at 12 000 rpm for 12 min at room temperature to allow for phase separation. The upper aqueous phase (150 -200 µl) was collected and 0.1 volumes of cooled RNase-free 3M sodium acetate (pH 5.2) (Sigma-Aldrich) and 500 µl cooled absolute (~95%) ethanol was added to the supernatants, respectively. The samples were vortexed and incubated overnight (4^{o}C) before the RNA was centrifuged (12 000 rpm, 20 min, 4^{o}C). The resulting pellets were washed with 500 µL of pre-cooled 75% ethanol followed by a centrifugation step. The 75% ethanol was then decanted and the RNA pellets were left to air-dry at room temperature for 10 min before being dissolved in 30 µl nuclease free H_2O (Qiagen). The RNA samples (extracted from the three above studied *M. tuberculosis* strains) were then stored in aliquots of 10 µl, (per each RNA sample) at -80^{o}C until further use.

RNA quality assessment. RNA quality was assessed as follows: PCR amplification was performed for *rpoB* region (437 bp fragment) using the extracted RNA as a template, the gDNA extracted from H37Rv ATCC27294 as positive control and electrophoretic mobility in non-denaturing 2% agarose gels. Briefly, 2 µl of DNase-treated RNA was added to the following PCR reaction mixture to assess gDNA contamination: 5 µl of 10X buffer (Qiagen), 1 µl of $MgCl_2$ (2.5 mM), 10 µl of 5X Q-solution (Qiagen), 4 µl deoxyribonucleotide triphosphates (dNTP's) (Promega) (0.2 mM of each dNTP), 0.25 µl of each forward and reverse *rpoB* primers (50 pmol/µl) (Table 3.2), 0.15 µl HotStart Taq polymerase (5 units/µl) (Qiagen) and H_2O to a final volume of 50 µl. Amplification was performed using the GeneAmp PCR System 2400 (Applied Biosystems) under the following conditions: 95^{o}C for 15 min; 40 cycles of 94^{o}C for 1 min, specific gene primer annealing at the (T_m) of 72^{o}C for 1 min, and 72^{o}C for 1 min; final cycle of 72^{o}C for 10 min. A 2 µl of 1 µg (0.284 µg/ml= 284 µl) of gDNA sample (positive template control) was included. To confirm successful PCR amplification of the *rpoB* gene, gel electrophoresis was performed for the obtained PCR products. Briefly, PCR amplicons were visualized in 1.5% agarose containing Tris/Borate/Ethylenediaminetetraacetic acid (EDTA) (TBE) and 2 µl of ethidium bromide (10 mg/ml in H_2O) (Sigma-Aldrich).

Bioanalyser analysis for assessing RNA integrity: A 3 µl aliquot of DNase-free RNA (15 samples) was sent to the Centre for Proteomic & Genomic Research (CPGR) (CPGR, Cape Town, South Africa) to determine the integrity and concentration of the RNA using the Agilent Bioanalyser system (Applied Biosystems). Bioanalyser analysis generates an RNA integrity number (RIN) score for evaluation of RNA integrity. A value of 10 indicates intact RNA, while a value of less than 7.0 could result in high variation during gene expression analysis (34). RNA samples with a RIN score of 7.0 and higher were used for further analysis. Visual inspection was performed for RNA samples with RIN scores between 6.5 and 7.0 to assess their RNA quality. The RNA 260/280 and 260/230 ratios were determined to further evaluate the RNA purity and quality using Nanodrop.

3.2.5. cDNA synthesis

The QuantiNova™ Reverse Transcriptase Kit (Qiagen) was used to synthesize cDNA from purified RNA according to manufacturer's instructions. The genomic DNA (gDNA) wipe out step was implemented to remove any possible residual gDNA from the purified RNA. Although the control PCR did not show gDNA contamination from our RNA samples, this step was included as an extra precautionary measure. Briefly, 2 µl gDNA removal mix and 1 µl internal control RNA was added to 1 µg of RNA. RNase-free H_20 was added to ensure a final reaction volume of 15 µl. The gDNA wipe-out reaction was incubated at 45^{o}C for 2 min. Following this, 4 µl of QuantiNova RT mix (consisting of oligo-dTs and random RT primers) and 1 µl Reverse Transcriptase enzyme was added to the gDNA removal reaction. The reverse-transcription reaction was incubated at 25^{o}C for 3 min (annealing step), followed by incubation at 45^{o}C for 10 min (reverse-transcription step) and at 85^{o}C for 5 min to inactivate the Reverse Transcriptase. A negative control, which consists of cDNA synthesis reaction without the Reverse Transcriptase enzyme, was included for each sample reaction. The reverse transcription was then assessed by qPCR.

3.2.6 Gene expression analysis using RT-qPCR (quality control step)

Previous studies reported several genes that were differentially expressed in *M. tuberculosis* after 24h of INH treatment, including *kasA* and *accD6*, (4,35). Therefore, these 2 genes were selected to validate the INH treatment conditions used in our study. This was achieved by assessing their gene expression using RT-qPCR, after 24h treatment with a sub-lethal concentration of INH in the selected *M. tuberculosis*

strains ($K636^{WT}$, $K636^{RIF}$ and $H37Rv^{WT}$). The genome sequence of *M. tuberculosis* H37Rv reference strain (http://genolist.pasteur.fr/TubercuList) and Primer3plus software version 0.4.0 (http://www.bioinformatics.nl/cgi-bin/primer3plus/primer3plus.cgi) were used to design primers to amplify fragments smaller than 200 bp for the candidate genes, *kasA* and *accD6* (Table 3.2). The designed primers were synthesized by Integrated DNA Technologies (Coralville, Iowa, United States) and purchased from Whitehead Scientific (Winelands Close, Stikland, Cape Town, South Africa). Two housekeeping genes, *sigA* and 16S ribosomal RNA (*16S rRNA*), which have previously been shown to be stable under various conditions in *M. tuberculosis* gene expression, (36) were selected and primers were obtained from the primer databank at Stellenbosch University. The T_m of selected candidate and reference genes was further optimized by running a gradient PCR at various temperatures (58 – 65^{0}C) using the CFX96 Touch™ Real-Time PCR detection system (Bio-Rad Laboratories, USA). The amplification efficiency of each qPCR reaction was determined by standard curve analysis. Briefly, 1 µg of extracted gDNA (0.284 µg/ml = 284 µl) sample of H37Rv *M. tuberculosis* (23) was subjected to 10-fold serial dilutions. Then, qPCR of the diluted gDNA samples was performed using the CFX96 Touch™ Real-Time PCR Detection System (Bio-Rad Laboratories) for the candidate and housekeeping genes.

Following optimization, the iTaq™ Universal SYBR® Green kit was used to set up all RT-qPCR reactions as per manufacturer's instructions (Bio-Rad Laboratories). Briefly, 1 µg of gDNA was added to 5 µl SYBR Green mix, 50 µM of each forward and reverse primer and water was added to a final volume of 10 µl. A template free control was included to assess extraneous nucleic acid contamination and a no reverse transcription control was included to assess possible products that can arise from gDNA contamination. RT-qPCR was done using the CFX96 Touch™ Real-Time PCR Detection System (Bio-Rad Laboratories). The following reaction conditions were used: 95^{0}C for 30 seconds, 40 cycles of 95^{0}C for 5 seconds, 61^{0}C for 30 seconds and last step, of 65^{0}C for 5 min. The *16S rRNA* and *sigA* gene were included as housekeeping/reference genes for each RT-qPCR reaction. To assess reproducibility, each RT-qPCR experiment was performed on three biological samples that were each assayed in duplicate. The level of gene expression was quantified and analysed by the delta-delta Ct calculation (equation: $R=2^{-(\text{delta CT sample} - \text{delta CT control})}$) in which the

relative abundance of the target genes was normalized to the relative abundance of the housekeeping genes (37). The standard deviation (SD) of ≤ 0.5 as cut-off was used for the normalisation and analysis of the data. Identified genes that were differentially expressed by ≥ 2 fold were considered significantly expressed under the various conditions (38).

3.2.7 RNA-Seq analysis

High quality RNA extracted from untreated *M. tuberculosis* strains and *M. tuberculosis* strains treated with a sub-lethal INH concentration was analysed by the Agricultural Research Council (ARC) Biotechnology Platform, Next Generation Sequencing, Onderstepoort, South Africa. RNA was sequenced on the TruSeq 2500 System platform using the TruSeq® Stranded Total Sample Preparation v2 kit with Ribo-Zero ribosomal RNA reduction chemistry (Illumina, CA, USA) generating 5-10 million, of paired end reads with about 123bp per read length. RNA library construction from the purified total RNA of studied *M. tuberculosis* culture was prepared for Illumina (TruSeq®) as per manufacturer's guide (TruSeq RNA Sample Preparation v2 Guide, Illumina).

3.2.8 RNA-Seq bioinformatics analysis

Bioinformatics analysis of all Illumina RNA sequencing data was done in consultation with a biostatistician, Dr Stuart Meier from the University of Cape Town. Figure 3.2 below illustrates all steps followed for performing differential gene expression analysis using the Bioconductor software package EdgeR and the bioinformatics analysis pipeline. FastQC software (v0.115) was used to analyse the quality of the original FASTQ files (http://www.bioinformatics.babraham.ac.uk/projects/fastqc/). The "Trimmomatic software and TruSeq3-PE.fa" in R programming language (free software platform for statistical computing) (Appendix B) was used to remove adapters and low quality reads (27). The trimmed reads were re-analysed with FastQC to confirm improvement in the quality of the reads and the removal of adapters. The trimmed reads were mapped to the *M. tuberculosis* H37Rv genome ASM19595v2, http://bacteria.ensembl.org/Mycobacterium_tuberculosis_H37Rv) using the STAR (v2.5.3a) aligner. Raw counts for the negative strand were extracted from STAR gene count output file for each sample and combined to make a raw count table. Following

this, the Bioconductor software package EdgeR was used to determine the differential gene expression (39,40) (Figure 3.2), using the raw count table. Genes were removed that did not have a count per million (cpm) of at least six (raw count around 8 in low count samples) in at least two samples. The remaining genes were normalized using EdgeR. The trimmed mean of M-values normalization method (TMM method) and dispersion estimates (DE) analysis was subsequently performed using both the generalized linear model (GLM) likelihood ratio test (glmLRT) and the quasi-likelihood (QL) F-test (glmQLF). The fold change ratios are very similar for both methods however the QLF-test is considerably more stringent for significance testing. The false discovery rate (FDR) and p-value < 0.05 was considered significant.

All significant differentially expressed genes were searched through the Tuberculist (http://svitsrv8.epfl.ch/tuberculist/), UniProt (https://www.uniprot.org/) and NCBI (https://www.ncbi.nlm.nih.gov/) databases for annotation and identity. These databases were also used to describe and explain the characteristics of the identified genes. To investigate the relationship, biological interpretation or association between differentially expressed genes, we applied the Gene Ontology Enrichment Analysis Software Toolkit (GOEAST) (http://omicslab.genetics.ac.cn/GOEAST/faq.php) to generate a significantly enriched gene ontology (GO) terms lists for the different comparison groups (41). Gene Ontology helps narrow the number of differentially expressed genes to the most important based on functional categories. GOEAST is a free web-based tool which employs various statistical methods to determine significantly enriched GO terms. Significance was based on the FDR which was calculated using the Benjamini–Yekutieli model (41). The different comparison groups included $K636^{WT}$ vs $H37Rv^{WT}$ as group A; $K636^{WT}$ vs $K636^{RIF}$ as group B; $K636^{WT}$ (untreated) vs $K636^{WT}$ (INH treated) as group C and $K636^{RIF}$ (untreated) vs $K636^{RIF}$ (INH treated) as group D. The denoted names, group A-D will be used in the results section for the different comparisons referral.

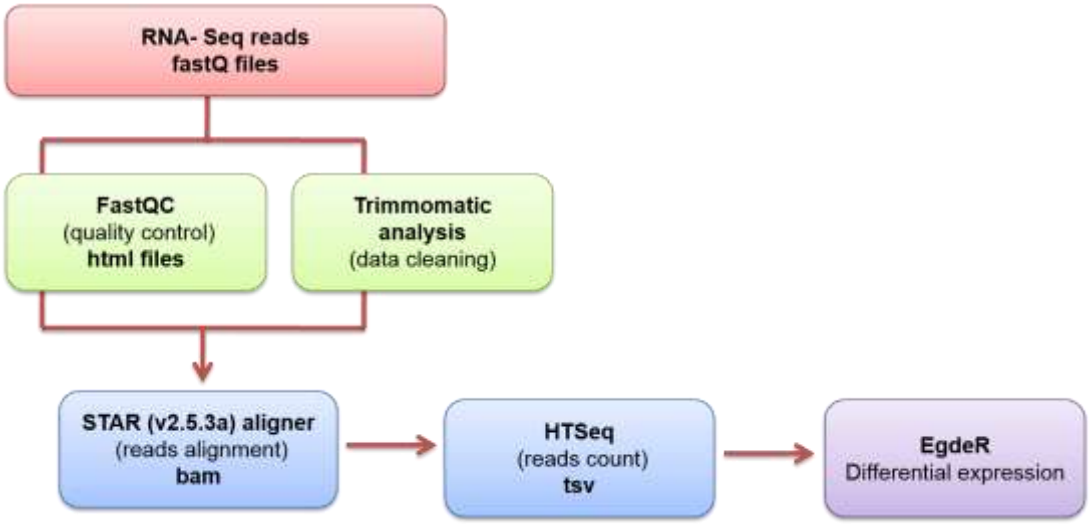

Figure 3.6 Illustration on the bioinformatic pipeline used to assess differential gene expression.

3.2.9 Validation by RT-qPCR of differentially expressed genes identified by RNA-Seq

After the identification of genes that were significantly differentially expressed under the various conditions by RNA-Seq, candidate genes (n=5) were selected for validation of gene expression levels by RT-qPCR. The selection criteria of the 5 candidate genes included: 1) ≥ 4-fold change differential gene expression with significant false discovery rate (FDR) < 0.05; and 2.00) functional categories which included genes involved in cellular and cell wall processes, lipid metabolism and regulatory processes. In addition, *kasA* and *accD6* previously known to be differentially expressed upon INH treatment (42) were included for validation.

3.3 Results

3.3.1 Quality control of *M. tuberculosis* strains: genotypic and phenotypic characterization

Genotypic and phenotypic characterization of the selected *M. tuberculosis* strains (K636^{WT}; K636^{RIF,} and H37Rv^{WT}) was performed to rule out contamination (refer to Appendix C: Figure S3.1). The confirmed RIF MICs for K636^{WT} and H37Rv^{WT} were 0.5 µg/ml and 0.2 µg/ml (Table 3.3), respectively, which confirmed the sensitive phenotype for *M. tuberculosis* strains without an *rpoB* mutation. The strain with the *rpoB* Ser531Leu mutation, denoted as K636^{RIF}, showed a MIC of 200 µg/ml RIF which indicates high level resistance to RIF (Table 3.3). This suggests that the level of RIF resistance correlated with the presence of the *rpoB* Ser531Leu mutation as shown by targeted sequencing results (Appendix C: Figure S3.2).

Table 3.6 Phenotypic and genotypic characterization of *M. tuberculosis* strains

Strain background	**RIF MIC (µg/ml)**	***rpoB* Ser531Leu mutation present?**
K636^{WT}	0.5	No
K636^{RIF}	200	Yes
H37Rv^{WT}	0.2	No

3.3.2 Whole genome sequencing (WGS) analysis of *M. tuberculosis* strains

The comparative analysis of K636^{WT} and K636^{RIF} (with *rpoB* mutation) *M. tuberculosis* strains sequence data showed variation in the read depth between the two strains and that the level of confidence in calling variants was low for K636^{RIF} (with *rpoB* mutation) unless they were fixed variants. The presence of *rpoB* Ser531Leu mutation was confirmed as well as a synonymous substitution in the *malQ* gene (Table 3.4) and therefore, no effect on the K636^{RIF} transcriptome is expected. Additionally, 2 other variants were also observed in the *glpK* and *Rv1285* genes, respectively (Table 3.4). The re-culturing of K636^{WT} and K636^{RIF} (with *rpoB* mutation) *M. tuberculosis* strains could have influenced the relative ratios these variants by possibly introducing some heterogeneity or causing their accumulation. The comparative analysis of K636^{WT} and H37Rv^{WT} *M. tuberculosis* strains sequence

data identified more than 1000 fixed variants. These variants were filtered with the heterogeneity frequency of 0.7 and the minimum number of reads at the variant position was set to 30. Out of the identified variants, 30 variants were unique to $K636^{WT}$ (Table 3.5). The synonymous variants were excluded from the data shown because of no protein changes and only non-synonymous (nonSyn) variants were incorporated (Table 3.5). Briefly, 6 genes with variants belonged to the lipid metabolism functional category; 6 to conserved hypotheticals; 4 to intermediary metabolism and respiration; 3 to virulence, detoxification, adaptation, 3 to regulatory proteins, 1 to cell wall and cell processes and 8 to PE/PPE functional categories.

Table 3.4 WGS analysis of $K636^{WT}$, $H37Rv^{WT}$and $K636^{RIF}$ (with *rpoB* Ser531Leu mutation) *M. tuberculosis* strains

Strain background	Average % depth of coverage	Average % mapped reads	Variants identified in comparison to progenitor (WGS)	Variant frequency
$K636^{WT}$	98	99	-	-
$K636^{RIF}$	28	97	*rpoB* TCG 1349 TTG (S531L/S450L)	100%
			malQ GTG 1221 GTA	100%
			glpK	
			Rv1285	
$K636^{WT}$ vs $H37Rv^{WT}$	98	99	30 variants (Table 3.6)	Heterogeneity frequency (0.7)

.

Table 3.5 Variants identified for K636^{WT} *M. tuberculosis* strain with respect to H37Rv^{WT} (reference genome) using WGS

K636^{WT} (with respect to H37Rv^{WT})							
No.	**Gene position**	**Gene Name**	**Product/Function**	**Functional Category**	**Mutation**	**Amino acid change and position**	**Synonymous/nonSynonymous•**
1	563	*mce1D Rv0172*	Mce-family protein Mce1D	Virulence, detoxification, adaptation	ATC - ACC	I188T	nonSyn
2	137	*vapC47 Rv3408*	Possible toxin VapC47	Virulence, detoxification, adaptation	TCG- TTG	S46L	nonSyn
3	1109	*mce1F Rv0174*	Mce-family protein Mce1F	Virulence, detoxification, adaptation	CTG- CCG	L370P	nonSyn
4	334	*Rv0078A*	Hypothetical protein	Conserved hypotheticals	GAG- AAG	E112K	nonSyn
5	660	*Rv3081*	Conserved hypothetical protein	Conserved hypotheticals	TTC- TTG	F220L	nonSyn
6	287	*Rv3424c*	Hypothetical protein	Conserved hypotheticals	GTG- GCG	V96A	nonSyn
7	217	*Rv2562*	Conserved hypothetical protein	Conserved hypotheticals	GCC- ACC	A73T	nonSyn
8	785	*Rv2017*	Transcriptional regulatory protein	Regulatory proteins	GCG- GAG	A262E	nonSyn
9	989	*Rv3399*	Possible S-adenosylmethionine-dependent methyltransferase	Lipid metabolism	GCG- GAG	A330E	nonSyn
10	670	*oxcA Rv0118c*	Probable oxalyl-CoA decarboxylase OxcA	Intermediary metabolism and respiration	AGC- GGC	S224G	nonSyn
11	623	*Rv3830c*	Transcriptional regulatory protein (probably TetR-family)	Regulatory proteins	G- GA	INDEL	INDEL
12	160	*sdhD Rv3317*	Probable succinate dehydrogenase SdhD	Intermediary metabolism and respiration	GTG- CTG	V54L	nonSyn
13	6013	*Rv2940c*	Probable multifunctional mycocerosic acid synthase membrane-associated Mas	Lipid metabolism	ACT- CCT	T2005P	nonSyn
14	316	*Rv0465c*	Probable transcriptional regulatory protein	Regulatory proteins	TGC- CGC	C106R	nonSyn
15	4205	*pks6 Rv0405*	Probable membrane bound polyketide synthase Pks6	Lipid metabolism	CGG- CCG	R1402P	nonSyn

16	395	*idsB Rv3383c*	Possible polyprenyl synthetase IdsB	Lipid metabolism	GTC- GGC	V132G	nonSyn
17	448	*fadA Rv0859*	Possible acyl-CoA thiolase FadA	Lipid metabolism	AGC- GGC	S150G	nonSyn
18	239	*Rv3282*	Conserved hypothetical protein	Conserved hypotheticals	GCC- GAC	A80D	nonSyn
19	448	*Rv1461*	Conserved protein	Conserved hypotheticals	GTA- ATA	V150I	nonSyn
20	757	*lldD2 Rv1872c*	Possible L-lactate dehydrogenase (cytochrome) LldD2	Intermediary metabolism and respiration	GTG- ATG	V253M	nonSyn
21	644	*Rv3884c*	ESX conserved component EccA2. ESX-2 type VII secretion system protein.	Cell wall and cell processes	GAG- GGG	E215G	nonSyn
22	245	*Rv0457c*	Probable peptidase	Intermediary metabolism and respiration	CGC- CCC	R82P	nonSyn
23	6320	*Rv3343c*	PPE family protein PPE54	PE/PPE	GCC- GTC	A2107V	nonSyn
24	769	*Rv0280*	PPE family protein PPE3	PE/PPE	GAA- AAA	E257K	nonSyn
25	382	*Rv3425*	PPE family protein PPE57	PE/PPE	ACT- GCT	T128A	nonSyn
26	2026	*Rv1917c*	PPE family protein PPE34	PE/PPE	TCA- GCA	S676A	nonSyn
27	808	*Rv2769c*	PE family protein PE27	PE/PPE	GTG- ATG	V270M	nonSyn
28	336	*Rv1089*	PE family protein PE10	PE/PPE	ATT- AT	INDEL335	INDEL
29	846	*Rv2328*	PE family protein PE23	PE/PPE	AGT- AGG	S282R	nonSyn
30	303	Rv3738c	PPE family protein PPE66	PE/PPE	TTG- TTC	L101F	nonSyn

3.3.3 Growth assessment of *M. tuberculosis* strains

Growth assessed by OD_{600nm} measurement indicated a mid-log phase at an OD_{600nm} = 0.8 (day 14) for $K636^{WT}$, OD_{600nm} = 0.8 (day 14) for $H37Rv^{WT}$ and at an OD_{600nm} = 0.9 (day 14) for $K636^{RIF}$ *M. tuberculosis* strains (Figure 3.3). CFU assessment at day 14 showed 1.8 x 10^9 CFU/ml for $K636^{WT}$, 2.0 x 10^9 CFU/ml $H37Rv^{WT}$ and 3.1 x10^9 CFU/ml for $K636^{RIF}$ *M. tuberculosis* strains (Figure 3.3). However, no statistical analysis was done and it could not be concluded whether the slight differences observed in the growth patterns of studied *M. tuberculosis* strains were statistically significant or not, which is one of the limitations.

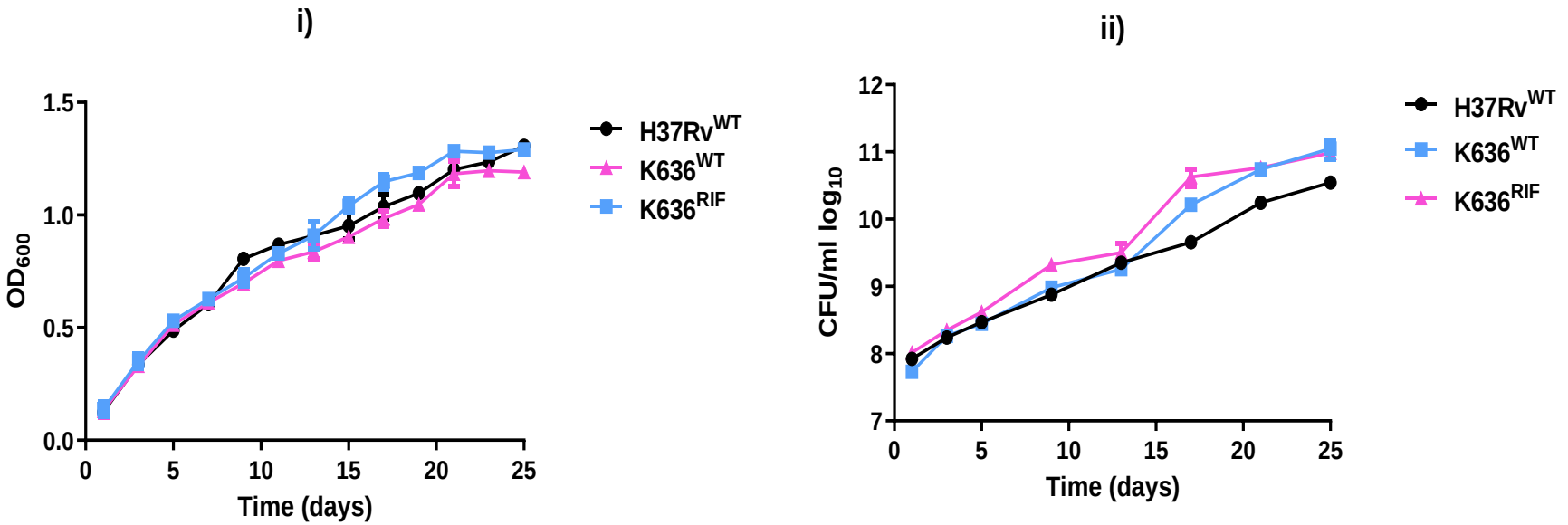

Figure 3.7 The growth curves of the studied *M. tuberculosis* strains. The growth of H37Rv^{WT}; K636^{WT} and K636^{RIF} were assessed every second day for 25 days by i) OD_{600nm} measurements starting with an OD_{600nm} of 0.1 and, ii) colony forming unit (CFU) determination. These experiments are a representation of 3 biological triplicates for H37Rv^{WT}; K636^{WT} and K636^{RIF}. The plots represent the mean values and standard deviation (SD) of the biological triplicates.

The INH titration experiments were performed by treating H37Rv^{WT} and K636^{WT} *M. tuberculosis* strains with various ranges of INH concentrations (0.02 µg/ml, 0.03 µg/ml and 0.05 µg/ml) to determine the INH concentration that shows less than 10% reduction in bacterial growth within 24h of treatment of the respective *M. tuberculosis* strains (Figure 3.4i). The INH titration curve revealed that an INH concentration of 0.05 µg/ml resulted in 8.7% bacterial growth inhibition in K636^{WT} and 7.6% H37Rv^{WT} *M. tuberculosis* strains at 24h exposure (day 1 on Figure 3.4i) compared to K636^{WT} and H37Rv^{WT} that were unexposed to INH. These % calculations were done by dividing the day 1 (24h) mean values (obtained from Figure 3.4i) of K636^{WT} and H37Rv^{WT} INH exposed over K636^{WT} and H37Rv^{WT} unexposed x 100%, respectively. The % growth inhibition values at 0.02 µg/ml and 0.03 µg/ml INH after 24h exposure (day 1 on Figure 3.4i) for K636^{WT} and H37Rv^{WT} were lower than 5.5%; therefore suggesting lower growth inhibition than at 0.05 µg/ml INH 24h exposure. In addition, 89.6% of mycobacterial growth inhibition was observed for K636^{WT} 7 days after exposure to 0.05 µg/ml INH (Figure 3.4i). Similarly, 85.1% H37Rv^{WT} inhibition of growth was observed after 7 days of INH treatment relative to the untreated cultures (Figure 3.4i). These results indicate that exposure of *M. tuberculosis* strains to 0.05 µg/ml INH results in an increased inhibition of bacterial growth over time. The CFU/ml over time plots indicate the culturability of the K636^{WT} and H37Rv^{WT} *M. Tuberculosis* strains in the presence of 0.05 µg/ml INH (Figure 3.4ii). Subsequent experiments were done by exposing the selected *M. tuberculosis* strains with 0.05 µg/ml INH concentrations for 24h and followed by RNA extraction.

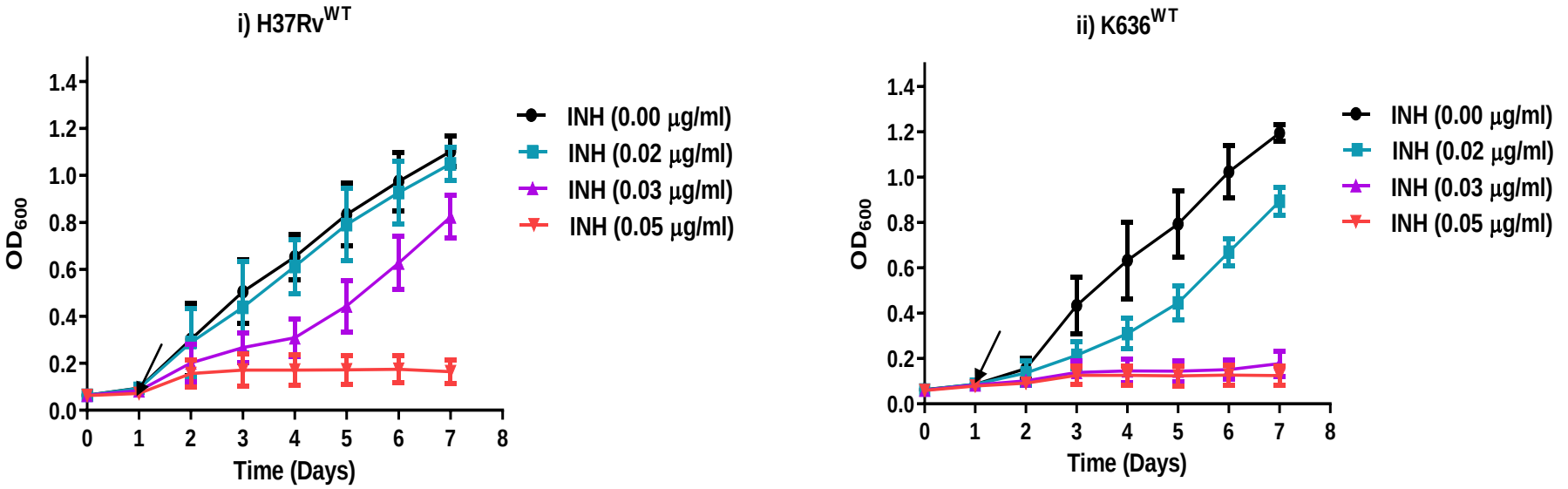

Figure 3.8i The INH titration of studied *M. tuberculosis* strains (OD_{600nm}/time). The INH titration experiments were performed by treating *M. tuberculosis* strains (i) $H37Rv^{WT}$ ii) $K636^{WT}$ with various concentrations of INH to determine the INH concentrations of that shows 10% reduction in bacterial growth after 1 day (24h) exposure of *M. tuberculosis* strains. The ⟶= 1 day (24h) mark. These experiments are a representation of 3 biological triplicates. The plots represent the mean values of OD_{600nm} over time and standard deviation (SD) of the biological triplicates.

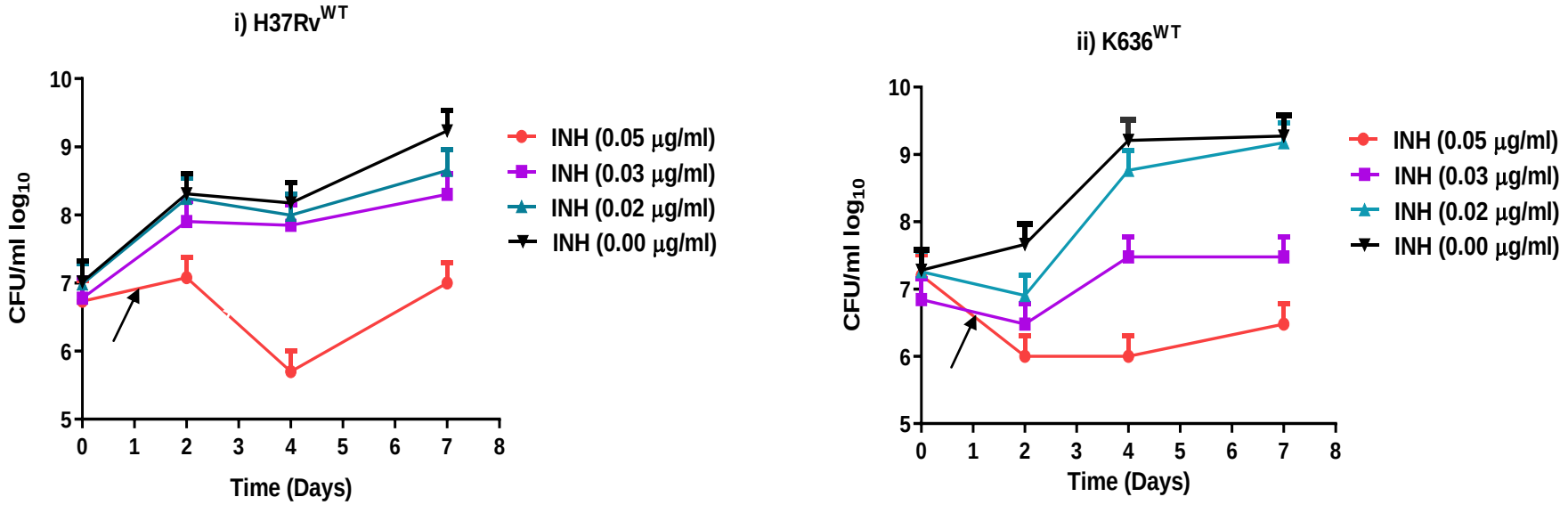

Figure 3.4ii The INH titration of studied *M. tuberculosis* strains (CFU/time). The INH titration experiments were performed by treating *M. tuberculosis* strains (i) H37Rv^{WT}; ii) K636^{WT} with various concentrations of INH to determine the INH concentrations of that shows 10% reduction in bacterial growth after 1 day (24h) exposure of *M. tuberculosis* strains. The ⟶= 1 day (24h) mark. The plots represent the mean values of CFU/ml over time. These experiments are a representation of 3 biological triplicates.

3.3.4 RNA quality control

3.3.4.1 RNA quality assessment

The integrity and concentration of the extracted RNA samples (n=15) was determined by the Agilent Bioanalyser (Figure 3.5) and the Nanodrop system. The generated 260/280 ratios (from Nanodrop) of the RNA samples ranged from 1.8 to 2.0 (Table 3.6). In addition, the 260/230 ratios ranged from 2.1 to 2.3 (Table 3.6); indicating that high quality RNA was extracted from $K636^{WT}$, $K636^{RIF}$ and $H37Rv^{WT}$ *M. tuberculosis* strains. The RIN scores of RNA extracted from $K636^{WT}$, $K636^{RIF}$ and $H37Rv^{WT}$ strains ranged from 6.7 to 8.1, indicating intact RNA (Table 3.6). The ranges of RNA concentrations for the 3 biological samples were from 1) $K636^{WT}$ (untreated): 199 to 246 ng/µl; 2) $K636^{WT}$ (treated): 275 to 353 ng/µl; 3) $K636^{RIF}$ (untreated): 141 to 225 ng/µl; 4) $K636^{RIF}$ (treated): 208 to 242 ng/µl and 5) $H37Rv^{WT}$(untreated): 332 to 536 ng/µl) (Table 3.6), indicating good RNA yield. PCR amplification of the *rpoB* region confirmed the absence of gDNA in the extracted RNA templates, by showing no amplification for this region. A positive PCR amplification of *rpoB* region was confirmed in the H37Rv DNA. These results therefore confirmed the suitability of the extracted RNA samples (n=15) for RNA-Seq analysis and subsequent RT-qPCR.

Table 3.6 Quality and quantity values of the RNA extracted from the studied *M. tuberculosis* strains

Sample ID	RNA conc. (ng/µl)	260/280	260/230	PCR amplification of (*inh*A promoter)	RIN value (Bioanalyser)
Biological 1					
$K636^{WTuntreated}$	246	1.8	2.2	Negative	6.8
$K636^{WTtreated}$	307	1.8	2.2	Negative	7.2
$K636^{RIFuntreated}$	141	1.9	2.1	Negative	6.7
$K636^{RIFtreated}$	208	1.9	2.1	Negative	6.9
$H37Rv^{WTuntreated}$	332	1.8	2.2	Negative	7.5
Biological 2					
$K636^{WTuntreated}$	199	1.9	2.2	Negative	7.6
$K636^{WTtreated}$	353	1.9	2.2	Negative	7.7
$K636RIF^{untreated}$	222	2.0	2.2	Negative	8.1
$K636^{RIFtreated}$	242	2.0	2.2	Negative	8.0
$H37Rv^{WTuntreated}$	407	1.9	2.3	Negative	7.8
Biological 3					
$K636^{WTuntreated}$	203	1.9	2.1	Negative	7.8
$K636^{WTtreated}$	275	2.0	2.3	Negative	8.3
$K636^{RIFuntreated}$	225	1.9	2.3	Negative	7.4
$K636^{RIFtreated}$	224	1.8	2.2	Negative	7.6
$H37Rv^{WTuntreated}$	536	1.9	2.2	Negative	8.1

$K636^{WTuntreated}$; $K636^{RIFuntreated}$; $H37Rv^{WTuntreated}$ and $K636^{WTtreated}$; $K636^{RIFtreated}$ (treated with 0.05µg/ml INH for 24h)

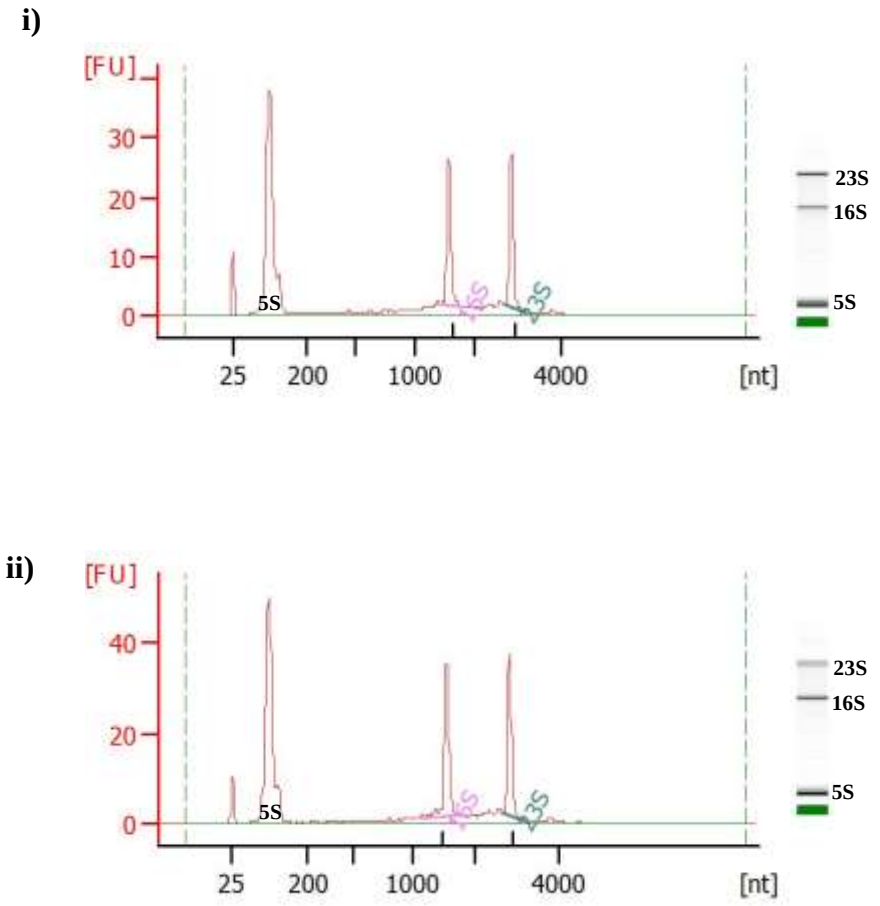

Figure 3.5 Representative example of a typical electropherogram and gel electrophoresis of the extracted RNA samples by the Agilent Bioanalyser system. The graphs indicate the 16S and 23S RNA signal peaks in i) $K636^{RIF}$ *M. tuberculosis* strain treated with 0.05 µg/ml INH for 24h and ii) $K636^{WT}$ not treated with INH.

Optimization of the qPCR amplification conditions. A temperature gradient PCR was performed using H37Rv DNA as a template to optimise the qPCR amplification conditions. The T_m gradient PCR of H37Rv DNA revealed that the annealing temperature of the primers for the amplification of *kasA* and *accD6* was 60.4 – 61.8^{0}C for both primers' sets (section 3.2.2.2). Subsequently, standard curves were generated to assess the amplification efficiency of the primer sets for *kasA* and *accD6* and the housekeeping genes, *sigA* and *16S rRNA*. The amplification curve showed Ct values of *kasA*, *accD6*, *sigA* and *16S rRNA* ranging from 15 – 30 cycles for 1:10 diluted H37Rv DNA (Appendix C: Figure S3.4). The amplification efficiency per primer set was calculated from the generated standard curves using H37Rv DNA as a template

and was 102% and 114% for *kasA* and *accD6*, respectively (Table 3.7). In addition, it was observed that the amplification efficiency for the housekeeping genes *sigA* and *16S rRNA* was 99.8% and 97.3%, respectively (Table 3.7). Melting curve analysis confirmed the specificity of the primers to amplify *kasA*, *accD6*, *sigA* and 16S rRNA and the absence of primer dimers and non-specific binding (data not shown).

Table 3.7 The amplification efficiency of the candidate genes selected for RT-qPCR before RNA-Seq

Type of gene	Gene	Amplification efficiency (%)
Housekeeping genes	*sigA*	99.8
	16S rRNA	97.3
Candidate genes	*kasA*	102
	accD6	114

3.3.4.2 Validation of gene expression of *kasA* and *accD6* for quality control purposes

Prior to performing RNA-Seq analysis on the extracted RNA from the respective *M. tuberculosis* strains, two candidate genes, *kasA* and *accD6*, were selected for RT-qPCR assessment, as these genes were previously shown to be up-regulated upon INH (0.1 and 0.2 µg/ml) treatment for 24h (3,5,35). High-level up-regulation was observed for *kasA* and *accD6* when normalised to *16S rRNA* and *sigA* (housekeeping genes) in $K636^{WT}$ and $K636^{RIF}$ *M. tuberculosis* strains, respectively after 24h exposure to 0.05 µg/ml INH [Figure 3.6 (i–ii)]. This was demonstrated by varying fold-changes for *kasA* (1.8-2-fold) and *accD6* (2.5 -2.7-fold) in $K636^{WT}$ and for *kasA* (2.5-2.8-fold) and *accD6* (1.8 -2.3-fold) in $K636^{RIF}$, respectively [Figure 3.6 (i–ii)]. In contrast, low-level up-regulation was observed for *kasA* and *accD6* when normalised to *16S rRNA* and *sigA* (housekeeping genes) in $H37Rv^{WT}$ *M. tuberculosis* strain, after 24h exposure to 0.05 µg/ml INH. This was demonstrated by lower than 1.0-fold-changes for *kasA* and *accD6* in $H37Rv^{WT}$ [Figure 3.6 (i–ii)]. This suggests that the induction of *kasA* and *accD6* was different between $K636^{WT}$, $K636^{RIF}$ and $H37Rv^{WT}$ strains [Figure3.6 (i-ii)]. However, no statistical analysis was done and it could not be concluded whether the observed differences were statistical significant and for this reason, as the

limitation of the study, H37Rv^{WT} (INH-treated) strain was excluded for the RNA-Seq analysis.

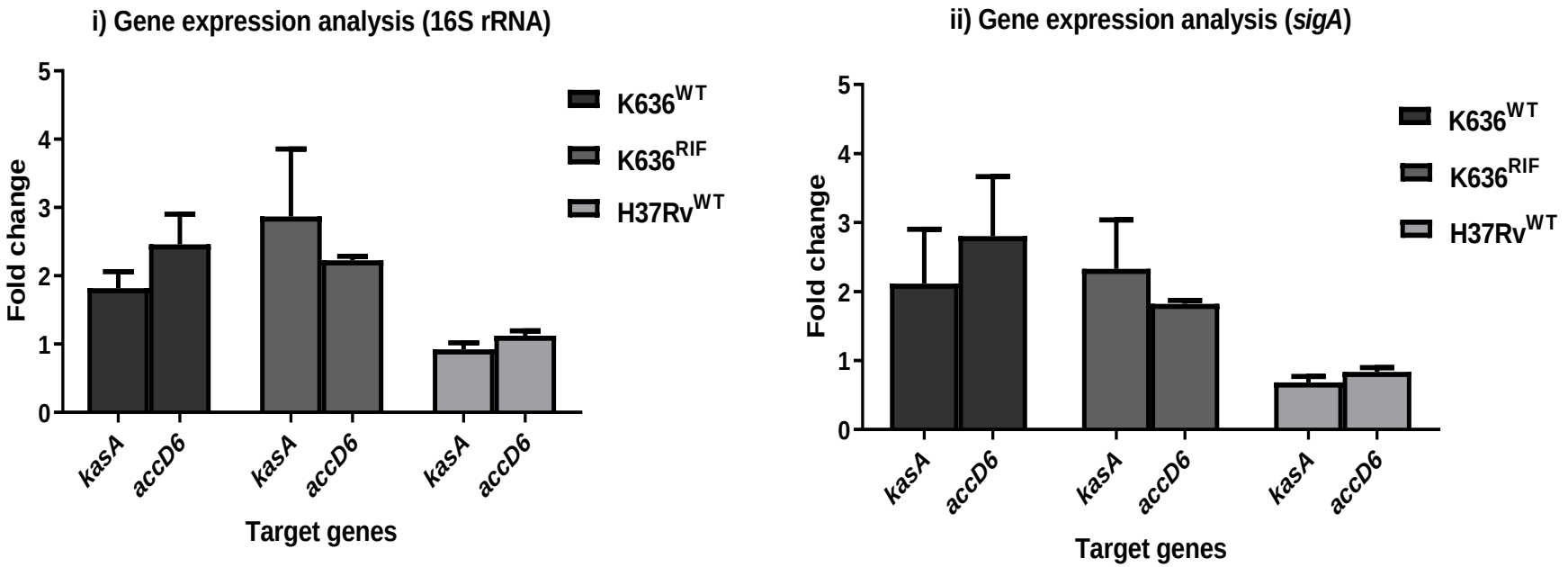

Figure 3.6 (i-ii) Differential gene expressions of *kasA* and *accD6* in the K636^{RIF} and K636^{WT} *M. tuberculosis* strains after 24h treatment with or without 0.05 µg/ml INH and for H37Rv^{WT} without 0.05 µg/ml INH. i) Differential expression of *kasA* and *accD6* normalised to *16S rRNA*, ii) Differential gene expression of *kasA* and *accD6* normalised to *sigA*. Data shown is representative of 3 biological repeats of the INH-treated K636^{RIF} and K636^{WT} strains and untreated H37Rv^{WT}, K636^{RIF} and K636^{WT} strains and the plots of mean values of 3 biological replicates and SDs.

3.3.5 RNA-Seq analysis

3.3.5.1 RNA-Seq bioinformatics analysis

The RNA-Seq analysis was performed for 3 biological samples in triplicates (n= 5x3= 15) and approximately 5-10 million reads were generated for each sample using paired end sequencing. A FastQC report was generated for each raw FASTQ file using the FastQC software program to assess the quality of the reads. Good quality reads with 36-28 high quality scores (indicated by the green colour scale) and 100% coverage were observed as shown in Figure 3.7i. Furthermore, a good base quality of the reads from 1bp to 123bp as shown in the tile graph in Figure 3.7ii (indicated by a clear blue colour scale) was observed. Read quality was greatly improved after removal of adapters by trimming the reads. No adapters were present after trimming and Phred Scores showed a 0.2% error rate [Figure 3.7 (iii and iv)]. The biological coefficient of the variation (BCV) plot (which is a square root of the negative binomial dispersion) was calculated using the generalized GLM (Figure 3.7 (v)). This was performed to de-prioritize genes with inconsistent results and allow the main analysis to focus on changes that are consistent between biological replicates (43).

(i)

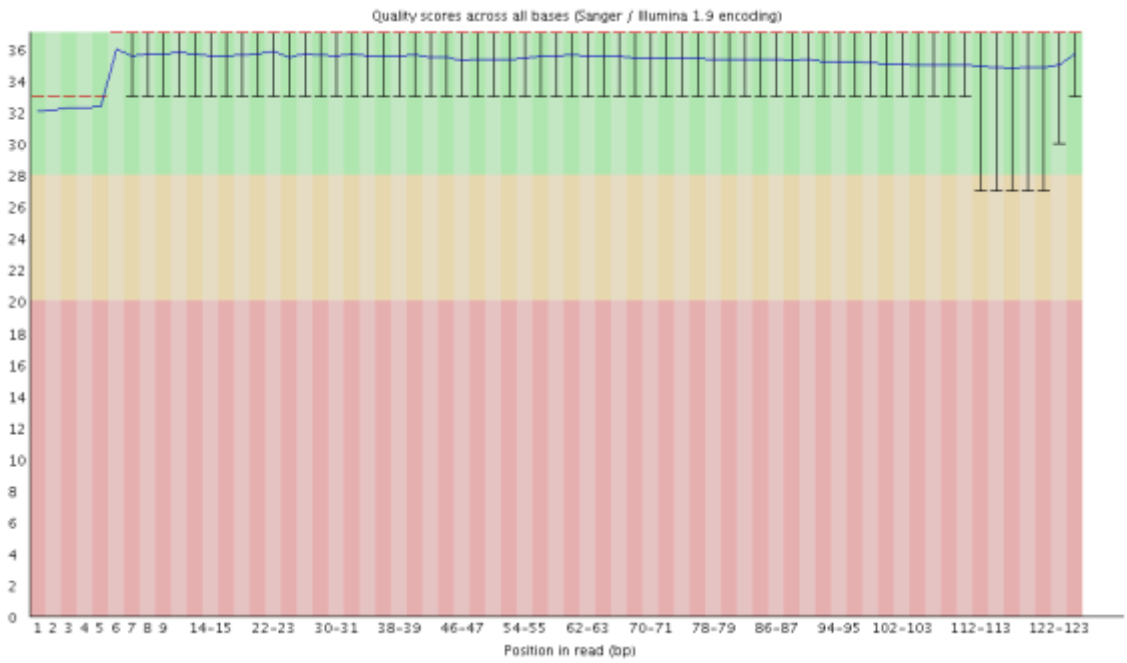

(ii)

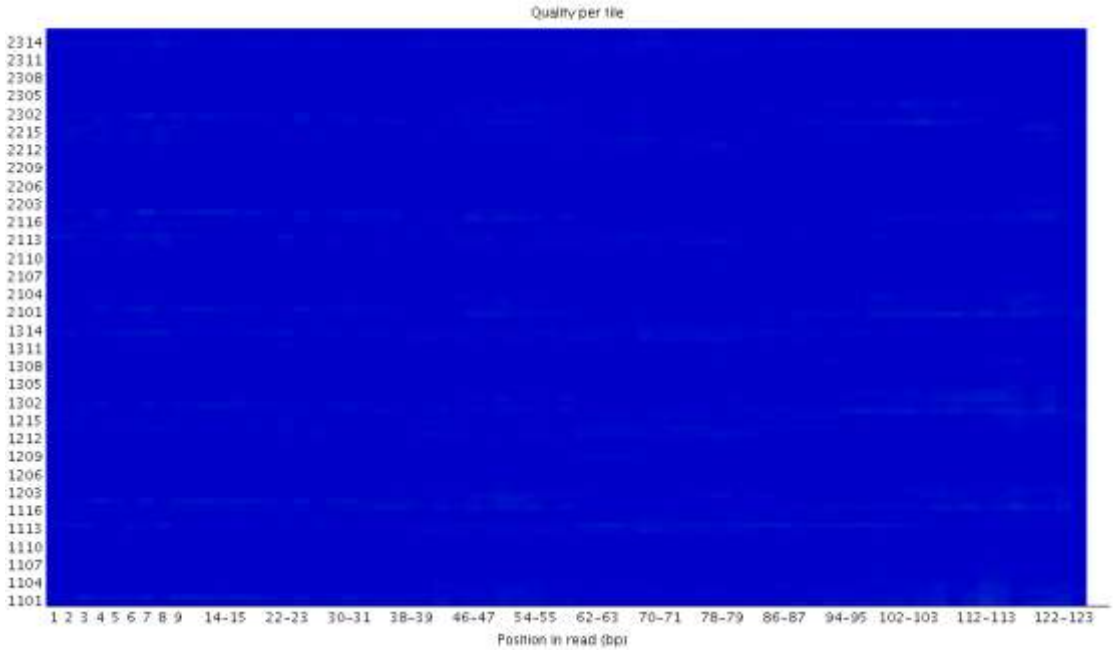

(iii)

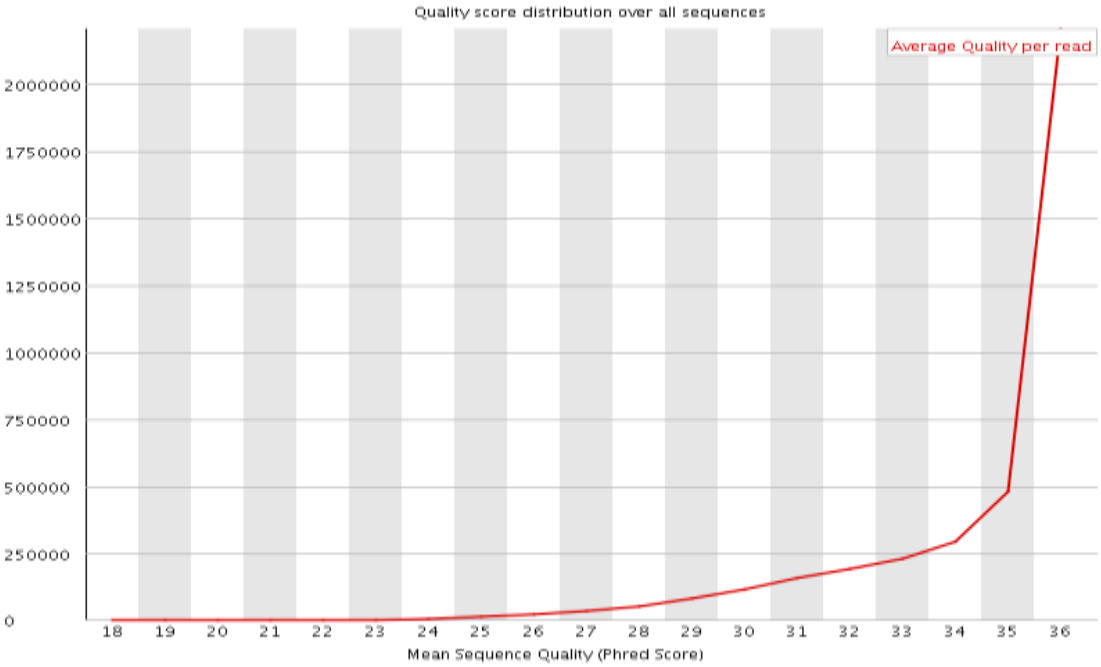

(iv)

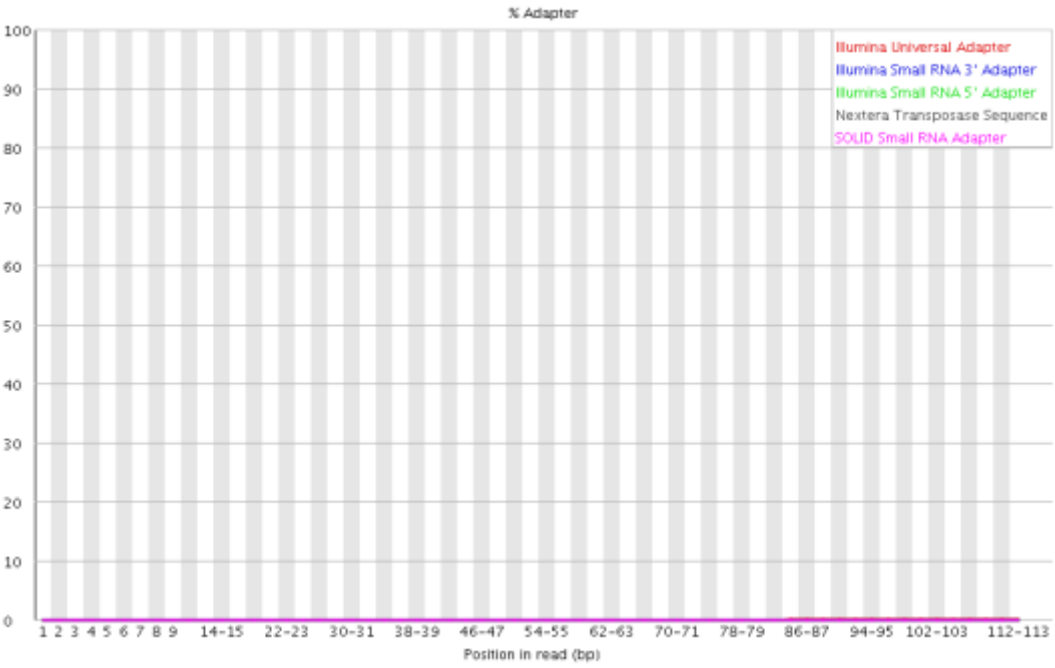

(v)

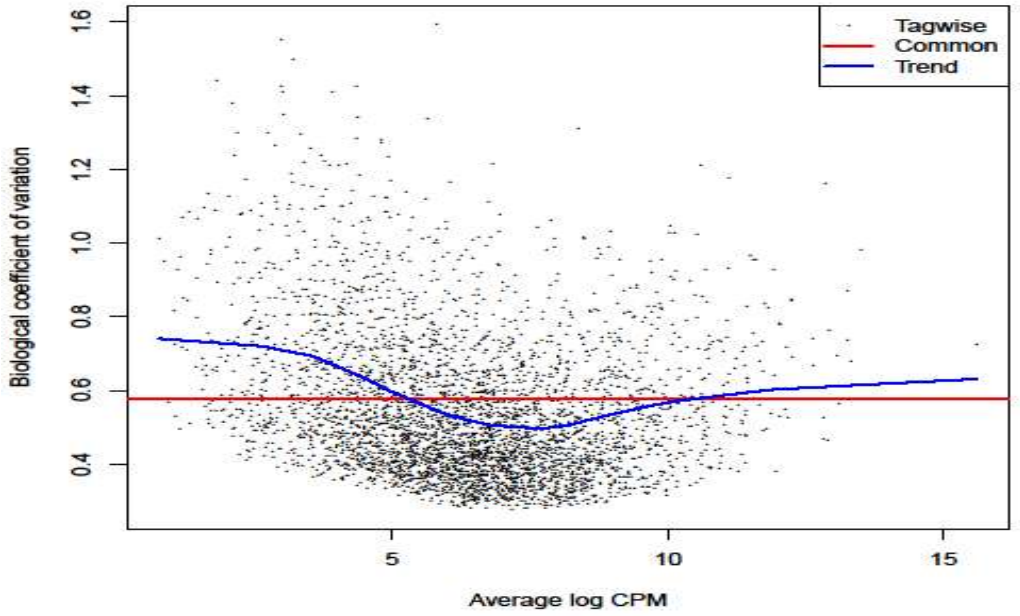

Figure 3.7 Quality score of sequence reads calculated by FastQC software program and the biological coefficient of variation (BCV) plot calculated by GLMs. A quality assessment in a form of a FastQC report was generated for each raw FASTQ file using FastQC software **(i)** Illustration of the quality of the reads with sections ranging from good (green), to intermediate (orange) and poor quality (red). The quality will decrease as the run progresses. The blue line represents the mean quality. **(ii)** A tile graph specific to Illumina libraries where the blue colour scale represents good base quality. The graph is a representation of the original flowcell tiles for each read from the sequencer. **(iii)** Phred Score showing 0.2 % error rate being calculated when the mean quality is below 27 and a 1 % error rate if the mean quality is below 20. **(iv)** A depiction of the % adapter content for the trimmed reads. **(v)** The BCV plot statistics to allow de-prioritizing of genes with inconsistent results

and allowing the main analysis to focus on changes that are consistent between transcriptomes of the analysed biological replicates.

3.3.5.2 Comparative transcriptomic profiles of drug resistant and susceptible *M. tuberculosis* strains

Table 3.8 shows the number of genes that were identified by RNA-Seq analysis to be significantly differentially expressed based on FDR value cut-off of ≤ 0.05 and LogFC value of 2.5 fold in the different comparison groups (A-D). Data sets were analysed to assess (i) the effect of genetic background, (ii) the effect of the resistance-conferring mutation (*rpoB* Ser531Leu mutation) and (iii) the effect of the INH treatment on transcriptional profiles. The assessment of the effect of the genetic background on the transcriptional profile of $K636^{WT}$ (untreated) vs $H37Rv^{WT}$ (untreated) *M. tuberculosis* strains, revealed that 348 genes were significantly differentially expressed [group A, (Table 3.8)]. These genes were grouped into functional categories and 66 genes belonged to cell wall and cellular processes, 56 genes to intermediary metabolism and respiration and 95 genes were categorised as conserved hypotheticals (Table 3.9). In addition, 17 genes belonged to lipid metabolism, 16 genes to regulatory proteins and the remaining genes belonged to either virulence, detoxification, adaptation (24 genes), insertion seqs and phages (32 genes), information pathways (16 genes) and PE/PPEs (28 genes) functional categories (Table 3.9).

The assessment of the effect of the *rpoB* Ser531Leu mutation on the transcriptional profiles of $K636^{WT}$ (untreated) vs $K636^{RIF}$ (untreated) *M. tuberculosis* strains, revealed that 192 genes were significantly differentially expressed [group B, (Table 3.8)]. These genes were grouped into functional categories and 28 genes belonged to cell wall and cellular processes, 31 genes to intermediary metabolism and respiration and 65 genes were categorised as conserved hypotheticals (Table 3.10). In addition, 12 genes belonged to lipid metabolism, 7 genes to regulatory proteins and the remaining genes belonged to either virulence, detoxification, adaptation (9 genes), insertion seqs and phages (14 genes), information pathways (6 genes) and PE/PPEs (20 genes) functional categories (Table 3.10). However, WGS analysis also revealed 3 variants (*malQ*, *Rv2185* and *glpK*) (Table 3.4). Interestingly, the assessment of the effect of INH treatment on transcriptional profiles in Group C [$K636^{WT}$ (treated*) vs

K636^{WT} (untreated)] and group D [K636^{RIF} (treated*) vs K636^{RIF} (untreated) (Group D)] revealed no significant differentially expressed genes (Table 3.8). For this reason, group C and D had to be excluded, which is one of the study limitations (see discussion section 3.4.5).

Table 3.8 Comparison of significantly differentially expressed genes of *M. tuberculosis* strains

***M. tuberculosis* strains comparison groups**	**Number of differentially expressed genes**
K636^{WT} (untreated) vs H37Rv^{WT} (untreated) (Group A)	348 genes
K636^{WT} (untreated) vs K636^{RIF} (untreated) (Group B)	192 genes
******K636^{WT} (treated*) vs K636^{WT} (untreated) (Group C)	0 genes
******K636^{RIF} (treated*) vs K636^{RIF} (untreated) (Group D)	0 genes

******* *Exposure to 0.05 µg/ml INH for 24h*

***In Group C and D no significant differential expression was observed and therefore these groups were excluded from further analysis.*

Table 3.9 Genes (n= 348) that were significantly differentially expressed between *M. tuberculosis* strains K636^{WT} (untreated) vs H37Rv^{WT} (untreated), (Group A.)

Functional category	Gene no.	Gene name	Function/Product	P-value	FDR	LogFC
Cell wall and cell processes	1	*Rv0987*	Thought to be involved in active transport of adhesion component across the membrane: involved in attachment and virulence. Responsible for the translocation of the substrate across the membrane.	1,92E-05	4,70E-04	3,80
	2	*Rv1115*	Function unknown.	3,66E-05	6,26E-04	4,47
	3	*Rv0986*	Thought to be involved in active transport of adhesion component across the membrane: involved in attachment and virulence. Responsible for energy coupling to the transport system.	4,68E-05	7,06E-04	4,23
	4	*Rv0010c*	Function unknown, probable conserved membrane protein.	3,39E-05	6,06E-04	3,48
	5	*esxO*	Function unknown, putative ESAT-6 like protein EsxO (ESAT-6 like protein 6).	2,57E-05	5,51E-04	3,42
	6	*Rv0988*	Function unknown, possible conserved exported protein.	1,12E-05	3,64E-04	3,87
	7	*Rv1435c*	Function unknown, probable conserved proline, glycine, valine-rich secreted protein.	6,55E-06	3,05E-04	3,43
	8	*drrC*	Probably involved in active transport of antibiotic and phthiocerol dimycocerosate (dim) across the membrane (export).	2,51E-05	5,47E-04	3,60
	9	*lppC*	Function unknown, probable lipoprotein LppC.	1,37E-06	1,89E-04	3,75
	10	*mmpL2*	Function unknown, hought to be involved in fatty acid transport.	7,71E-05	8,67E-04	3,22
	11	*Rv0011c*	Function unknown, probable conserved transmembrane protein.	4,60E-05	7,02E-04	3,03
	12	*lppL*	Function unknown, probable conserved lipoprotein LppL.	1,73E-04	1,36E-03	3,07
	13	*espE*	Function unknown, ESX-1 secretion-associated protein EspE.	5,25E-06	2,85E-04	4,55
	14	*pitA*	Involved in low-affinity inorganic phosphate transport across the membrane. Responsible for the translocation of the substrate across the membrane.	1,39E-05	3,88E-04	2,83
	15	*Rv1230c*	Function unknown, possible membrane protein.	4,38E-06	2,66E-04	2,95
	16	*Rv0426c*	Function unknown, possible transmembrane protein.	2,21E-06	2,57E-04	2,83
	17	*mmpS4*	Function unknown, probable conserved membrane protein MmpS4.	6,25E-06	3,03E-04	4,53
	18	*Rv1517*	Function unknown.	7,02E-06	3,06E-04	3,09
	19	*mmpL4*	Function unknown, thought to be involved in fatty acid transport.	5,36E-06	2,85E-04	3,65
	20	*lppT*	Function unknown, probable lipoprotein LppT	4,04E-04	2,30E-03	2,87
	21	*espK*	ESX-1 secretion-associated protein EspK.	4,55E-06	2,72E-04	3,16
	22	*Rv0188*	Function unknown, probable conserved transmembrane protein.	3,93E-05	6,36E-04	2,98
	23	*esxB*	Function unknown, exported protein cotranscribed with Rv3875|MT3989|MTV027.10.	2,84E-05	5,77E-04	3,68
	24	*Rv1371*	Function unknown, probable conserved membrane protein.	2,81E-06	2,59E-04	3,85
	25	*mmpL6*	Function unknown, thought to be involved in fatty acid transport.	1,35E-05	3,88E-04	3,24
	26	*Rv1672c*	Thought to be involved in transport across the membrane. Responsible for the translocation of undetermined substrate across the membrane.	3,56E-05	6,15E-04	-10,24
	27	*Rv1761c*	Function unknown, possible exported protein.	2,73E-04	1,81E-03	-9,01
	28	*esxR*	Secreted ESAT-6 like protein EsxR (TB10.3) (ESAT-6 like protein 9).	8,00E-03	2,00E-02	-7,65
	29	*ctpD*	Cation-transporting ATPase; possibly catalyzes the transport of a cation (possibly cadmium) with the hydrolyse of ATP.	2,11E-04	1,52E-03	-2,99
	30	*lprE*	Function unknown, probable lipoprotein LprE.	3,13E-04	1,95E-03	-2,87
	31	*Rv2687c*	Thought to be involved in active transport of unidentified antibiotic across the membrane (export): antibiotic	9,06E-05	9,51E-04	-2,87

			resistance by an export mechanism. Responsible for the translocation of the substrate across the membrane.			
	32	*Rv1217c*	Thought to be involved in active transport of tetronasin across the membrane (export): tetronasin resistance by an export mechanism. Responsible for the translocation of the substrate across the membrane.	3,58E-05	6,15E-04	-3,13
	33	*Rv1024*	Function unknown, possible conserved membrane protein.	1,69E-03	6,20E-03	-2,83
	34	*Rv2597*	Function unknown, probable membrane protein.	1,18E-05	3,69E-04	-2,79
	35	*Rv0528*	Function unknown, probable conserved transmembrane protein.	4,24E-05	6,66E-04	-2,98
	36	*Rv0073*	Thought to be involved in active transport of glutamine across the membrane (import). Responsible for the translocation of the substrate across the membrane. Probable glutamine-transport transmembrane protein ABC transporter.	8,97E-07	1,48E-04	-13,58
	37	*Rv0072*	Thought to be involved in active transport of glutamine across the membrane (import). Responsible for the translocation of the substrate across the membrane. Probable glutamine-transport transmembrane protein ABC transporter.	8,32E-07	1,48E-04	-13,80
	38	*Rv2306A*	Function unknown, possible conserved membrane protein.	1,60E-01	2,68E-02	-2,84
	39	*Rv2049c*	Function unknown, possible conserved membrane protein.	1,18E-02	2,86E-02	-3,04
	40	*Rv0666*	Function unknown, possible membrane protein.	4,81E-04	2,57E-03	-2,85
	41	*Rv3658c*	Function unknown, probable conserved transmembrane protein.	2,40E-02	8,04E-03	-3,02
	42	*kdpF*	Thought to be involved in stabilization of the KDP complex.	6,56E-03	1,71E-02	-3,38
	43	*esxF*	Putative ESAT-6 like protein EsxF (hypothetical alanine and glycine rich protein) (ESAT-6 like protein 13).	2,74E-03	8,80E-03	-8,38
	44	*Rv3888c*	Function unknown, probable conserved membrane protein.	1,11E-04	1,06E-03	2,71
	45	*eccA2*	ESX conserved component EccA2. ESX-2 type VII secretion system protein. Probable CbxX/CfqX family protein.	2,10E-05	4,90E-04	2,61
	46	*Rv1903*	Function unknown, probable conserved membrane protein.	4,23E-06	2,66E-04	2,61
	47	*Rv0364*	Function unknown, probable conserved membrane protein.	1,25E-05	3,72E-04	2,62
	48	*rpfA*	May be promote the resuscitation and growth of dormant, nongrowing cell. Possible resuscitation-promoting factor RpfA	1,21E-04	1,10E-03	2,56
	49	*esxD*	Possible ESAT-6 like protein EsxD.	1,08E-05	3,53E-04	2,71
	50	*Rv2209*	Function unknown, probable conserved integral membrane protein.	3,29E-05	5,98E-04	2,67
	51	*espF*	ESX-1 secretion-associated protein EspF.	1,04E-05	3,50E-04	2,74
	52	*Rv2169c*	Function unknown, probable conserved transmembrane protein.	3,58E-06	2,66E-04	2,68
	53	*mmpL13b*	Thought to be involved in fatty acid transport. Probable conserved transmembrane transport protein MmpL13b.	3,61E-06	2,66E-04	2,54
	54	*Rv2617c*	Function unknown, probable transmembrane protein.	8,17E-05	8,95E-04	2,53
	55	*Rv3454*	Function unknown, probable conserved integral membrane protein.	1,85E-04	1,43E-03	2,67
	56	*esxA*	Elicits high level of inf-gamma from memory effector cells during the first phase of a protective immune response. 6 kDa early secretory antigenic target EsxA (ESAT-6).	2,91E-04	1,87E-03	2,57
	57	*Rv3312A*	Function Unknown, secreted protein antigen.	2,88E-03	9,12E-03	-2,66
	58	*Rv2864c*	Function unknown, possibly involved in cell wall biosynthesis. Possible penicillin-binding lipoprotein.	6,32E-04	3,10E-03	-2,71

	59	*Rv2164c*	Function unknown, probable conserved proline rich membrane protein.	2,17E-05	4,93E-04	-2,60
	60	*murF*	Involved in cell wall formation; peptidoglycan biosynthesis.	1,62E-03	6,00E-03	-2,63
	61	*eccE3*	ESX conserved component EccE3. ESX-3 type VII secretion system protein.	6,73E-03	1,74E-02	-2,76
	62	*dacB2*	Involved in peptidoglycan synthesis (at final stages). Hydrolyzes the bound D-alanyl-D-alanine.	3,30E-03	1,01E-02	-2,66
	63	*Rv0476*	Function unknown, possible conserved transmembrane protein.	1,39E-06	1,89E-04	-2,61
	64	*cfp6*	Function unknown, low molecular weight protein antigen 6 (CFP-6).	1,23E-04	1,11E-03	-2,57
	65	*Rv0621*	Function unknown, possible membrane protein.	4,43E-04	2,43E-03	-2,70
	66	*lprM*	Thought to be involved in host cell invasion. Possible Mce-family lipoprotein LprM (Mce-family lipoprotein Mce3E).	9,87E-03	2,35E-02	-2,66
Lipid metabolism	**1**	*idsB*	Involved in biosynthesis of membrane ether-linked lipids.	1,89E-03	6,74E-03	3,53
	2	*pks6*	Polyketide synthase possibly involved in lipid synthesis.	1,64E-04	1,32E-03	4,20
	3	*umaA*	Involved in mycolic acid modification or synthesis.	5,28E-05	7,42E-04	3,63
	4	*mmaA1*	Involved in mycolic acids modification. Catalyzes unusual S-adenosyl-methionine-dependent transformation of a cis-olefin mycolic acid into a secondary alcohol.	7,25E-07	1,43E-04	4,12
	5	*tesA*	Probably involved in biosynthesis of phthiocerol dimycocerosate (PDIM).	8,80E-05	9,43E-04	3,66
	6	*fadA5*	Function unknown, but involved in lipid degradation.	1,10E-04	1,05E-03	3,20
	7	*fadD30*	Function unknown, but involved in lipid degradation.	2,10E-04	1,52E-03	3,18
	8	*mbtK*	Involved in the biogenesis of the hydroxyphenyloxazoline-containing siderophore mycobactins.	1,22E-03	4,89E-03	3,88
	9	*papA2*	Involved in sulfolipid-1 (SL-1) biosynthesis.	6,74E-05	8,28E-04	2,89
	10	*fadD26*	Involved in phthiocerol dimycocerosate (dim) biosynthesis, possibly by activating substrates for the PPS polyketides synthase.	8,52E-06	3,33E-04	3,48
	11	*fadA*	Function unknown, but involvement in lipid degradation.	1,10E-06	1,67E-04	3,15
	12	*mbtI*	Involved in the biogenesis of the hydroxyphenyloxazoline-containing siderophore mycobactins. Possibly plays a role in the conversion of chorismate to salicilate (the starter unit for mycobactin siderophore construction).	1,23E-02	2,79E-02	3,32
	13	*pks9*	Potentially involved in some intermediate steps for the synthesis of a polyketide molecule, which may be involved in secondary metabolism.	7,56E-06	3,11E-04	3,11
	14	*Rv2261c*	Function unknown; thought to be involved in lipid metabolism.	2,00E-03	7,01E-03	-2,83
	15	*Rv1760*	May be involved in synthesis of triacylglycerol.	1,25E-05	3,72E-04	-12,06
	16	*acpM*	Involved in fatty acid biosynthesis (mycolic acids synthesis); involved in meromycolate extension.	3,88E-03	1,15E-02	2,62
	17	*Rv2262c*	Function unknown; thought to be involved in lipid metabolism.	1,82E-02	3,77E-02	-2,63
Regulatory Proteins	**1**	*lrpA*	Involved in transcriptional mechanism.	4,77E-05	7,10E-04	3,30
	2	*Rv0078*	Possibly involved in transcriptional mechanism.	1,03E-05	3,50E-04	2,92
	3	*Rv2506*	Involved in transcriptional mechanism.	1,66E-05	4,28E-04	3,41
	4	*whiB1*	Involved in transcriptional mechanism. Transcriptional regulatory protein WhiB-like WhiB1.	2,75E-05	5,69E-04	3,24
	5	*whiB6*	Involved in transcriptional mechanism. Possible transcriptional regulatory protein WhiB-like WhiB6.	1,30E-08	9,82E-06	7,90
	6	*Rv3583c*	Involved in transcriptional mechanism.	6,82E-04	3,24E-03	2,81
	7	*Rv3143*	Function unknown, but could be involved in regulatory mechanism.	1,09E-07	3,31E-05	3,55
	8	*Rv2160A*	Conserved hypothetical protein.	4,62E-03	1,31E-02	-3,80

	9	*Rv2017*	Thought to be involved in transcriptional mechanism.	1,51E-08	9,82E-06	-6,52
	10	*Rv2912c*	Thought to be involved in transcriptional mechanism. Probable transcriptional regulatory protein (probably TetR-family).	9,04E-05	9,51E-04	-3,23
	11	*Rv3066*	Involved in transcriptional mechanism. Probable transcriptional regulatory protein (probably DeoR-family).	1,59E-04	1,29E-03	-2,93
	12	*furA*	Acts as a global negative controlling element, employing FE(2+) as a cofactor to bind the operator of the repressed genes. Seems to regulate transcription of KATG|Rv1908c gene.	7,50E-06	3,11E-04	2,55
	13	*Rv0081*	Involved in transcriptional mechanism. Probable transcriptional regulatory protein.	9,34E-05	9,67E-04	2,67
	14	*devR*	Regulator part of the two component regulatory system DEVR/DEVS/dost. Controls HSPX|Rv2031|ACR expression.	2,34E-04	1,63E-03	2,64
	15	*Rv2989*	Involved in transcriptional mechanism, probable transcriptional regulatory protein.	6,24E-05	7,94E-04	-2,80
	16	*prrA*	Transcriptional regulator part of the two component regulatory system PRRA/PRRB. Thought to be involved in the environmental adaptation, specifically in an early phase of the intracellular growth.	5,49E-05	7,54E-04	-2,55
Intermediary metabolism and respiration	**1**	*Rv3378c*	Produces isotuberculosinol (nosyberkol) from halimadienyl diphosphate.	5,15E-05	7,34E-04	5,51
	2	*udgA*	Possibly involved in polysaccharide biosynthesis.	4,40E-05	6,81E-04	4,15
	3	*Rv2959c*	Thought to cause methylation.	1,48E-05	4,04E-04	4,49
	4	*Rv3377c*	Produces halimadienyl diphosphate (tuberculosinyl diphosphate) from geranylgeranyl diphosphate (GGPP).	6,41E-05	8,05E-04	4,14
	5	*Rv2949c*	Catalyzes the conversion of chorismate to 4-hydroxybenzoate.	8,79E-06	3,37E-04	4,20
	6	*Rv1500*	Function unknown, probable glycosyltransferase.	3,19E-05	5,98E-04	3,77
	7	*moaD1*	Involved in molybdenum cofactor biosynthesis.	3,00E-04	1,91E-03	3,49
	8	*atpF*	This is one of the three chains of the nonenzymatic component (cf(0) subunit) of the ATPase complex.	7,91E-06	3,15E-04	5,76
	9	*kshB*	Predicted to be involved in lipid catabolism, reductase component of 3-ketosteroid-9-alpha-hydroxylase KshB.	3,75E-06	2,66E-04	3,72
	10	*metK*	Involved in the activated methyl cycle. Catalyzes the formation of S-adenosylmethionine from methionine and ATP.	6,26E-06	3,03E-04	3,47
	11	*moaA1*	Involved in molybdenum cofactor biosynthesis; involved in the biosynthesis of molybdopterin precursor Z from guanosine.	3,74E-05	6,31E-04	3,11
	12	*Rv1714*	Function unknown; probably involved in cellular metabolism	8,12E-05	8,92E-04	2,99
	13	*ctaC*	Involved in aerobic respiration. Subunit I and II form the functional core of the enzyme complex.	3,22E-05	5,98E-04	3,05
	14	*Rv0691A*	Electron carrier, mycofactocin precursor protein.	1,13E-05	3,64E-04	3,02
	15	*sdhD*	Involved in tricarboxylic acid cycle. Putative hydrophobic component of the succinate dehydrogenase complex.	1,24E-04	1,11E-03	2,96
	16	*Rv0306*	Function unknown; probably involved in cellular metabolism.	1,15E-05	3,66E-04	2,84
	17	*moeW*	Involved in molybdoptenum cofactor biosynthesis; thought to be involved in the biosynthesis of a demolybdo-cofactor (molybdopterin), necessary for molybdo-enzymes.	7,97E-05	8,83E-04	2,87
	18	*glbN*	Oxygen transport, product Hemoglobin GlbN	7,70E-03	1,94E-02	4,13
	19	*Rv0111*	Function unknown; probably involved in cellular metabolism.	2,46E-04	1,67E-03	2,81
	20	*Rv3829c*	Function unknown; probably involved in cellular metabolism.	2,77E-09	5,56E-06	6,79
	21	*ptrBb*	Cleaves peptide bonds on the C-terminal side of lysyl and argininyl residues.	1,74E-08	9,82E-06	5,16
	22	*Rv2277c*	Function unknown; possible glycerolphosphodiesterase.	5,64E-08	2,07E-05	3,96
	23	*plcD*	Hydrolyzes sphingomyelin in addition to phosphatidylcholine. Probable virulence factor implicated in the pathogenesis of M.tuberculosis at the level of intracellular survival, by the alteration of cell signaling events or by direct cytotoxicity.	1,32E-03	5,13E-03	-9,09
	24	*Rv2913c*	Hydrolyzes specific D-amino acid.	1,38E-04	1,19E-03	-2,94

	25	*ispF*	Involved in the deoxyxylulose-5-phosphate pathway (DXP) of isoprenoid biosynthesis (at the fifth step). Converts 4-diphosphocytidyl-2C-methyl-D-erythritol 2-phosphate into 2C-methyl-D-erythritol 2,4-cyclodiphosphate and CMP.	1,99E-05	4,77E-04	-3,83
	26	*oxcA*	Involved in catabolism of oxalic acid [catalytic activity: oxalyl-CoA = formyl-CoA + CO2].	4,16E-04	2,33E-03	-2,87
	27	*Rv1257c*	Function unknown; probably involved in cellular metabolism.	5,64E-04	2,84E-03	-3,08
	28	*Rv0763c*	Ferredoxins are iron-sulfur proteins that transfer electrons in a wide variety of metabolic reactions. Probably involved in electron transport for cytochrome P-450 system.	2,47E-02	4,87E-02	-2,99
	29	*Rv1104*	In combination with MTV017.58|Rv1105 catalyzes hydrolysis of several beta-lactam antibiotic PNB esters to the corresponding free acid and PNB alcohol.	1,92E-04	1,45E-03	-2,91
	30	*che1*	Possibly involved in inserting FE2+ into sirohydrochlorin to produce siroheme, required for SIRA (Rv2391) function	1,14E-03	4,67E-03	-2,95
	31	*hycQ*	Possibly involved in hydrogen metabolism.	1,94E-04	1,45E-03	-2,99
	32	*Rv3712*	Function unknown; probably involved in cellular metabolism.	1,26E-03	5,02E-03	-3,18
	33	*Rv2074*	May be involved in biosynthesis of pyridoxine (vitamin B6) and pyridoxal phosphate.	5,07E-06	2,85E-04	-3,04
	34	*Rv2766c*	Function unknown, possibly involved in cellular metabolism.	1,46E-04	1,23E-03	-3,01
	35	*Rv0765c*	Function unknown; probably involved in cellular metabolism, possibly electron transfer.	7,11E-06	3,06E-04	-3,44
	36	*frdD*	Involved in interconversion of fumarate and succinate (anaerobic respiration). This hydrophobic component may be required to anchor the catalytic components of the fumarate reductase complex to the cytoplasmic membrane.	2,85E-02	5,45E-02	-3,18
	37	*Rv0097*	Function unknown; probably involved in cellular metabolism.	2,37E-04	1,64E-03	2,56
	38	*cyp130*	Cytochromes P450 are a group of heme-thiolate monooxygenases. They oxidize a variety of structurally unrelated compounds, including steroids, fatty acids, and xenobiotics.	3,75E-04	2,18E-03	2,52
	39	*bioF2*	Could be involved in biotin biosynthesis (at the first step).	2,83E-05	5,77E-04	2,57
	40	*ppk2*	Catalyzes the reversible transfer of phosphate from polyphosphate (polyp) to form GTP.	3,80E-04	2,20E-03	2,51
	41	*gca*	Possibly involved in synthesis of a-band common antigen lipopolysaccharide. First of the three steps in the biosynthesis of GDP-fucose from GDP-mannose.	7,74E-06	3,12E-04	2,73
	42	*sahH*	Thioester hydrolase which acting on ether bounds. Could be involved in methionine and selenoamino acid metabolisms. Also involved in activated methyl.	4,16E-04	2,33E-03	2,51
	43	*Rv0805*	Hydrolyzes cyclic nucleotide monophosphate to nucleotide monophosphate. Shown to hydrolyze 2',3'-cNMP and 3',5'-cNMP.	4,44E-04	2,43E-03	2,52
	44	*moaX*	Thought to be involved in molybdenum cofactor biosynthesis. Probable MoaD-MoaE fusion protein MoaX.	5,14E-05	7,34E-04	2,61
	45	*frdC*	Involved in interconversion of fumarate and succinate (anaerobic respiration). This hydrophobic component may be required to anchor the catalytic components of the fumarate reductase complex to the cytoplasmic membrane.	4,97E-04	2,62E-03	2,58
	46	*fdxA*	Involved in electron transfer. Ferredoxin FdxA.	2,46E-03	8,15E-03	2,62
	47	*Rv2263*	Oxidoreduction, possible oxidoreductase.	5,42E-04	2,77E-03	-2,63
	48	*trpD*	Tryptophan biosynthesis. Probable anthranilate phosphoribosyltransferase TrpD.	1,57E-03	5,89E-03	-2,65
	49	*pyrE*	Involved in pyrimidine biosynthesis (at the fifth step).	4,87E-06	2,78E-04	-2,62
	50	*suhB*	Involved in inositol phosphate metabolism. It is responsible for the provision of inositol required for synthesis of phosphatidylinositol and polyphosphoinositides. Key enzyme of the phosphatidyl inositol signaling pathway.	9,99E-04	4,25E-03	-2,70
	51	*Rv2739c*	Function unknown; probably involved in cellular metabolism.	8,96E-03	2,17E-02	-2,53
	52	*folB*	Involved in folate biosynthesis. Catalyzes the conversion of 7,8-dihydroneopterin to 6- hydroxymethyl-7,8-dihydropterin.	1,48E-04	1,24E-03	-2,74
	53	*Rv2966c*	Thought to cause methylation. Possible methyltransferase (methylase).	5,14E-03	1,42E-02	-2,55
	54	*ppdK*	Catalyzes the reversible phosphorylation of pyruvate and phosphate. Probable pyruvate, phosphate dikinase PpdK.	1,40E-05	3,88E-04	-2,54

	55	*Rv0375c*	Function unknown; probably involved in cellular metabolism. Probable carbon monoxyde dehydrogenase (medium chain).	5,37E-03	1,46E-02	-2,74
	56	*Rv0097*	Function unknown; probably involved in cellular metabolism.	2,37E-04	1,64E-03	2,56
Conserved hypotheticals	**1**	*Rv3415c*	Function unknown.	1,00E-03	4,25E-03	4,19
	2	*Rv2425c*	Function unknown.	1,56E-04	1,28E-03	4,66
	3	*Rv3528c*	Function unknown.	5,34E-06	2,85E-04	4,87
	4	*Rv2492*	Function unknown.	1,81E-05	4,48E-04	4,60
	5	*Rv1501*	Function unknown.	3,14E-05	5,98E-04	4,26
	6	*Rv3282*	Function unknown.	2,05E-04	1,50E-03	3,89
	7	*Rv1507A*	Function unknown.	3,72E-05	6,30E-04	4,36
	8	*Rv1765c*	Function unknown.	2,95E-04	1,89E-03	-5,31
	9	*Rv3902c*	Function unknown.	1,02E-04	1,01E-03	4,15
	10	*Rv1291c*	Function unknown.	3,82E-05	6,36E-04	3,87
	11	*Rv2023A*	Function unknown.	3,95E-06	2,66E-04	6,07
	12	*Rv3192*	Function unknown.	7,26E-06	3,06E-04	3,57
	14	*Rv1507c*	Function unknown.	1,14E-04	1,06E-03	3,84
	15	*Rv3766*	Function unknown.	2,41E-06	2,57E-04	4,20
	16	*Rv2808*	Function unknown.	6,29E-06	3,03E-04	4,09
	17	*Rv2660c*	Function unknown.	3,23E-06	2,66E-04	4,18
	18	*Rv3351c*	Function unknown.	1,05E-05	3,50E-04	3,82
	19	*Rv1948c*	Function unknown.	7,55E-05	8,66E-04	3,73
	20	*Rv1374c*	Function unknown.	1,69E-04	1,35E-03	2,90
	21	*Rv3766*	Function unknown.	2,48E-05	5,44E-04	3,12
	22	*Rv1268c*	Function unknown.	4,60E-08	2,01E-05	5,33
	23	*Rv2960c*	Function unknown.	3,25E-06	2,66E-04	3,51
	24	*Rv2432c*	Function unknown.	1,56E-04	1,28E-03	4,74
	25	*Rv2956*	Function unknown.	2,75E-06	2,59E-04	4,24
	26	*Rv1461*	Function unknown.	7,71E-06	3,12E-04	4,40
	27	*Rv2901c*	Function unknown.	1,01E-04	1,01E-03	3,01
	28	*octT*	Function unknown.	4,00E-06	2,66E-04	3,25
	29	*Rv2067c*	Function unknown.	1,59E-05	4,15E-04	3,05
	30	*Rv1794*	Function unknown.	5,91E-05	7,75E-04	2,84
	31	*Rv3424c*	Function unknown.	5,52E-05	7,56E-04	3,90
	32	*Rv2182c*	Transfer of fatty acyl groups.	7,26E-06	3,06E-04	2,95
	33	*Rv1509*	Function unknown.	8,19E-07	1,48E-04	3,73
	34	*Rv2629*	Function unknown.	5,60E-04	2,83E-03	3,42
	35	*Rv1508A*	Function unknown.	1,57E-06	2,00E-04	3,40
	36	*Rv3126c*	Function unknown.	6,95E-04	3,28E-03	2,90
	37	*Rv0826*	Function unknown.	2,97E-08	1,46E-05	5,50
	38	*Rv0569*	Function unknown.	3,83E-03	1,13E-02	3,06
	39	*Rv1813c*	Function unknown.	9,38E-04	4,07E-03	3,22
	40	*Rv2819c*	Function unknown.	1,50E-07	4,24E-05	-8,70

	41	*Rv2818c*	Function unknown.	1,86E-06	2,30E-04	-7,00
	42	*Rv2817c*	Function unknown.	2,00E-03	6,99E-03	-2,84
	43	*Rv2159c*	Function unknown.	1,19E-04	1,09E-03	-4,56
	44	*Rv1762c*	Function unknown.	2,19E-05	4,93E-04	-10,97
	45	*Rv2816c*	Function unknown.	2,94E-05	5,81E-04	-11,00
	46	*Rv1673c*	Function unknown.	1,12E-04	1,06E-03	-10,11
	47	*Rv3612c*	Function unknown.	7,40E-05	8,53E-04	-3,02
	48	*Rv2762c*	Function unknown.	7,59E-03	1,92E-02	-2,85
	49	*Rv3659c*	Function unknown.	2,13E-03	7,35E-03	-3,51
	50	*Rv0185*	Function unknown; probably involved in a cellular metabolism.	7,28E-06	3,06E-04	-3,09
	51	*Rv3678c*	Function unknown.	5,38E-05	1,45E-03	-3,13
	52	*Rv2288*	Function unknown.	4,24E-04	2,36E-03	-2,93
	53	*Rv3672c*	Function unknown.	5,71E-05	7,65E-04	-3,13
	54	*Rv3753c*	Function unknown.	2,64E-04	1,77E-03	-3,08
	55	*Rv0790c*	Function unknown.	5,04E-03	1,40E-02	-3,11
	56	*Rv3899c*	Function unknown.	4,97E-05	7,25E-04	-3,73
	57	*Rv1443c*	Function unknown.	1,24E-04	1,11E-03	-3,36
	58	*Rv0459*	Function unknown.	2,43E-03	8,04E-03	-3,02
	59	*Rv1888A*	Function unknown.	2,06E-02	4,19E-02	-3,85
	60	*Rv1505c*	Function Unknown.	3,49E-03	1,06E-02	2,79
	61	*Rv1954c*	Function Unknown.	9,01E-04	3,96E-03	2,75
	62	*Rv0057*	Function Unknown.	3,51E-04	2,10E-03	2,54
	63	*Rv2734*	Function Unknown.	3,79E-04	2,20E-03	2,58
	64	*Rv1535*	Function Unknown.	5,49E-04	2,80E-03	2,74
	65	*Rv1950c*	Function Unknown.	5,84E-05	7,71E-04	2,71
	66	*Rv3179*	Function Unknown.	4,29E-05	6,70E-04	2,51
	67	*Rv2468A*	Function Unknown.	2,42E-04	1,66E-03	2,52
	68	*Rv2309A*	Function Unknown.	1,17E-04	1,08E-03	2,54
	69	*Rv2548A*	Function Unknown.	1,32E-06	1,89E-04	2,66
	70	*Rv2267c*	Function Unknown.	3,32E-05	5,98E-04	3,16
	71	*Rv2307B*	Function Unknown.	8,82E-05	9,43E-04	2,79
	72	*Rv0909*	Function Unknown.	3,59E-05	6,15E-04	2,79
	73	*Rv2190c*	Function Unknown.	4,51E-04	2,46E-03	2,56
	74	*Rv2179c*	Function Unknown.	1,30E-05	3,81E-04	2,51
	75	*Rv2722*	Function Unknown.	7,19E-05	8,45E-04	2,52
	76	*Rv0047c*	Function Unknown.	4,71E-04	2,53E-03	2,68
	77	*Rv1804c*	Function Unknown.	2,24E-04	1,57E-03	2,72
	78	*Rv1754c*	Function Unknown.	1,20E-05	3,69E-04	2,85
	79	*Rv0756c*	Function Unknown.	3,00E-05	5,81E-04	-2,70
	80	*Rv1251c*	Function Unknown.	1,56E-03	5,85E-03	-2,55
	81	*Rv1186c*	Function Unknown.	1,91E-04	1,45E-03	-2,55
	82	*Rv2681*	Function Unknown.	8,08E-04	3,65E-03	-2,66

	83	*Rv0607*	Function Unknown.	1,68E-03	6,17E-03	-2,59
	84	*Rv2680*	Function Unknown.	1,19E-05	3,69E-04	-2,67
	85	*Rv3856c*	Function Unknown.	1,70E-04	1,35E-03	-2,76
	86	*Rv1025*	Function Unknown.	2,27E-03	7,72E-03	-2,78
	87	*Rv1590*	Function Unknown.	1,66E-02	3,51E-02	-2,78
	89	*Rv2255c*	Function Unknown.	2,88E-06	2,59E-04	-2,63
	90	*Rv2532c*	Function Unknown.	8,51E-05	9,19E-04	-2,70
	91	*Rv2898c*	Function Unknown.	3,76E-03	1,12E-02	-2,61
	92	*Rv2102*	Function Unknown.	1,39E-05	3,88E-04	-2,55
	93	*Rv0500A*	Function Unknown.	9,38E-07	1,48E-04	-2,52
	94	*Rv3031*	Function Unknown.	2,37E-03	7,95E-03	-2,55
	95	*Rv2133c*	Function Unknown.	4,28E-06	2,66E-04	-2,70
Virulence, detoxification, adaptation	**1**	*mazE1*	Function unknown, possible antitoxin MazE1.	3,54E-05	6,15E-04	3,91
	2	*mazE6*	Function unknown, possible antitoxin MazE6.	9,89E-06	3,50E-04	3,30
	3	*vapB2*	Function unknown, possible antitoxin VapB2.	9,14E-06	3,39E-04	3,07
	4	*parE2*	Function unknown, possible toxin ParE2.	2,91E-04	1,87E-03	3,12
	5	*VapB17*	Function unknown, possible antitoxin VapB17.	1,03E-05	3,50E-04	3,82
	6	*Rv0590A*	Function unknown, but could be involved in host cell invasion.	9,30E-06	3,40E-04	3,51
	7	*mymT*	Coordinates Cu(I) ions into a Cu(I)-thiolate core, protects cell from copper toxicity.	1,27E-03	5,02E-03	3,06
	8	*Rv1996*	Function unknown, universal stress protein family protein.	5,32E-03	1,45E-02	3,10
	9	*Rv2005c*	Function unknown, universal stress protein family protein.	1,27E-03	5,03E-03	2,80
	10	*mce2D*	Function unknown, but thought to be involved in host cell invasion. Mce-family protein Mce2D.	5,77E-08	2,07E-05	3,72
	11	*vapC17*	Function unknown, possible toxin VapC17.	7,07E-06	3,06E-04	3,46
	12	*bpoA*	Supposedly involved in detoxification reactions. Possible peroxidase BpoA.	2,44E-04	1,67E-03	2,89
	13	*vapC47*	Function unknown, possible toxin VapC47. Contains PIN domain.	4,73E-07	1,04E-04	-5,46
	14	*vapB5*	Function unknown, possible ribonuclease.	1,96E-02	4,01E-02	-3,09
	15	*vapC31*	Function unknown, possible toxin VapC31.	4,02E-06	2,66E-04	-2,94
	16	*vapB4*	Function unknown, possible antitoxin VapB4.	3,98E-04	2,28E-03	-3,44
	17	*mazF7*	Function unknown, possible toxin MazF7.	1,86E-03	6,62E-03	-3,80
	18	*oxyR'*	Function unknown, transcriptional regulator OxyR', pseudogene.	3,91E-05	6,36E-04	2,62
	19	*cspA*	Possibly involved in cold acclimation processes (the production of the protein is supposedly predominantly induced at low temperatures).	2,14E-05	4,93E-04	2,63
	20	*vapC1*	Possible toxin VapC1.	2,98E-03	9,34E-03	2,57
	21	*vapB32*	Possible antitoxin VapB32.	4,01E-05	6,43E-04	2,54
	22	*Rv1478*	Function unknown, but supposedly involved in virulence.	2,68E-05	5,60E-04	-2,51
	23	*vapB14*	Possible antitoxin VapB14.	1,08E-04	1,04E-03	-2,65
	24	*aac*	Confers resistance to aminoglycosides (gentamicin, tobramycin, dibekacin, netilmicin, and 6'-N-ethylnetilmicin).	1,91E-04	1,45E-03	-2,76
Insertion seqs and phages	**1**	*Rv2646*	Sequence integration. Integrase is necessary for integration of a phage into the host genome by site-specific recombination. In conjunction with excisionase, integrase is also necessary for excision of the prophage from the host genome.	8,31E-06	3,28E-04	3,59
	2	*Rv2106*	Required for the transposition of the insertion element IS6110.	5,34E-05	7,46E-04	6,24
	3	*Rv0829*	Required for the transposition of the insertion element IS1605'.	1,39E-04	1,19E-03	4,15

	4	*Rv3185*	Involved in the transposition in the insertion sequence IS6110.	2,58E-06	2,59E-04	9,11
	5	*Rv3770A*	Possibly required for the transposition of an insertion element.	4,28E-06	2,66E-04	3,36
	6	*Rv0795*	Required for the transposition of the insertion element IS6110.	2,62E-04	1,76E-03	3,60
	7	*Rv3474*	Involved in the transposition of the insertion sequence IS6110.	1,50E-05	4,04E-04	5,80
	8	*Rv0850*	Required for the transposition of an insertion element.	2,72E-04	1,80E-03	3,72
	9	*Rv0797*	Required for the transposition of the insertion element IS1547.	2,82E-09	5,56E-06	7,87
	10	*Rv1370c*	Possibly required for the transposition of the insertion element IS6110.	9,08E-07	1,48E-04	7,05
	11	*Rv2659c*	Sequence integration. Integrase is necessary for integration of a phage into the host genome by site-specific recombination. In conjunction with excisionase, integrase is also necessary for excision of the prophage from the host genome.	2,87E-04	1,86E-03	-3,55
	12	*Rv2168c*	Required for the transposition of the insertion element IS6110.	1,60E-03	5,95E-03	-3,26
	13	*Rv1585c*	Possible phage PhiRv1 protein.	3,42E-05	6,07E-04	-11,35
	14	*Rv1577c*	Probable PhiRv1 phage protein.	6,09E-05	7,89E-04	-12,35
	15	*Rv1586c*	Integration of phiRv1 into chromosome.	9,02E-05	9,51E-04	-12,44
	16	*Rv1584c*	Possible PhiRv1 phage protein.	3,05E-04	1,93E-03	-11,36
	17	*Rv1579c*	Possible PhiRv1 phage protein.	5,06E-04	2,65E-03	-9,96
	18	*Rv1582c*	Possible PhiRv1 phage protein.	6,46E-04	3,14E-03	-11,79
	19	*Rv1573*	Possible PhiRv1 phage protein.	7,49E-04	3,46E-03	-8,99
	20	*Rv1578c*	Possible PhiRv1 phage protein.	8,44E-04	3,78E-03	-8,56
	21	*Rv1574*	Possible PhiRv1 phage protein.	9,45E-04	4,09E-03	-8,99
	22	*Rv1580c*	Possible PhiRv1 phage protein.	3,35E-03	1,03E-02	-8,94
	23	*Rv1575*	Possible PhiRv1 phage protein.	1,07E-02	2,49E-02	-7,40
	24	*Rv2658c*	Possible prophage protein.	7,71E-05	8,67E-04	-3,51
	25	*Rv3381c*	Involved in the transposition of the insertion sequence IS6110.	4,26E-03	1,23E-02	-7,97
	26	*Rv1576c*	Probable PhiRv1 phage protein.	2,60E-05	5,51E-04	-13,16
	27	*Rv2085*	Conserved hypothetical protein.	8,96E-05	9,50E-04	-4,17
	28	*Rv2424c*	Required for the transposition of the insertion element IS1558.	1,99E-03	6,96E-03	-4,04
	29	*Rv1036c*	Possibly required for the transposition of the insertion element IS1560.	5,35E-04	2,75E-03	2,57
	30	*Rv1765A*	Possibly required for the transposition of an insertion element.	2,94E-05	5,81E-04	2,68
	31	*Rv1313c*	Possibly required for the transposition of the insertion element IS1557.	1,66E-03	6,15E-03	2,67
	32	*Rv3191c*	Involved in the transposition of an insertion sequence.	7,76E-04	3,55E-03	2,60
PE/PPE	**1**	*ppe58*	Function unknown.	3,37E-04	2,05E-03	4,95
	2	*ppe46*	Function unknown.	5,65E-05	7,65E-04	4,35
	3	*ppe57*	Function unknown.	3,17E-04	1,97E-03	4,89
	4	*ppe47*	Function unknown.	4,63E-05	7,03E-04	4,87
	5	*ppe3*	Function unknown.	4,29E-05	6,70E-04	4,18
	6	*ppe66*	Function unknown.	3,62E-04	2,15E-03	3,20
	7	*PE_PGRS19*	Function unknown.	8,70E-04	3,86E-03	4,02
	8	*ppe12*	Function unknown.	3,91E-05	6,36E-04	3,43
	9	*ppe4*	Function unknown.	1,40E-04	1,19E-03	3,16
	10	*pe35*	Function unknown.	2,32E-04	1,63E-03	3,74
	11	*pe27*	Function unknown.	3,93E-05	6,36E-04	3,71

	12	*ppe11*	Function unknown.	3,83E-06	2,66E-04	4,14
	13	*ppe39*	Function unknown.	7,23E-07	1,43E-04	10,05
	14	*pe22*	Function unknown.	6,57E-09	8,64E-06	8,75
	15	*ppe36*	Function unknown.	1,70E-08	9,82E-06	7,37
	16	*ppe22*	Function unknown.	4,55E-07	1,04E-04	3,35
	17	*PE_PGRS25*	Function unknown.	1,89E-03	6,73E-03	3,05
	18	*pe19*	Function unknown.	2,39E-06	2,57E-04	3,15
	19	*ppe7*	Function unknown.	3,83E-05	6,36E-04	3,06
	20	*ppe5*	Function unknown.	7,19E-05	8,45E-04	2,94
	21	*wag22*	Function unknown.	4,86E-03	1,37E-02	-3,16
	22	*pe21*	Function unknown.	5,28E-04	2,72E-03	-3,80
	23	*Rv0201c*	Function unknown.	1,02E-04	1,01E-03	-3,13
	24	*Rv3748*	Function unknown.	7,14E-05	8,45E-04	-3,48
	25	*ppe33*	Function Unknown.	8,21E-04	3,70E-03	2,71
	26	*ppe24*	Function Unknown.	9,10E-05	9,52E-04	2,64
	27	*ppe34*	Function Unknown.	1,02E-05	3,50E-04	3,20
	28	*pe23*	Function Unknown.	2,95E-05	5,81E-04	2,53
Information Pathways	**1**	*recF*	The RECF protein is involved in DNA metabolism and recombination; it is required for DNA replication and normal sos inducibility.	4,90E-05	7,19E-04	3,11
	2	*Rv3644c*	DNA polymerase is a complex, multichain enzyme responsible for most of the replicative synthesis in bacteria.	4,38E-06	2,66E-04	5,02
	3	*lysS*	Involved in translation.	1,08E-04	1,04E-03	3,16
	4	*rhlE*	Has a helix-destabilizing activity, probable ATP-dependent RNA helicase RhlE.	2,10E-04	1,52E-03	3,35
	5	*rpsQ*	Protein S17 binds specifically to the 5' end of 16S ribosomal RNA.	2,50E-04	1,70E-03	2,83
	6	*Rv0071*	Function unknown, possible maturase.	1,73E-04	1,36E-03	-4,81
	7	*rimI*	Acetylates the N-terminal alanine of ribosomal protein S18.	2,70E-05	5,60E-04	-3,95
	8	*ruvB*	forms a complex with RUVA. RUVB could possess weak ATPase activity, which will be stimulated by the RUVA protein in the presence of DNA.	1,62E-03	6,00E-03	-3,24
	9	*gatC*	Component of the translational apparatus. Furnishes a means for formation of correctly charged GLN-tRNA(GLN) through the transamidation of misacylated GLU- tRNA(GLN) in organisms which lack glutaminyl-tRNA synthetase.	1,37E-02	3,05E-02	-3,09
	10	*sigM*	The sigma factor is an initiation factor that promotes attachment of the RNA polymerase to specific initiation sites and then is released.	7,21E-03	1,84E-02	-3,02
	11	*rpmA*	Involved in translation mechanisms. 50S ribosomal protein L27 RpmA.	1,05E-04	1,03E-03	-3,38
	12	*nrdF2*	Involved in the DNA replication pathway. Catalyzes the biosynthesis of deoxyribonucleotides from the corresponding ribonucleotides, precursors that are necessary for DNA synthesis.	1,63E-04	1,63E-04	2,74
	13	*priA*	Recognizes a specific hairpin sequence on PHIX SSDNA; this structure is then recognized and bound by proteins PRIB and PRIC.	2,38E-06	2,57E-04	2,60
	14	*nrdF1*	Involved in the DNA replication pathway. Catalyzes the biosynthesis of deoxyribonucleotides from the corresponding ribonucleotides, precursors that are necessary for DNA synthesis.	3,69E-05	6,28E-04	2,64
	15	*rplW*	Binds to a specific region on the 23S rRNA. 50S ribosomal protein L23 RplW.	2,60E-06	2,59E-04	2,72
	16	*recD*	Involved in homologous recombination. Probable exonuclease V (alpha chain) RecD.	2,38E-03	7,96E-03	-2,53

* Gene name, function and category indicated by TubercuList, v 2.6.
# p-value, q-value/FDR and log fold change obtained from Star Bioinformatics software and edger

(i)

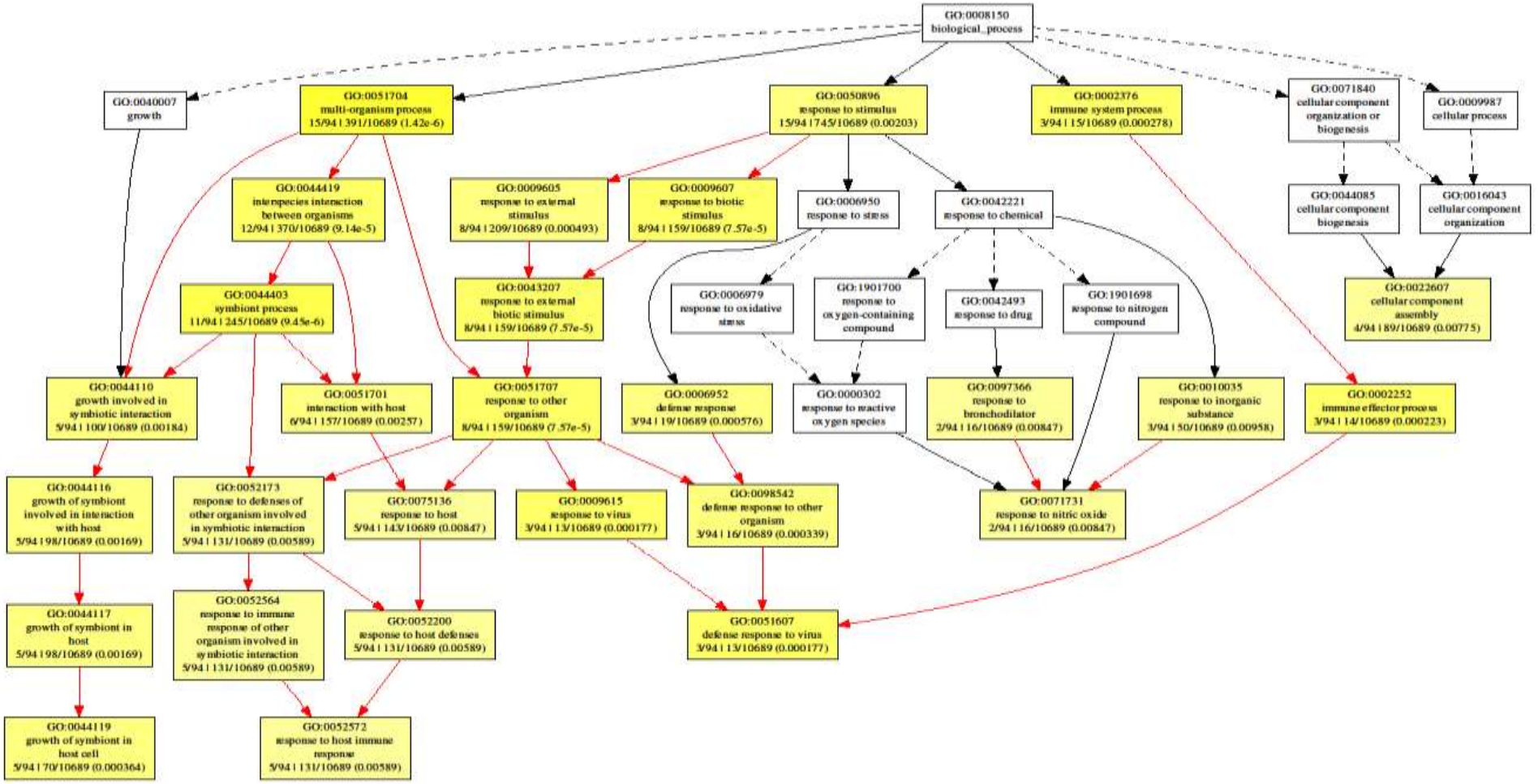

(ii)

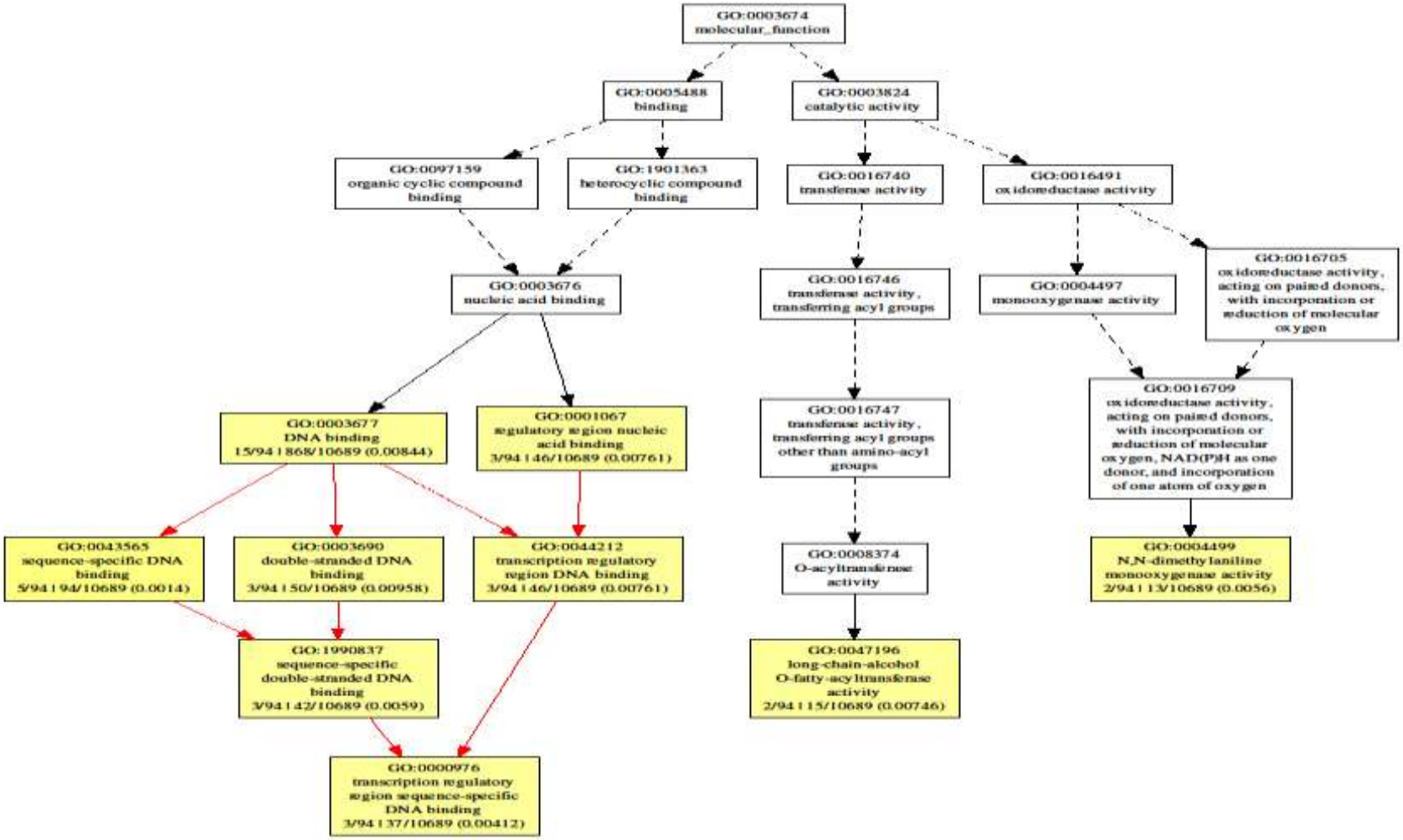

(iii)

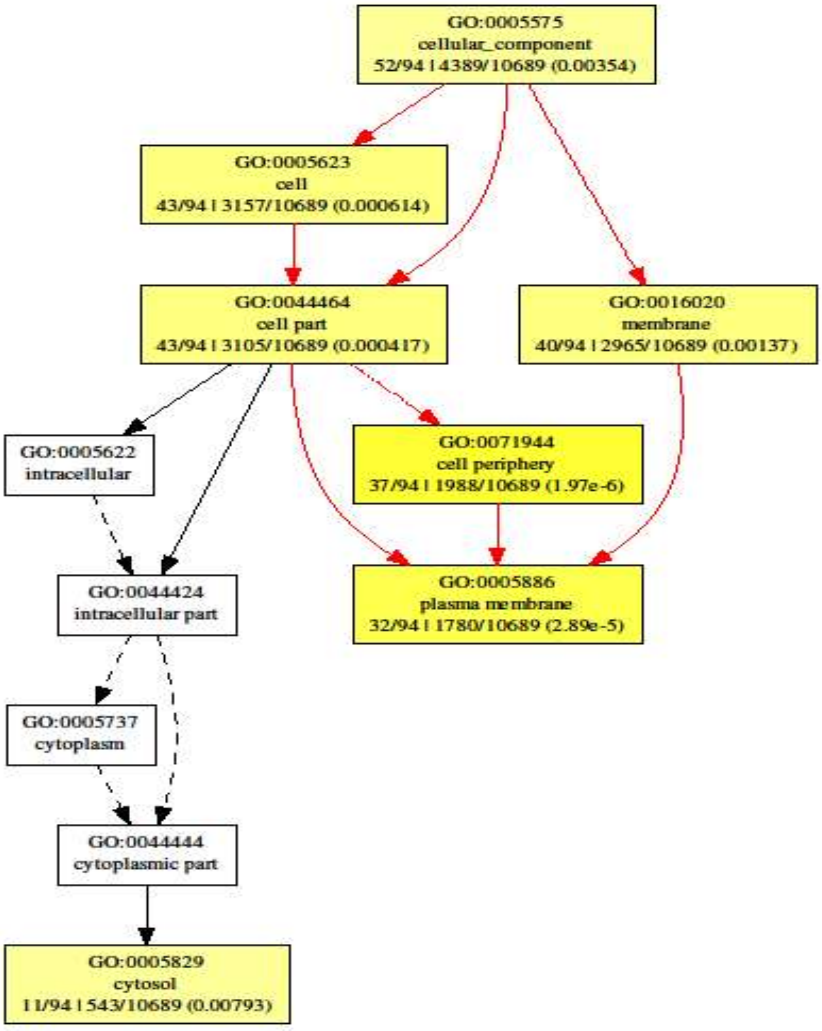

Figure 3.8 (i-iii) A graphical output of enriched GO terms for the differentially expressed genes from comparison Group A in different GO categories (i) biological process, (ii) molecular function and (iii) cellular component category. Significantly enriched GO terms are illustrated by the yellow boxes, whereas the white boxes represent non-significant GO terms. The red arrows represent an association between the significantly enriched terms and the black arrows represent an association between enriched and unenriched GO terms. The dashed black arrows illustrate the relationship between two unenriched GO terms.

Table 3.10 Genes (n= 192) that were significantly differentially expressed between *M. tuberculosis* strains K636^{WT} (untreated) vs K636^{RIF} (untreated) (Group B).

Functional category	Gene no.	Gene name	Function/Product	P-value	FDR	LogFC
Cell wall and cell processes	1	*Rv0986*	Thought to be involved in active transport of adhesion component across the membrane: involved in attachment and virulence. Responsible for energy coupling to the transport system.	1,39E-04	3,57E-03	4,41
	2	*Rv0010c*	Function unknown. Probable conserved membrane protein.	1,26E-04	3,57E-03	3,48
	3	*esxO*	Function unknown. Putative ESAT-6 like protein EsxO (ESAT-6 like protein 6).	8,72E-05	3,54E-03	3,47
	4	*Rv0988*	Function unknown. Possible conserved exported protein.	9,94E-05	3,57E-03	3,45
	5	*Rv1435c*	Function unknown. Probable conserved proline, glycine and valine-rich secreted protein.	2,78E-05	3,24E-03	3,39
	6	*Rv0987*	Thought to be involved in active transport of adhesion component across the membrane: involved in attachment and virulence. Responsible for the translocation of the substrate across the membrane.	1,73E-04	3,69E-03	3,35
	7	*drrC*	Probably involved in active transport of antibiotic and phthiocerol dimycocerosate across the membrane. Probably responsible for the translocation of the substrate across the membrane and localization of dim into the cell wall.	1,63E-04	3,68E-03	3,32
	8	*murD*	Involved in cell wall formation; peptidoglycan biosynthesis. Probable UDP-N-acetylmuramoylalanine-D-glutamate ligase MurD.	1,42E-05	3,05E-03	2,95
	9	*Rv3888c*	Function unknown. Probable conserved membrane protein.	2,22E-04	3,98E-03	2,90
	10	*lppC*	Function unknown. Probable lipoprotein LppC.	4,02E-05	3,28E-03	2,89
	11	*kdpF*	Thought to be involved in stabilization of the KDP complex.	6,18E-03	2,42E-02	-3,52
	12	*esxF*	Putative ESAT-6 like protein EsxF (hypothetical alanine and glycine rich protein) (ESAT-6 like protein 13).	7,37E-03	2,70E-02	-7,79
	13	*Rv0011c*	Function unknown. Probable conserved transmembrane protein.	2,83E-04	4,16E-03	2,78
	14	*lppL*	Function unknown. Probable conserved lipoprotein LppL.	1,12E-03	8,14E-03	2,75
	15	*espE*	ESX-1 secretion-associated protein EspE.	6,92E-04	6,17E-03	2,74
	16	*pitA*	Involved in low-affinity inorganic phosphate transport across the membrane. Responsible for the translocation of the substrate across the membrane.	6,39E-05	3,28E-03	2,73
	17	*Rv1230c*	Function unknown. Possible membrane protein.	2,98E-05	3,24E-03	2,73
	18	*Rv0426c*	Function unknown. Possible transmembrane protein.	1,23E-05	3,05E-03	2,70
	19	*mmpS4*	Function unknown. Probable conserved membrane protein MmpS4.	1,02E-03	7,70E-03	2,62
	20	*Rv2719c*	Function unknown. Possible conserved membrane protein.	1,55E-02	4,47E-02	2,62
	21	*Rv1517*	Function unknown. Conserved hypothetical transmembrane protein.	1,01E-04	3,57E-03	2,58
	22	*Rv0556*	Function unknown. Probable conserved transmembrane protein.	1,55E-05	3,05E-03	2,58
	23	*mmpL4*	Function unknown. Thought to be involved in fatty acid transport. Probable conserved transmembrane transport protein MmpL4.	3,01E-04	4,30E-03	2,53
	24	*Rv0779c*	Function unknown. Possible conserved transmembrane protein.	1,08E-02	3,52E-02	-2,51
	25	*cfp6*	Function unknown (putative secreted protein). Low molecular weight protein antigen 6 (CFP-6).	1,90E-04	3,73E-03	-2,54
	26	*Rv0621*	Function unknown. Possible membrane protein.	9,36E-04	7,30E-03	-2,55
	27	*lprM*	Function unknown. But thought to be involved in host cell invasion. Possible Mce-family lipoprotein LprM (Mce-family lipoprotein Mce3E).	1,45E-02	4,28E-02	-2,59
	28	*mmpL2*	Thought to be involved in fatty acid transport. Probable conserved transmembrane transport protein MmpL2.	5,79E-04	5,71E-03	2,85
Lipid metabolism	1	*idsB*	Involved in biosynthesis of membrane ether-linked lipids. Catalyzes the trans-addition of the three molecules of IPP onto DMAPP to form geranylgeranyl pyrophosphate which is a precursor of the ether-linked lipids.	1,20E-03	8,44E-03	4,67

	2	*pks6*	Polyketide synthase possibly involved in lipid synthesis.	4,06E-04	4,95E-03	4,47
	3	*umaA*	Involved in mycolic acid modification or synthesis. Possible mycolic acid synthase UmaA.	1,17E-04	3,57E-03	3,92
	4	*mmaA1*	Involved in mycolic acids modification. Catalyzes unusual S-adenosyl-methionine-dependent transformation of a cis-olefin mycolic acid into a secondary alcohol. Catalyzes introduction of a hydroxyl group at the distal position on mycolic acid chains to produce the hydroxyl mycolate.	5,87E-06	3,05E-03	3,81
	5	*tesA*	Probably involved in biosynthesis of phthiocerol dimycocerosate (PDIM).	3,39E-04	4,57E-03	3,61
	6	*fadA5*	Function unknown, but involved in lipid degradation.	1,82E-04	3,73E-03	3,57
	7	*fadD30*	Function unknown, but involved in lipid degradation. Fatty-acid-AMP ligase FadD30.	4,09E-04	4,97E-03	3,44
	8	*acpM*	Involved in fatty acid biosynthesis (mycolic acids synthesis); involved in meromycolate extension.	4,57E-03	1,98E-02	3,00
	9	*mbtK*	Involved in the biogenesis of the hydroxyphenyloxazoline-containing siderophore mycobactins. Lysine N-acetyltransferase MbtK.	1,35E-02	4,08E-02	2,94
	10	*papA2*	Involved in sulfolipid-1 (SL-1) biosynthesis.	2,79E-04	4,16E-03	2,80
	11	*fadD28*	Involved in phthiocerol dimycocerosate (dim) biosynthesis. Thought to be involved in the release and transfer of mycoserosic acid from mas onto the DIOLS.	1,12E-03	8,15E-03	2,78
	12	*fadD26*	Involved in phthiocerol dimycocerosate (dim) biosynthesis, possibly by activating substrates for the PPS polyketides synthase.	3,25E-04	4,48E-03	2,53
Regulatory Proteins	**1**	*whiB7*	Involved in transcriptional mechanism. Probable transcriptional regulatory protein WhiB-like WhiB7.	6,45E-03	2,48E-03	5,91
	2	*lrpA*	Involved in transcriptional mechanism. Probable transcriptional regulatory protein LrpA (Lrp/AsnC-amily).	1,37E-04	3,57E-03	3,42
	3	*Rv0078*	Possibly involved in transcriptional mechanism.	2,01E-05	3,05E-03	3,20
	4	*Rv2506*	Involved in transcriptional mechanism. Probable transcriptional regulatory protein (probably TetR-family).	1,28E-04	3,57E-03	3,08
	5	*whiB1*	Involved in transcriptional mechanism. Transcriptional regulatory protein WhiB-like WhiB1. Contains [4FE-4S]2+ cluster.	4,22E-04	5,00E-03	2,62
	6	*whiB6*	Involved in transcriptional mechanism. Possible transcriptional regulatory protein WhiB-like WhiB6.	1,88E-04	3,73E-03	2,58
	7	*Rv3066*	Involved in transcriptional mechanism. Probable transcriptional regulatory protein (probably DeoR-family).	4,57E-04	5,15E-03	-2,68
Intermediary metabolism and respiration	**1**	*Rv3378c*	Produces isotuberculosinol (nosyberkol) from halimadienyl diphosphate. Some has also showed production of tuberculosinol.	2,21E-04	3,98E-03	5,48
	2	*udgA*	Possibly involved in polysaccharide biosynthesis.	8,68E-05	3,54E-03	4,62
	3	*Rv2959c*	Thought to cause methylation. Possible methyltransferase (methylase).	1,10E-04	3,57E-03	4,12
	4	*Rv3377c*	Produces halimadienyl diphosphate (tuberculosinyl diphosphate) from geranylgeranyl diphosphate (GGPP).	2,59E-04	4,16E-03	4,09
	5	*Rv2949c*	Catalyzes the conversion of chorismate to 4-hydroxybenzoate.	6,06E-05	3,28E-03	3,91
	6	*Rv1500*	Function unknown: probable glycosyltransferase	1,42E-04	3,57E-03	3,68
	7	*moaD1*	Involved in molybdenum cofactor biosynthesis.	7,89E-04	6,71E-03	3,64
	8	*atpF*	This is one of the three chains of the nonenzymatic component (cf (0) subunit) of the ATPase complex.	7,07E-04	6,22E-03	3,57
	9	*kshB*	Predicted to be involved in lipid catabolism	2,18E-05	3,05E-03	3,56
	10	*metK*	Involved in the activated methyl cycle. Catalyzes the formation of S-adenosylmethionine from methionine and ATP. The overall synthetic reaction is composed of two sequential steps, AdoMet formation and the subsequent tripolyphosphate hydrolysis, which occurs prior to release of AdoMet from the enzyme.	4,16E-05	3,28E-03	3,23
	11	*moaA1*	Involved in molybdenum cofactor biosynthesis; involved in the biosynthesis of molybdopterin precursor Z from guanosine.	1,36E-04	3,57E-03	3,10
	12	*Rv1714*	Function unknown; probably involved in cellular metabolism	2,21E-04	3,98E-03	3,09

	13	*ctaC*	Involved in aerobic respiration. Subunit I and II form the functional core of the enzyme complex. Electrons originating in cytochrome C are transferred via heme a and Cu (A) to the binuclear center formed by heme A3 and Cu (B).	1,21E-04	3,57E-03	3,02
	14	*Rv0097*	Function unknown; probably involved in cellular metabolism. Possible oxidoreductase.	2,75E-04	4,16E-03	2,95
	15	*Rv0691A*	Electron carrier. Mycofactocin precursor protein.	5,55E-05	3,28E-03	2,91
	16	*proC*	Involved at the terminal (third) step in proline biosynthesis.	1,18E-04	3,57E-03	2,88
	17	*sdhD*	Involved in tricarboxylic acid cycle. Putative hydrophobic component of the succinate dehydrogenase complex. Could be required to anchor the catalytic components to the cytoplasmic membrane.	4,83E-04	5,19E-03	2,87
	19	*Rv0765c*	Function unknown; probably involved in cellular metabolism, possibly electron transfer.	5,59E-05	3,28E-03	-2,80
	20	*frdD*	Involved in interconversion of fumarate and succinate (anaerobic respiration). This hydrophobic component may be required to anchor the catalytic components of the fumarate reductase complex to the cytoplasmic membrane.	7,85E-03	2,80E-02	-4,01
	21	*cyp130*	Cytochromes P450 are a group of heme-thiolate monooxygenases. They oxidize a variety of structurally unrelated compounds, including steroids, fatty acids, and xenobiotics.	6,20E-04	5,95E-03	2,75
	22	*bioF2*	Could be involved in biotin biosynthesis (at the first step) [catalytic activity: 6-carboxyhexanoyl-CoA + L-alanine = 8-amino-7-oxononanoate + CoA + CO2].	7,77E-05	3,54E-03	2,64
	23	*cyp141*	Cytochromes P450 are a group of heme-thiolate monooxygenases. They oxidize a variety of structurally unrelated compounds, including steroids, fatty acids, and xenobiotics.	4,00E-04	4,91E-03	2,63
	24	*ppk2*	Catalyzes the reversible transfer of phosphate from polyphosphate (polyp) to form GTP [catalytic activity: GDP + {phosphate} (N) = GTP + {phosphate} (N-1)].	1,03E-03	7,70E-03	2,54
	25	*che1*	Possibly involved in inserting FE2+ into sirohydrochlorin to produce siroheme, required for SIRA (Rv2391) function.	4,23E-03	1,88E-02	-2,50
	26	*hycQ*	Possibly involved in hydrogen metabolism. Possible hydrogenase HycQ	1,04E-03	7,78E-03	-2,51
	27	*Rv3712*	Function unknown; probably involved in cellular metabolism.	7,17E-03	2,66E-02	-2,55
	28	*Rv2074*	May be involved in biosynthesis of pyridoxine (vitamin B6) and pyridoxal phosphate.	2,83E-05	3,24E-03	-2,56
	29	*ppdK*	Catalyzes the reversible phosphorylation of pyruvate and phosphate.	1,61E-05	3,05E-03	-2,62
	30	*Rv2766c*	Function unknown, possibly involved in cellular metabolism.	4,87E-04	5,21E-03	-2,68
	31	*Rv0375c*	Function unknown; probably involved in cellular metabolism.	6,25E-03	2,43E-02	-2,78
Conserved Hyphothetic als	**1**	*Rv3415c*	Function unknown.	1,63E-03	9,96E-03	4,79
	2	*Rv1115*	Function unknown.	1,26E-04	3,57E-03	4,59
	3	*Rv2452c*	Function unknown.	7,09E-04	6,23E-03	4,49
	4	*Rv3528c*	Function unknown.	5,93E-05	3,28E-03	4,25
	5	*Rv2492*	Function unknown.	1,37E-04	3,57E-03	4,20
	6	*Rv1501*	Function unknown.	1,38E-04	3,57E-03	4,19
	7	*Rv3282*	Function unknown.	4,66E-04	5,16E-03	4,17
	8	*Rv1507A*	Function unknown.	2,54E-04	4,16E-03	4,00
	9	*Rv1505c*	Function unknown.	1,29E-03	8,79E-03	3,99
	10	*Rv3902c*	Function unknown.	5,06E-04	5,29E-03	3,95
	11	*Rv3738c*	Function unknown.	3,23E-04	4,48E-03	3,94
	12	*Rv1067c*	Function unknown.	2,97E-03	1,48E-02	3,93
	14	*Rv1291c*	Function unknown.	1,64E-04	3,68E-03	3,83
	15	*Rv2023A*	Function unknown.	3,86E-04	4,90E-03	3,75

	16	*Rv3192*	Function unknown.	2,09E-05	3,05E-03	3,74
	17	*Rv1507c*	Function unknown.	4,75E-04	5,16E-03	3,74
	18	*Rv3766*	Function unknown.	2,43E-05	3,09E-03	3,74
	19	*Rv3395c*	Function unknown.	5,82E-03	2,32E-02	3,61
	20	*Rv2808*	Function unknown.	6,80E-05	3,31E-03	3,57
	21	*Rv2660c*	Function unknown.	4,85E-05	3,28E-03	3,50
	22	*Rv3351c*	Function unknown.	8,04E-05	3,54E-03	3,49
	23	*Rv1948c*	Function unknown.	4,55E-04	5,15E-03	3,44
	24	*Rv1374c*	Function unknown.	2,06E-04	3,84E-03	3,37
	25	*Rv1268c*	Function unknown.	9,74E-06	3,05E-03	3,21
	26	*Rv1506c*	Function unknown.	1,57E-04	3,63E-03	3,19
	27	*Rv2960c*	Function unknown.	3,13E-05	3,24E-03	3,12
	28	*Rv2432c*	Function unknown.	5,59E-03	2,27E-02	3,12
	29	*Rv2956*	Function unknown.	1,35E-04	3,57E-03	3,01
	30	*Rv3218*	Function unknown.	9,09E-04	7,21E-03	2,95
	31	*Rv1954c*	Function unknown.	1,76E-03	1,05E-02	2,92
	32	*Rv2147c*	Function unknown.	2,69E-03	1,40E-02	2,91
	33	*Rv1954c*	Function unknown.	1,76E-03	1,05E-02	2,92
	34	*Rv2147c*	Function unknown.	2,69E-03	1,40E-02	2,91
	35	*Rv0057*	Function unknown.	4,25E-04	5,00E-03	2,91
	36	*Rv1461*	Function unknown.	5,37E-04	5,48E-03	2,90
	37	*Rv2734*	Function unknown.	5,87E-04	5,74E-03	2,85
	38	*Rv1535*	Function unknown.	1,31E-03	8,84E-03	2,83
	39	*Rv2901c*	Function unknown.	5,24E-04	5,39E-03	2,81
	40	*Rv3753c*	Function unknown.	6,75E-04	6,15E-03	-2,80
	41	*Rv0790c*	Function unknown.	1,00E-02	3,33E-02	-2,85
	42	*Rv3899c*	Function unknown.	6,35E-04	6,02E-03	-2,88
	43	*Rv0201c*	Function unknown.	2,38E-04	4,14E-03	-2,92
	44	*Rv3748*	Function unknown.	3,30E-04	4,49E-03	-2,98
	45	*Rv1443c*	Function unknown.	2,89E-04	4,17E-03	-3,13
	46	*Rv1904*	Function unknown.	1,61E-04	3,66E-03	-3,19
	47	*Rv0459*	Function unknown.	1,73E-03	1,04E-02	-3,29
	48	*Rv1888A*	Function unknown.	1,88E-02	5,08E-02	-4,02
	49	*Rv2735c*	Function unknown.	6,01E-03	2,37E-02	2,78
	50	*octT*	Transfers octanoate to glucosylglycerate (GG) and diglucosylglycerate (DGG), the earliest intermediates in methylglucose lipopolysaccharides (MGLP) biosynthesis.	5,12E-05	3,28E-03	2,77
	51	*Rv2067c*	Function unknown.	1,17E-04	3,57E-03	2,77
	52	*Rv2369c*	Function unknown.	2,52E-04	4,16E-03	2,75
	53	*Rv1950c*	Function unknown.	1,80E-04	3,72E-03	2,74
	54	*Rv3749c*	Function unknown.	9,32E-04	7,28E-03	2,63

	55	*Rv1724c*	Function unknown.	1,90E-04	3,73E-03	2,58
	56	*Rv1794*	Function unknown.	4,19E-04	4,99E-03	2,55
	57	*Rv3179*	Function unknown.	1,33E-04	3,57E-03	2,53
	58	*Rv1504c*	Function unknown.	2,05E-03	1,16E-02	2,51
	59	*Rv2133c*	Function unknown.	1,19E-05	3,05E-03	-2,50
	60	*Rv0750*	Function unknown.	1,70E-04	3,69E-03	-2,54
	61	*Rv2292c*	Function unknown.	1,69E-02	4,76E-02	-2,59
	62	*Rv1558*	Function unknown.	1,35E-04	3,57E-03	-2,62
	63	*Rv1684*	Function unknown.	1,10E-03	8,11E-03	-2,64
	64	*Rv2288*	Function unknown.	1,14E-03	8,20E-03	-2,66
	65	*Rv3672c*	Function unknown.	2,46E-04	4,16E-03	-2,70
Virulence, detoxification, adaptation	**1**	*mazE1*	Possible antitoxin MazE1.	3,48E-04	4,59E-03	3,39
	2	*mazE6*	Antitoxin MazE6.	6,48E-05	3,28E-03	3,07
	3	*aac*	Confers resistance to aminoglycosides (gentamicin, tobramycin, dibekacin, netilmicin, and 6'-N-ethylnetilmicin).	2,00E-04	3,80E-03	-2,86
	4	*vapB4*	Possible antitoxin VapB4.	1,33E-03	8,93E-03	-3,09
	5	*mazF7*	Possible toxin MazF7.	1,11E-02	3,58E-02	-3,10
	6	*vapB2*	Possible antitoxin VapB2.	8,74E-05	3,54E-03	2,70
	7	*vapB22*	Possible antitoxin VapB22.	1,23E-03	8,54E-03	2,58
	8	*parE2*	Possible toxin ParE2.	2,99E-03	1,49E-02	2,55
	9	*vapB14*	Possible antitoxin VapB14.	1,91E-04	3,73E-03	-2,58
Insertion seqs and phages	**1**	*Rv2106*	Required for the transposition of the insertion element IS6110.	1,98E-03	1,13E-02	4,12
	2	*Rv2646*	Sequence integration. Integrase is necessary for integration of a phage into the host genome by site-specific recombination. In conjunction with excisionase, integrase is also necessary for excision of the prophage from the host genome.	4,16E-05	3,28E-03	3,48
	3	*Rv3770A*	Possibly required for the transposition of an insertion element.	6,46E-05	3,28E-03	3,29
	4	*Rv0829*	Required for the transposition of the insertion element IS1605'.	2,08E-03	1,17E-02	3,15
	5	*Rv3185*	Involved in the transposition in the insertion sequence IS6110.	5,37E-04	5,48E-03	3,10
	6	*Rv2657c*	Probable PhiRv2 prophage protein.	6,14E-05	3,28E-03	-2,82
	7	*Rv2424c*	Required for the transposition of the insertion element IS1558.	1,44E-02	4,26E-02	-3,19
	8	*Rv3380c*	Involved in the transposition of the insertion sequence IS6110.	4,91E-03	2,07E-02	-5,01
	9	*Rv3325*	Involved in the transposition of the insertion sequence element IS6110.	1,23E-02	3,82E-02	2,78
	10	*Rv0795*	Required for the transposition of the insertion element IS6110.	3,57E-03	1,65E-02	2,71
	11	*Rv3474*	Involved in the transposition of the insertion sequence IS6110.	2,76E-03	1,41E-02	2,70
	12	*Rv1036c*	Possibly required for the transposition of the insertion element IS1560.	1,19E-03	8,41E-03	2,67
	13	*Rv1765A*	Possibly required for the transposition of an insertion element.	1,32E-04	3,57E-03	2,58
	14	*Rv2085*	Conserved hypothetical protein	6,82E-03	2,56E-02	-2,55
PE/PPE	**1**	*ppe58*	Function unknown.	8,10E-04	6,82E-03	5,32
	2	*ppe46*	Function unknown.	1,13E-04	3,57E-03	4,92
	3	*ppe57*	Function unknown.	1,17E-03	8,34E-03	4,85
	4	*ppe47*	Function unknown.	2,19E-04	3,98E-03	4,79
	5	*ppe3*	Function unknown.	1,41E-04	3,57E-03	4,30

	6	*ppe66*	Function unknown.	3,23E-04	4,48E-03	3,94
	7	*PE_PGRS19*	Function unknown.	2,97E-03	1,48E-02	3,93
	8	*ppe12*	Function unknown.	1,22E-04	3,57E-03	3,51
	9	*ppe4*	Function unknown.	2,73E-04	4,16E-03	3,43
	10	*ppe54*	Function unknown.	1,89E-03	1,10E-02	3,21
	11	*pe35*	Function unknown.	1,08E-03	8,02E-03	3,20
	12	*p27*	Function unknown.	3,95E-04	4,91E-03	3,19
	13	*ppe39*	Function unknown.	4,59E-03	1,98E-02	2,93
	14	*pe22*	Function unknown.	8,45E-05	3,54E-03	2,88
	15	*pe21*	Function unknown.	5,78E-03	2,32E-02	-2,90
	16	*ppe36*	Function unknown.	9,08E-05	3,57E-03	2,80
	17	*ppe40*	Function unknown.	4,89E-03	2,07E-02	2,62
	18	*ppe22*	Function unknown.	1,44E-05	3,05E-03	2,59
	19	*ppe33*	Function unknown.	3,10E-03	1,52E-02	2,56
	20	*PE_PGRS25*	Function unknown.	1,17E-02	3,73E-02	2,56
Information Pathways	**1**	*Rv3644c*	DNA polymerase is a complex, multichain enzyme responsible for most of the replicative synthesis in bacteria.	7,01E-05	3,37E-03	4,14
	2	*lysS*	Involved in translation.	9,94E-05	3,57E-03	3,45
	3	*recF*	The RECF protein is involved in DNA metabolism and recombination; it is required for DNA replication and normal sos inducibility. RECF binds preferentially to single-stranded, linear DNA.	1,76E-04	3,69E-03	3,10
	4	*rhlE*	Has a helix-destabilizing activity. Probable ATP-dependent RNA helicase RhlE.	1,25E-03	8,61E-03	4,03
	5	*rpmA*	Involved in translation mechanisms. 50S ribosomal protein L27 RpmA.	1,27E-04	3,57E-03	-3,43
	6	*sigM*	The sigma factor is an initiation factor that promotes attachment of the RNA polymerase to specific initiation sites and then is released. Possible alternative RNA polymerase sigma factor SigM.	1,56E-02	4,49E-02	-2,75

* Gene name, function and category indicated by TubercuList, v 2.6.
# p-value, q-value/FDR and log fold change obtained from Star Bioinformatics software and edgeR

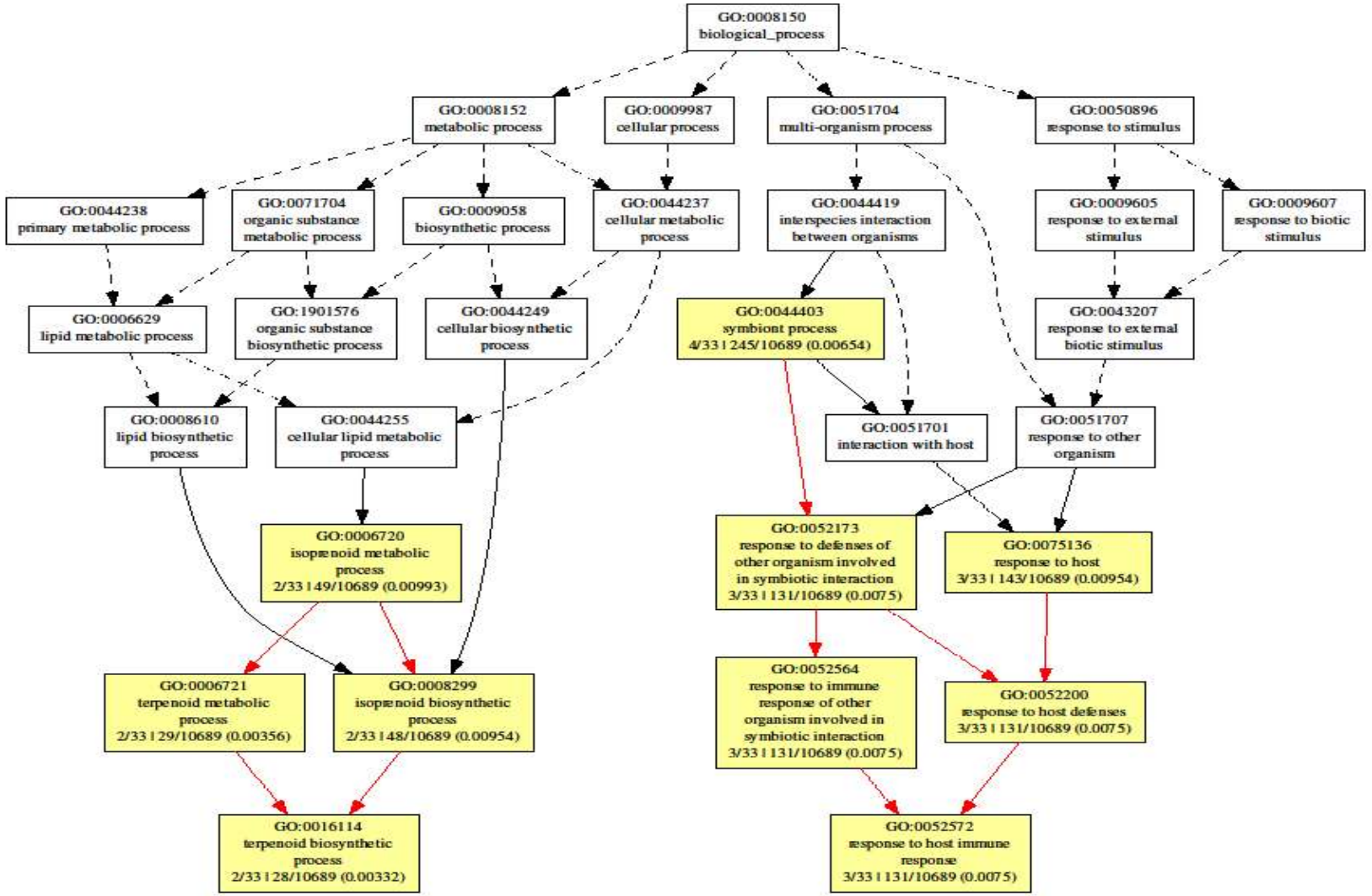

(i)

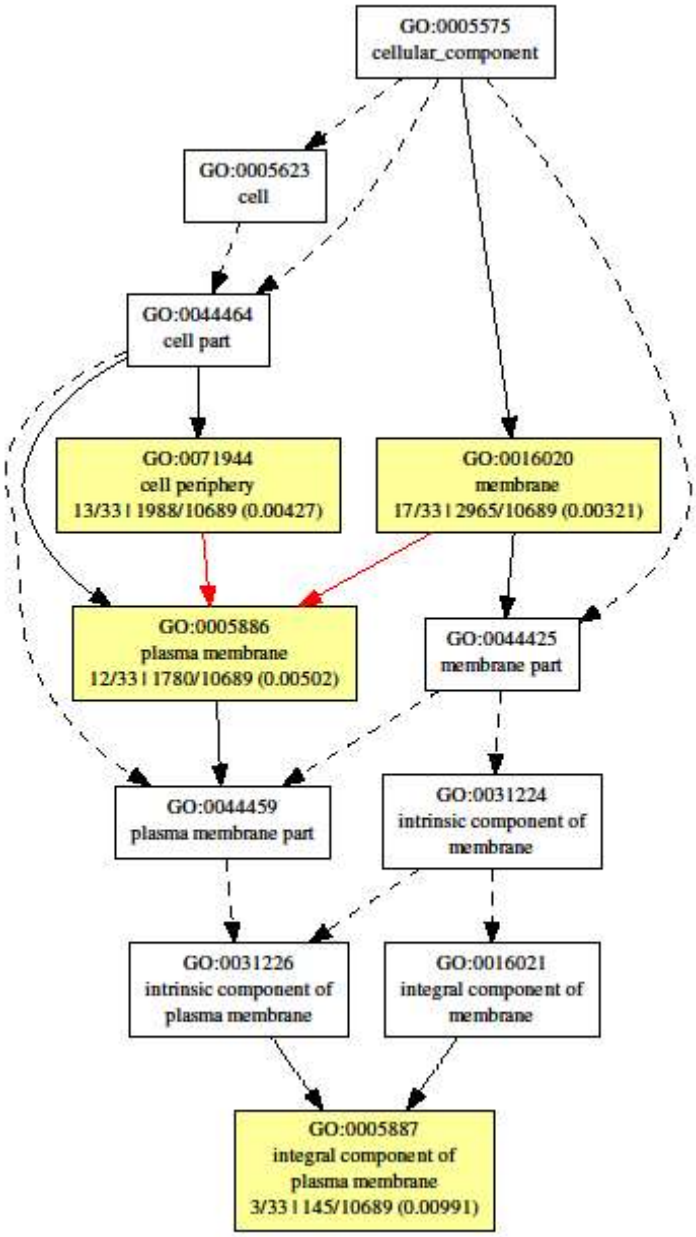

(ii)

Figure 3.9 (i-ii) A graphical output of enriched GO terms for the differentially expressed genes from comparison Group B in different GO categories (i) biological process and (ii) cellular component category. Significantly enriched GO terms are illustrated by the yellow boxes whereas the white boxes represent non-significant GO terms. The red arrows represent an association between the significantly enriched terms and the black arrows represent an association between enriched and unenriched GO terms. The dashed black arrows illustrate the relationship between two unenriched GO terms.

3.3.5.3 GO terms (group A and B)

The total number of the differentially expressed list was too large to discuss in this thesis, hence a simplified significantly enriched GO terms list was generated using GOEAST for the purpose of this discussion (see 3.2.7 methods section). The significance was based on the FDR which is calculated using the Benjamini–Yekutieli model (44). The majority of the identified enriched genes in group A (Figure 3.8 (i-iii); Table 3.11) and in group B (Figure 3.9 (i-ii); Table 3.11) belonged to cell wall and cell processes and regulatory proteins. The level of significance (FDR ≤ 3,73E-03), the cell wall, cell processes and regulatory proteins functional categories were used to refine the selection criteria of genes for discussion. In group A, 9 genes belonging to cell wall and cell processes that were significantly up-regulated were selected for discussion. These genes included (*esxA*, *esxB*, *esxD*, *esxO*, *espE espF* and *espK*) and significant down-regulation of *Rv0072*, *Rv0073* genes (Table 3.11). In group B, 7 genes belonging to cell wall and cell processes and regulatory proteins that were significantly up-regulated were selected for discussion. These genes included (*whiB1*, *whiB6*, *whiB7*, *Rv0078*, *mmpL4*, *mmpS4 and mmpL2*) (Table 3.11).

Table 3.11 Classification of group A and B genes subsets selected for discussion

Group A (K636^{WT} vs H37Rv^{WT})			**Group B (K636^{WT} vs K636^{RIF})**		
Functional category	**Gene name**	**FDR value**	**Functional category**	**Gene name**	**FDR value**
Cell wall and cell processes	*Rv0072*	1,48E-04	**Regulatory proteins**	*whiB1*	3,73E-03
	Rv0073	1,48E-04		*whiB6*	5,00E-03
	esxA	1,87E-03		*whiB7*	2,48E-03
	esxB	5,77E-04		*Rv0078*	3,05E-03
	esxD	3,53E-04	**Cell wall and cell processes**	*mmpL4*	4,30E-03
	esxO	5,51E-04		*mmpS4*	7,70E-03
	espE	2,85E-04		*mmpL2*	5,71E-03
	espF	3,50E-04		-	-
	espK	2,72E-04		-	-

3.3.6 Validation of RNA-Seq analysis by RT-qPCR assessment

The RT-qPCR validation of *kasA, accD6* and 5 candidate genes (*whiB7, Rv1760, pks6, Rv3211* and *Rv0073*) that were selected (as per criteria explained in methods section 3.2.8) from the list of significant differentially expressed genes revealed varying gene expression patterns compared to that of RNA-Seq data; when normalised to *16S rRNA* and *sigA* (housekeeping genes), respectively in $K636^{WT}$, $K636^{RIF}$ and $H37Rv^{WT}$ *M. tuberculosis* strains [Table 3. 13 (i-iii); Figure 3.10 (i-ii)]. Briefly, low-level up-regulation was observed for *whiB7* (1.0-fold) and *pks6* (2.24-fold) compared to these genes high-level up-regulation in RNA-Seq data. Subsequently, we observed the up-regulation of *Rv1760* (1.97-fold) and *Rv0073* (1.43-fold) compared to these genes down-regulation in RNA-Seq data. Interestingly, we observed similar high-level up-regulation for *Rv3211* (4.92-fold) when normalized against *16S rRNA*, *kasA* (6.19-fold) and *accD6* (3.96-fold) compared to these genes high-level up-regulation in RNA-Seq data except for *kasA* (2.05-fold). The amplification efficiencies for housekeeping genes were observed as 98% for *sigA* and 95% for *16S rRNA* (Table 3.12). PCR efficiencies for the candidate genes ranged from 85% to 123% and they are classified below in Table 3.12.

Table 3.12 The amplification efficiency of the candidate genes selected after RNA-Seq identification

Type of a gene	Gene	Amplification efficiency (%)
Housekeeping genes	*sigA*	98.0
	16S rRNA	95.0
Candidate genes	*whiB7 (Rv3197A)*	85.0
	Rv3211	90.0
	pks6 (Rv0405)	123
	Rv0073	111
	Rv1760	121.0

Table 3.13 (i-iii) The comparison of RT-qPCR data and RNA-Seq data for the validated genes (n=7) in *M. tuberculosis* strains

(i) $K636^{WT\ (treated\ vs\ untreated)}$			
Gene name	**RNA-Seq analysis**	**RT-qPCR analysis**	
	Fold change	**Fold change (16S rRNA)**	**Fold change (*sigA*)**
kasA	2.05	6.19	5.30
accD6	3.13	3.96	3.40
(ii) $K636^{WT(untreated)}$ vs $H37Rv^{WT(untreated)}$			
Gene name	**RNA-Seq analysis**	**RT-qPCR analysis**	
	Fold change	**Fold change (16S rRNA)**	**Fold change (*sigA*)**
Rv1760	-12.06	1.97	1.00
Rv0073	-13.58	1.43	1.55
(iii) $K636^{WT\ (untreated)}$ vs $K636^{RIF\ (untreated)}$			
Gene name	**RNA-Seq analysis**	**RT-qPCR analysis**	
	Fold change	**Fold change (16S rRNA)**	**Fold change (*sigA*)**
pks6 (Rv0405)	4.47	2.24	1.50
whiB7 (Rv3197A)	5.91	1.00	1.01
Rv3211	4.03	4.92	1.43

i) $K636^{WT}$ treated vs untreated, ii) $K636^{WT}$ (untreated) vs $K636^{RIF}$ (untreated) and iii) $K636^{WT}$ vs $H37Rv^{WT}$ M. tuberculosis strains.

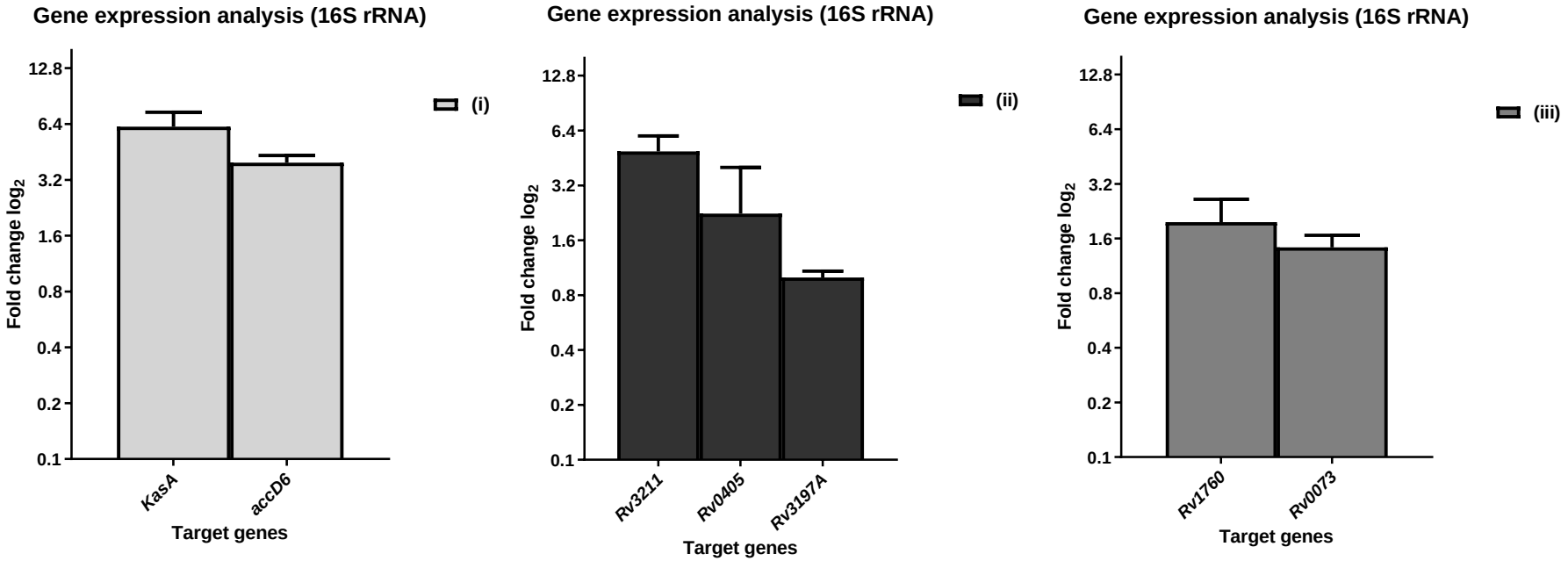

Figure 3.10i Differential gene expression (*16S rRNA*) of the candidate genes (n=7) validated by RT-qPCR in the studied *M. tuberculosis* strains. i) $K636^{WT}$ (treated vs untreated) for the candidate genes; ii) $K636^{WT}$ (untreated) vs $H37Rv^{WT}$ (untreated) and iii) $K636^{WT}$ (untreated) vs $K636^{RIF}$ (untreated) *M. tuberculosis* strains. Data is shown as mean values plots of 3 biological replicates and their standard deviations (SDs) of various samples per group descriptions.

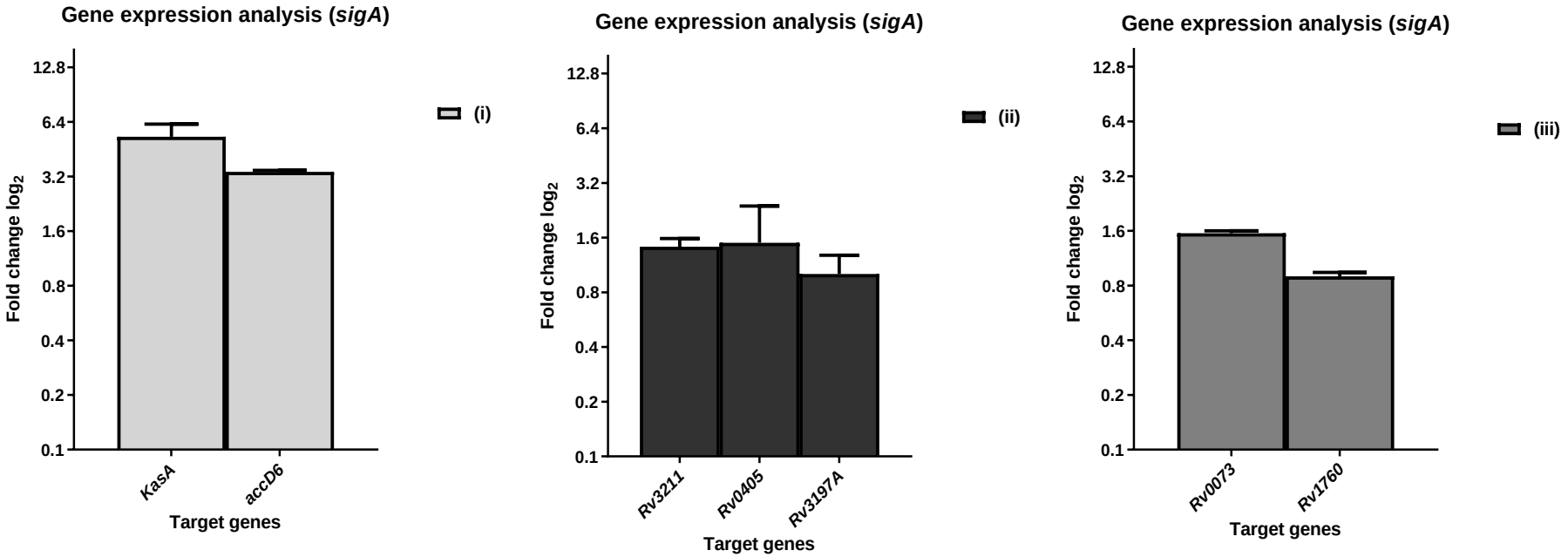

Figure 3.10ii Differential gene expression (*sigA*) of the candidate genes (n=7) validated by RT-qPCR in the studied *M. tuberculosis* strains. i) $K636^{WT}$ (treated vs untreated) for the candidate genes; ii) $K636^{WT}$ (untreated) vs $H37Rv^{WT}$ (untreated) and iii) $K636^{WT}$ (untreated) vs $K636^{RIF}$ (untreated) *M. tuberculosis* strains. Data is shown as mean values plots of 3 biological replicates and their standard deviations (SDs) of various samples per group descriptions.

.

3.4 Discussion

3.4.1 INH titration experiments of K636^{WT}, K636^{RIF} (with *rpoB* Ser531Leu mutation) and H37Rv^{WT} *M .tuberculosis* strains

The INH titration experiments were performed to investigate the concentration of INH that will elicit a transcriptional response and the 0.05 µg/ml INH concentration was chosen. It was demonstrated that 0.05 µg/ml INH induces the high-level up-regulation of *kasA* (≥ 2-fold) and *accD6* (≥ 2-fold) in K636^{WT} *M. tuberculosis* strain (Figure 3.6i and Figure 3.6ii). Numerous studies employing micro-array technology studied the influence of 0.1, 0.125 and 0.2 µg/ml INH concentration treatment (24h) in *M. tuberculosis* and *M. smegmatis*. (3,5,20,35,45). These studies reported that the treatment of susceptible and resistant *M. tuberculosis* strains with 0.1 µg/ml INH concentration for 24h demonstrated differential gene expression of *kasA*, *acpM* and *accD6* genes (46). Similarly, differential gene expression was induced after treatment of susceptible *M. tuberculosis* clinical strains with 0.2 µg/ml INH for 24h (3). In addition, treatment of a susceptible *M. smegmatis* strain with 0.125 µg/ml INH for 24h induced differential gene expression (5). In contrast, our results demonstrate that 0.05 µg/ml INH induced a very low-level regulation of *kasA* (≤ 1.0- fold) and *accD6* (≤ 1.0- fold) when normalised to *16S rRNA* and *sigA* in H37Rv^{WT} *M. tuberculosis* strain, after 24h treatment with 0.05 µg/ml INH (Figure 3.6i and Figure 3.6ii). It can be speculated that maybe if H37Rv^{WT} was treated with 0.05 µg/ml INH for a longer (28h) period or maybe increasing the INH treatment concentration, it could have resulted in an increased *kasA* and *accD6* gene expression. For this reason, as the limitation of the study, H37Rv^{WT} (INH-treated) strain was excluded for the RNA-Seq analysis.

3.4.2 Comparative analysis of K636^{WT}, K636^{RIF} (with *rpoB* mutation) and H37Rv^{WT} *M. tuberculosis* strains by WGS data

Comparative analysis of K636^{WT} and K636^{RIF} (with *rpoB* mutation) showed variation in the number of reads of these two strains and confirmed the presence of the *rpoB* Ser531Leu mutation, a *malQ* (Val1221Val) variant in the *malQ* protein and 2 other variants that accumulated in the *glpK* and *Rv1285* genes (Table 3.4). Nevertheless, these were synonymous changes suggesting no effect on the transcriptome of this strain. Therefore, it can be suggested that their accumulation could be a possible consequence of re-culturing K636^{WT} and K636^{RIF} *M. tuberculosis* strains and this, in turn, having an effect on their relative fold-change ratios; as reflected by their accumulation. The comparative analysis of

K636^{WT} and H37Rv^{WT} WGS sequence data identified variants unique and relevant to the genetic background differences of these two *M. tuberculosis* strains, thus in agreement with our transcriptomic data (Table 3.5). Interestingly, from the 30 identified variants between K636^{WT} and H37Rv^{WT} comparative sequence analysis, 7 of these variants accumulated in the 7 genes (*sdhD, VapC47, pks6, idsB, fadA, oxcA* and *Rv2017*) (Table 3.9) that were shown to be differentially expressed as reflected by the transcriptomic data. This observation suggests that the differences in K636^{WT} and H37Rv^{WT} *M. tuberculosis* genetic backgrounds had an effect on both the genome and transcriptome.

3.4.3 Validation of RNA-Seq analysis by RT-qPCR assessment for differentially expressed genes in studied *M. tuberculosis* strains.

The RT-qPCR validation of *kasA, accD6* and 5 candidate genes (*whiB7, Rv1760, pks6, Rv3211* and *Rv0073*) that were selected from the list of significant differentially expressed genes, revealed discrepant gene expression (up- and down-regulation) patterns in K636^{WT}, K636^{RIF} and H37Rv^{WT} *M. tuberculosis* strains compared to that of RNA-Seq data (results section 3.5). For example, RT-qPCR validation data showed the low-level up-regulation of *whiB7*and *pks6* compared to their high-level up-regulation in RNA-Seq data. Subsequently, RT-qPCR validation data showed the up-regulation of *Rv1760* and *Rv0073* compared to their down-regulation in RNA-Seq data (results section 3.5). The observed discrepancies between the RT-qPCR validation and RNA-Seq data could be due to various reasons. For example, the differences between the two methods of estimating the levels of gene expression; for RNA-Seq data the EdgeR software package was used to determine the differential gene expression (methods section 3.2.7), while for RT-qPCR, the delta-delta Ct calculation was used to determine the level of gene expression (methods section 3.2.7). The EdgeR software package uses R-programming language and the analysis is automated, with optional steps you can select to improve the analysis. In contrast, the delta-delta Ct calculation is done using the equation in excelsheet and therefore, possible low chances of the evident results similarities between the two methods. Secondly, the discrepancy could be due to a technical issue. Specifically, cDNA from different RNA batches was used for RT-qPCR and RNA sequencing analysis.

In support, Yu *et al*. (2015) DNA microarray study showed similar discrepancy between RT-qPCR validation and RNA-Seq data, was observed; in their gene expression profiles in resistant *M. tuberculosis* strains relative to susceptible H37Rv strain (20). The differences they observed was technical; a consequence of using different batches of RNA for their RT-

qPCR validation experiment compared to the batch used for their microarray analysis (20). Of importance, besides the discrepant results; we also observed similarities in the level of gene expression for some genes; similar high-level up-regulation for *Rv3211, kasA* and *accD6* in RT-qPCR data compared to these genes high-level up-regulation in RNA-Seq data (results section 3.5).

3.4.4 The effect of genetic background diversity on the transcriptomic profiles of K636^{WT} vs H37Rv^{WT} *M. tuberculosis* strains (group A)

Our transcriptomic data revealed the significant down-regulation of genes involved in cell wall and cell processes; two putative amino acid transporters *Rv0072* (FDR: 1,48E-04) and *Rv0073* (FDR: 1,48E-04) in K636^{WT} relative to H37Rv^{WT} *M. tuberculosis* strains (refer to Table 3.11). Both Rv0072 and Rv0073 proteins form part of the putative glutamine importing system(s) (15,47) and they are organized in an operon that encodes a putative glutamine ABC transporter (Figure 3.11) (48). Together with *Rv2563-GlnQ* operon and *GlnH* (encoding a putative glutamine-binding lipoprotein), they are involved in the acquisition of inorganic and organic nitrogen sources in *M. tuberculosis* (Figure 3.11) (48). Therefore, the significant down-regulation of these genes in K636^{WT} relative to H37Rv^{WT} is indicative of their important role in *M. tuberculosis* nitrogen metabolism and this need to be explored further. Previously, it was demonstrated that *M. tuberculosis* auxotrophic mutants of glutamine are severely attenuated *in vivo;* indicating that the biosynthesis of glutamine is required for *M. tuberculosis* growth in the intracellular environment (49). Therefore, the down-regulation of *Rv0072* and *Rv0073* in K636^{WT} relative to H37Rv^{WT} suggests two things; (i) that glutamine was possibly not transferred into the cell in the clinical Beijing strain compared to the lab strain or (ii) that the regulation of glutamine biosynthesis *in vitro* was important for the survival and growth of the clinical Beijing strain.

Interestingly, a comparative proteomics analysis showed that Rv0072 protein was present in the proteome of H37Rv strain and absent in the proteome of Beijing B0/W148 strain; this was a consequence of an insertion mutation (Rv888: 987586 insGG) in the coding region of this gene (50). Furthermore, it showed that *Rv0072* mapped to chromosome regions showing differences between these two strains (50). Therefore, in agreement with our speculations, the down-regulation of *Rv0072* and *Rv0073* genes was indicative of physiological differences between K636^{WT} and H37Rv^{WT} *M. tuberculosis* strains (Beijing and H37Rv). No genomic variants were identified associated with *Rv0072* and *Rv0073* in our WGS data of K636^{WT} compared to H37Rv^{WT}.

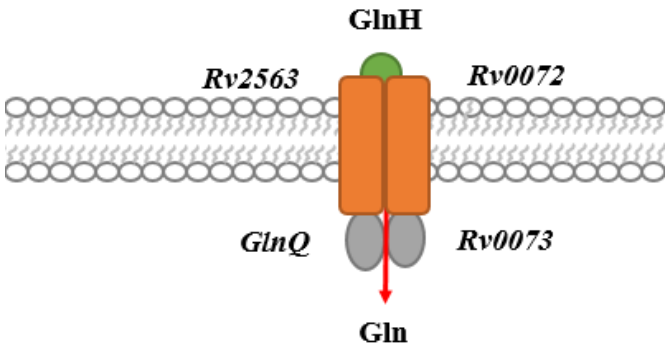

Figure 3.11 The involvement of *Rv0072* and *Rv0073* putative transporters in the acquisition organic nitrogen sources. The both *Rv0072-Rv0073* and *Rv2563-glnQ* operons encodes a putative glutamine ABC transporter, while *glnH* depicted in the image encodes a putative glutamine-binding lipoprotein.

Our transcriptomic data revealed the over-expression of the ESX-1 secretion system genes in K636^{WT} relative to H37Rv^{WT} *M. tuberculosis* strains. This showed significant up-regulation of *espE* (FDR: 2,85E-04), *espF* (FDR: 3,50E-04) and *espK* (FDR: 2,72E-04) genes (refer to Table 3.11). The virulence-associated ESX-1 secretion system is required for mycobacterial pathogenesis in *M. tuberculosis* (51) and is used by *M tuberculosis* to export protein across the cell wall using specific secreted proteins *espE*, *espF* and *espK* (52). Studies report that genes encoding ESX-1 substrates are directly regulated by numerous transcription factors such as PhoP, EspR, and WhiB6 in *M. tuberculosis* (51,53–55). Consistent with our findings, the regulatory protein *whiB6* (FDR: 9,82E-06) was also significantly up-regulated in K636^{WT} relative to H37Rv^{WT} in the current study. This confirms what has been shown in literature that WhiB6 is positively auto-regulated and it directly regulates the transcription of genes encoding several ESX-1 substrates and components in both *M. tuberculosis* and *M. marinum* (56–58). Furthermore, it was demonstrated that the transcription regulator *whiB6* regulates the expression of ESX-1 via the PhoP regulon in *M. tuberculosis* (56). With this in mind, it can be suggested that K636^{WT} might be more likely to form pores than H37Rv^{WT}, because it produces more *ESX-1* genes, making it more virulent. However, Bosserman *et al.* (2017) revealed that this transcriptional regulation might be dependent on the presence or absence of the ESX-1 export system that functions in virulence (ESX-1) or essential physiologic processes (ESX-3) (51,59). ESX-1 was the first system found facilitating the secretion of ESAT-6 and its chaperone protein culture filtrate 10-kDa (CFP-10) out of the cell envelope (60).

Interestingly, our data also revealed the significant up-regulation of the ESAT-6 like genes, *esxA* (1,87E-03), *esxB* (FDR: 5,77E-04), *esxD* (FDR: 3,53E-04), and *esxO* (FDR:5,51E-04) in an operon-like structure and are transcribed as polycistronic RNA, in $K636^{WT}$ relative to $H37Rv^{WT}$ *M. tuberculosis* strains (refer to Table 3.12). ESAT-6 is a pore-forming toxin required for virulence and modulating host immune response modulation (61–64). Therefore, the up-regulation of the ESAT-6 like genes suggests increased virulence in clinical Beijing strain compared to the lab strain. This is indicative of physiological differences between the two *M. tuberculosis* strains (Beijing and H37Rv) and their role in virulence and mycobacterial pathogenesis.

3.4.5 The effect of the *rpoB* mutation on the transcriptomic profiles of $K636^{WT}$ vs $K636^{RIF}$ *M. tuberculosis* strains (group B)

Our transcriptomic data revealed the significant up-regulation of genes involved in cell wall and cell processes; *mmpL4* (*Rv0450c*) (FDR: 4,30E-03), *mmpS4* (FDR: 7,70E-03) and *mmpL2* (FDR: 5,71E-03) in $K636^{WT}$ relative to $K636^{RIF}$ (with *rpoB* Ser531Leu mutation) *M. tuberculosis* strains (refer to Table 3.11). The MmpL transporters play a role in drug efflux and INH intrinsic resistance in *M. tuberculosis* (65–67). *MmpL2* is involved in fatty acids transport (65) and its up-regulation suggests an efflux-pump associated mechanism that *M. tuberculosis* can adapt for intrinsic resistance and stress response. According to literature, MmpL4 and MmpL5 proteins usually form complexes with smaller accessory proteins (MmpS) associated with RND efflux pumps proteins, to export cell wall constituents and aid *M tuberculosis* under low iron conditions (65,68). These *MmpS4* and *mmpS5* genes are the major components of the siderophore export system that is critical for the survival of *M. tuberculosis* in its host (60). It is important to note that, both *mmpL4/mmpS4* and *mmpL5/mmpS5* are similar transport systems required for biosynthesis, export and recycling of siderophores used by *M. tuberculosis* (Figure 3.12) (68–70).

It was previously reported that *mmpL4* (*Rv0450c*)/*mmpS4* and *mmpL5/mmpS5* siderophores export pumps play a role in iron-scavenging mechanism (Figure 3.12) (68–70). Therefore the up-regulation *mmpL4/mmpS4* transport system in $K636^{WT}$ relative to $K636^{RIF}$ *M. tuberculosis* strains is indicative of efflux-pumps mechanism associated with the regulation of iron metabolism for the survival and growth of *M. tuberculosis* under a nutrient limiting intracellular environment. A microarray assay reported the overexpression of *mmpL4* and *mmpL5* after RIF exposure to RIF-resistant *M. tuberculosis* strains (71). Therefore, it can be speculated that the presence of the *rpoB* mutation might influence the regulation of *mmpL4*

and *mmpS4* by different regulators (*Rv0452* or *Rv0678*, respectively) (71). It has been reported that *mmpL4* plays a role in virulence in mice and is essential for the normal replication of *M. tuberculosis* during the active-growth phase in a murine TB model (65). This *mmpL4*/*mmpS4* operon is regulated by *Rv0452* (68) and therefore, the expression (up-regulation) of *mmpL4* (*Rv0450c*) further suggests the modulation of bacterial growth and differences in the iron metabolism of the $K636^{WT}$ relative to $K636^{RIF}$ *M. tuberculosis* strains.

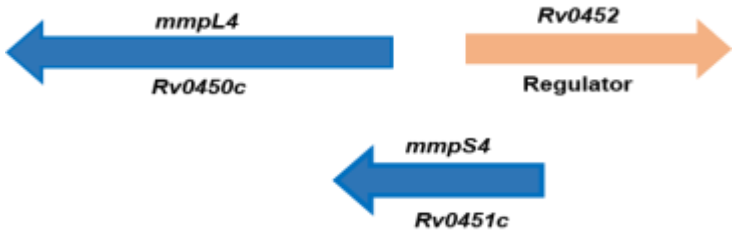

Figure 3.12 The illustration of *mmpL4* (*Rv0450c*) and other linked genes that plays a role in iron-scavenging by functioning as siderophores export pumps together with *mmpS4* and *mmpL5* – *mmpS5* in *M. tuberculosis.*

Transcription regulation predominantly directs and brings balance in the transcriptome profile by means of rapidly driving and regulating gene expression. Our transcriptomic data revealed the overexpression of genes involved in regulatory proteins; of significant up-regulation of *whiB7* (FDR: 2,48E-03), *whiB6* (FDR: 5,00E-03) and *whiB1* (FDR: 3,73E-03) in $K636^{WT}$ relative to $K636^{RIF}$ (with *rpoB* mutation) *M. tuberculosis* strains (refer to Table 3.11). *WhiB7*, *whiB6* and *whiB1* forms part of the seven *whiB*-like family genes that are distinctive to *Actinomycetes* (72–75). They are known to play essential roles in cell adaption, physiology and cell division of *M. tuberculosis* (76). Therefore, the up-regulation of these genes is indicative of the transcriptional physiological changes influenced by the presence of *rpoB* mutation in $K636^{RIF}$ compared to $K636^{WT}$ *M. tuberculosis* strains. *WhiB1* plays an essential role as a transcriptional repressor under *in vivo* conditions and is co-expressed with *whiB7* transcriptional activator (76,77). Moreover, *whiB1* is set to possess a [4Fe-4S]2+ cluster that is sensitive to nitric oxide which is produced by infected lung macrophages (77,78). Therefore the up-regulation of *whiB1* is indicative of its involvement in activating dormancy signals, which may lead to latency in resistant *M. tuberculosis* strains (79). *WhiB6* and *whiB5* are involved in macrophage infection and virulence (80). *WhiB6* (regulated by MntR) regulates *espACD* and some *devR* (formerly known as *dosR*) regulated genes (81). This is

interesting, because *devR* is the main regulator of dormancy and *espACD* is involved in pore formation (58). A previous study in *M. marinum* showed that apo-WhiB6 induces the *devR* regulon, which results in the suppression of ESX-1, while the *whiB6* [4Fe-4S]2+ cluster negatively controls the *devR* regulon and positively controls the ESX-1 secretion system (81). It is tempting to speculate that the up-regulation of *whiB6* influenced by the presence of the *rpoB* mutation might cause K636^{RIF} *M. tuberculosis* to go into a dormancy state as part of survival strategy.

Previous studies have shown *M. tuberculosis* to auto-regulate *whiB7* expression in the presence of RIF(76). Furthermore, it was previously revealed that the overexpression of *whiB7* results in increased drug resistance, while its deletion results in increased drug susceptibility (67). Therefore, the up-regulation of *whiB7* in K636^{WT} relative to K636^{RIF} *M. tuberculosis* strains could contribute to intrinsic resistance in *M. tuberculosis* (82). This explains the significant physiological role *whiB7* plays in *M. tuberculosis*, in both strengthening the intrinsic resistance of cells and maintaining low level drug resistance (82,83). Interestingly, the overexpression of *whiB7* and *Rv1258c* was reported in MDR *M. tuberculosis* clinical strains treated with INH and RIF (84,85). Therefore, it can be speculated that the upregulation of *whiB7* in K636^{WT} relative to K636^{RIF} *M. tuberculosis* strains is indicative of the role that *whiB7* plays in the mechanism of *M. tuberculosis* drug resistance.

Another transcriptional regulator, *Rv0078* was significantly up-regulated (FDR: 3,05E-03) in K636^{WT} relative to K636^{RIF} (with *rpoB* mutation) *M. tuberculosis* strains (refer to Table 3.11). *Rv0078* is a transcriptional repressor and its up-regulation of *Rv0078* suggests an underlying mechanism of resistance in the resistant *M. tuberculosis* strains, as *Rv0078* is mostly induced upon drug treatment. It forms part of the TetR family transcriptional regulators; a family of proteins that regulate a large array of cellular activities, including multidrug resistance, carbon catabolism and virulence (86). Additionally, STRING networks show a relationship between expression of *Rv0078, Rv0077* and *ethR* (87). Therefore, it could further be speculated that the presence of the *rpoB* mutation had an effect on the *Rv0078* expression; however this remains to be further explored. This suggests that *Rv0078* might play an important role in the physiology of K636^{WT} and K636^{RIF} *M. tuberculosis* strains.

3.4.6 INH treatment had no effect on the transcriptomic profiles of K636^{WT} and K636^{RIF} *M. tuberculosis* strains (group C and D)

The assessment of the effect of INH treatment on transcriptional profiles in Group C [K636^{WT} (treated*) vs K636^{WT} (untreated)] and group D [K636^{RIF} (treated*) vs K636^{RIF} (untreated) (Group D)] revealed no significantly differentially expressed genes (refer to Table 3.8). To investigate this discrepancy we performed a RNA-Seq data analysis check and there were no significant differences in gene expression. Hence, the subsequent analysis and discussion were focused on genes that were significantly differentially expressed in group A and B. As a consequence, we could not confirm the effect of INH treatment on transcriptional profiles of INH treated *M. tuberculosis* strains, making this one of our study limitations. It was demonstrated in the current study that 0.05 µg/ml INH induces the high-level up-regulation of *kasA* (≥ 2-fold) and *accD6* (≥ 2-fold) in K636^{WT} *M. tuberculosis* strain (see discussion 3.4.1), even though it did not induce transcriptional responses in this case. For this reason, maybe we should have exposed for 48h instead of 24h as well, since it was clear the exposure of *M. tuberculosis* strains to 0.05 µg/ml INH resulted in an increase in inhibition of bacterial growth over time. Future work would be to conduct similar RNA-Seq experiments, treating the *M. tuberculosis* strains with the optimized 0.05 µg/ml INH but for a longer time period (28h) and then to reassess the effect of INH treatment on transcriptional profiles of INH treated *M. tuberculosis* strains.

3.5 Conclusion

In conclusion, the current study confirmed the effect of genetic background and the effect the resistance-conferring mutation (*rpoB* Ser531Leu mutation) on transcriptional profiles of various *M. tuberculosis* strains. This was demonstrated by identified 348 genes found to be significantly differentially expressed between K636^{WT} vs H37Rv^{WT} *M. tuberculosis* strains. Additionally, 192 genes found to be significantly differentially expressed between K636^{WT} vs K636^{RIF} *M. tuberculosis* strains. The differential gene expression between K636^{WT} vs H37Rv^{WT} and between K636^{WT} vs K636^{RIF} showed the up-regulation and down-regulation of cell wall and regulatory genes; which play a role in transcription regulation and *M. tuberculosis* survival under stressful conditions. These findings broadened our knowledge about molecular mechanisms and genes involved in the physiology of RIF resistant (K636^{RIF}) and susceptible (K636^{WT} and H37Rv^{WT}) *M. tuberculosis* strains. The latter knowledge, if further extrapolated can help provide more insight on the identification of potential anti-TB drug targets. In the current study, we were only able to use differential gene expression data

obtained from two biological samples, one of our limitations. We investigated why the specific biological sample did not work and discovered that there were some differences in the number of reads between this specific biological sample and the other two that worked well. For this reason, normalization is recommended as it can account for some of the differences, nevertheless not for all differences.

3.6 References

1. **Yew WW, Lange C, Leung CC.** 2011. Treatment of tuberculosis: update 2010. Eur Respir J. **37**:441–62.

2. **Somoskovi A, Parsons LM, Salfinger M.** 2001. The molecular basis of resistance to isoniazid, rifampin, and pyrazinamide in *Mycobacterium tuberculosis.* Respir Res. **2**:164.

3. **Wilson M, DeRisi J, Kristensen H-H, Imboden P, Rane S, Brown PO, *et al.*** 1999. Exploring drug-induced alterations in gene expression in *Mycobacterium tuberculosis* by microarray hybridization. Proc Natl Acad Sci USA. **96**:12833–8.

4. **Waddell SJ, Stabler RA, Laing K, Kremer L, Reynolds RC, Besra GS.** 2004. The use of microarray analysis to determine the gene expression profiles of *Mycobacterium tuberculosis* in response to anti-bacterial compounds. Tuberculosis. **84**:263–74.

5. **Niki M, Niki M, Tateishi Y, Ozeki Y, Kirikae T, Lewin A, *et al.*** A Novel mechanism of growth phase-dependent tolerance to isoniazid in mycobacteria. J Biol Chem. **287**:27743–52.

6. **Betts JC, McLaren A, Lennon MG, Kelly FM, Lukey PT, Blakemore SJ, *et al.*** 2003. Signature gene expression profiles discriminate between isoniazid-, thiolactomycin-, and triclosan-treated *Mycobacterium tuberculosis*. Antimicrob Agents Chemother. **47**:2903–13.

7. **Alland D, Kramnik I, Weisbrod TR, Otsubo L, Cerny R, Miller LP, *et al.*** 1998. Identification of differentially expressed mRNA in prokaryotic organisms by customized amplification libraries (DECAL): the effect of isoniazid on gene expression in *Mycobacterium tuberculosis.* Proc Natl Acad Sci USA. **95**:13227–32.

8. **Vilchèze C, Jacobs WR.** 2007. The mechanism of isoniazid killing: clarity through the scope of genetics. Annu Rev Microbiol. **61**:35–50.

9. **Niemann S, Supply P.** 2014. Diversity and evolution of *Mycobacterium tuberculosis*: moving to whole-genome-based approaches. Cold Spring Harb Perspect Med.

10. **Al-Ghafli H, Kohl TA, Merker M, Varghese B, Halees A, Niemann S, *et al.*** 2018. Drug-resistance profiling and transmission dynamics of multidrug-resistant *Mycobacterium tuberculosis* in Saudi Arabia revealed by whole genome sequencing. Infect Drug Resist. **11**:2219–29.

11. **Holt KE, McAdam P, Thai PVK, Thuong NTT, Ha DTM, Lan NN, *et al.*** 2018. Frequent transmission of the *Mycobacterium tuberculosis* Beijing lineage and positive selection for the EsxW Beijing variant in Vietnam. Nat Genet. **50**:849–56.

12. **European Concerted Action.** 2006. New generation genetic markers and techniques for the epidemiology and control of tuberculosis. Beijing/W genotype *Mycobacterium tuberculosis* and drug resistance. Emerg Infect Dis. **12**:736–43.

13. **Ramazanzadeh R, Sayhemiri K.** 2014. Prevalence of Beijing family in *Mycobacterium tuberculosis* in world population: systematic review and meta-analysis. Int J Mycobacteriology. **3**:41–5.

14. **Niemann S, Diel R, Khechinashvili G, Gegia M, Mdivani N, Tang Y-W**. 2010. *Mycobacterium tuberculosis* Beijing lineage favors the spread of multidrug-resistant tuberculosis in the republic of Georgia. J Clin Microbiol. **48**:3544–50.

15. **Cole ST, Brosch R, Parkhill J, Garnier T, Churcher C, Harris D, *et al.*** 1998. Deciphering the biology of *Mycobacterium tuberculosis* from the complete genome sequence. Nature. **393**:537–44.

16. **Betts JC. 2002.** Transcriptomics and proteomics: tools for the identification of novel drug targets and vaccine candidates for tuberculosis. IUBMB Life. **53**:239–42.

17. **Leisching G, Pietersen R-D, van Heerden C, van Helden P, Wiid I, Baker B.** 2016. RNAseq reveals hypervirulence-specific host responses to *M. tuberculosis* infection. Virulence. **8**:848–58.

18. **Welzen L de, Eldholm V, Maharaj K, Manson AL, Earl AM, Pym AS.** 2017. Whole-transcriptome and -genome analysis of extensively drug-resistant *Mycobacterium tuberculosis* clinical isolates identifies downregulation of *ethA* as a mechanism of ethionamide resistance. Antimicrob Agents Chemother. **61**:01461-17.

19. **Deep A, Tiwari P, Agarwal S, Kaundal S, Kidwai S, Singh R, *et al.*** 2018. Structural, functional and biological insights into the role of *Mycobacterium tuberculosis VapBC11* toxin–antitoxin system: targeting a tRNase to tackle mycobacterial adaptation. Nucleic Acids Res. **46**:11639–55.

20. **Yu G, Cui Z, Sun X, Peng J, Jiang J, Wu W, *et al.*** 2015. Gene expression analysis of two extensively drug-resistant tuberculosis isolates show that two-component response systems enhance drug resistance. Tuberculosis. **95**:303–14.

21. **Finotello F, Di Camillo B.** 2015. Measuring differential gene expression with RNA-seq: challenges and strategies for data analysis. Brief Funct Genomics. **14**:130–42.

22. **Nagalakshmi U, Wang Z, Waern K, Shou C, Raha D, Gerstein M, *et al.*** The 2008. transcriptional landscape of the yeast genome defined by RNA sequencing. Science. **320**:1344–9.

23. **Warren R, de Kock M, Engelke E, Myburgh R, Gey van Pittius N, Victor T, *et al.*** 2006. Safe *Mycobacterium tuberculosis* DNA extraction method that does not compromise integrity. J Clin Microbiol. **44**:254–6.

24. **Dippenaar A, Parsons SDC, Sampson SL, van der Merwe RG, Drewe JA, Abdallah AM, *et al.*** 2015. Whole genome sequence analysis of *Mycobacterium suricattae*. Tuberc Edinb Scotl. **95**:682–8.

25. **Babraham Bioinformatics** - FastQC a quality control tool for high throughput sequence data.

26. **Bolger AM, Lohse M, Usadel B.** 2014. Trimmomatic: a flexible trimmer for Illumina sequence data. Bioinforma Oxf Engl. **30**:2114–20.

27. **USADELLAB.org** - Trimmomatic: A flexible read trimming tool for Illumina NGS data.

28. **Li H, Durbin R.** 2009. Fast and accurate short read alignment with Burrows-Wheeler transform. Bioinforma Oxf Engl. **25**:1754–60.

29. **Ponstingl H, Ning.** 2010. SMALT – A new mapper for DNA sequencing reads . F1000Research.

30. **McKenna A, Hanna M, Banks E, Sivachenko A, Cibulskis K, Kernytsky A, *et al.*** 2010. The Genome Analysis Toolkit: A MapReduce framework for analyzing next-generation DNA sequencing data. Genome Res. **20**:1297–303.

31. **Lew JM, Kapopoulou A, Jones LM, Cole ST**. 2011. TubercuList--10 years after. Tuberc Edinb Scotl. **91**:1–7.

32. **Siddiqi S, Ahmed A, Asif S, Behera D, Javaid M, Jani J, *et al.*** 2012. Direct drug susceptibility testing of *Mycobacterium tuberculosis* for rapid detection of multidrug resistance using the Bactec MGIT 960 System: a multicenter study. J Clin Microbiol. **50**:435–40.

33. **Springer B, Lucke K, Calligaris-Maibach R, Ritter C, Böttger EC.** 2009. Quantitative drug susceptibility testing of *Mycobacterium tuberculosis* by use of MGIT 960 and EpiCenter instrumentation. J Clin Microbiol. **47**:1773–80.

34. **Jahn CE, Charkowski AO, Willis DK.** 2008. Evaluation of isolation methods and RNA integrity for bacterial RNA quantitation. J Microbiol Methods. **75**:318–24.

35. **Karakousis PC, Williams EP, Bishai WR.** 2008. Altered expression of isoniazid-regulated genes in drug-treated dormant *Mycobacterium tuberculosis.* J Antimicrob Chemother. **61**:323–31.

36. **Hu Y, Coates ARM.** 1999. Transcription of two sigma 70 homologue genes, *sigA* and *sigB*, in stationary-phase *Mycobacterium tuberculosis*. J Bacteriol. **181**:469–76.

37. **Livak KJ, Schmittgen TD.** 2001. Analysis of relative gene expression data using real-time quantitative PCR and the 2(-Delta Delta C (T)) method. Methods. **25**:402–8.

38. **Bustin SA, Benes V, Garson JA, Hellemans J, Huggett J, Kubista M, *et al.*** 2009. The MIQE guidelines: minimum information for publication of quantitative real-time PCR experiments. Clin Chem. **55**:611–22.

39. **Trapnell C, Hendrickson DG, Sauvageau M, Goff L, Rinn JL, Pachter L.** 2013. Differential analysis of gene regulation at transcript resolution with RNA-seq. Nat Biotechnol. **31**:46–53.

40. **Robinson MD, McCarthy DJ, Smyth GK. 2010.** *edgeR*: a Bioconductor package for differential expression analysis of digital gene expression data. Bioinforma Oxf Engl. **26**:139–40.

41. **Zheng Q, Wang X-J.** 2008. GOEAST: a web-based software toolkit for Gene Ontology enrichment analysis. Nucleic Acids Res. **36**:358-363.

42. J**ohnson R, Streicher EM, Louw GE, Warren RM, van Helden PD, Victor TC.** 2006. Drug resistance in *Mycobacterium tuberculosis*. Curr Issues Mol Biol. **78**:97–111.

43. **McCarthy DJ, Chen Y, Smyth GK.** 2012. Differential expression analysis of multifactor RNA-Seq experiments with respect to biological variation. Nucleic Acids Res **40**:4288–97.

44. **Zheng Q, Wang X-J.** 2009. GOEAST: a web-based software toolkit for Gene Ontology enrichment analysis. Nucleic Acids Res. 36:W358–63.

45. **Waddell SJ, Laing K, Senner C, Butcher PD.** 2008. Microarray analysis of defined *Mycobacterium tuberculosis* populations using RNA amplification strategies. BMC Genomics. **9**:94.

46. **Johnson R.** 2007. Understanding the mechanisms of drug resistance in enhancing rapid molecular detection of drug resistance in *Mycobacterium tuberculosis*. Thesis. Stellenbosch : University of Stellenbosch;

47. **Braibant M, Gilot P, Content J.** 2000. The ATP binding cassette (ABC) transport systems of *Mycobacterium tuberculosis*. FEMS Microbiol Rev. **24**:449–67.

48. **Gouzy A, Poquet Y, Neyrolles O.** 2014. Nitrogen metabolism in *Mycobacterium tuberculosis* physiology and virulence. Nat Rev Microbiol. **12**:729–37.

49. **Borah K, Beyß M, Theorell A, Wu H, Basu P, Mendum TA, *et al.*** 2019. Intracellular *Mycobacterium tuberculosis* exploits multiple host nitrogen sources during growth in human macrophages. Cell Rep. **29**:3580-3591.

50. **Bespyatykh J, Shitikov E, Butenko I, Altukhov I, Alexeev D, Mokrousov I, *et al.* 2016.** Proteome analysis of the *Mycobacterium tuberculosis* Beijing B0/W148 cluster. Sci Rep. **6:**28985.

51. **Bosserman RE, Nguyen TT, Sanchez KG, Chirakos AE, Ferrell MJ, Thompson CR, *et al.*** 2017. *WhiB6* regulation of *ESX-1* gene expression is controlled by a negative feedback loop in *Mycobacterium marinum.* Proc Natl Acad Sci. **114**:E10772–81.

52. **Solomonson M, Setiaputra D, Makepeace KAT, Lameignere E, Petrotchenko EV, Conrady DG, *et al.*** 2015. Structure of *espB* from the ESX-1 type VII secretion system and insights into its export mechanism. Struct Lond Engl 1993. **23**:571–83.

53. **Raghavan S, Manzanillo P, Chan K, Dovey C, Cox JS.** 2008. Secreted transcription factor controls *Mycobacterium tuberculosis* virulence. Nature. **454**:717–21.

54. **Anil Kumar V, Goyal R, Bansal R, Singh N, Sevalkar RR, Kumar A, *et al.*** 2016. *EspR*-dependent ESAT-6 protein secretion of *Mycobacterium tuberculosis* requires the presence of virulence regulator PhoP. J Biol Chem. **291**:19018–30.

55. **Minch KJ, Rustad TR, Peterson EJR, Winkler J, Reiss DJ, Ma S, *et al.*** 2015. The DNA-binding network of *Mycobacterium tuberculosis.* Nat Commun. **6**:5829.

56. **Solans L, Aguiló N, Samper S, Pawlik A, Frigui W, Martín C, *et al.*** 2014. A specific polymorphism in *Mycobacterium tuberculosis* H37Rv causes differential ESAT-6 expression and identifies WhiB6 as a novel ESX-1 component. Infect Immun. **82**:3446–56.

57. **Rustad TR, Minch KJ, Ma S, Winkler JK, Hobbs S, Hickey M, *et al.*** 2014. Mapping and manipulating the *Mycobacterium tuberculosis* transcriptome using a transcription factor overexpression-derived regulatory network. Genome Biol. **15**:502.

58. **Chen Z, Hu Y, Cumming BM, Lu P, Feng L, Deng J, *et al.*** 2016. Mycobacterial WhiB6 differentially regulates ESX-1 and the Dos regulon to modulate granuloma formation and virulence in zebrafish. Cell Rep. **16**:2512–24.

59. **Feltcher ME, Sullivan JT, Braunstein M.** 2010. Protein export systems of *Mycobacterium tuberculosis*: novel targets for drug development? Future Microbiol. **5**:1581–97.

60. **Bitter W, Houben ENG, Bottai D, Brodin P, Brown EJ, Cox JS, *et al.*** 2009. Systematic genetic nomenclature for Type VII secretion systems. PLoS Pathog. **5**:1000507.

61. **Sreejit G, Ahmed A, Parveen N, Jha V, Valluri VL, Ghosh S, *et al.*** 2014. The ESAT-6 protein of *Mycobacterium tuberculosis* interacts with Beta-2-Microglobulin (β2M) affecting antigen presentation function of macrophage. PLOS Pathog. **10**:1004446.

62. **Hsu T, Hingley-Wilson SM, Chen B, Chen M, Dai AZ, Morin PM, *et al.*** 2003. The primary mechanism of attenuation of bacillus Calmette-Guerin is a loss of secreted lytic function required for invasion of lung interstitial tissue. Proc Natl Acad Sci USA. **100**:12420–5.

63. **Gey Van Pittius NC, Gamieldien J, Hide W, Brown GD, Siezen RJ, Beyers AD.** 2001. The ESAT-6 gene cluster of *Mycobacterium tuberculosis* and other high G+C Gram-positive bacteria. Genome Biol. **2**:0044.

64. **Pym AS, Brodin P, Majlessi L, Brosch R, Demangel C, Williams A, *et al.* 2003.** Recombinant BCG exporting ESAT-6 confers enhanced protection against tuberculosis. Nat Med. **9**:533–9.

65. **Domenech P, Reed MB, Barry CE.** 2005. Contribution of the *Mycobacterium tuberculosis* MmpL protein family to virulence and drug resistance. Infect Immun. 73:3492–501.

66. V**arela C, Rittmann D, Singh A, Krumbach K, Bhatt K, Eggeling L, *et al.*** 2012. MmpL genes are associated with mycolic acid metabolism in mycobacteria and corynebacteria. Chem Biol. **19**:498–506.

67. **Minnikin DE, Kremer L, Dover LG, Besra GS.** 2002. The methyl-branched fortifications of *Mycobacterium tuberculosis*. Chem Biol. **9**:545–53.

68. **Wells RM, Jones CM, Xi Z, Speer A, Danilchanka O, Doornbos KS, *et al.*** 2013. Discovery of a siderophore export system essential for virulence of *Mycobacterium tuberculosis.* PLoS Pathog. **9**:1003120.

69. R**ichard M, Gutiérrez AV, Viljoen AJ, Ghigo E, Blaise M, Kremer L.** 2018. mechanistic and structural insights into the unique TetR-dependent regulation of a drug efflux pump in *Mycobacterium abscessus*. Front Microbiol.

70. **Delmar JA, Chou T-H, Wright CC, Licon MH, Doh JK, Radhakrishnan A, *et al.*** Structural basis for the regulation of the MmpL transporters of *Mycobacterium tuberculosis*. J Biol Chem **290**:28559–74.

71. **de Knegt GJ, Bruning O, ten Kate MT, de Jong M, van Belkum A, Endtz HP, *et al.*** 2013. Rifampicin-induced transcriptome response in rifampicin-resistant *Mycobacterium tuberculosis.* Tuberc Edinb Scotl. **93**:96–101.

72. **Larsson C, Luna B, Ammerman NC, Maiga M, Agarwal N, Bishai WR.** 2012. Gene expression of *Mycobacterium tuberculosis* putative transcription factors *whiB1-7* in redox environments. PLoS ONE. **7**:37516.

73. **Jakimowicz P, Cheesman MR, Bishai WR, Chater KF, Thomson AJ, Buttner MJ**. 2005. Evidence that the *Streptomyces* developmental protein WhiD, a member of the WhiB family, binds a [4Fe-4S] cluster. J Biol Chem. **280**:8309–15.

74. **Crack J, Green J, Thomson AJ.** 2004. Mechanism of oxygen sensing by the bacterial transcription factor fumarate-nitrate reduction (FNR). J Biol Chem. **279**:9278–86.

75. **Kiley PJ, Beinert H.** 1998. Oxygen sensing by the global regulator, FNR: the role of the iron-sulfur cluster. FEMS Microbiol Rev. **22**:341–52.

76. **Burian J, Yim G, Hsing M, Axerio-Cilies P, Cherkasov A, Spiegelman GB, *et al.*** 2013. The mycobacterial antibiotic resistance determinant w*hiB7* acts as a transcriptional activator by binding the primary sigma factor *sigA* (RpoV). Nucleic Acids Res. **41**:10062–76.

77. **Smith LJ, Stapleton MR, Fullstone GJM, Crack JC, Thomson AJ, Le Brun NE, *et al.*** 2010. *Mycobacterium tuberculosis* WhiB1 is an essential DNA-binding protein with a nitric oxide-sensitive iron-sulfur cluster. Biochem J. **432**:417–27.

78. **Stapleton MR, Smith LJ, Hunt DM, Buxton RS, Green J.** 2012. *Mycobacterium tuberculosis* WhiB1 represses transcription of the essential chaperonin GroEL2. Tuberc Edinb Scotl. 92:328–32.

79. **Voskuil MI, Schnappinger D, Visconti KC, Harrell MI, Dolganov GM, Sherman DR, et al.** 2003. Inhibition of respiration by nitric oxide induces a *Mycobacterium tuberculosis* dormancy program. J Exp Med. **198**:705–13.

80. **Casonato S, Cervantes Sánchez A, Haruki H, Rengifo González M, Provvedi R, Dainese E, *et al*.** 2012. WhiB5, a transcriptional regulator that contributes to *Mycobacterium tuberculosis* virulence and reactivation. Infect Immun. **80**:3132–44.

81. **Pang X, Samten B, Cao G, Wang X, Tvinnereim AR, Chen X-L, *et al*.** 2013. MprAB regulates the *espA* operon in *Mycobacterium tuberculosis* and modulates ESX-1 function and host cytokine response. J Bacteriol. **195**:66–75.

82. **Burian J, Ramón-García S, Howes CG, Thompson CJ**. 2012. WhiB7, a transcriptional activator that coordinates physiology with intrinsic drug resistance in *Mycobacterium tuberculosis*. Expert Rev Anti Infect Ther. **10:**1037–47.

83. **Morris RP, Nguyen L, Gatfield J, Visconti K, Nguyen K, Schnappinger D, *et al.*** 2005. Ancestral antibiotic resistance in *Mycobacterium tuberculosis*. Proc Natl Acad Sci USA. **102**:12200–5.

84. **Ramón-García S, Martín C, Aínsa JA, Rossi ED. 2006**. Characterization of tetracycline resistance mediated by the efflux pump Tap from *Mycobacterium fortuitum*. J Antimicrob Chemother. **57**:252–9.

85. **Ramón-García S, Mick V, Dainese E, Martín C, Thompson CJ, De Rossi E, *et al.*** 2012. Functional and genetic characterization of the Tap efflux pump in *Mycobacterium bovis* BCG. Antimicrob Agents Chemother. **56**:2074–83.

86. **Balhana RJC, Singla A, Sikder MH, Withers M, Kendall SL.** 2015. Global analyses of TetR family transcriptional regulators in mycobacteria indicates conservation across species and diversity in regulated functions. BMC Genomics.

87. **Rv0078 protein** (*Mycobacterium tuberculosis* H37Rv) - STRING interaction network. https://string-db.org/network/83332.Rv0078

CHAPTER 4

Evaluation of host immune response to genetically resistant and susceptible *Mycobacterium tuberculosis* strains in a RAW264.7 macrophage model

---

My contribution:

- Project planning
- Bacterial strain culturing and tissue culture
- Macrophage infections experiments
- Sample preparation
- Luminex assay and ELISA with the assistance of immunology group
- Interpretation of results
- Statistical analysis in consultation with a statistician
- Writing and editing of the chapter

4.1 Introduction

Transmission of MDR- and XDR-TB and the ineffectiveness of the *M. bovis* BCG vaccine necessitates an in-depth evaluation of the host-pathogen interaction and the associated factors that could contribute to prolonged treatment, TB disease outcome and differences in transmission (1–3). The ability of *Mycobacterium tuberculosis* to evade killing mechanisms of macrophages is critical to the pathogen's survival upon infection (4). The stages of infection are determined by the ability of the host's innate and adaptive immune systems to eradicate or control *M. tuberculosis* (5). A wide range of specific and nonspecific host immune responses contribute to the differential outcomes of exposure and infection (5). These include the secretion of cytokines and chemokines essential for the activation of macrophages, which function to detect and destroy pathogens, including *M. tuberculosis* (5). Macrophages are the first line of defence in the lungs when *M. tuberculosis* is encountered (5), therefore the innate immune response of macrophages plays an essential role in host defence (5,6). Ingestion of mycobacteria by macrophages induces the release of pro-inflammatory cytokines and chemokines, which leads to the induction of an adaptive immune response (6). Failure to activate macrophages results in the inability to contain and kill *M. tuberculosis* and this subsequently leads to overt disease followed by transmission (4,5).

Literature shows that different *M. tuberculosis* strains exhibit differences in virulence/immunogenicity and antibiotic susceptibility (7–9). Various studies have shown that infection of human macrophages with genetically different *M. tuberculosis* strains from distinct lineages, such as CDC1551 and Erdman and the laboratory (lab) strains H37Rv and H37Ra results in statistically significant difference in cytokines and chemokines secretion (10–13). In addition, infection with genetically distinct *M. tuberculosis* strains induce variable host responses in different host cells, such as THP-1 cells, human monocytes and cell lines (10,14,15). The infection (48h) of human peripheral blood monocyte-derived macrophages (MDM) (isolated from active TB patients and healthy volunteers) with H37Rv, H37Ra lab strains and clinical MDR *M. tuberculosis* strain resulted in increased secretion levels of interleukin (IL-12), using enzyme-linked immunosorbent assay (ELISA) (3). Previous studies reported that *M. tuberculosis* Beijing strains elicit a reduced pro-inflammatory Th_1 type cytokine response in macrophages and peripheral blood mononuclear cells (PBMCs) compared to non-Beijing strains and *M. tuberculosis* H37Rv (11,16). In addition, previous reports demonstrate the differential secretion of tumour necrosis factor-alpha (TNF-γ) and interferon-gamma (IFN-γ) after infection with susceptible *M. bovis* BCG,

M. tuberculosis H37Rv and *M. tuberculosis* clinical strains (10,11). These findings suggest that the genetic differences in *M. tuberculosis* strains play a fundamental role in the host-pathogen interaction and cytokine/chemokine response.

Few studies have reported about macrophage response to drug resistant *M. tuberculosis* strains (17). The aim of the current study was to characterise the cytokine and chemokine profile of RAW264.7 macrophages following infection with a pan-susceptible clinical progenitor from the Beijing family ($K636^{WT}$), an *in vitro* rifampicin (RIF) resistant *M. tuberculosis* strain, harbouring the Ser531Leu mutation in *rpoB* gene, derived from the pan-susceptible clinical strain ($K636^{RIF}$), the laboratory strain ($H37Rv^{WT}$) and the *in vitro* RIF resistant *M. tuberculosis* strain, harbouring the Ser531Leu mutation in *rpoB* gene, derived from the laboratory strain ($H37Rv^{RIF}$).

We **hypothesised** that the infection of RAW264.7 macrophages with clinical *M. tuberculosis* strains from the Beijing family (susceptible ($K636^{WT}$) and RIF resistant ($K636^{RIF}$)) with *rpoB* Ser531Leu mutation, susceptible laboratory strain ($H37Rv^{WT}$) and resistant laboratory strain ($H37Rv^{RIF}$) with the *rpoB* Ser531Leu mutation, would result in differential secretion of murine cytokines and chemokines. The **objective** of this study was to determine the secretion of the cytokines (TNF-α, IL-1 beta (IL-1β), IL-10, IFN-γ, IL-4, IL-6 and IL-12 subunit p40 (IL-12p40) and chemokines ((granulocyte-macrophage colony-stimulating factor (GM-CSF), chemokine (C-C motif) ligand 5 (RANTES/CCL5) and chemokine (C-C motif) ligand 2 (MCP-1)) by macrophages following infection with $K636^{WT}$, $K636^{RIF}$, $H37Rv^{WT}$ and $H37Rv^{RIF}$ *M. tuberculosis* strains. The results from these analyses provided insightful knowledge about the function of the RAW264.7 macrophage in response to infection with these strains and how *M. tuberculosis* survived the host immunity. Multiplex and ELISA analyses provided an indication of essential secreted cytokines and chemokines that can aid in determining and designing novel TB detection biomarkers. Additionally, the presence of Ser531Leu *rpoB* mutation in the RIF resistant *M. tuberculosis* strains provided information on how an altered mycobacterial physiology may influence the host pathogen interaction.

4.2 Materials and methods

4.2.1 Mycobacterial strain selection and culture conditions

A clinical $K636^{WT}$ *M. tuberculosis* strain was selected from the Beijing family that is prevalent in the Western Cape region, as described in Chapter 3. A $K636^{RIF}$ *in vitro* mutant (harbouring the *rpoB* Ser531Leu mutation) derived from the $K636^{WT}$ strain was selected

(Table 4.1). The *rpoB* Ser531Leu mutation is known to frequently occur in RIF resistant clinical strains (18). In addition, H37Rv^{WT} [American Type Culture Collection (ATCC 27294)] (ATCC, Johannesburg, South Africa) and H37Rv^{RIF} *in vitro* mutant (harbouring the *rpoB* Ser531Leu mutation), derived from the H37Rv^{WT} strain were also selected. A volume of 1 ml freezer stocks of each *M. tuberculosis* strains (K636^{WT}, K636^{RIF}, H37Rv^{WT} and H37Rv^{RIF}) were subcultured in 9 ml 7H9 Middlebrook medium (BD Biosciences, New Jersey, USA), supplemented with 10% Oleic acid-albumin-dextrose-catalase (OADC), 0.2% (v/v) glycerol (Merck Laboratories, Cape Town, SA) and 0.05% Tween 80 (BD Biosciences) (7H9-OGT) in filtered screw cap tissue culture flasks (Greiner Bio-one, Maybachstreet, Germany). These sub-cultures were incubated at 37°C without shaking until an optical density (OD_{600nm}) of 0.7- 0.8 was reached. The OD_{600nm} was measured on the spectrophotometer by taking an OD_{600nm} reading of 7H9-OGT for the blank sample and followed by the OD_{600nm} reading of the tested culture sample. These cultures were assessed for contamination by Ziehl Nielsen staining and culturing on blood agar plates. Glass beads and glycerol stocks (1:1 v/v, 500 µl culture and 500 µl 50% glycerol) were prepared, following similar procedures as described in chapter 3 (material and methods) and stored at -80°C.

Table 4.3 Mycobacterial strains used in this study

Name of strains	**Description**	**Source/Reference**
***M. tuberculosis* K636 ^{WT} (denoted to as K636^{WT})**	*M. tuberculosis* susceptible clinical strain from the Beijing Family Cluster 203	In-house strain collection
***M. tuberculosis* K636 ^{RIF} (denoted to as K636^{RIF})**	*M. tuberculosis in vitro* generated RIF resistant mutant, derived from the clinical strain, harbouring the Ser531Leu mutation in the *rpoB* gene	A kind gift from Dr M de Vos
***M. tuberculosis* H37Rv (ATCC 27294) (denoted to as H37Rv^{WT})**	*M. tuberculosis* laboratory strain	In-house strain collection
***M. tuberculosis* H37Rv^{RIF} (denoted to as H37Rv^{RIF})**	*M. tuberculosis in vitro* generated RIF resistant mutant, derived from the lab strain, harbouring the Ser531Leu mutation in the *rpoB* gene	A kind gift from Dr M de Vos

4.2.2 Techniques used to assess cytokines/chemokines response:

Luminex x multi-analyte profiling (xMAP) technology: Luminex xMAP and the Bio-Plex Pro Mouse Cytokine 1 10plex Bio-Rad kit (Bio-Rad Laboratories, Switzerland) were used to measure cytokine and chemokine secretion in the current study. This luminex technology is a combination of flow cytometry, digital signal processing, biological chemistry and microsphere tools, based on the use of polystyrene or paramagnetic 5.6-micron microspheres (beads) that are dyed internally with red and infrared fluorophores of different intensities (19). A bead region is assigned to each dyed bead and this allows for individual differentiation of the beads that are coated with antibodies, receptors, peptides and streptavidin specific for an analyte. Multiple analyte specific beads can therefore be incubated with a small heterogeneous sample volume to allow capturing and detection in a 96 well microplate.

ELISA: A 96-well plate-based assay ELISA technique and mouse IFN-gamma, TNF-alpha and RANTES Quantikine ELISA kits (Whitehead Scientific, Stickland, South Africa) were exploited to validate and assess the secretion of selected cytokine and chemokine analytes (TNF-α, IFN-γ and RANTES). Briefly, in ELISA, an antigen is immobilized on a solid surface and then complexed with an antibody that is linked to an enzyme. Detection is accomplished by assessing the conjugated enzyme activity via incubation with a substrate to produce a measureable product (20).

4.2.3 Mammalian cell culture conditions and macrophage infection

The RAW264.7 murine macrophage cell line selected for infection experiments was obtained from the ATCC TIB-71. RAW264.7 macrophages were cultured and prepared for infection with *M. tuberculosis*. Briefly, the RAW264.7 macrophage cell line was cultured in monolayers in Dulbecco's Modified Eagle Medium (DMEM) (Sigma-Aldrich, St Louis, Missouri, USA) containing heat-inactivated 10% fetal bovine serum (FBS) (Sigma-Aldrich) (D10) in 75 cm^2 cell culture flasks and visualized under a light microscope to assess confluency and cell quality before incubation in a 5% CO_2 incubator at 37^0C (Figure 4.1).

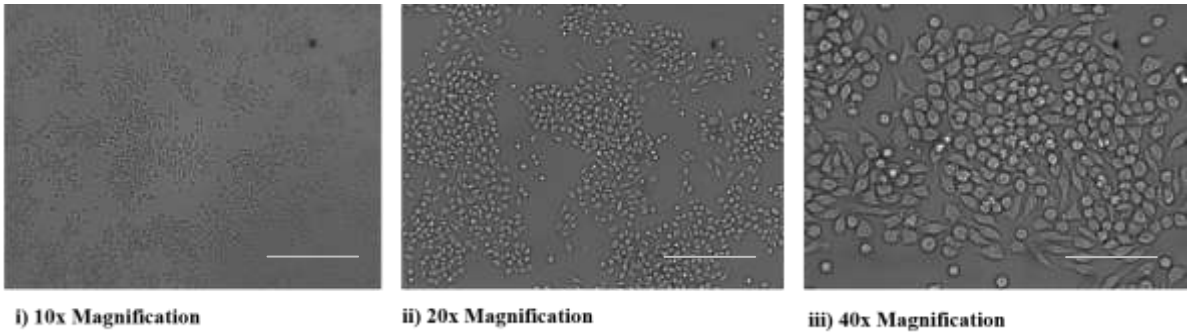

Figure 4.5 Microscopic images of the RAW264.7 macrophage cell line at (i) 10x, ii) 20x and, iii) 40x magnifications. The RAW264.7 macrophages were cultured in D10, incubated in a 5% CO_2 incubator at 37^0C in 75 cm^2 culture flasks and passaged every 2 -3 days. The scale bar: 0.2 µm. The images were taken the day before infection with *M. tuberculosis*.

Subsequently, the cells were inspected daily to assess confluency and passaged every 2-3 days to maintain healthy cells. One day prior to infection, RAW264.7 macrophages (5 x 10^5 macrophages macrophages/well) were seeded into 24-well plates with 0.4 mL of D10 per well and incubated for 24h in a 5% CO_2 incubator at 37°C (Figure 4.2). For macrophage infections, *M. tuberculosis* strains were cultured in 7H9-OGT media by incubating at 37°C until an OD_{600nm} of approximately 0.8-1.0. The 10 ml cultures were sonicated in an ultrasonic bath (UC-ID; Zeus Automation) at 37 kHz for 12 min (to minimize clumping) at room temperature and then filtered using a 40 µm cell strainer (Sigma-Aldrich, St Louis, Missouri, USA) to minimize clumping, before the OD_{600nm} was measured. Following this, *M. tuberculosis* cells were washed twice with an equal volume of D10 by centrifugation (4000 rpm, 10 min) at room temperature before the pellet was resuspended in D10 to adjust the OD_{600nm} to 1.0 (~10^8 CFU/ml). The mycobacterial culture was then diluted to 2.5 x 10^7 CFU/ml in D10. One hundred microliters of the diluted *M. tuberculosis* was added to macrophages to achieve a multiplicity of infection (MOI) of 5:1. Infected cells were incubated at 37°C, 5% CO_2 for 3h (Figure 4.2). Infected macrophages were then washed once with PBS and the medium was replaced with D10 containing penicillin (pen) (10 000 units/ml)/streptomycin (strep) (10 000 µg/ml) (Sigma-Aldrich) in a 100-fold working concentration (1:100) and incubated for 1h at 37°C, 5% CO_2.to kill extracellular bacteria followed by 2x wash steps. Uninfected macrophages were included as a negative control. Lipopolysaccharide (LPS) (Sigma-Aldrich) was added at a final concentration of 0.05 µg/ml to monolayers of 2 wells as positive controls.

To determine the percentage uptake of *M. tuberculosis* at 0h by CFU assessment,

macrophages were lysed after the initial infection. Briefly, following removal of the supernatant, 0.5 ml filtered milliQ water was added to infected macrophages and allowed to stand for 1 min. Following this, macrophages were loosened from the cell surface using a pipette tip and the mixture was pipetted up and down 5-6 times to ensure lysis of macrophages. Serial dilutions of the lysates were then plated onto Middlebrook 7H10 (BD Biosciences) agar plates and incubated at 37ºC for 21 days, for CFU determination. All experiments were performed in technical duplicates and in 3 biological replicates.

To monitor cytokine production by macrophages in response to *M. tuberculosis* infection, 200 to 300 µl of the culture supernatants were removed from each well at 24h and 48h post-infection, into a 24-well plate. Removed supernatants were filtered separately into 0.22 µm low protein binding cellulose/acetate centrifuge 2 ml tube filters (Sigma-Aldrich), then sealed and stored at -20ºC until further processing (Figure 4.2).

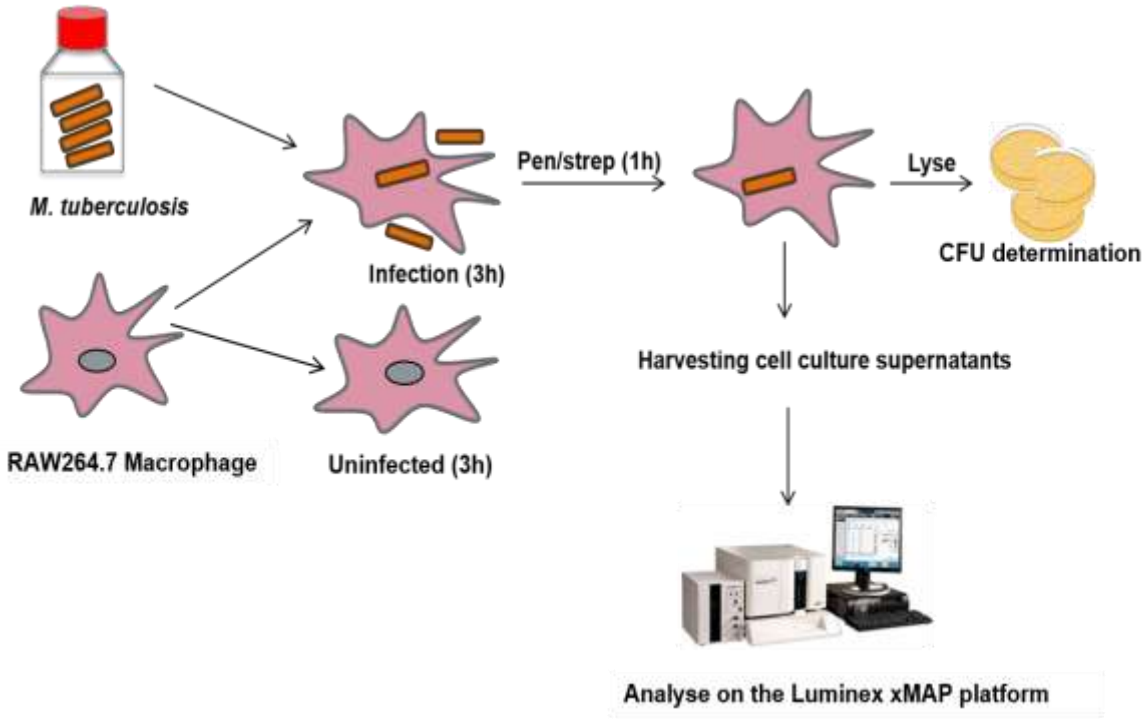

Figure 4.6 Schematic representation of RAW264.7 macrophage infection with *M. tuberculosis*. Approximately 5 x 10^5 macrophages in each well with 0.4 ml D10, were infected with 100 µl of 2.5x10^7 CFU/ml of bacteria at MOI of 5:1 in 24 well plates to a final volume of 400 µl for a period of 3h, uninfected macrophages was also included as a control. The infected and uninfected macrophages were then treated with pen (10 000 units/ml)/strep (10 000 µg/ml) in a (1:100) concentration for 1h to remove extracellular bacteria and then washed 3 times with PBS. Following this, cell culture supernatants were harvested after 24h and 48h of infection and analysed on the Luminex xMAP platform. After harvesting of cell culture supernatants, the infected macrophages were lysed by adding 0.5 ml distilled water. Intracellular bacteria were obtained from lysed macrophages for CFU plating.

4.2.4 Detection of secreted mouse cytokines and chemokines

To examine the host immune response of RAW264.7 macrophages infected with $K636^{WT}$, $K636^{RIF}$, $H37Rv^{WT}$ and $H37Rv^{RIF}$ *M. tuberculosis* strains, the mouse cytokines and chemokines secretion, following 24h and 48h infection were assessed in cell culture supernatants (Figure 4.2) using the Luminex xMAP platform (section 4.2.2). The cell culture supernatants were probed with a selected multiplex mouse Luminex panel (Bio-Rad, Hercules, CA, USA) according to the manufacturer's instructions. This panel included the following cytokines (tumor necrosis factor alpha (TNF-α), interleukin 1 beta (IL-1β), interleukin 10 (IL-10), interferon gamma (IFN-γ), interleukin 4 (IL-4), interleukin 6 (IL-6) and interleukin-12 subunit p40 (IL-12p40) and chemokines [(granulocyte-macrophage colony-stimulating factor (GM-CSF), chemokine (C-C motif) ligand 5 (RANTES/CCL5) and chemokine (C-C motif) ligand 2 (MCP-1)]. Moreover, the levels of RANTES, IFN-γ and

TNF-α secretion were validated by an ELISA platform as per manufacturer's instructions (R&D systems, Minneapolis, Minnesota, USA) using SpectraMax Plus 384 software. Table 4.2 describes the characteristics and functions of all analysed cytokines and chemokines. All experiments were performed in 3 biological replicates and each biological replicate was assayed in 2 technical duplicates of *M. tuberculosis* strains. Furthermore, this was done on the same day but the experiments were done on different luminex assay plates (X3 plates) per each run per biological replicate. Fluorescent intensities for each cytokine and chemokine were acquired using BioPlex™ 200 Luminex xMAP technology data analysis software (Bio-Rad).

Table 4.4 Characteristics of various secreted cytokines, chemokines and their functions relevant to this study

	Names	Anti- and pro-inflammatory cytokines	Functions	References
Cytokines	**IL-6**	pro- and anti-inflammatory	- Important mediator of inflammation response and of the acute phase response - Secreted by macrophages and T cells to stimulate immune response	(21)
	IL-12p40	pro-inflammatory	- Mediator for Th_1 response - Involved in the regulation of the T helper type 1 (Th_1)/Th_2 characterization of the lymphocyte response	(22)
	IL-1β	pro-inflammatory	- Multifunctional cytokine that plays a role in the regulation of immune and inflammatory responses to infection	(21,23)
	IL-4	anti-inflammatory	- IgE class switching during the development of immune responses - Pleiotropic cytokine with regulatory effects on B cell growth, T cell growth, and function	(24,25)
	TNFα	pro-inflammatory	- Plays a role in macrophage activation and controlling granuloma formation in mice - Responsible for inflammation response	(11,23)
	IFNγ	pro-inflammatory	- Responsible for Th_1 response - Plays a role in macrophage activation and controlling granuloma formation in mice	(11,21)
	IL-10	anti-inflammatory	- Critically involved in the regulation of the T helper type 1 (Th_1)/Th_2 characterization of the lymphocyte response and suppression	(22)
Chemokines	**MCP-1**	-	- Key chemokine that regulates migration and infiltration of monocytes/macrophages and chemotactic for monocytes and lymphocytes - Mediator of acute and chronic inflammation	(26–29)
	RANTES	-	- Chemotactic for monocytes and lymphocytes - Mediator of acute and chronic inflammation	(26,28,29)
	GM-CSF	anti-inflammatory	- Part of the IL-4 lymphokines family	(25,30)

4.2.5 Statistical analysis

The statistical analysis of acquired secreted cytokines and chemokines analytes concentrations was perfomed. The concentrations of the secreted cytokines and chemokines were determined from observed standard curve using BioPlex™ 200 Luminex xMAP technology data analysis software (Bio-Rad, Hercules, CA, USA). The secreted cytokines and chemokines analytes concentrations (shown as absorbance concentrations from the Luminex assay) were analysed by plotting the mean with standard deviation (SD) the analytes' 3 biological replicate samples over time in GraphPad Prism version 7.03. For inferential statistics, one-way ANOVA analyses were used to assess differences in mean values for the secretion of cytokines and chemokines after 24h and 48h of RAW264.7 macrophages infection with $K636^{WT}$, $K636^{RIF}$, $H37Rv^{WT}$ and $H37Rv^{RIF}$ *M. tuberculosis* strains. After one-way ANOVA analysis, the Tukey's honestly significant difference (HSD) post hoc tests were done to determine the difference between treatments. The p-value ≤ 0.05 was considered statistically significant. Analyses of normally distributed data were performed using STATISTICA software version 13.3 by Prof. M Kidd from the Centre for Statistical Consultation, at the Department of Statistics and Actuarial Sciences, Stellenbosch University.

4.3 Results

4.3.1 Macrophage infection and CFU determination

The inoculum sizes (CFU/well) and percentage (%) uptake of $K636^{WT}$, $K636^{RIF}$, $H37Rv^{WT}$ and $H37Rv^{RIF}$ *M. tuberculosis* strains were determined by serial dilution plating and CFU enumeration. A similar inoculum size was confirmed for the 4 strains [$K636^{WT}$ (1.2×10^7 CFU), $H37Rv^{WT}$ (1.4×10^7 CFU), $K636^{RIF}$ (1.3×10^7 CFU) and $H37Rv^{RIF}$ (1.2×10^7 CFU] at (Figure 4.3). This was indicated by the observed viable count CFUs of these strains in infected RAW264.7 macrophages from 0h-48h (Figure 4.3). Similar range of mycobacterial cells percentage (%) uptake numbers were confirmed for the 4 strains [$K636^{WT}$ (8.5% mycobacterial cells uptake), $H37Rv^{WT}$ (8% mycobacterial cells), $K636^{RIF}$ (8% mycobacterial cells) and $H37Rv^{RIF}$ (9% mycobacterial cells)] (Appendix C: Figure S4.1). The latter observations were expected. The RAW264.7 macrophages were separately infected with similar mycobacterial cell doses of the tested *M. tuberculosis* strains (refer to Figure 4.3).

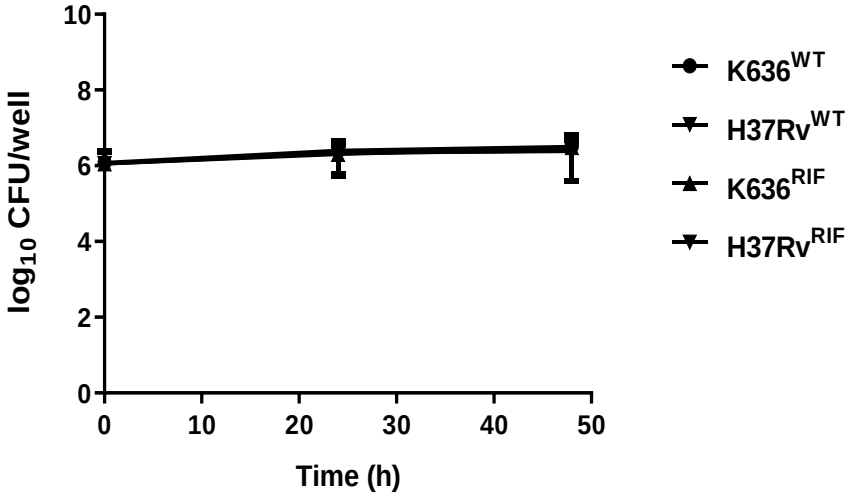

Figure 4.7 The viable count of *M. tuberculosis* strains in RAW264.7 macrophages post infection. This figure depicts the viable count in CFU/well for the $K636^{WT}$, $K636^{RIF}$, $H37Rv^{WT}$ and $H37Rv^{RIF}$ *M. tuberculosis* strains in RAW264.7 macrophages from 0h, 24h and 48h. The data is depicted as mean (viable count) with standard deviation (SD) and are a representation of 3 biological replicates, (each with three technical replicates).

4.3.2 Cytokines and chemokines response of *M. tuberculosis* infected RAW264.7 macrophages

A ten-plex multiplex assay was performed to quantify the levels of IL-6, IL-4, IL-1β, IL-10, IL-12p40, GM-CSF, IFN-γ, TNF-α, MCP-1 and RANTES (Appendix C: S4.3) secreted by RAW264.7 macrophages uninfected and infected with $K636^{WT}$, $K636^{RIF}$, $H37Rv^{WT}$ and $H37Rv^{RIF}$ *M. tuberculosis* strains. Of the 10 cytokines and chemokines assessed, IL-10, IL-1β, GM-CSF and IFN-γ had secretion concentrations less than 5 pg/ml and IL-4 was secreted below the limit of detection (< 0 pg/ml) (Appendix C: Figure S4.3). The remaining 5 analytes (cytokines IL-6, IL-12p40 and TNF-α, and chemokines RANTES and MCP-1) were secreted at detectable concentrations, as shown in Figure 4.4 (i-v). The LPS-treated (positive control) and uninfected RAW264.7 macrophages (negative control) were included in the cytokine and chemokine secretion analysis. Their responses for IL-6, IL-12p40, TNFα, MCP-1 and RANTES (chemokine) were as expected (31); the LPS-treated RAW264.7 macrophages demonstrated high secretion levels of IL-6, IL-12p40, TNFα, MCP-1 and RANTES compared to uninfected macrophage response as anticipated [refer to Figure 4.4 (i-v)].

IL-6, IL-12p40 and RANTES showed similar patterns of secretion by infected RAW264.7 macrophages. Lower levels of these cytokines/chemokines were observed in RAW264.7 macrophages infected with $K636^{RIF}$, than by those infected with $K636^{WT}$, $H37Rv^{WT}$ and $H37Rv^{RIF}$ [refer to Figure 4.4 (i-iv)]. The IL-6 and IL-12 (p40) secretion levels in RAW264.7 macrophages infected with $K636^{WT}$ ranged from 74.2 -124.7 pg/ml and 19.61 -42.67 pg/ml, respectively. The IL-6 and IL-12 (p40) secretion levels in RAW264.7 macrophages infected with $H37Rv^{WT}$ ranged from 38.51 – 89.29 pg/ml and 16.19 - 47.70 pg/ml, respectively [refer to Figure 4.4 (i-iv)]. The IL-6 and IL-12 (p40) secretion levels in RAW264.7 macrophages infected with $H37Rv^{RIF}$ ranged from 28.64 -47.59 pg/ml and 13.83 – 40.98 pg/ml, respectively. Levels of IL-6 and IL-12 (p40) were significantly lower, in RAW264.7 macrophages infected with $K636^{RIF}$ and ranged from 1. 09 -5.96 pg/ml ($p \leq 0.00004$) and 2.47 -12.15 pg/ml ($p \leq 0.00045$), respectively compared to LPS induced and uninfected RAW264.7 macrophages, over a period of 24h and 48h [refer to Figure 4.4 (i-iv)].

Even though luminex xMAP technology assesses cytokines and chemokines secretion levels, by its nature is multiplexed and therefore, may be subject to any perturbations that arise from analysing multiple ligands simultaneously, such as cross-reactivities (32). This might have an impact on the observed results, which might have been the case in the current study (32). Two of our analytes (TNF-α and RANTES) showed discrepant results as reflected by their

lower secretion level than that in literature. For this reason, we repeated the secretion analysis of TNF-α and RANTES analytes using ELISA. ELISA was selected based on the its advantage of assessing the secretion levels of one specific analyte at a time and thus avoiding any concerns that could arise from multiplexing (20,32). Therefore, the secretion level results presented for TNF-α and RANTES were obtained from this assay. TNF-α secretion was higher in RAW264.7 macrophages infected with either $K636^{WT}$ ranging from 696.3 -566.5 pg/ml or with $K636^{RIF}$ ranging from 320.5 -352.5 pg/ml or with $H37Rv^{WT}$ ranging from 655.5 -627.7 pg/ml, and with $H37Rv^{RIF}$ ranging from 572.9 -507.9 pg/ml, respectively [refer Figure 4.4 (iii)] compared to LPS induced and uninfected RAW264.7 macrophages over a period of 24h and 48h. Notably, TNF-α secretion in RAW264.7 macrophages infected with $K636^{RIF}$ (resistant Beijing strain) was lower compared to $K636^{WT}$ [Figure 4.4 (iii)], however this was not statistically significant.

RANTES secretion was higher in RAW264.7 macrophages infected with either $K636^{WT}$ ranging from 1806 -1707 pg/ml, or with $H37Rv^{WT}$ ranging from 1387 -1477 pg/ml and with $H37Rv^{RIF}$ ranging from 811.0 -1091 pg/ml, respectively [Figure 4.4 (iv)] compared to LPS induced and uninfected RAW264.7 macrophages, over a period of 24h and 48h. Furthermore, the secretion level of RANTES was significantly lower ($p \leq 0.00001$) (Appendix C: Figure S4.2 (i-v)) in RAW264.7 macrophages infected with $K636^{RIF}$ ranging from 163.7 -190.3 pg/mL, compared to its counterpart $K636^{WT}$ [Figure 4.4 (iv)]. This observation suggests that the secretion of RANTES in RAW264.7 macrophages was influenced by the specific strain genotypes. Additionally, the MCP-1 secretion levels were similar in response to all tested strains ($K636^{WT}$ was (33604 -39531 pg/ml), $K636^{RIF}$ (25085 -40682 pg/ml), $H37Rv^{WT}$ (37107 -41933 pg/ml) and $H37Rv^{RIF}$ (32800 -43582 pg/ml) Figure 4.4, (v)).

i) IL-6

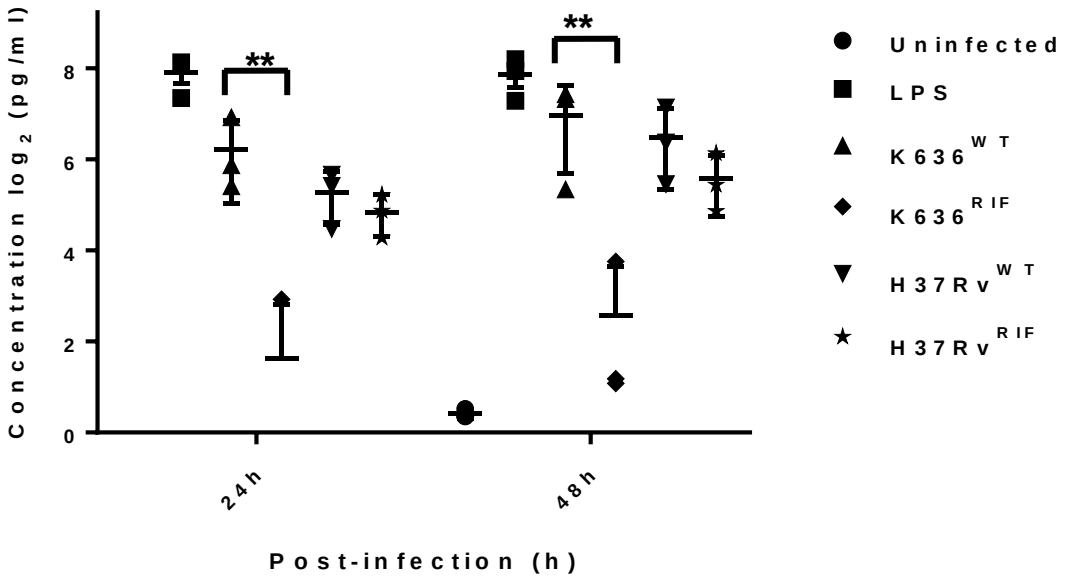

ii) IL-12(p40)

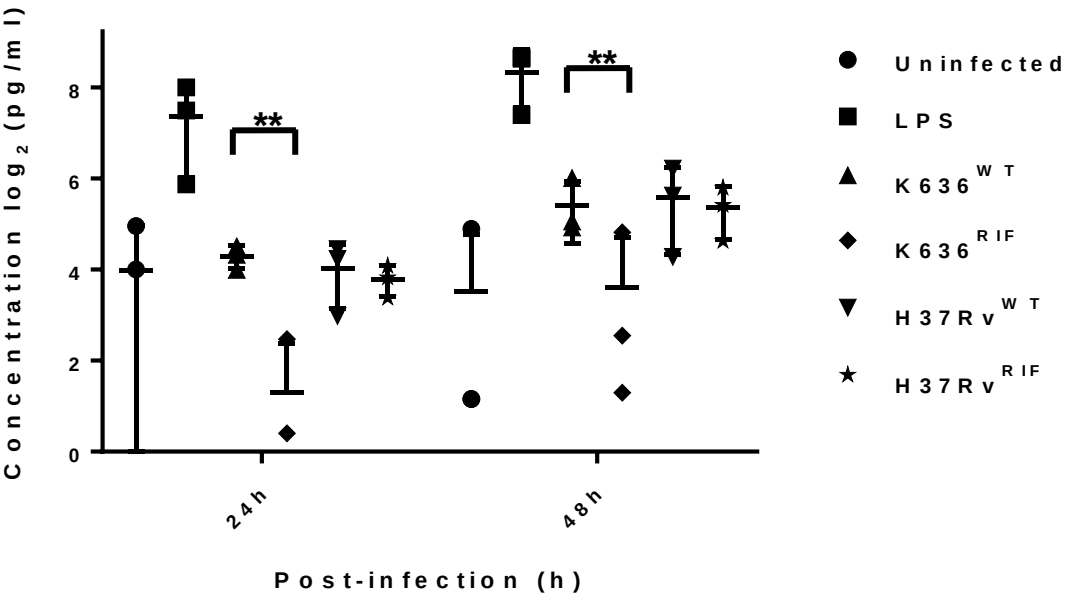

iii) TNFα

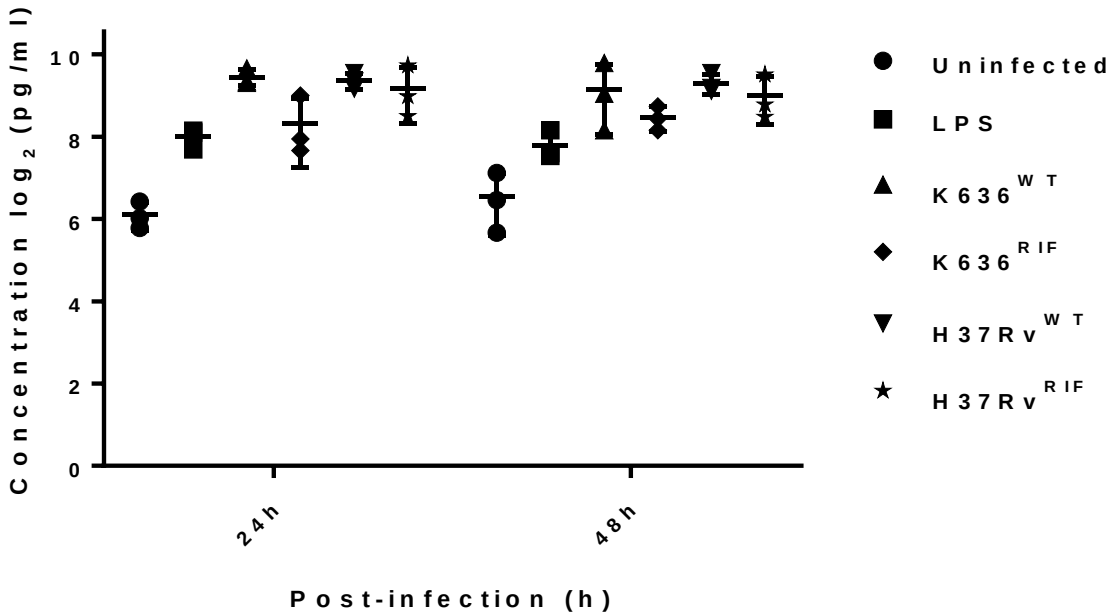

iv) RANTES

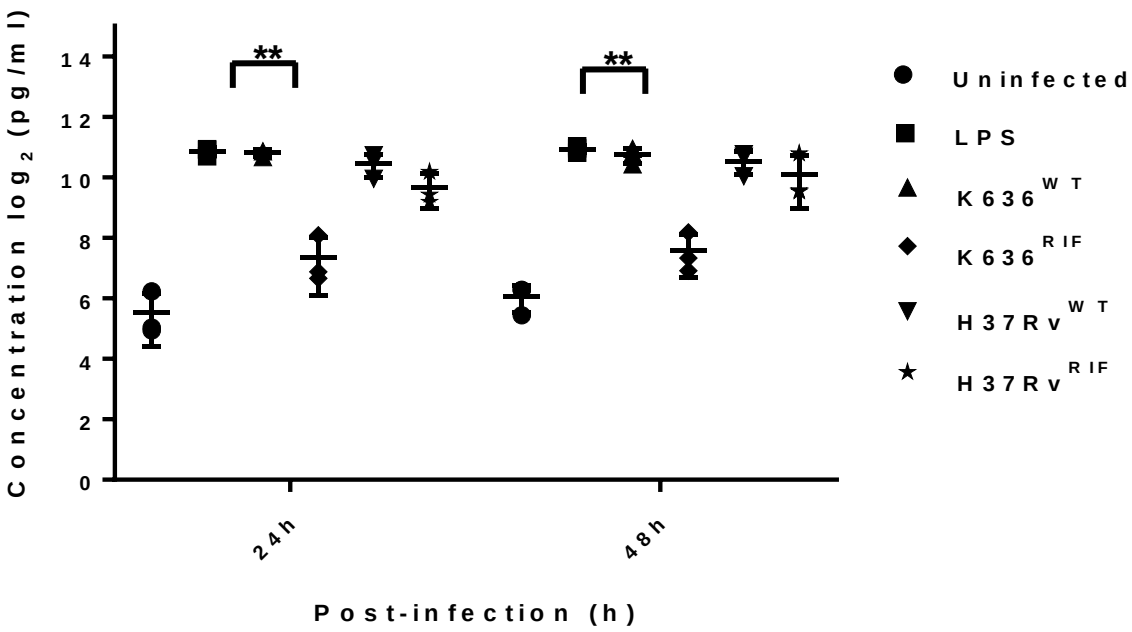

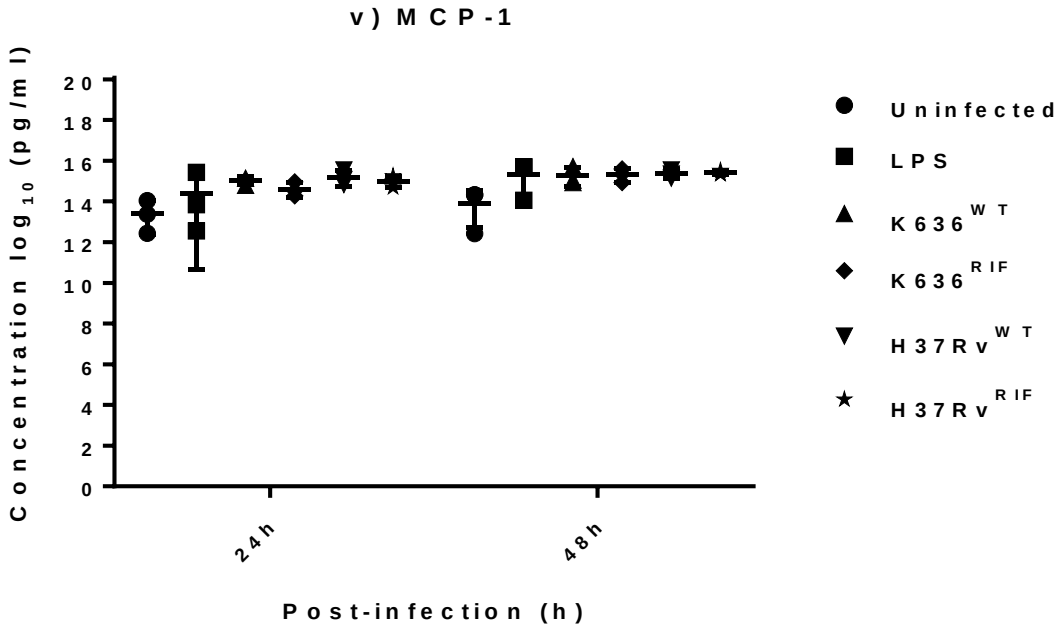

Figure 4.8 (i-v) Normalized concentrations of the secreted cytokines and chemokines. The graphs above show the following cytokines (i) IL-6, ii) IL-12p40, iii) TNFα and chemokines (iv) RANTES and v) MCP1)), which were secreted in the supernatants of RAW264.7 macrophages infected with ($K636^{WT}$, $K636^{RIF}$, $H37Rv^{WT}$ and $H37Rv^{RIF}$ *M.tuberculosis* strains compared to LPS induced and uninfected macrophages, over a period of 24h and 48h. TNFα and RANTES plot are from ELISA data. The data is depicted as mean [of the secreted cytokine and chemokines (pg/ml)] with standard deviation (SD) and are a representation of 3 biological replicates. ** = $p \leq 0.001$ indicates statistical significance.

4.4 Discussion

The limited knowledge of the immune response that mediates protection or steers disease progression during MDR *M. tuberculosis* infections is an important obstacle to the current efforts to prevent global emergence of MDR *M. tuberculosis*. The current study evaluated the host immune response to infection with susceptible and RIF resistant *M. tuberculosis* strains in a RAW264.7 macrophage model. The stages of *M. tuberculosis* infection are influenced by the ability of the host's innate and adaptive immune systems to eradicate or control *M. tuberculosis* (5). For this reason, the current study focused on providing understanding of the host macrophage's response to infection with *M. tuberculosis* strains from different genetic backgrounds, as reflected by the secretion of cytokines/chemokines.

Important key findings from the current study include the significantly reduced secretion levels of IL-6, IL-12p40 cytokines and RANTES chemokine in response to infection with $K636^{RIF}$ compared to levels elicited by $K636^{WT}$ and $H37Rv^{WT}$, $H37Rv^{RIF}$. Published literature indicates that IL-6 is both pro- and anti-inflammatory and is an important mediator of inflammation and acute phase immune responses in TB infection (21). Moreover, IL-12p40 is pro-inflammatory and a mediator for Th_1 response, which is critically involved in the regulation of the (Th_1)/Th_2 and characterization of the lymphocyte response to TB infection (22). RANTES is chemotactic for monocytes and lymphocytes and is a mediator of acute and chronic inflammation (26,28,29). This suggests that the host response was highly pro-inflammatory towards infection with $K636^{WT}$, $H37Rv^{WT}$ and $H37Rv^{RIF}$ *M. tuberculosis* strains. However, infection with the $K636^{RIF}$ strain elicited lower secretion levels of IL-6, IL-12p40 and RANTES.

Our results suggest that the secretion of IL-6, IL-12p40 and RANTES is independent of the specific strain genotypes. No differences were observed in immune response between $K636^{WT}$ and $H37Rv^{WT}$ *M. tuberculosis* strains from different genetic backgrounds (Section 4.3.2). In contrast, differences were observed in the host response between $K636^{WT}$ and $K636^{RIF}$ *M. tuberculosis* strains; reduced secretion IL-6, IL-12p40 cytokines and RANTES chemokine was confirmed. Interestingly, the genomic differences between $K636^{WT}$ and $K636^{RIF}$ strains revealed another three variants (*malQ*, *glpK*, *Rv2185*) besides *rpoB* Ser531Leu mutation present in $K636^{RIF}$. Nevertheless, these were synonymous changes suggesting no effect on the transcriptome of this strain. Additionally, it was suggested that their accumulation could have been a possible consequence of re-culturing $K636^{WT}$ and $K636^{RIF}$ *M. tuberculosis* strains, and this, in turn, having an effect on their relative fold

change ratios; as reflected by their accumulation (chapter 3 discussion. section 3.4.2). Therefore, it can be speculated that this observation was indicative of *rpoB* Ser531Leu mutation present in K636^{RIF} in combination with the genetic background of the Beijing *M. tuberculosis* strain. Nonetheless, the RNA-Seq showed a significant number of genes were differentially expressed in K636^{WT} relative to the K636^{RIF} strain (chapter 3 RNA-Seq results section). Therefore, it is possible that some of the differentially expressed genes might have been responsible for the difference in abundance of IL-6, IL-12p40 cytokines and RANTES chemokine secretion profiles observed between these strains.

To confirm our speculation, we determined exactly from our RNA-Seq data (chapter RNA-Seq results) which genes were uniquely differentially expressed that could have modulated the release of the IL-6, IL-12p40 cytokines and RANTES chemokine resulting in the different immune responses between K636^{WT} and K636^{RIF} *M. tuberculosis* strains. Our transcriptomic data demonstrated significant differential expression, the up-regulation of *mmpL4* and *mmpS4* in K636^{WT} relative to K636^{RIF} (with *rpoB* Ser531Leu mutation) *M. tuberculosis* strains. It is not surprising that *mmpS4* was also up-regulated because it is one of the major components of siderophore export system that is critical for the survival of *M. tuberculosis* in its host (60). Interestingly, *mmpS* forms complexes with *mmpL4* (*mmpL4 – mmpS4* operon) to export cell wall constituents and aid *M tuberculosis* under low iron conditions (33,34). Therefore, it can be speculated that the up-regulation of the *mmpL4 – mmpS4* operon in K636^{WT} relative to K636^{RIF} (with *rpoB* Ser531Leu mutation) was indicative of *M. tuberculosis* using iron metabolism to survive macrophage immune response and continue to grow. In return, modulating the release of the IL-6, IL-12p40 cytokines and RANTES chemokine and resulting in varying immune responses between these two strains.

The virulence gene *pks6* was significantly up-regulated in K636^{WT} relative to K636^{RIF} (with *rpoB* Ser531Leu mutation) *M. tuberculosis* strains., The *pks6* plays a role in *M. tuberculosis* metabolism *in vivo*, which is influenced by the host response to infection by modulating cytokine/chemokine secretion (35), in agreement with our speculations. Our transcriptomic data also demonstrated the overexpression of the three *whiB*-like family genes (*whiB1*, *whiB6* and *whiB7*) in K636^{WT} relative to K636^{RIF} (with *rpoB* Ser531Leu mutation) *M. tuberculosis* strains, of which all were significantly up-regulated. Interestingly, *whiB1*, *whiB6* and *whiB7* have shown to play a role in macrophage infection and virulence (36). *WhiB1* plays an essential role as a transcriptional repressor under *in vivo* conditions and it possesses a [4Fe-4S]2+ cluster) that is sensitive to nitric oxide which is produced by infected lung

macrophages (37,38). While *whiB7* transcriptional activator is suggested to play a role in host pathogen interactions (39,40) and is co-expressed with *WhiB1* (37,38). Therefore, the up-regulation of these *whiB*-like family genes suggests a possible modulation in the release of the IL-6, IL-12p40 cytokines and RANTES chemokine as a consequence of *M. tuberculosis* surviving macrophage immune responses.

IL-6 is a key player in mediating the Th_1 response and is crucial in the development of protective immunity against TB in mouse and human studies (3,21) (Table 4.2). Our results show decreased IL-6 secretion levels in RAW264.7 macrophages after infection with $K636^{RIF}$ compared to $K636^{WT}$ and $H37Rv^{WT}$ and $H37Rv^{RIF}$. Previously, reduced IL-6 secretion levels were demonstrated in murine macrophages infected *ex vivo* with a hypervirulent *M. tuberculosis mce1* mutant compared to the WT susceptible strain (41). This finding suggests that $K636^{RIF}$ suppressed the release of IL-6 in macrophages (42). A recent study demonstrated significant increase relative to uninfected macrophages in the secretion of IL-6 (120 -1900 pg/ml) in RAW264.7 macrophages infected with susceptible *M. bovis* BCG (43), in agreement with our study in terms of $K636^{WT}$ and $H37Rv^{WT}$ susceptible strains.

IL-12 (p40) is involved in the induction of Th_1 response and is essential in the development of protective immunity against TB in mouse and human studies (22). Chakraborty *et al*. showed lower levels of IL-12 in THP-1 cells when infected with a Beijing strain compared with infection with an EAI-5 strain from an ancient lineage 1 (44). In contrast, higher secretion levels of IL-12 was demonstrated in human monocytes at 24h post infection with CDC1551, compared to H37Rv *M. tuberculosis* (12). These observations are in agreement with the secretion levels of IL-12 (p40) in our study. TNF-α plays a critical role in macrophage activation, control of mycobacterial replication and granuloma formation in humans and mice (11,45). Literature reports that classically activated macrophages are responsible for sustained levels of TNF-α signals after infection with *M. tuberculosis* (46). Our results showed a slight decrease in TNF-α secretion levels in RAW264.7 macrophages after infection with $K636^{RIF}$ compared to $K636^{WT}$ and $H37Rv^{WT}$, $H37Rv^{RIF}$. Consistent with our observations, decreased secretion levels of TNF-α to infection with hypervirulent *M. tuberculosis* Beijing strains (H107, H108, H112) compared to H37Rv in murine macrophages and THP-1 (40,47).

RANTES and MCP-1 are chemotactic and small immunoregulatory cytokines of approximately 8 ~14 kDa in size (26,48). They form part of the β-chemokine subfamily and

are critical in mediating constitutive and inflammatory leukocyte recruitment (Table 4.2) from the blood into tissues (26,48–50), functions essential for the immune response to *M. tuberculosis*. Our results show increased RANTES secretion levels in RAW264.7 macrophages after infection with K636^{WT} and H37Rv^{WT} and H37Rv^{RIF} compared to K636^{RIF}. Literature reports high secretion of RANTES in the murine RAW264.7 macrophage cells after stimulation with *M. tuberculosis* (51), consistent with our observations. The infection of alveolar macrophages with *M. tuberculosis* strains (H37Rv and H37Ra) released significantly high levels of RANTES (by 2.1-fold) and MCP-1 (by 6.90-fold) ($p< 0.05$) (28), 24h post infection compared to uninfected controls. Interestingly, in our study, we also observed high secretion levels of RANTES, except for the infection with K636^{RIF} resistant *M. tuberculosis* strain.

Literature has shown that the higher levels of MCP-1 enhance the Th_2 response (52); in our study MCP-1 was secreted in high concentrations in K636^{WT} and H37Rv^{WT}, H37Rv^{RIF} and K636^{RIF} *M. tuberculosis* strains. Infection of RAW264.7 macrophages with BCG resulted in high secretion levels of MCP-1 (13 000 pg/ml) after 72h infection (43). Interestingly, it was found that the expression of MCP-1 in macrophages mediates the protective immunity against *M. tuberculosis* infection (26,53). Limited studies report the secretion of RANTES and MCP-1 in macrophages in response to *M. tuberculosis* (43,48,54), but work in other infection models could shed light on its role in response to *M. tuberculosis* infection.

Our findings revealed five cytokines that were secreted at levels lower than the limit of detection, namely, IFN-γ, IL-1β, IL-10, IL-4 and GM-CSF (Appendix A: Figure S4.3). This could be due to multiple reasons, such as selected model of infection (we worked with an immortalized cell line), time of infection and/or inactivated RAW264.7 macrophages (10,11,44). With regards to the latter, the activation of macrophages prior to infection helps sustain the secretion of IFN-γ (55,56). In the current study, RAW264.7 macrophages were not activated prior to infection, which could explain the extremely low levels of IFN-γ observed.

In conclusion, this study provided evidence that host response *in vitro* is influenced by *M. tuberculosis* strain genotype. That infection with K636^{WT} and H37Rv^{WT} and H37Rv^{RIF} *M. tuberculosis* strains will result in the secretion of pro-inflammatory cytokines/chemokines while infection with K636^{RIF} *M. tuberculosis* strain (with *rpoB* Ser531Leu mutation) might induce secretion of anti-inflammatory cytokines (second line of host defense). We

demonstrated some of the genes which were uniquely differentially expressed that could have modulated the release of the IL-6, IL-12p40 cytokines and RANTES chemokine resulting in the different immune responses between $K636^{WT}$ and $K636^{RIF}$ *M. tuberculosis* strains. We further confirmed that the high MCP-1 secretion levels observed in all tested *M. tuberculosis* strains could be indicative of MCP-1 ability to enhance the Th_2 response. Nevertheless, this remains to be explored further. This knowledge accentuates the importance of understanding the mechanisms of pathogenesis, the host-pathogen interactions and host response to infection with drug susceptible and resistant *M. tuberculosis* strains. Furthermore, this knowledge sheds light on how the drug-resistant *M. tuberculosis* strain's ability to reduce inflammatory responses might necessitate the need for prolonged anti-TB treatment, in return resulting in the emergence and spread of MDR-TB. Therefore, these study findings add value towards research being done to find better strategies to prevent the spread of emerging MDR, as well as extensively drug resistant *M. tuberculosis*.

4.5 References

1. **BASU S, GALVANI AP.** 2008. The transmission and control of XDR TB in South Africa: an operations research and mathematical modelling approach. Epidemiol Infect. **136**:1585–98.

2. **Zenteno-Cuevas R.** 2017. Successes and failures in human tuberculosis vaccine development. Expert Opin Biol Ther. **17**:1481–91.

3. **Sharma M, Bose M, Abhimanyu, Sharma L, Diwakar A, Kumar S, *et al.*** 2012. Intracellular survival of *Mycobacterium tuberculosis* in macrophages is modulated by phenotype of the pathogen and immune status of the host. Int J Mycobacteriology. **1**:65–74.

4. **Delogu G, Sali M, Fadda G.** 2013. The Biology of *Mycobacterium Tuberculosis* Infection. Mediterr J Hematol Infect Dis. **5**:e2013070

5. **O'Garra A, Redford PS, McNab FW, Bloom CI, Wilkinson RJ, Berry MPR.** 2013. The immune response in tuberculosis. Annu Rev Immunol. **31**:475–527.

6. **Cooper AM, Khader SA.** 2008. The role of cytokines in the initiation, expansion, and control of cellular immunity to tuberculosis. Immunol Rev. **226**:191–204.

7. **Lan NTN, Lien HTK, Tung LB, Borgdorff MW, Kremer K, van Soolingen D.** 2003. *Mycobacterium tuberculosis* Beijing genotype and risk for treatment failure and relapse, Vietnam. Emerg Infect Dis. **9**:1633–5.

8. **Bifani PJ, Mathema B, Kurepina NE, Kreiswirth BN.** 2002. Global dissemination of the *Mycobacterium tuberculosis* W-Beijing family strains. Trends Microbiol.**10**:45–52.

9. **Dormans J, Burger M, Aguilar D, Hernandez-Pando R, Kremer K, Roholl P, *et al.*** 2004. Correlation of virulence, lung pathology, bacterial load and delayed type hypersensitivity responses after infection with different *Mycobacterium tuberculosis* genotypes in a BALB/c mouse model. Clin Exp Immunol. **2137**:460–8.

10. **Hoal-van Helden EG, Stanton LA, Warren R, Richardson M, van Helden PD.** 2001. Diversity of in vitro cytokine responses by human macrophages to infection by *Mycobacterium tuberculosis* strains. Cell Biol Int. **25**:83–90.

11. **Tanveer M, Hasan Z, Kanji A, Hussain R, Hasan R.** 2009. Reduced TNF-alpha and IFN-gamma responses to Central Asian strain 1 and Beijing isolates of *Mycobacterium tuberculosis* in comparison with H37Rv strain. Trans R Soc Trop Med Hyg. **103**:581–7.

12. **Manca C, Tsenova L, Barry CE, Bergtold A, Freeman S, Haslett PAJ, *et al.*** 1999. *Mycobacterium tuberculosis* CDC1551 induces a more vigorous host response *in vivo* and *in vitro*, but is not more virulent than other clinical isolates. J Immunol. **162**:6740–6.

13. **Bosio CM, Gardner D, Elkins KL.** 2000. Infection of B cell-deficient mice with CDC 1551, a clinical isolate of *Mycobacterium tuberculosis*: delay in dissemination and development of lung pathology. J Immunol. **164**:6417–25.

14. **López B, Aguilar D, Orozco H, Burger M, Espitia C, Ritacco V, *et al.*** 2003. A marked difference in pathogenesis and immune response induced by different *Mycobacterium tuberculosis* genotypes. Clin Exp Immunol. 133:30–7.

15. **Manca C, Reed MB, Freeman S, Mathema B, Kreiswirth B, Barry CE, *et al.*** 2004. Differential monocyte activation underlies strain-specific *Mycobacterium tuberculosis* pathogenesis. Infect Immun. **72**:5511–4.

16. **Portevin D, Gagneux S, Comas I, Young D.** 2011. Human macrophage responses to clinical isolates from the *Mycobacterium tuberculosis* complex discriminate between ancient and modern lineages. PLoS Pathog. **7**:1001307.

17. **Howard NC, Marin ND, Ahmed M, Rosa BA, Martin J, Bambouskova M, *et al.*** 2008. *Mycobacterium tuberculosis* carrying a rifampicin drug resistance mutation reprograms macrophage metabolism through cell wall lipid changes. Nat Microbiol. **3**:1099–108.

18. **Telenti A.** 1998. Genetics of drug resistant tuberculosis. Thorax. **53**:793–7.

19. **Surenaud M, Manier C, Richert L, Thiébaut R, Levy Y, Hue S, *et al.*** 2016. Optimization and evaluation of Luminex performance with supernatants of antigen-stimulated peripheral blood mononuclear cells. BMC Immunol. **17**(1):44.

20. **Overview of ELISA - NG**. https://www.thermofisher.com/ng/en/home/life-science/protein-biology/protein-biology-learning-center/protein-biology-resource-library/pierce-protein-methods/overview-elisa.html

21. **Dinarello CA.** 2000. Proinflammatory cytokines. Chest. **118**:503–8.

22. **Mosmann TR, Sad S.** 1996. The expanding universe of T-cell subsets: Th1, Th2 and more. Immunol Today. **17**:138–46.

23. **Soromou LW, Zhang Z, Li R, Chen N, Guo W, Huo M, *et al.*** 2012. Regulation of inflammatory cytokines in lipopolysaccharide-stimulated RAW 264.7 murine macrophage by 7-O-methyl-naringenin. Mol Basel Switz. **17**:3574–85.

24. **Mukherjee S, Chen L-Y, Papadimos TJ, Huang S, Zuraw BL, Pan ZK**. 2009. Lipopolysaccharide-driven Th2 cytokine production in macrophages is regulated by both MyD88 and TRAM. J Biol Chem. **284**:29391–8.

25. **Paul WE**. 1991. Interleukin-4: a prototypic immunoregulatory lymphokine. Blood. **77**:1859–70.

26. **Slight SR, Khader SA.** 2013. Chemokines shape the immune responses to tuberculosis. Cytokine Growth Factor Rev. **24**:105–13.

27. **Deshmane SL, Kremlev S, Amini S, Sawaya BE.** 2009. Monocyte chemoattractant protein-1 (MCP-1): an overview. J Interferon Cytokine Res Off J Int Soc Interferon Cytokine Res. **29**:313–26.

28. **Sadek MI, Sada E, Toossi Z, Schwander SK, Rich EA.** 1998. Chemokines induced by infection of mononuclear phagocytes with mycobacteria and present in lung alveoli during active pulmonary tuberculosis. Am J Respir Cell Mol Biol. **19**:513–21.

29. **Conti P, DiGioacchino M.** 2001. MCP-1 and RANTES are mediators of acute and chronic inflammation. Allergy Asthma Proc. **22**:133–7.

30. **Bergamini A, Bolacchi F, Bongiovanni B, Cepparulo M, Ventura L, Capozzi M, *et al.*** 2000. Granulocyte–macrophage colony-stimulating factor regulates cytokine production in cultured macrophages through CD14-dependent and -independent mechanisms. Immunology. **101**:254–61.

31. **Domingo-Gonzalez R, Prince O, Cooper A, Khader S.** 2016. Cytokines and chemokines in *Mycobacterium tuberculosis* infection. Microbiol Spectr.**4**(5):1128-10

32. **Elshal MF, McCoy JP.** 2006. Multiplex bead array assays: performance evaluation and comparison of sensitivity to ELISA. Methods San Diego Calif. **38:**317–23.

33. **Wells RM, Jones CM, Xi Z, Speer A, Danilchanka O, Doornbos KS, *et al.*** 2013. Discovery of a siderophore export system essential for virulence of *Mycobacterium tuberculosis.* PLoS Pathog. 9:1003120.

34. **Domenech P, Reed MB, Barry CE.** 2005. Contribution of the *Mycobacterium tuberculosis* MmpL protein family to virulence and drug resistance. Infect Immun. **73**:3492–501.

35. **Hisert KB, Kirksey MA, Gomez JE, Sousa AO, Cox JS, Jacobs WR, *et al*.** 2004. Identification of *Mycobacterium tuberculosis* counterimmune (cim) mutants in immunodeficient mice by differential screening. Infect Immun. **72**:5315–21.

36. **Casonato S, Cervantes Sánchez A, Haruki H, Rengifo González M, Provvedi R, Dainese E, *et al.*** 2012. WhiB5, a transcriptional regulator that contributes to *Mycobacterium tuberculosis* virulence and reactivation. Infect Immun. **80**:3132–44.

37. **Burian J, Yim G, Hsing M, Axerio-Cilies P, Cherkasov A, Spiegelman GB, *et al*.** 2013. The mycobacterial antibiotic resistance determinant *whiB7* acts as a transcriptional activator by binding the primary sigma factor *sigA* (RpoV). Nucleic Acids Res. **41**:10062–76.

38. **Smith LJ, Stapleton MR, Fullstone GJM, Crack JC, Thomson AJ, Le Brun NE, *et al.*** 2010. *Mycobacterium tuberculosis* WhiB1 is an essential DNA-binding protein with a nitric oxide-sensitive iron-sulfur cluster. Biochem J. **432**:417–27.

39. **Rohde KH, Abramovitch RB, Russell DG.** 2007. *Mycobacterium tuberculosis* invasion of macrophages: linking bacterial gene expression to environmental Cues. Cell Host Microbe. **2**:352–64.

40. **Krishnan N, Malaga W, Constant P, Caws M, Thi Hoang Chau T, Salmons J, *et al.*** 2011. *Mycobacterium tuberculosis* lineage influences innate immune response and virulence and is associated with distinct cell envelope lipid profiles. PLoS ONE. **6**:23870.

41. **Shimono N, Morici L, Casali N, Cantrell S, Sidders B, Ehrt S, *et al.*** 2003. Hypervirulent mutant of *Mycobacterium tuberculosis* resulting from disruption of the mce1 operon. Proc Natl Acad Sci USA. **100**:15918–23.

42. **Wu Y, Guo Z, Yao K, Miao Y, Liang S, Liu F, *et al*.** 2016. The transcriptional foundations of Sp110-mediated macrophage (RAW264.7) resistance to *Mycobacterium tuberculosis* H37Ra. Sci Rep.**6**: 22041.

43. **N L, Vesin D, Martinvalet D, Garcia I.** 2016. Low dose BCG infection as a model for macrophage activation maintaining cell viability. Journal of Immunology Research. **10**:1155

44. **Chakraborty P, Kulkarni S, Rajan R, Sainis K.** 2013. Drug resistant clinical isolates of *Mycobacterium tuberculosis* from different genotypes exhibit differential host responses in THP-1 cells. PLoS ONE. **8**(5):e62966.

45. **Cooper AM.** 2009. Cell mediated immune responses in tuberculosis. Annu Rev Immunol. **27**:393–422.

46. **Mosser DM, Zhang X.** 2008. Activation of murine macrophages. Curr Protoc Immunol Ed John E Coligan Al. **14**(2):1002-10.

47. **Reed MB, Domenech P, Manca C, Su H, Barczak AK, Kreiswirth BN, *et al.*** 2004. A glycolipid of hypervirulent tuberculosis strains that inhibits the innate immune response. Nature. **431**:84–7.

48. **Lee J-S, Kim KH, Lee D-Y, Choi H-H, Lee H-M, Son JW, *et al.*** 2008. Depressed CCL5 expression in human pulmonary tuberculosis. J Bacteriol Virol. **38**:97–107.

49. **Mehrad B, Keane MP, Strieter RM.** 2007. Chemokines as mediators of angiogenesis. Thromb Haemost. **97**:755–62.

50. **Zlotnik A, Yoshie O, Nomiyama H.** 2006. The chemokine and chemokine receptor superfamilies and their molecular evolution. Genome Biol. **7**:243.

51. J**ones BW, Heldwein KA, Means TK, Saukkonen JJ, Fenton MJ.** 2001. Differential roles of Toll-like receptors in the elicitation of proinflammatory responses by macrophages. Ann Rheum Dis. **3**:6-12.

52. **Karpus WJ, Lukacs NW, Kennedy KJ, Smith WS, Hurst SD, Barrett TA**. 1997. Differential CC chemokine-induced enhancement of T helper cell cytokine production. J Immunol Baltim Md 1950. **158**:4129–36.

53. **Peters W, Cyster JG, Mack M, Schlöndorff D, Wolf AJ, Ernst JD, *et al.*** 2004. CCR2-dependent trafficking of F4/80dim macrophages and CD11cdim/intermediate dendritic cells is crucial for T cell recruitment to lungs infected with *Mycobacterium tuberculosis*. J Immunol Baltim Md 1950. **172:**7647–53.

54. **Skwor TA, Sedberry Allen S, Mackie JT, Russell K, Berghman LR, McMurray DN.** 2006. BCG vaccination of guinea pigs modulates *Mycobacterium tuberculosis*-induced CCL5 (RANTES) production in vitro and in vivo. Tuberc Edinb Scotl. **86**:419–29.

55. S**ibley LD, Krahenbuhl JL.** 1988. Induction of unresponsiveness to gamma interferon in macrophages infected with *Mycobacterium leprae*. Infect Immun. **56**:1912–9.

56. **Herbst S, Schaible UE, Schneider BE.** 2011. Interferon gamma activated macrophages kill mycobacteria by nitric oxide induced apoptosis. PLoS ONE. **6**:19105.

CHAPTER 5

The contribution of a viable but non-replicating bacterial population to genetic resistance in *Mycobacterium smegmatis*

My contribution:

- Project planning
- Bacterial strain culturing
- INH treatment experiments
- Flow cytometry and sorting sample preparation
- DNA sequencing sample preparation
- Data analysis and interpretation of results on FlowJo
- Statistical analysis in consultation with a statistician
- Writing and editing of the chapter

5.1 Introduction

Tuberculosis (TB) continues to be a major public health problem worldwide (1). A key goal for enhancing the efficacy of TB treatment is to shorten the length of anti-TB treatment without increasing relapse rates or boosting the development of drug-resistant strains (2). However, this is hindered by inadequate knowledge about bacterial drug tolerance (2). A drug-tolerant bacterium is phenotypically, but not genotypically, resistant to anti-TB drugs (3,4). As with most other bacteria, in any *Mycobacterium tuberculosis* population, there is expected to be a small sub-population of viable but non-replicating (VBNR) persister bacteria (5). It has been speculated in *in vitro* models, that these VBNR bacteria enter a drug-tolerant state, possibly decreasing their metabolic activity or becoming metabolically inactive (6). This bacterial subpopulation may tolerate prolonged drug treatment and contribute to treatment failure and subsequent evolution of drug resistant strains. These drug-tolerant bacteria are difficult to eradicate completely as most drugs are designed to target metabolic pathways in actively replicating cells. Therefore, there is an urgent need for new agents that can induce growth of VBNR populations to actively replicating bacteria. Understanding the physiology of drug-tolerant persisters would advance knowledge of the mechanisms these bacteria exploit to survive drug treatment.

Little is known about persistent mycobacteria, mainly because our knowledge about the physiology of persistent *M. tuberculosis* has been limited by the lack of suitable tools to successfully identify and isolate persistent populations. Recently, a fluorescence dilution (FD) reporter system was applied to study the replication dynamics of a persistent *Salmonella enterica* serovar Typhimurium (*S.* Typhimurium) population in murine macrophages (7,8). The FD technique was used to show that upon entry into macrophages, numerous bacteria do not replicate, but appear to enter a dormant-like state, in order to adapt to and survive macrophage killing activities (7). This approach has been adapted for use in *M. tuberculosis* and *Mycobacterium smegmatis* (9). Briefly, the FD reporter system approach exploits two fluorescent reporters; a constitutive green fluorescent reporter (GFP) that allows the tracking of viable bacteria, while an inducible red fluorescent reporter enables the measurement of bacterial replication (Figure 5.1) (9).

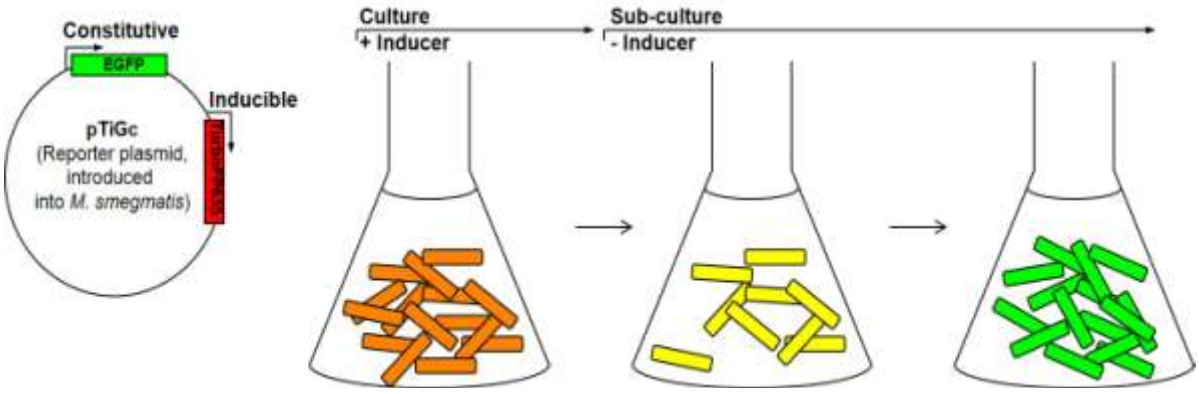

Figure 5.5 Principle of the FD reporter system to explore the replication dynamics of *M. smegmatis*. The figure depicts the FD reporter system where the GFP (green) reporter serves as a marker for viability and the TurboFP635 (red) reporter, under regulation of an inducible promoter, is able to track bacterial replication (9). In the presence of the inducer (Theophylline), GFP (green) and TurboFP635 (red) are maximally expressed. Upon removal of the inducer, the TurboFP635 signal is diluted (as shown in orange) in an actively growing culture.

Literature reports suggest that persistent *M. tuberculosis* bacteria might reside within the granuloma, a lesion of immune cells that creates a microenvironment that supports or suppresses the survival of these bacteria (10,11). As a result of the low numbers and slow growth of bacterial persisters, these bacteria are hard to study. The bacteria experience stressful conditions in the granuloma which include low pH, nitric oxide (NO), hypoxia, and restricted nutrients (12,13) and these conditions have been shown to produce a VBNR (persister) state *in vitro* (6,14–17). Persister formation have been demonstrated *in vivo*, in murine macrophages using a dual reporter system based on FD techniques (9). Furthermore, pre-existing *M. tuberculosis* persistent cells have been revealed in human sputum using dual-reporter mycobacteriophages (Φ^2DRMs) (18,19). Previous studies have reported that drug treatment at high concentrations induces the formation of VBNR persister bacteria (5,9). In the current study, isoniazid (INH) drug treatment at a high concentration was used to select for this VBNR persister *M. smegmatis* and the FD reporter system was exploited to separate VBNR *M. smegmatis* sup-population from actively replicating (AR) bacteria. This was done in order to determine whether *M. smegmatis* sub-populations, when exposed to high INH concentrations, may provide a reservior of INH resistance from which genetic resistant mutants can emerge.

In the current study we **hypothesised** that treating *M. smegmatis* with INH at high concentrations will result in the emergence of a sup-population of VBNR persisters. Additionally, that VBNR persister *M. smegmatis* sup-population will likely provide a reservoir of INH resistance from which genetic resistant mutants can arise. To address this,

we **aimed** to determine the mutation frequency of the VBNR persister *M. smegmatis* sup-population relative to the AR *M. smegmatis* population. The **objectives** of the current study was (i) to detect and quantify VBNR and actively replicating (AR) *M. smegmatis* bacterial populations following INH treatment at high concentrations using a combination of FD and flow cytometry, (ii) to isolate *M. smegmatis* VBNR from AR populations using fluorescence-activated cell sorting (FACS), following INH treatment at high concentrations (30x MIC) for 72h, and (iii) to identify the proportion of genetic INH resistant *M. smegmatis* that can emerge from a VNBR subpopulation that was exposed to 30x MIC INH, by amplification of *katG* and *inhA* promoter and identification of mutations in these genes that are predominantly associated with INH resistance. This was done using polymerase reaction chain (PCR) amplification and Sanger sequencing for *katG* and *inhA* promoter regions in order to identify INH resistant mutants. The findings were expected to provide more knowledge of the influence of VBNR *M. smegmatis* sub-population on the evolution of drug resistance in mycobacteria. This knowledge shed light about the potential mechanisms of tolerance in *M. tuberculosis* driving the emergence of drug resistant TB and necessitating the need for prolonged anti-TB treatment.

5.2 Material and methods

5.2.1 Mycobacterial strains

Mycobacterium smegmatis mc^2155 strains containing plasmids as listed in Table 5.1 were used in the current study. The pTiGc or FD reporter plasmid encodes two fluorescent reporter proteins (constitutive GFP and inducible TurboFP635). Control strains carried the pST5552 plasmid encoding inducible GFP and the pSTCHARGE plasmid with an inducible red fluorescent reporter (TurboFP635).

Table 5.4 Strains and plasmids used in this study

Strain	**Description**	**Source/Reference**
M. smegmatis pTiGc	*M. smegmatis* reporter strain carrying pTiGc plasmid, *hsp60(ribo)-turboFP635 hsp60-gfp*, Kanamycin resistant (Kan^R), episomal	Addgene plasmid number: 78314, (9)

M. smegmatis pST5552	*M. smegmatis* reporter strain carrying pST5552 plasmid, *hsp60(ribo)-egfp* (inducible EGFP under control of theophylline-inducible riboswitch), Kan^R, episomal	Addgene plasmid number 36255, (20)
M. smegmatis pSTCHARGE	*M. smegmatis* reporter strain carrying pSTCHARGE plasmid, *hsp60(ribo)-turboFP635* (inducible TurboFP635 under control of theophylline-inducible riboswitch), Kan^R, episomal	Addgene plasmid number 24658, (21)
M. smegmatis::katG	*M. smegmatis* deletion mutation (INH^R)	A gift from Dr Lynthia Paul
M. smegmatis mc^2155	*M. smegmatis* reporter strain, non-pathogenic, fast growing model organism	ATCC 700084

5.2.2 The determination of INH mutation frequency

To determine the INH (Sigma-Aldrich, St Louis, Missouri, USA) mutation frequency in *M. smegmatis* mc^2155, different bacterial strains were cultured in liquid media with and without INH for 24h. These strains included wild type (WT) *M. smegmatis*, INH pre-treated *M. smegmatis* (30x MIC) (*M. smegmatis*^{30x}) and *M. smegmatis::katG* mutant, carrying a *katG* deletion mutation, as a positive control. Briefly, *M. smegmatis* cultures were separately inoculated into 9 ml of 7H9 Middlebrook medium (BD Biosciences, New Jersey, USA), supplemented with 10% Oleic acid-albumin-dextrose-catalase (OADC), 0.2% (v/v) glycerol (Merck Laboratories, Cape Town, SA) and 0.05% Tween 80 (Becton Dickinson, Sparks, USA) (7H9-OGT) in 50 ml falcon tubes (Becton Dickinson), to obtain a starting OD_{600nm} = 0.1. The *M. smegmatis*^{WT} cultures were either treated with 150 µg/ml INH (30x MIC) or left untreated as the negative control. The *M. smegmatis::katG* mutant strain was not treated with 150 µg/ml INH (30x MIC) and served as the positive control. All cultures were incubated for 72h at 37°C, shaking at 180 rpm. After 72h of incubation, the *M. smegmatis*^{WT} treated with 150 µg/ml INH (30x MIC), *M. smegmatis*^{UNT} and untreated *M. smegmatis::katG* mutant

cultures were plated onto Luria-Bertani (LB) agar plates with and without previously determined 5.0 µg/ml INH (1x MIC) (Figure 5.2). Plates were incubated at 37^0C for 5 days (Figure 5.2) prior to CFU determination. Following this, the mutation frequency was calculated by dividing the number of colonies (of the tested strains) that emerged on solid media supplemented with 5.0 µg/ml INH (1x MIC), by the number of colonies that emerged on plates without INH. GraphPad Prism software version 7.03 (https://www.graphpad.com) was used to analyse CFU data. The estimated CFU/ml was a representative of 3 biological replicates in technical triplicate expressed as mean± standard deviation (SD).

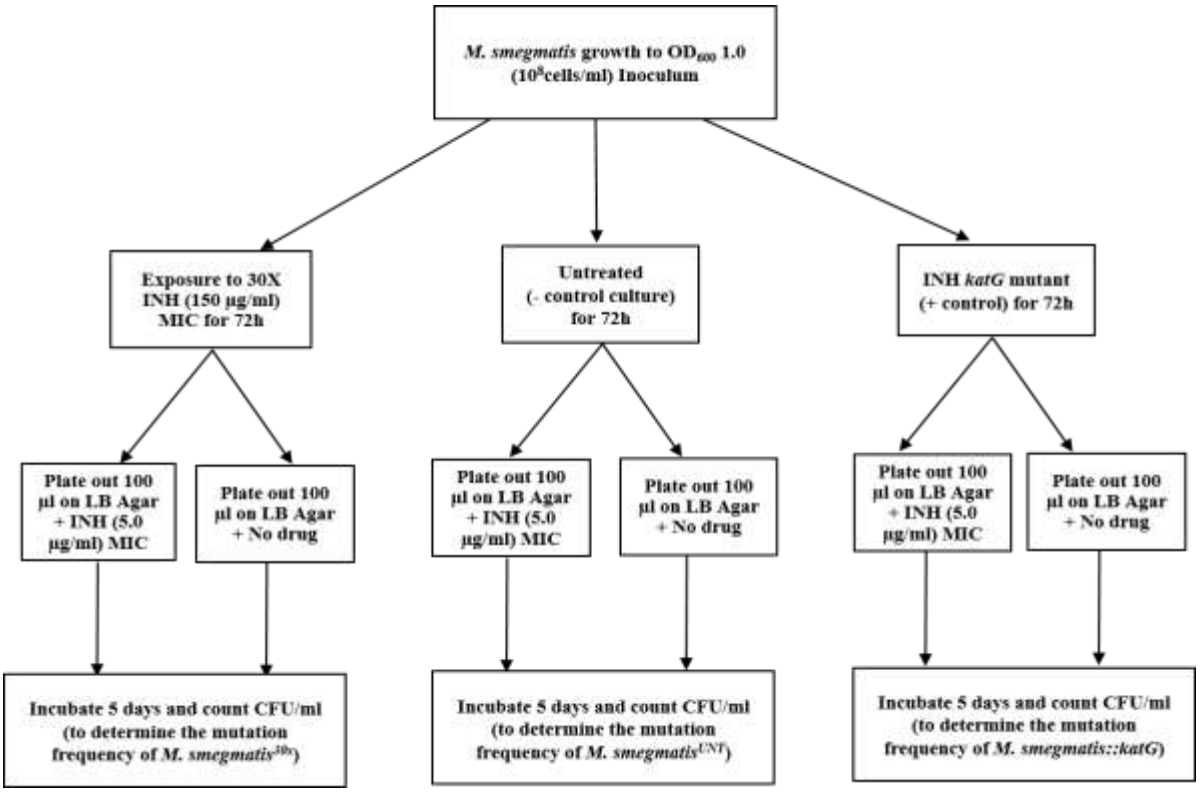

Figure 5.6 Schematic illustration of experimental set-up followed to determine the mutation frequencies of studied *M. smegmatis* strains on LB Agar plates supplemented with or without INH (1xMIC) treatment. Additionally, the INH *M. smegmatis::katG* mutant was untreated for 72h.

5.2.3 Flow cytometry and FACS

Flow cytometry is a powerful technique that can be used to analyse, count and examine individual cells within heterogeneous populations from a stream of a fluid (22–25). In the current study, flow cytometry was exploited to quantify the AR and VBNR persister bacterial populations. Following this, FACS was exploited to separate VBNR persisters from AR

bacterial populations in *M. smegmatis* after treatment with 150 µg/ml INH (30x MIC). The INH treatment concentration (30x MIC) used to induce VBNR persisters *M. smegmatis* in the current study, was previously determined by Keren *et al*.(5).

5.2.3.1 Sample preparation

To detect and quantify VBNR and AR *M. smegmatis* following INH treatment, a combination of the FD reporter system and flow cytometry was exploited. One millilitre of *M. smegmatis* containing pTiGc (*M. smegmatis::*pTiGc) and each of the single colour controls (*M. smegmatis* carrying pST5552 and pSTCHARGE) and *M. smegmatis*^{WT} strains were inoculated in 9 ml of 7H9-OGT, respectively (Table 5.2). *M. smegmatis::*pTiGc, *M. smegmatis::*pST5552 and *M. smegmatis*::pSTCHARGE were cultured in the presence of 25 µg/ml KAN and 2 mM Theophylline (Theo) (for the induction of TurboFP635 and EGFP reporters) (Sigma-Aldrich, St Louis, Missouri, USA) (Table 5.2).

Table 5.5 *M. smegmatis* culture conditions with and without induction with 2 mM Theophylline

Strain	**Theophylline induction**	**O/N culture (ml)**	**Kan (25 mg/ml)**	**7H9**	**10 mM Theophylline**
***M. smegmatis::* pTiGc**	2 mM induction	1.0 ml	10.0 µl	7.0 ml	2.0 ml
***M. smegmatis::*pST5552**	2 mM induction	1.0 ml	10.0 µl	7.0 ml	2.0 ml
***M. smegmatis*::pSTCHARGE**	2 mM induction	1.0 ml	10.0 µl	7.0 ml	2.0 ml
***M. smegmatis::*pTiGc**	NONE	1.0 ml	10.0 µl	9.0 ml	NONE
***M. smegmatis* mc^{2}155**	NONE	1.0 ml	NONE	9.0 ml	NONE

All cultures were incubated overnight at 37°C, shaking at 200 rpm. After 24h all tested cultures were removed from the incubator and one of the *M. smegmatis::*pTiGc cultures was prepared for INH treatment, while in parallel, the control culture samples (*M. smegmatis::*pST5552, *M. smegmatis*::pSTCHARGE and *M. smegmatis*^{WT}) were prepared as controls for flow cytometry analysis. Briefly, cultures were sonicated in an ultrasonic bath (UC-ID; Zeus Automation) at 37 kHz for 12 min to disperse clumps before filtering through a 40 µm cell strainer (BD Biosciences), to minimize clumping (without affecting bacterial viability). OD_{600nm} readings were recorded before cultures were readjusted to OD_{600nm} =1.0 by

centrifugation, washing and ultimately resuspension in an appropriate volume of 7H9-OGT. Following this, 1 ml of each culture was inoculated into 9 ml of 7H9-OGT in the presence of 2 mM Theo (for 24h) (for a starting OD_{600nm} = 0.1). Samples were then treated with 150 µg/ml INH (30x MIC), or left untreated before incubation for 72h at 37°C, shaking at 180 rpm. Theo was removed after 24h incubation from all cultures by centrifugation and washing before samples were resuspended in 7H9-OGT with and without INH (30x MIC) and re-incubated for a further 48h at 37°C, shaking at 180 rpm. After a total 72h of incubation, both treated and untreated *M. smegmatis::*pTiGc samples were processed for flow cytometry analysis. Briefly, 1-2 ml aliquots of the cultures were pelleted at room temperature (13 000 rpm, 5 min), resuspended in 200 µl 4% formaldehyde (Sigma-Aldrich) diluted with PBS and fixed for 30 min in the dark. After 30 min, 800 µl PBS-0.05% Tween 80 was added to the fixed samples to a final volume of 1 ml. Samples (3 technical replicates) were then centrifuged (13 000 rpm, 5 min) and the pellets were resuspended in 500 µl PBS without Tween 80 and passed through a 40 µm filter into flow cytometry tubes (BD Biosciences). Three technical replicates were included for each sample.

For FACS, bacterial samples were not fixed with 4% formaldehyde, instead they were analyzed live. After 72h incubation, 10 ml of both INH treated and untreated samples were sonicated in an ultrasonic bath (UC-ID; Zeus Automation) at 37 kHz for 12 min (to minimize clumping) and washed (with PBS twice to remove Tween 80) by centrifugation. Then, the pellets were resuspended into 5 ml of PBS and the OD_{600nm} was measured. After this, 300 µl aliquots were taken for CFUs determination analysis before FACS in order to later compare with the resulting CFUs determined after FACS. The remaining culture was supplemented with EDTA (2 mM) prior to sorting. The supplementation with EDTA was to prevent cation dependent cell-cell interactions, thus preventing the bacterial cells from sticking to the flow tubes (26). After FACS, the isolated and quantified (VBNR and AR) bacterial populations and the unsorted populations were plated onto LB agar plates with or without 5.0 µg/ml INH (1x MIC). For CFU determination, the plates were then incubated at 37^0C for 5 days (Figure 5.3). Three biological replicates were done per sample.

5.2.3.2 Flow cytometry, FACS acquisition and analysis

The BD LSRFortessa flow cytometer (BD Biosciences) was used for the analysis of fixed samples at different time points (0h, 24h and 72h). This was to quantify the VBNR and AR *M. smegmatis* populations following INH treatment (150 µg/ml INH, 30x MIC). The forward scatter (FSC) and side scatter (SSC) settings were adjusted so that the bacterial population

shifts to the middle of the plot; the GFP fluorescence intensity was captured by excitation at 488 nm, using a 530/30 filter, and TurboFP635 fluorescence intensity was captured by excitation at 561 nm, using a 610/20 filter. Furthermore, the acquisition mode signals were acquired using logarithmic scaling. A gate was set up around the total bacterial population based on FSC/SSC and a second gate for the live bacteria population based on GFP+ signal (Figure 5.3). Additionally, TurboFP635 signal within this population was assessed as a measure of bacterial replication or lack thereof. The compensation for each experiment was performed using unlabelled and single-colour controls. Between 10 000 events and 30 000 events in bacterial gates were captured for all samples.

The BD FACSJazz™ cell sorter (BD Biosciencs) was used to sort live bacterial samples in order to isolate the VBNR *M. smegmatis* population from the AR bacterial population following INH treatment. For sorting, a stringent gating strategy was set up to ensure the highest possible purity. The VBNR population was selected based on high TurboFP635 and GFP signal (TurboFP635++++, GFP++++) and AR was selected based on low TurboFP635 and high GFP signal (TurboFP635+,GFP++++), allowing selection of the extreme phenotypes. The 1 yield drop sorting mode was used for all biological replicates. Experiments and samples were sorted at a low sorting speed to ensure increased accuracy. In addition, the purity was between 68% - 98% and efficiency was between 72% - 92%. For sorting, between 10 000 events and 20 000 events in bacterial gates were captured for all samples. Statistical analysis was carried out using GraphPad Prism v6.04 software.

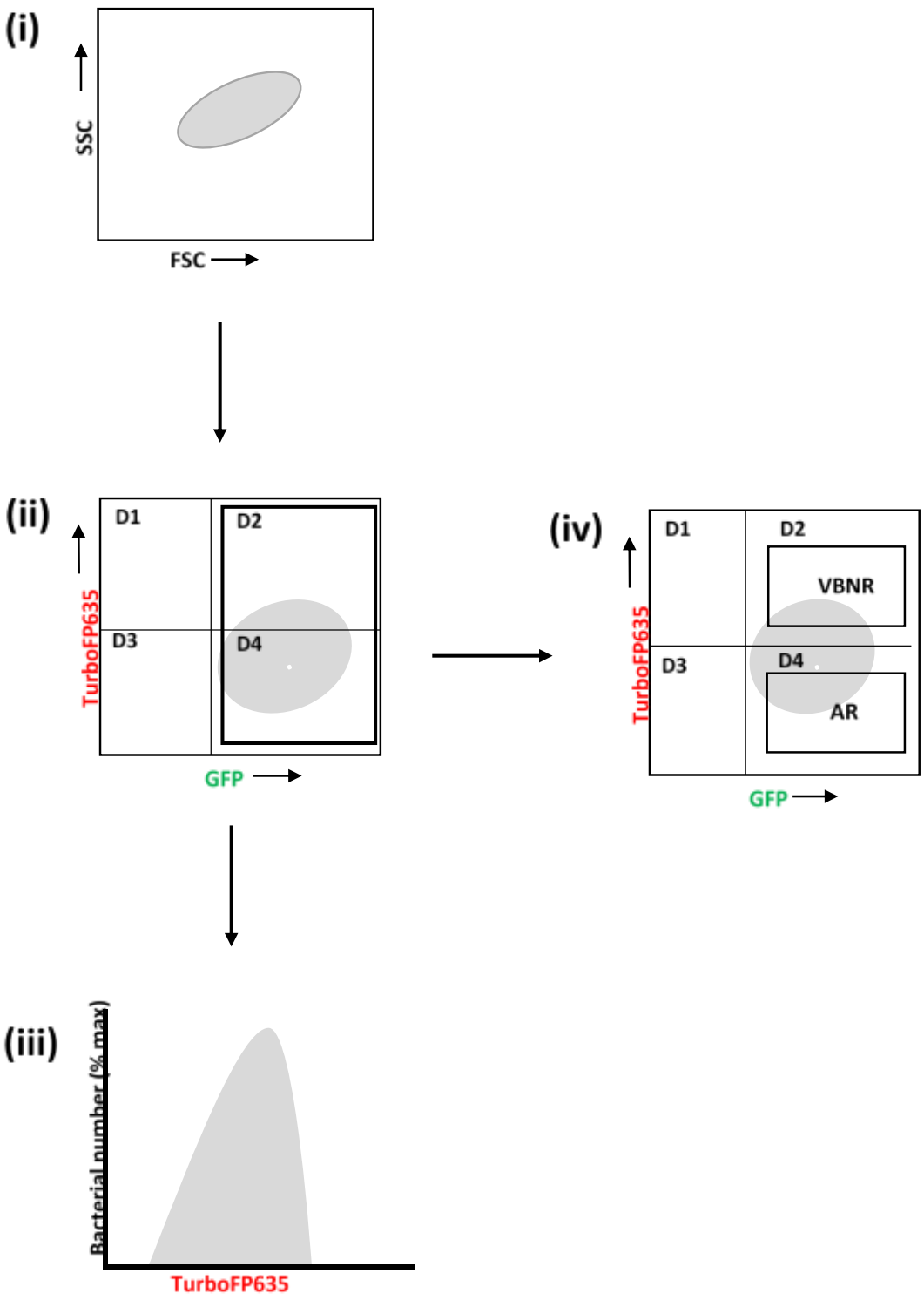

Figure 5.7 Schematic illustrations of FD and FACS gating strategies. The schematic depicts 4 steps which were followed for gating. Briefly (i) Selecting the bacterial population (ii) Gating on GFP+ to select for viable bacteria, (iii) The histogram depicts the TurboFP635 signal in live bacteria, which provides an indication about bacterial replication (loss in TurboFP635 signal) or lack of replication (high TurboFP635 signal), and (iv) Gating strategy for sorting AR (GFP+++++, TurboFP635+) from VBNR (GFP+++++, TurboFP635+++++) bacteria populations to show the position of the populations sorted.

5.2.4 DNA sequencing characterization of isolated drug tolerant bacterial populations

Targeted DNA sequencing was performed of *katG* and *inh*A regions known to harbour mutations that confer INH resistance in the isolated phenotypically INH drug tolerant (VBNR) *M. smegmatis* bacterial populations. This was done by PCR amplification and targeted gene Sanger sequencing to confirm the emergence of known *katG* and *inh*A promoter drug resistance conferring mutations.

5.2.4.1 Crude DNA extraction and colony screening

Colony screening of VBNR persisters and AR *M. smegmatis* populations was performed. Fifty (25 VBNR and 25 AR) colonies were randomly picked from VBNR and AR *M. smegmatis* LB agar plates containing 5.0 µg/ml INH (1x MIC) from FACS analysis experiments [experiment 1 (8 colonies), experiment 2 (16 colonies) and experiment 3 (16 colonies)], respectively. This was performed with sterile tips into 200 µl of ddH_2O (per colony) into 2.0 ml sterile tubes (Sigma-Aldrich). Picked colonies were mixed with the ddH_2O by pipetting up and down to resuspend. Following this, crude DNA was obtained by incubating 200 µl aliquots of the colonies at 100^0C for 30 min. The extracted crude DNA concentration was measured using NanoDrop™ 2000 (Thermo Fisher Scientific, Massachusetts, USA) (Appendix C: Table S5. 1) and the DNA was stored at 4^0C for subsequent analysis. The extracted crude DNA with concentrations ≥ 100 ng/µl for the 25 VBNR colonies and 25 AR colonies was PCR amplified for the *inh*A promoter and *katG* gene.

5.2.4.2 Primer design for PCR amplification of INH conferring resistance genes

The primers (Table 5.3) used for PCR amplification and targeted gene sequencing were obtained from an oligonucleotide bank maintained at Stellenbosch University, Western Cape, South Africa.

Table 5.6 Primers used for the amplification of anti-TB drug resistance conferring genes

Anti-TB drugs	Gene	Primer	Sequence (5'-3')	T_m (^{0}C)	Fragment length (bp)
INH	*katG*	RTB 59 RTB 38	TGGCCGCGGCGGTCGACATT GGTCAGTGGCCAGCATCGTC	62^{o}C	419 bp
	inhA prom	inhA P5 inhA P3	CGCAGCCAGGGCCTCGCTG CTCCGGTAACCAGGACTGA	55^{o}C	246 bp

5.2.4.3 PCR amplification conditions and fragment visualisation

The PCR master-mix comprised of 5 µl 10X buffer (Qiagen), 1 µl $MgCl_2$ (2.5 mM), 4 µl deoxyribonucleotide triphosphates (dNTP's) (Promega) (0.2 mM of each dNTP), (0.25 µl Forward primer (50 pmol/ µl), 0.25 µl Reverse primer (50 pmol/µl) (of specific gene amplified), 0.15 µl Hotstart Taq polymerase (5 units/µl) (Qiagen). Subsequently, 2.5 µl of the crude DNA template was added to 47.5 µl PCR master mix to a total of 50 µl. No template controls were included in each reaction to assess possible contamination. Additionally, DNA from the laboratory strain, H37Rv ATCC27294 was included as a positive control. The PCR reactions were carried out in the GeneAmp PCR System 2400 (Applied Biosystems, Foster City, California, USA) and were as follows: an initial denaturing step at 95^{0}C for 15 min, followed by 45 cycles of denaturation at 94^{0}C for 1 min, annealing at the T_m of the specific gene primer (Table 5.3) for 1 min, extension at 72^{0}C for 1 min and final extension step at 72^{0}C 15 min. Briefly, fragments were visualized on a 1.5% Tris/Borate/Ethylenediaminetetraacetic acid (TBE) agarose gel stained with 0.13 µg/µl of ethidium bromide (Sigma-Aldrich).

5.2.4.4 DNA sequencing, mutation detection and statistical analysis

The PCR products were submitted for PCR clean-up and sequencing at the Central Analytic Facility (CAF) of Stellenbosch University. Gene sequences (forward direction) for *inh*A promoter and *katG* primers were then aligned using DNA MAN Version 7.0 to the respective gene sequence of the *M. smegmatis* reference strain (https://www.ncbi.nlm.nih.gov) in order to detect the *inh*A (C-15T) promoter and *katG* (Ser315Thr) mutation known to cause INH genetic resistance. To determine whether there were statistically significant differences in the

proportion of identified *inh*A promoter and *katG* mutations between VBNR and AR colonies, statistical analysis and tests were performed in consultation with a biostatistician. Following this, 95% Poisson confidence intervals were calculated using a Pearson's Chi-Squared-test (X^2) (27,28).

5.3 Results

5.3.1 Overall INH mutation frequency determination

In the current study, INH drug treatment at a high concentration (30x MIC) was used to select for VBNR persister from AR bacteria by INH mutation frequency determination. The latter concentration was selected based on previous findings by Keren *et al.* (2011) which showed that high doses of INH induced persister formation (5). The INH mutation frequency was determined by dividing the number of colonies (of the different tested strains) that emerged on solid media supplemented with 5.0 µg/ml INH (1x MIC) to colonies that emerged from plates without INH. The INH mutation frequency was found to be 0.003% for *M. smegmatis*^{UNT}, 10.07% for *M. smegmatis::katG* and 14.75% for *M. smegmatis*^{30x} relative to untreated cultures (Figure 5.4). The mutation frequency of the *M. smegmatis*^{UNT} sample was significantly lower (0.003%) when compared to mutation frequencies for *M. smegmatis::katG* and *M. smegmatis*^{30x} as shown in Figure 5.4 below. This is in agreement with the literature, where mutations with frequencies of 0.001% (29) to 0.0000002% (30) were reported for *M. smegmatis* mc^{2}155.

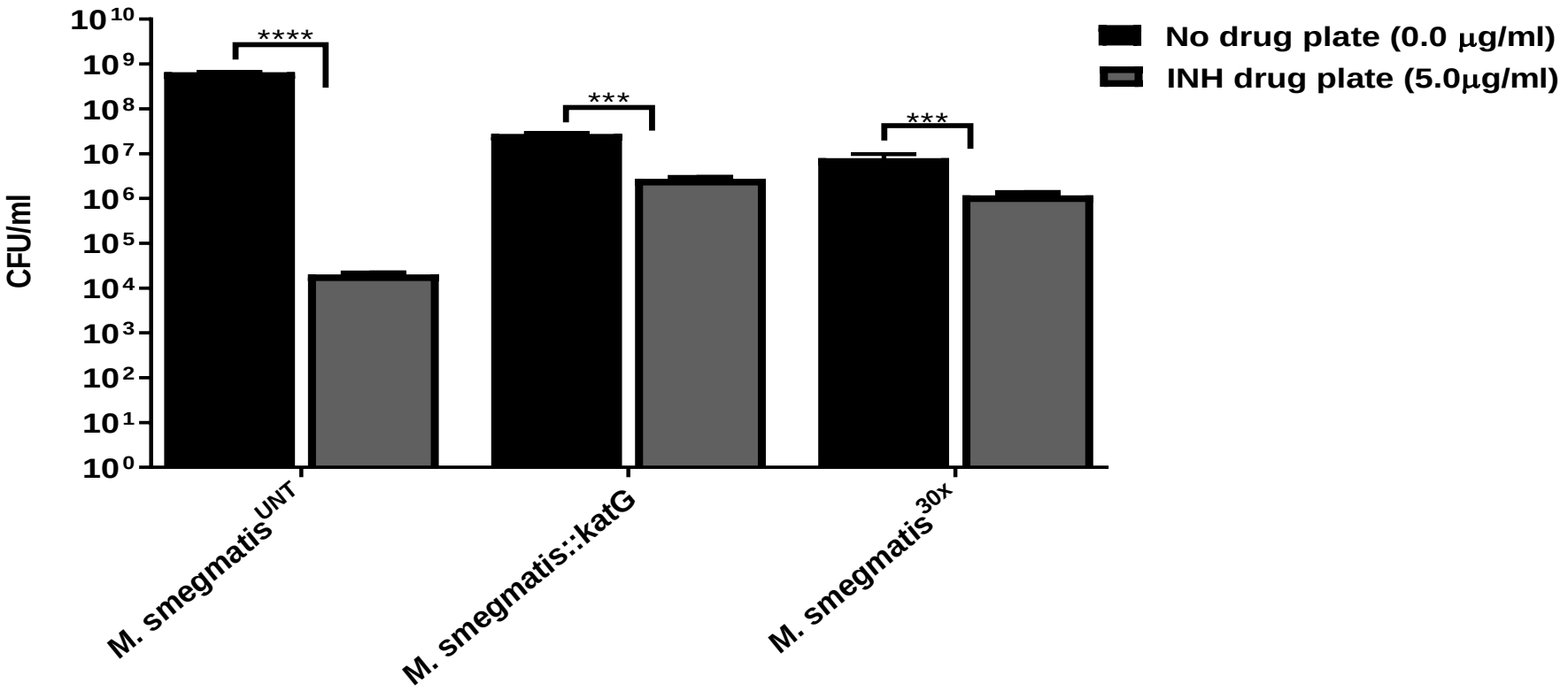

Figure 5.8 INH mutation frequencies in *M. smegmatis* following INH treatment. This graphical plot depicts the determined CFU/ml (*in vitro*) of studied *M. smegmatis* strains in the presence and absence of INH. The mutation frequency of (i) *M. smegmatis*^{UNT} was 2.02 x 10^4 (INH drug plate)/ 6.52 x 10^8 (no drug plate) = 0.003%; for (ii) *M. smegmatis::katG* was 2.76 x 10^6/2.74 x 10^7 = 10.07% and, for (iii) *M. smegmatis*^{30x} = 1.17 x 10^6/ 7.93 x 10^6 = 14.75%, respectively. Multiple t-tests were used and the *** (p= 0.0001) and **** (p= 0.00001) indicates statistical significance. Data shown are representative of three technical replicates and expressed as mean and standard deviation (SD).

5.3.2 Flow cytometry analysis: the detection of VBNR and AR bacterial populations in *M. smegmatis*::pTiGc following INH treatment

To discriminate between the VBNR and AR *M. smegmatis* bacterial populations following 150 µg/ml INH (30x MIC) treatment, the FD reporter system in combination with flow cytometry was exploited. *M. smegmatis*::pTiGc cultures were grown in 7H9-OGT in the presence of 2 mM theophylline (for 24h) and then treated with 150 µg/ml INH (30x MIC), or left untreated (see section 5.2.3.1). Following this, Theo was removed after 24h of INH or no treatment (see section 5.2.3.1) and samples were re-incubated for a further 48h with and without 150 µg/ml INH (30x MIC). After a total of 72h of incubation, samples were then analysed by flow cytometry. To define cut-off gates (black horizontal line) for AR and VBNR populations, untreated (0h and 24h) *M. smegmatis*::pTiGc samples were used to aid in identifying VBNR bacteria formation from 72h INH treated sample, Figure 5.5 (i-ii) depicts the flow cytometry plots for pre-treated bacteria (0h) and bacteria (72h) with and without INH treatment [data for technical replicates in Appendix C: Figure S5.2 (i-ii)].

From our results, we observed that the overall bacterial numbers after INH treatment drastically dropped and within those low bacterial numbers, a small population was high red (indicative of VBNR bacteria) while the majority of the population was low red (representing AR bacteria). The majority of the untreated population retained high GFP fluorescence (19 329/19 333 cells) (Table 5.4). Only 4/19 333 viable (high GFP) cells demonstrated high red fluorescence (Table 5.4). Additionally, a small proportion of AR bacteria stopped fluorescing GFP, suggestive of dead bacilli (5/249 cells). For samples treated with 150 µg/ml INH (30x MIC) for 72h, a small population [Figure 5.5 (ii)] retained a high TurboFP635 signal (14/249 cells) (Table 5.4), indicating that they had reduced replication and represent a distinct VBNR phenotype. The majority of the population [Figure 5.5 (ii)] had a much reduced TurboFP635 signal (235/249 cells) (Table 5.4), indicating that they continued to grow actively and represent AR population. Additionally, heterogeneity was observed in red fluorescence signal as illustrated in Figure 5.5 (ii).

Treatment with 150 µg/ml INH (30x MIC) for 72h, promoted the formation or selection of a VBNR, presumably drug tolerant, *M. smegmatis* population. This allowed us to estimate the frequency of VBNR *M. smegmatis* sub-populations in response to INH treatment at high concentrations, which in turn allowed us to estimate the required bacterial input number/volume for the FACS analysis. This was important to ensure that we were able to capture and sort sufficient VBNR and AR *M. smegmatis* numbers; for the assessment of the

VBNR *M. smegmatis* sub-populations likelihood to provide a reservoir of INH resistance from which genetic resistant mutants could emerge. This was achieved by calculating the percentage of resistant mutants of this population when plated on LB agar plates with and without 5.0 µg/ml INH (1x MIC).

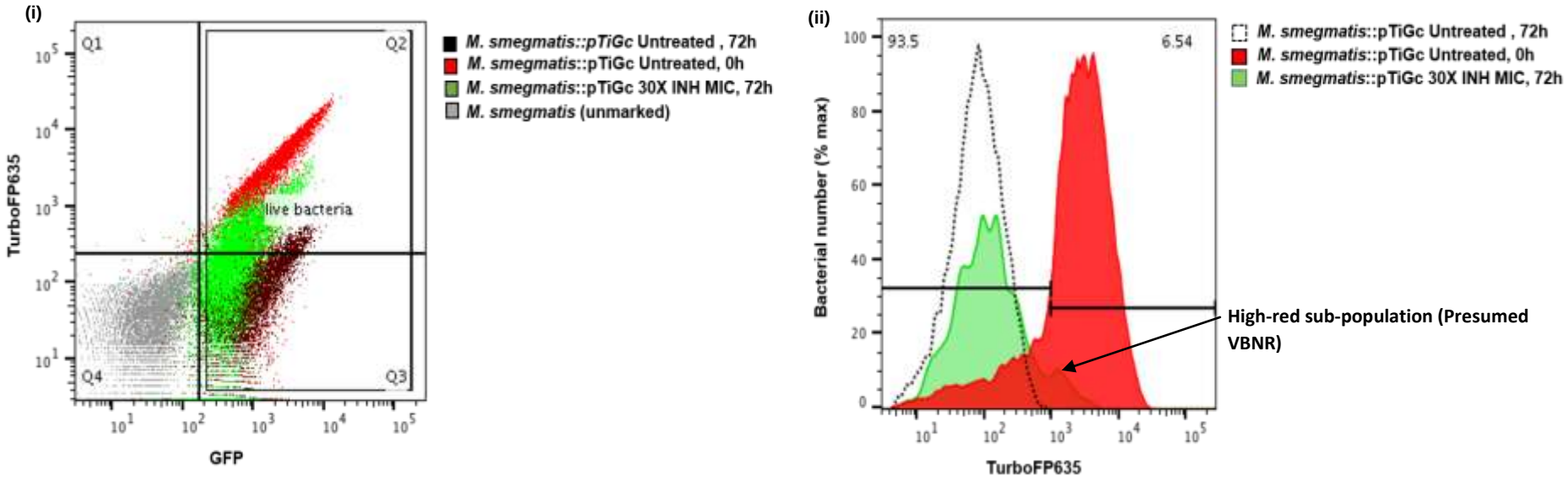

Figure 5.5 (i-ii) The detection of VBNR from AR bacterial population in *M. smegmatis*::*pTiGc* treated with high INH concentrations. The FD reporter system in combination with flow cytometry was exploited to *detect and quantify the* VBNR *in M. smegmatis*::pTiGc. *M. smegmatis*::pTiGc cultures were grown in 7H9-OGT in the presence of 2 mM theophylline for 24h. After 24h samples were prepared and treated with 150 µg/ml INH (30x MIC) for 72h, with theophylline being retained for another 24h before being withdrawn. Samples were then analysed by flow cytometry. Briefly, flow plot (i) represents the fluorescence intensities of the untreated *M. smegmatis*::pTiGc samples at 0h and 72h are depicted in red and black, respectively and treated (150 µg/ml INH (30x MIC)) *M. smegmatis*::pTiGc at 72h is depicted in green. The grey population represents unmarked *M. smegmatis*^{WT} bacteria. The histogram plot (represents the used time points/treatments for the selection of cut-off gates, as indicated by the black horizontal line (ii). The untreated (0h) as depicted by the red and untreated (72h) as depicted by dotted black lines, *M. smegmatis*::pTiGc samples were used to select the cut-off gate values (ii). The histogram plot (ii) depicts the INH-treated populations at 0h (red) and 72h (green), and the untreated population at 72h (black dotted line). The presence of VBNR bacteria following INH treatment is suggested by the high-red sub-population indicated by the arrow. Data shown are representative of the three technical replicates.

Table 5.4 Flow cytometric quantification of populations following treatment with high INH concentration

Condition	Total number live bacteria	Total number high red bacteria	Total number low red bacteria	% "VBNR"
Untreated, 0h	23 339	17 753	5586	N/A
	23 765	17 948	5817	N/A
	24 454	18 719	5735	N/A
Mean	**23 853**	**18 140**	**5713**	**N/A**
Untreated, 72h	23 563	3	23 560	0.01
	17 402	4	17 398	0.02
	17 034	4	17 030	0.02
Mean	**19 333**	**4**	**19 329**	**0.02**
30x INH MIC, 72h	419	28	391	6.68
	169	6	163	3.60
	158	8	150	5.06
Mean	**249**	**14**	**235**	**5.62**

5.3.3 FACS analysis: the isolation and quantification of VBNR from AR *M. smegmatis* in response to INH treatment

The BD FACSJazz™ cell sorter was used to separate the detected VBNR and AR populations following 150 µg/ml INH (30x MIC) treatment for 72h. After FACS, the isolated VBNR (drug tolerant) and AR bacterial populations were plated onto LB agar plates supplemented with and without 5.0 µg/ml INH (1x MIC). This was followed by calculating the INH mutation frequencies of the VBNR and AR *M. smegmatis* bacterial populations by dividing the number of mutants that emerged on the LB agar plates containing INH by the number of those that grew on the LB agar plates without INH. The determined mutation frequencies from the FACS analysis of these separated bacterial populations (*M. smegmatis*^{VBNR}, *M. smegmatis*^{AR} and *M. smegmatis* UNT) (i-iii) are tabulated in Table 5.5 (refer to Figure 5.6 for the values used for mutation frequency calculations). Additionally, the estimated mutation frequencies of the total treated bacterial populations for these different experiments (i-iii) before sorting are also tabulated in Table 5.5. Furthermore, Figure 5.6 illustrates the observed CFU/ml of the different *M. smegmatis* bacterial populations [*M. smegmatis*^{VBNR}, *M. smegmatis*^{AR}, *M. smegmatis* UNT and *M. smegmatis*^{30xmic} (before sort)]. There was no statistical difference for the mutation frequencies estimated from the observed

CFUs for *M. smegmatis*^{VBNR}, *M. smegmatis*^{AR}, *M. smegmatis* UNT populations (refer to Figure 5.6). The data represents three independent biological replicates.

Table 5.5 Summary of FACS analysis and estimated mutation frequencies for VBNR and AR populations in *M. smegmatis*

Number of sort exp.	Bacterial identification	Bacterial numbers captured after sort	Mutation frequency	Purity	Efficiency
i	**Total treated population (before sort)**	N/A	7.14%	-	-
	AR (after sort)	1 500 000	6.13%	74%	89%
	VBNR (after sort)	274 086	3.93%	74%	84%
	UNT (after sort)	1 029 467	0.02%	74%	86%
ii	**Total treated population (before sort)**	N/A	6.90%	-	-
	AR (after sort)	2 742 631	3.26%	94%	85%
	VBNR (after sort)	1 205 734	2.75%	68%	82%
	UNT (after sort)	1 605 905	0.02%	98%	82%
iii	**Total treated population (before sort)**	N/A	6.55%	-	-
	AR (after sort)	1 657 222	6.08%	74%	75%
	VBNR (after sort)	190 058	3.85%	74%	72%
	UNT (after sort)	405 951	0.02%	74%	92%

UNT= untreated M. smegmatis, VBNR (viable but non replicating) bacterial population, AR (actively replication) bacterial population; The total population (before sort) was calculated based on CFU/ml of treated M. smegmatis::pTiGc plated on agar plates supplemented with and without 5.0 µg/ml INH (1x MIC)

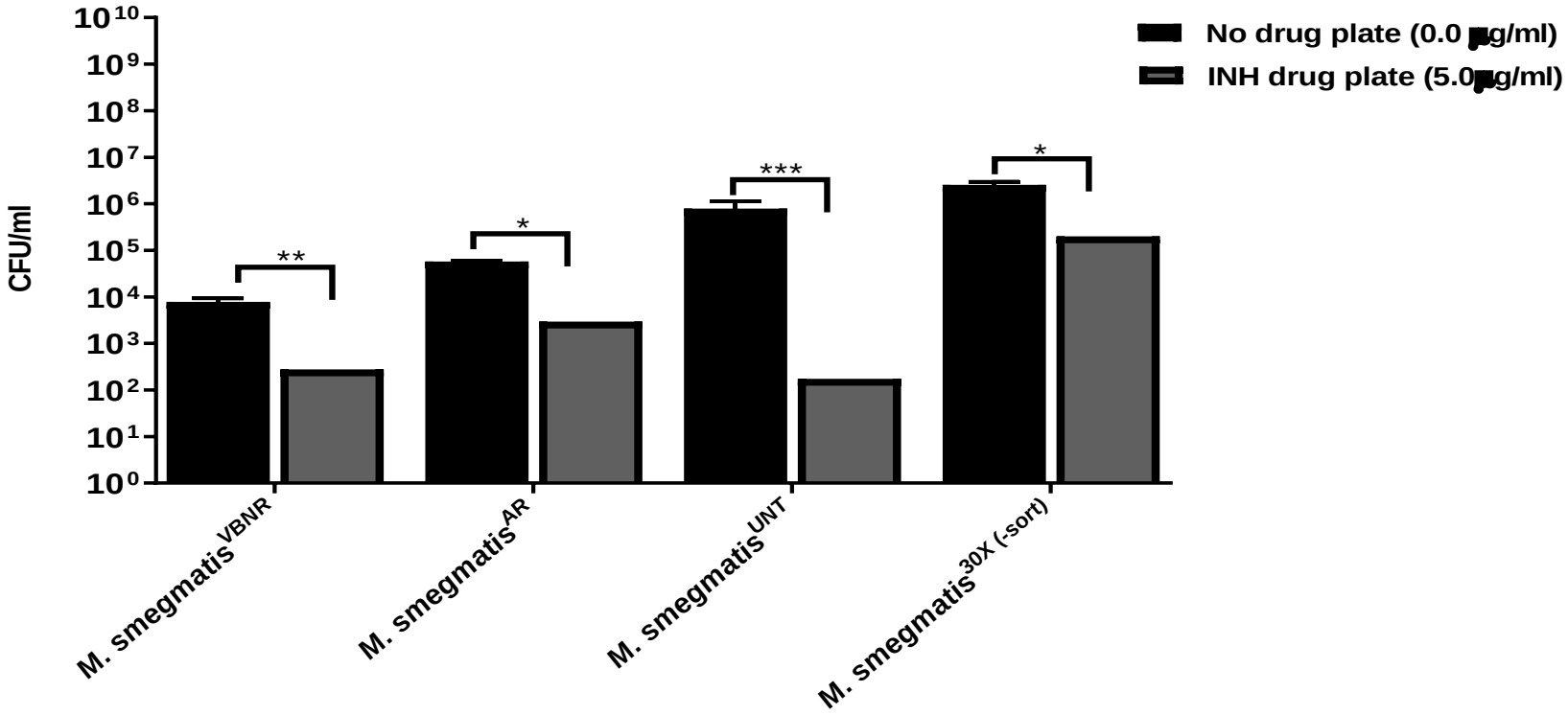

Figure 5.6 The overall INH mutation frequency of the VBNR and AR in *M. smegmatis* determined by CFU analyses following FACS. This graphical plot depicts the determined CFU/ml) of sorted VBNR and AR *M. smegmatis* populations and *M. smegmatis*^{30xmic} before sort in the presence and absence of INH. The mean mutation frequency of *M. smegmatis*^{VBNR} was found to be 277 CFU/ml (INH drug plate)/ 7883 CFU/ml (no drug plate) = 0.0351 x 100% = 3.51% compared to that of *M. smegmatis*^{AR}, which was found to be 2940 CFU/ml (INH drug plate)/ 57400 CFU/ml (no drug plate) = 0.0520 x 100% = 5.20%, but this difference was not statistically significant (p= 0.1). For *M. smegmatis* UNT was found to be 175 CFU/ml (INH drug plate)/ 787200 CFU/ml (no drug plate) = 0.00020 x 100% = 0.02% and for *M. smegmatis*^{30xmic} before sort (CFUs counted from LB agar plates and from FACSJazz run) was found to be 21000 CFU/ml (INH drug plate)/ 256667 CFU/ml (no drug plate) = 0.0690 x 100% = 6.90%. Multiple t tests were used and the * (p= 0.01), ** (p= 0.001), and *** (p= 0.0001) indicates statistical significance. Data shown are representative of three biological replicates and expressed as mean and standard deviation (SD).

5.3.4 Detection of INH resistance-causing mutations in VBNR and AR colonies

Studies have shown that mutations in *katG* and *inhA* promoter are the most frequent mutations associated with INH resistance in clinical settings (31–33). These mutations confer both low and high level INH resistance and for this reason (31–33), these genes were selected for targeted sequencing in the current study. Sequencing analysis of the *katG* and *inhA* promoter region identified mutations in AR and VBNR colonies. Briefly, 19/25 (76%) VBNR colonies harboured *inh*A promoter (C-15T) mutations, while 12/25 (48%) VBNR colonies harboured *katG* (Ser315Thr) mutations (Table 5.6). For AR colonies, 16/25 (64%) harboured *inh*A promoter (C-15T) mutations, while 11/25 (44%) AR colonies harboured *katG* (Ser315Thr) mutations (Table 5.6). Additionally, 10 VBNR and 5 AR colonies had both *inhA* and *katG* mutations (Table 5.6) and 4/25 VBNR and 3/25 AR colonies did not have variations in either of the target genes. We observed a higher number of mutations in the *inh*A promoter (C-15T) in both VBNR (76%) and AR (64%) colonies compared to mutations in the *katG* gene (VBNR, 48%; AR, 44%). However, the calculated 95% Poisson confidence intervals using a Pearson's chi-squared-test (X^2) estimation showed no statistically significant difference ($p > 0.1$) in the proportion of identified *katG* and *inhA* promoter mutations between VBNR and AR colonies (Appendix C: Figure S5.1).

Table 5.6 Identified INH resistance-causing mutations in colonies from VBNR and AR populations of *M. smegmatis*

	VBNR (from 5.0 µg/ml INH (1x MIC) plates)			AR (from 5.0 µg/ml INH (1x MIC) plates)		
Biological replicate 1	**Colony no.**	***inh*A promoter mutation** (C-15T)	***katG* mutation (**Ser315Thr)	**Colony no.**	***inh*A promoter mutation** (C-15T)	***katG* mutation (**Ser315Thr)
	1	+	+	**1**	+	+
	2	+	-	**2**	-	-
	3	+	-	**3**	+	-
	4	-	-	**4**	-	-
	5	-	+	**5**	-	-
	6	-	-	**6**	+	-
	7	+	-	**7**	+	-
	8	+	-	**8**	-	+
	Total no.	**5/8**	**2/8**		**4/8**	**2/8**
Biological replicate 2	**Colony no.**	***inh*A promoter mutation** (C-15T)	***katG* mutation (**Ser315Thr)	**Colony no.**	***inh*A promoter mutation** (C-15T)	***katG* mutation (**Ser315Thr)
	1	+	+	**1**	-	+
	2	+	+	**2**	-	+
	3	+	+	**3**	-	+
	4	+	+	**4**	-	+
	5	+	-	**5**	+	+
	6	+	-	**6**	+	-
	7	+	-	**7**	+	-
	8	-	-	**8**	+	-
Total (%)	**Total no.**	**7/8**	**4/8**		**4/8**	**5/8**
Biological replicate 3	**Colony no.**	***inh*A promoter mutation** (C-15T)	***katG* mutation (**Ser315Thr)	**Colony no.**	***inh*A promoter mutation** (C-15T)	***katG* mutation (**Ser315Thr)
	1	+	+	**1**	_	+
	2	+	+	**2**	+	+
	3	+	+	**3**	+	+
	4	+	-	**4**	+	-
	5	-	-	**5**	+	-
	6	+	+	**6**	+	-
	7	+	+	**7**	+	+
	8	-	+	**8**	+	-
	9	+	-	**9**	+	-
	Total no.	**7/9**	**6/9**		**8/9**	**4/9**
Overall	**Total (%)**	**19/25 (76%)**	**12/25 (48%)**		**16/25 (64%)**	**11/25 (44%)**

VBNR = viable but not replicating, AR= actively replicating, (+) = mutation present and (-) mutation absent

5.4 Discussion

Drug-tolerant bacteria are difficult to eradicate completely because of having developed a VBNR phenotype that restricts drug activity (34), as most drugs are designed to target actively replicating cells (34). VBNR (persisters) are subpopulations of cells that are not genetically resistant, but can phenotypically tolerate increased concentrations of drugs (4,35), and increased drug concentrations might render a VBNR population to potentially emerge with genetic resistance (34). For this reason, it is suggested that bacterial tolerance plays a role in drug resistance and treatment failure. However, this needs to be investigated further. The knowledge gaps in our understanding of the physiology of the persisters; is due to lack of tools to successfully identify, quantify and isolate these persistent populations. This is a challenge, because drug tolerance impacts the emergence of drug resistant TB and possibly, prolonged TB treatment (4).

To attempt to address these knowledge gaps, we first detected VBNR persisters from AR *M. smegmatis* populations using a combination of FD reporter system, flow cytometry and INH treatment at high concentrations. Once we detected and quantified VBNR persisters' sub-population, we isolated it from the AR population in *M. smegmatis::pTiGc*, using FACS in order, to determine the likelihood of the VBNR persisters' sub-population to provide a reservior of INH resistance from which genetic resistant mutants can emerge. We observed mutations in the promoter region of *inhA* (C-15T) and *katG* (Ser315Thr) genes (known to be predominantly associated with INH resistance) using a combination of PCR amplification and targeted DNA sequencing.

In literature, *M. smegmatis* has previously been used as a surrogate for *M. tuberculosis* in a variety of functional studies (36–40). For example, Xu *et al*. (2011) used *M. smegmatis* to confirm the role of mutations in INH (39). For this reason and a few bacterial growth limitations in using *M. tuberculosis*, all experiments in the current study were performed using *M. smegmatis*. In order to obtain quantifiable bacterial numbers, one would have needed to grow larger/cultures of *M. tuberculosis*, which would have had challenging implications because *M. tuberculosis* is a slow grower compared to *M. smegmatis*.

In the current study, the *M. smegmatis*^{UNT} sample demonstrated a low INH mutation frequency of 0.003% (Figure 5.4). Our results compared well to a previous report using a fluctuation assay, which showed mutation frequencies within a similar range of 0.001% (29) to 0.0000002% (30) in *M. smegmatis* mc^{2}155. Therefore, this suggest that the exposure of *M.*

smegmatis^{UNT} sample to 5.0 µg/ml INH (1x MIC) had an influence on the observed mutation frequency of the sample and the type of mutants that were selected on the LB agar plates (30,41). The *M. smegmatis::katG* deletion mutant sample demonstrated a lower proportion of cells that harboured resistance compared to the total number of cells that survived INH treatment. It can be speculated that INH might not have been effectively metabolized by *katG* and it had an off target effect, resulting in reduced growth, but this remains to be explored. Furthermore, this discrepancy could be due to variation in MICs; the observed MIC for *M. smegmatis::katG* deletion mutant is 8.0 µg/ml INH (42) higher than the predetermined (5.0 µg/ml INH MIC) we used in the current study (Figure 5.4). The *M. smegmatis*^{30x} sample demonstrated a high proportion of cells that harboured resistance compared to the total number of cells that survived INH treatment. The INH mutation frequency for *M. smegmatis*^{30x} was determined as 14.75% (Figure 5.4). In support of this, previous reports demonstrated that a subpopulation of the *M. smegmatis* bacterial population continues to grow after a 24h and 72h INH treatment at high 50 µg/ml and 80 µg/ml) INH concentrations respectively, which implicates increased bacterial resistance (43,44)

Our flow cytometry results showed successful detection of VBNR and AR bacterial populations in *M. smegmatis::pTiGc* following INH pre-treatment at high concentration (30x MIC) for 72h (Figure 5.5). The majority of the surviving population (high GFP) did not retain high TurboFP635 signal, suggestive of AR *M. smegmatis* population (Figure 5.5). A small population (5.26%) (Table 5.4) of the live bacterial cells retained a high TurboFP635 signal, suggesting that this population likely transitioned to a distinct tolerant (VBNR) phenotype. Previously, VBNR (persister cells) bacteria were reported in ampicillin pre-treated *E. coli*, using time-lapse microscopy (45). Additionally, Keren *et al*. (2011) confirmed the formation of a subpopulation of drug-tolerant persister cells in response to INH-treated *M. tuberculosis* at high INH concentrations (50x 0.135 µg/ml INH MIC) (5).

Since the VBNR (persisters) population were successfully detected and quantified in this study, we continued to estimate the mutation frequency of this population following INH treatment. This would aid in determining the required bacterial input number/volume for the FACS analysis. Our study was the first to successfully use a FACS analysis approach to isolate and quantify VBNR from AR *M. smegmatis* following INH pre-treatment at a high concentration. Mutation frequencies of different sorted populations were determined as 3.51% for *M. smegmatis*^{VBNR}, 5.20% for *M. smegmatis*^{AR} and 0.02% for *M. smegmatis* UNT (Figure 5.6). The mutation frequency of the total *M. smegmatis*^{30xmic} population before FACS

analyses was determined as 6.90% using CFU. As per Figure 5.6, no statistical significant differences were observed in the mutation frequencies between *M. smegmatis*^{VBNR} and *M. smegmatis*^{AR} bacterial populations (p= 0.1). However, we observed a statistical significant difference in the mutation frequency between *M. smegmatis* UNT and *M. smegmatis*^{30xmic} (p= 0.01) (Figure 5.6).

A loss in bacterial numbers was observed after FACS analyses; this is in line with what others have seen in the literature (25). This could be explained by (i) killing of bacterial cells during INH treatment (at 30x MIC) (ii) loss prior to FACS analyses by adhering to the flow tube, and (iii) during FACS analyses as a result of a stringent gating strategy to ensure the highest possible purity. To minimize the bacterial loss, culture tubes were rinsed with EDTA (2 mM) prior to FACS analyses. EDTA helps to prevent cation dependent cell-cell interactions; minimizing bacterial cells sticking to the flow tubes and thereby increasing bacterial yield (26). There is a lack of experimental techniques in mycobacterial studies to specifically quantify and characterize VBNR (persisters) populations at single cell level. Our approach is the first and allowed us to detect, separate and quantify the VBNR from AR bacterial populations using a combination of FD, flow cytometry and FACS. FACS has been reported in literature to successfully separate VBNR and AR population, in *E. coli* (46–48). Improving our FACS analysis methodology and experimental set-up to account for the loss in bacterial numbers post INH treatment prior to sorting, could render this strategy more efficient.

We determined the likelihood of VBNR *M. smegmatis* sub-population to provide a reservoir of INH resistance from which genetic resistant mutants could emerge, when exposed to high (30x MIC) concentrations of INH using PCR and Sanger sequencing. Sanger sequencing data demonstrated successful detection of INH resistance-causing mutations in the promoter of the *inhA* and *katG* genes from *M. smegmatis* VBNR and AR colonies (selected from INH containing plates). When comparing the percentages of identified resistant mutants between the two genes in both VBNR and AR colonies, we observed a high percentage of mutations in the *inh*A promoter (C-15T) (76% in VBNR; 64% in AR) compared to mutations in the *katG* gene (48% in VBNR; 44% in AR). However, the difference was not statistically significant (p> 0.1). Similar observations have been reported in *M. tuberculosis* strains, where targeted sequencing data revealed approximately 11/40 (27.5%) samples harbouring *katG* (Ser315Thr) mutation*s* (49). Nevertheless, our sample size was limited to 50 colonies (25 VBNR and 25 AR), which may also have impacted the similar proportion of the INH

resistant mutants we observed. It can be further speculated that VBNR *M. smegmatis* population could potentially harbour underlying resistant mutants, driving the emergence of INH genetic resistance, but this remains to be explored further.

Studies have shown that mutations in *katG* and *inhA* promoter are the most frequent ones that are associated with INH resistance in the clinical settings (31–33); conferring low and high levels of INH resistance. In our study both mutations were simultaneously observed in VBNR and AR colonies (10 and 5, respectively, Table 5.6), In contrast, some VBNR and AR colonies selected from INH containing plates (4 and 3, respectively), did not have either of the two targeted mutations. This raises the possibility of other novel INH resistance causing mutations identified by Torres *et al*. (2015) who revealed 23 novel mutations with a previously undocumented role in INH drug resistance in *M. tuberculosis* (36). Moreover, other mutations in genes besides *katG* and *inhA* (*kasA*, *oxyR* and *ahpC*) associated with INH resistance have been reported in clinical *M. tuberculosis* strains (50,51). This suggests that other INH resistant mutants, other than the ones explored in the current study, could have been possibly evident, a limitation of the current study. Interestingly, studies that have shown that there is substantial heterogeneity in drug responses within a *M. smegmatis* population and that various mechanisms underlie the emergence of drug tolerant and drug-resistant subpopulations (4,34,52,53). For example, Levin-Reisman *et al.*, proposed a mathematical population-genetics model that revealed how tolerance enhances the likelihood for resistant mutations to spread in the population (54). This is in agreement with our speculations that VBNR *M. smegmatis* sub-population is more likely to provide a pool of INH resistance from which genetic resistant mutants can arise.

In conclusion, this study was the first to successfully use a FACS analysis in combination with the FD reporter system to detect, isolate and quantify VBNR from AR *M. smegmatis*, following INH pre-treatment at high concentrations (30x MIC). Our study showed that INH resistant mutants emerged from VBNR populations following INH treatment at high 30x MIC concentrations. Data from this study provides evidence that a VBNR *M. smegmatis* population could potentially harbour underlying resistant mutants, driving the emergence of INH genetic resistance, but this remains to be further explored. This has some clinical implications in lengthening the drug resistant TB treatment. Understanding the implication of VBNR *M. smegmatis* sub-populations in the emergence of drug resistance will provide important knowledge for research work done on the underlying mechanism of these cells. Additionally, findings of the current study emphasises the need for development of new

approaches to further explore and eradicate such phenotypically drug-recalcitrant subpopulations in *M. tuberculosis*.

5.5 References

1. **WHO**. 2019. Global tuberculosis report 2019. World Health Organization.

2. **Conde MB, Lapa e Silva JR.** 2011. New regimens for reducing the duration of the treatment of drug-susceptible pulmonary tuberculosis. Drug Dev Res. 2011. **72**:501–8.

3. **Sacchettini JC, Rubin EJ, Freundlich JS.** 2008. Drugs versus bugs: in pursuit of the persistent predator *Mycobacterium tuberculosis.* Nat Rev Microbiol. **6**:41–52.

4. **Brauner A, Fridman O, Gefen O, Balaban NQ.** 2016. Distinguishing between resistance, tolerance and persistence to antibiotic treatment. Nat Rev Microbiol. 14:320–30.

5. **Keren I, Minami S, Rubin E, Lewis K.** 2011. Characterization and transcriptome analysis of *Mycobacterium tuberculosis* persisters. mBio. **2**:00100-11.

6. **Wayne LG, Hayes LG.** 1999. An in vitro model for sequential study of shiftdown of *Mycobacterium tuberculosis* through two stages of nonreplicating persistence. Infect Immun. 64:2062–9.

7. **Helaine S, Thompson JA, Watson KG, Liu M, Boyle C, Holden DW.** 2010. Dynamics of intracellular bacterial replication at the single cell level. Proc Natl Acad Sci. **107**(8):3746-51.

8. **Helaine S, Cheverton AM, Watson KG, Faure LM, Matthews SA, Holden DW.** 2014. Internalization of Salmonella by macrophages induces formation of nonreplicating persisters. Science. **343**:204–8.

9. **Mouton JM, Helaine S, Holden DW, Sampson SL.** 2016. Elucidating population-wide mycobacterial replication dynamics at the single-cell level. Microbiology. **162**(6):966-978.

10. **Barry CE, Boshoff HI, Dartois V, Dick T, Ehrt S, Flynn J, *et al*.** 2017. The spectrum of latent tuberculosis: rethinking the biology and intervention strategies. Nat Rev Microbiol. 7:845–55.

11. **Connolly LE, Edelstein PH, Ramakrishnan L.** 2007. Why Is Long-Term Therapy Required to Cure Tuberculosis? PLoS Med. 4(3).

12. **Höner zu Bentrup K, Russell DG.** 2001. Mycobacterial persistence: adaptation to a changing environment. Trends Microbiol. 9:597–605.

13. **Wayne LG, Sohaskey CD.** 2001. Nonreplicating persistence of *Mycobacterium tuberculosis*. Annu Rev Microbiol. **55**:139–63.

14. **Betts JC, Lukey PT, Robb LC, McAdam RA, Duncan K.** 2002. Evaluation of a nutrient starvation model of *Mycobacterium tuberculosis* persistence by gene and protein expression profiling. Mol Microbiol. **43**:717–31.

15. **Rustad TR, Harrell MI, Liao R, Sherman DR.** 2008. The Enduring hypoxic response of *Mycobacterium tuberculosis*. PLoS ONE. **3**:1502.

16. **Voskuil MI, Visconti KC, Schoolnik GK.** 2004. *Mycobacterium tuberculosis* gene expression during adaptation to stationary phase and low-oxygen dormancy. Tuberc Edinb Scotl. 84:218–27.

17. **Voskuil MI, Schnappinger D, Visconti KC, Harrell MI, Dolganov GM, Sherman DR, *et al.*** 2003. Inhibition of respiration by nitric oxide induces a *Mycobacterium tuberculosis* dormancy program. J Exp Med. 198:705–13.

18. **Jain P, Weinrick BC, Kalivoda EJ, Yang H, Munsamy V, Vilcheze C, *et al.*** 2016. Dual-reporter mycobacteriophages (Φ2DRMs) reveal preexisting *Mycobacterium tuberculosis* Persistent Cells in Human Sputum. mBio. **7**:01023-16.

19. **Jain P, Hartman TE, Eisenberg N, O'Donnell MR, Kriakov J, Govender K, *et al.*** 2012. ϕ2GFP10, a high-Intensity fluorophage, enables detection and rapid drug susceptibility testing of *Mycobacterium tuberculosis* directly from sputum samples. J Clin Microbiol. **50**:1362–9.

20. **Seeliger JC, Topp S, Sogi KM, Previti ML, Gallivan JP, Bertozzi CR.** 2012. A Riboswitch-Based inducible gene expression system for mycobacteria. PLOS ONE. **7**:29266.

21. **Carroll P, Schreuder LJ, Muwanguzi-Karugaba J, Wiles S, Robertson BD, Ripoll J, *et al.*** 2010. Sensitive detection of gene expression in mycobacteria under replicating and non-replicating conditions using optimized far-red reporters. **5**:9823.

22. **Practical Flow Cytometry** - Beckman Coulter. https://www.beckman.com/resources/reading-material/ebooks/practical-flow-cytometry/

23. **Picot J, Guerin CL, Le Van Kim C, Boulanger CM**. 2012. Flow cytometry: retrospective, fundamentals and recent instrumentation. Cytotechnology. **64**:109–30.

24. **Hendon-Dunn CL, Doris KS, Thomas SR, Allnutt JC, Marriott AAN, Hatch KA, *et al.*** 2016. A flow cytometry method for rapidly assessing *M. tuberculosis* responses to antibiotics with different modes of action. Antimicrob Agents Chemother. **60**(7):3869-3883.

25. **Givan AL.** 2011. Flow Cytometry: an introduction. Methods Mol Biol. **699**:1-29

26. **Cossarizza A, Chang H-D, Radbruch A, Acs A, Adam D, Adam-Klages S, *et al.* 2019.** Guidelines for the use of flow cytometry and cell sorting in immunological studies (second edition). Eur J Immunol. **49**:1457–973.

27. **Kucukyildirim S, Long H, Sung W, Miller SF, Doak TG, Lynch M.** 2016. The Rate and Spectrum of Spontaneous mutations in *Mycobacterium smegmatis*, a bacterium Naturally Devoid of the postreplicative mismatch repair pathway. G3 Genes Genomes Genetics. **6**:2157–63.

28. **Univariate Discrete Distributions, 3rd Edition** | Probability & mathematical statistics | General & Introductory Statistics | Subjects | Wiley.com.

29. **Karunakaran P, Davies J.** 2000. Genetic antagonism and hypermutability in *Mycobacterium smegmatis*. J Bacteriol. **182**:3331–5.

30. **Nyinoh IW.** 2019. Spontaneous mutations conferring antibiotic resistance to antitubercular drugs at a range of concentrations in *Mycobacterium smegmatis*. Drug Dev Res. **80**:147–54.

31. **Vilchèze C, Jacobs WR.** 2014. Resistance to isoniazid and ethionamide in *Mycobacterium tuberculosis*: Genes, mutations, and causalities. Microbiol Spectr. **2**:2-0014–2013.

32. **Böttger EC.** 2011. The ins and outs of *Mycobacterium tuberculosis* drug susceptibility testing. Clin Microbiol Infect Off Publ Eur Soc Clin Microbiol Infect Dis. **17**:1128–34.

33. **Lempens P, Meehan CJ, Vandelannoote K, Fissette K, Rijk P de, Deun AV, *et al.*** 2018. Isoniazid resistance levels of *Mycobacterium tuberculosis* can largely be predicted by high-confidence resistance-conferring mutations. Sci Rep. **8**:3246.

34. **Keren I, Kaldalu N, Spoering A, Wang Y, Lewis K.** 2004. Persister cells and tolerance to antimicrobials. FEMS Microbiol Lett. **230**:13–8.

35. **Gefen O, Balaban NQ.** 2009. The importance of being persistent: heterogeneity of bacterial populations under antibiotic stress. FEMS Microbiol Rev. 33:704–17.

36. **Torres JN, Paul LV, Rodwell TC, Victor TC, Amallraja AM, Elghraoui A, *et al.*** 2015. Novel *katG* mutations causing isoniazid resistance in clinical *M. tuberculosis* isolates. Emerg Microbes Infect. **4**:42.

37. **Zhang Y, Heym B, Allen B, Young D, Cole S.** 1992. The catalase-peroxidase gene and isoniazid resistance of *Mycobacterium tuberculosis*. Nature. **1358**:591–3.

38. **Borrell S, Teo Y, Giardina F, Streicher EM, Klopper M, Feldmann J, *et al.*** 2013. Epistasis between antibiotic resistance mutations drives the evolution of extensively drug-resistant tuberculosis. Evol Med Public Health. **2013**(1):65-74.

39. **Xu X, Vilchèze C, Av-Gay Y, Gómez-Velasco A, Jacobs WR.** 2011. Precise null deletion mutations of the mycothiol synthesis genes reveal their role in isoniazid and ethionamide resistance in *Mycobacterium smegmatis* ▽. Antimicrob Agents Chemother **55:**3133–9.

40. **Shcherbakov D, Akbergenov R, Matt T, Sander P, Andersson DI, Böttger EC. 2010.** Directed mutagenesis of *Mycobacterium smegmatis* 16S rRNA to reconstruct the *in vivo* evolution of aminoglycoside resistance in *Mycobacterium tuberculosis*. Mol Microbiol. **77**:830–40.

41. **Hughes D, Andersson DI.** 1997. Carbon starvation of *Salmonella typhimurium* does not cause a general increase of mutation rates. J Bacteriol **179**:6688–91.

42. **de Steenwinkel JEM, de Knegt GJ, ten Kate MT, van Belkum A, Verbrugh HA, Kremer K, *et al***. 2010. Time–kill kinetics of anti-tuberculosis drugs, and emergence of resistance, in relation to metabolic activity of *Mycobacterium tuberculosis*. J Antimicrob Chemother **65**:2582–9.

43. **Elitas M.** 2017 Isoniazid killing of *Mycobacterium smegmatis* NADH pyrophosphatase mutant at single-cell level using microfluidics and time-lapse microscopy. Sci Rep. **7**:10770.

44. **Teng R, Dick T.** 2003. Isoniazid resistance of exponentially growing *Mycobacterium smegmatis* biofilm culture. FEMS Microbiol Lett. 1 **227**:171–4.

45. **Balaban NQ, Merrin J, Chait R, Kowalik L, Leibler S.** 2004. Bacterial persistence as a phenotypic switch. Science. **305**:1622–5.

46. **Orman MA, Brynildsen MP.** 2013. Dormancy is not necessary or sufficient for bacterial persistence. Antimicrob Agents Chemother. 57:3230–9.

47. **Zhu J-H, Wang B-W, Pan M, Zeng Y-N, Rego H, Javid B.** 2018. Rifampicin can induce antibiotic tolerance in mycobacteria via paradoxical changes in *rpoB* transcription. Nat Commun. **9**:1–13.

48. **Henry TC, Brynildsen MP.** 2016. Development of Persister-FACSeq: a method to massively parallelize quantification of persister physiology and its heterogeneity. Sci Rep. **6**:25100.

49. **Li D, Song Y, Zhang C-L, Li X, Xia X, Zhang A-M.** 2017. Screening mutations in drug-resistant *Mycobacterium tuberculosis* strains in Yunnan, China. J Infect Public Health. **10**:630–6.

50. **Ling DI, Zwerling AA, Pai M.** 2008. GenoType MTBDR assays for the diagnosis of multidrug-resistant tuberculosis: a meta-analysis. Eur Respir J. **32:**1165–74.

51. **Farooqi JQ, Khan E, Alam SMZ, Ali A, Hasan Z, Hasan R.** 2012. Line probe assay for detection of rifampicin and isoniazid resistant tuberculosis in Pakistan. JPMA J Pak Med Assoc. **62**:767–72.

52. **Handwerger S, Tomasz A.** 1985. Antibiotic tolerance among clinical isolates of bacteria. Annu Rev Pharmacol Toxicol. **25**:349–80.

53. **Kester JC, Fortune SM.** 2014. Persisters and beyond: mechanisms of phenotypic drug resistance and drug tolerance in bacteria. Crit Rev Biochem Mol Biol. **49**:91–101.

54. **Levin-Reisman I, Ronin I, Gefen O, Braniss I, Shoresh N, Balaban NQ.** 2017. Antibiotic tolerance facilitates the evolution of resistance. Science. **355**(6327):826–30.

CHAPTER 6

General Conclusion

6.1 Conclusion

The current study was designed to explore key knowledge gaps concerning *Mycobacterium tuberculosis* physiology; investigating the influence of *M. tuberculosis* genetic diversity and resistance conferring mutations on the transcriptome, host response and whether induced mycobacterial tolerance can give rise to a reservoir of genetic resistance. Exploring some of these key knowledge gaps was imperative, given the fact that, lengthy anti-TB drug treatment is required to entirely eradicate *M. tuberculosis*, while incomplete treatment may lead to the emergence of MDR-TB.

Our review of the literature (Chapter 2) highlighted the *M. tuberculosis* cell wall, a target of the key anti-TB drug, isoniazid (INH). Specifically, INH targets mycolic acids biosynthesis. *M. tuberculosis* is able to exploit the complexity of its cell wall to adapt and survive INH treatment. The cell wall acts as a permeability barrier to limit influx of INH (and RIF) into the bacterial cell. This results in insufficient INH intracellular concentration which is required for prodrug activation with the catalase-peroxidase, KatG. Thus the mycolic acids biosynthesis is not disrupted and the cellular structure remains intact allowing *M. tuberculosis* to continue to grow. The latter may also be a consequence of *M. tuberculosis* INH resistance (mostly mutations in *katG* gene and *inhA* promoter). This confirms that mycolic acids biosynthesis is an essential component of the cell wall that needs to be explored further; for identifying potential anti-TB drug targets and genes able to shut down this pathway.

Our review also highlighted different mechanisms of INH resistance associated with *M. tuberculosis* clinical strains, which are not only limited to prominent resistance-conferring mutations in *katG* (high-level of INH resistance) and *inhA* (low-level of INH resistance). It provided evidence that there are other rare compensatory mutations (*ahpC, oxyR, furA* and *kasA* etc) accounting for low-level INH resistance in *M. tuberculosis*. It provided an overview of other underlying mechanisms that play an important role in low-level INH resistance in *M. tuberculosis*. For example, (i) Fitness cost associated with INH resistance (1,2), (ii) metabolic pathways (degradation pathway of alkanes) associated with INH resistance (3), (iii) efflux pump mechanisms (*iniABC* and *efpA*) (4,5), and (iv) the drug tolerance accounting for intrinsic resistance (6).

We know that transmission of RIF resistant *M. tuberculosis* strains fuels the MDR-TB epidemic, however it is not clear whether INH resistant *M. tuberculosis* strains contribute similarly. Epidemiological studies from different settings reviewed in the current study,

provided contrasting evidence. Certain studies have shown a correlation between the prevalence of INH-monoresistance and MDR-TB transmission, while other reports showed this to a certain extent. For example, Denkinger *et al*. (2014) demonstrated that adding the detection of INH-resistance to a rapid test for TB plus RIF-resistance, had minimal impact on the transmission of INH-monoresistant and MDR-TB strains (7). Nevertheless, *in vitro* evidence suggested that the nature of pre-existing INH resistant allele can influence the spectrum of subsequent *rpoB* mutations (8). Therefore, it can be suggested that maybe there is somehow an epistatic interaction between INH resistant and RIF resistant mutations, which might influence the success of MDR-TB strains. For this reason, more knowledge about the prevalence of both INH and RIF-monoresistance could provide insight into the continuing spread and evolution of drug-resistant TB.

Our differential gene expression data (Chapter 3) highlighted that *M. tuberculosis* strains genetic background influences the total transcriptome. Additionally, there is a significant difference in the physiological state of clinical *M. tuberculosis* strains compared to the H37Rv laboratory strain, as reflected in their transcriptomes. The overexpression of multiple genes belonging to cell wall components and intermediary metabolism and respiration functional categories, suggests potential identification of novel cell wall metabolism pathways in *M. tuberculosis*. We demonstrated that *rpoB* Ser531Leu mutation has an impact on the transcriptional responses of $K636^{WT}$ relative to $K636^{RIF}$ *M. tuberculosis* strains. This was made evident by the transcriptional profile signature we observed, showing differential expression of important regulatory proteins and genes belonging to the cell wall and cell processes category; all of which play a role in transcription regulation and *M. tuberculosis* survival under stressful conditions. Therefore, further exploration of specifically identified genes involved in transcriptional regulation in $K636^{RIF}$ *M. tuberculosis* strain and genes in cell wall and cell processes functional category associated with the presence of *rpoB* Ser531Leu mutation will aid in the identification of potential anti-TB drug targets. Interestingly, similar transcriptional data comparison patterns between $K636^{WT}$ vs $H37Rv^{WT}$ and $K636^{WT}$ vs $K636^{RIF}$ *M. tuberculosis* strains were observed in terms of host response data (Chapter 4).

Our host response data (Chapter 4) highlighted that there was no differences in immune response to $K636^{WT}$ and $H37Rv^{WT}$ *M. tuberculosis* strains despite their different genetic backgrounds. In contrast, there were differences in immune responses between $K636^{WT}$ and $K636^{RIF}$ *M. tuberculosis* strains in a RAW264.7 macrophage model of infection. This was

confirmed by the varying levels of secretion of cytokines and chemokine (IL-6, IL-12p40 and RANTES) following infection with *M. tuberculosis* for 24-48h. We concluded that the host response is highly pro-inflammatory towards infection with these tested *M. tuberculosis* strains, as reflected by vast majority of cytokines and chemokines belonging to this group. Our results further demonstrated that *rpoB* Ser531Leu mutation might have influenced the RAW264.7 macrophages response to infection with $K636^{RIF}$ *M. tuberculosis* strain. We confirmed this by demonstrating some of the genes which were uniquely differentially expressed that could have modulated the release of the IL-6, IL-12p40 cytokines and RANTES chemokine resulting in the different immune responses between $K636^{WT}$ and $K636^{RIF}$ *M. tuberculosis* strains. For example, this included the *whiB*-like family genes (*whiB1*, *whiB6* and *whiB7*), *mmpL4 – mmpS4* operon and *pks6.* This knowledge accentuates the importance of understanding the mechanisms of pathogenesis, the host-pathogen interactions and host response to infection with drug susceptible and resistant *M. tuberculosis* strains. One of the confounding factors that makes it difficult for the host to completely kill drug resistant *M. tuberculosis*; is the existence of drug-tolerant bacterial population that has developed a VBNR phenotype that restricts drug activity (9), as most drugs are designed to target actively replicating cells (9).

Our study findings (Chapter 5) highlighted successful characterization of VBNR (persisters) sub-population from AR population in *M. smegmatis.* We confirmed that a combination of FD reporter system and flow cytometry techniques can successfully aid in the detection and isolation of VBNR from AR in *M. smegmatis*, following pre-exposed to high INH (30x MIC) concentrations. We highlighted certain challenges that we observed during the sorting process, which could account for the possible loss in bacterial numbers i.e. bacterial cells being killed during INH treatment, loss of bacterial cells prior to sorting by sticking to the flow tube, and during sorting (FACSJazz run) resulting in fewer cells being captured. We show that the VBNR persisters' sub-population could provide a reservoir of INH resistance from which genetic resistant mutants can emerge. However, we can't fully confirm this because we observed a similar number of mutants in VBNR and AR *M. smegmatis*, therefore future work needs to explore this further to validate these results. The importance of understanding the implications of VBNR persisters' sub-population in the emergence of drug resistance will provide important knowledge for research work done on the underlying mechanisms of VBNR persisters mycobacterial sub-populations.

6.2 Limitations and future work

For future work, the differential expression needs to be confirmed in other RIF resistant and susceptible clinical *M. tuberculosis* strains. This will help to determine whether some the identified differntially-expressed genes belonging to cell wall and cell processes and regulatory proteins, can be studied further for identifying potential novel anti-TB drugs targets. In the current study, we were only able to use differential gene expression data obtained from two biological samples. We investigated (with the help of our bioinformatician) why the specific biological sample did not work, we discovered that there was some difference in the number of reads between this specific biological sample and the other two that worked well. Therefore, suggesting that this variation in read numbers between samples may have affected the results and resulting in increased variation between this biological sample counts; in turn, decreasing the sensitivity of detecting differential expression genes. For this reason, normalization is recommended as it can account for some of the differences, nevertheless not for all differences. Hence, for future work would be to perform RNA-Seq for another biological sample and the data to be added to our differential gene expression analysis. Our biggest limitation was that, we could not demonstrate the effect of INH treatment on the transcriptomes of *M. tuberculosis* strains from different genetic backgrounds. This could possibly be explained by the 24h exposure time not being longer enough for INH treatment to induce transcriptional responses. Future work would be to conduct similar RNA-Seq experiments, treating the *M. tuberculosis* strains with the same optimized 0.05 µg/ml INH but for a longer time period (48h) and then to reassess the effect of INH treatment on transcriptional profiles of INH treated *M. tuberculosis* strains.

In terms of host immune responses, future work would be to validate the cytokines and chemokine that were significantly secreted at high levels; by performing ELISA and multiplex assay experiments in well-defined bone marrow derived macrophages (BMDM) following infection with genetically resistant and susceptible *M. tuberculosis* strains. BMDM model of infection will give us a better representation of the cytokines and chemokines secretion signatures than in RAW264.7 macrophages (cell line). Additionally, for future work purposes, increasing the number of clinical *M. tuberculosis* strains (sample size) would be beneficial and increase the confidence and power of our secreted cytokines and chemokines data statistical analysis.

This study was the first to use FACS analysis in combination with the FD reporter system to detect, isolate and quantify VBNR from AR *M. smegmatis*, following INH pre-treatment at

high concentrations. This means, the experimental set-up was applied for the first time and a few challenges and limitations with the optimization of methods were experienced. Other limitations included only looking at targeted sequencing of the most prominent INH resistance-causing mutations that had been reported in literature, of which some of the sequenced INH resistant VBNR and AR colonies happened to not have either of these two targeted mutations. Another limitation was the restricted sample size (number of colonies that were sequenced). Therefore, future work would be to consider increasing the sample size of VBNR/AR *M. smegmatis* colonies and to consider performing WGS deep sequencing of VBNR/AR *M. smegmatis* colonies. Then potentially optimizing this study in *M. tuberculosis* model (most important), starting with H37Rv laboratory strain and potentially transitioning into clinical *M. tuberculosis* strains.

Overall, this study contributed knowledge to the research field. It provided more knowledge and evidence about (i) the current state of INH resistance in *M. tuberculosis*, (ii) the influence of the *M. tuberculosis* strains from different genetic backgrounds on the transcriptome, (iii) the RAW264.7 macrophages response to infection with *M. tuberculosis* strains, (iv) the role played by VBNR persisters bacterial sub-populations in the emergence of INH genetic resistance and, (v) the potential use of FACS in combination with FD and flow cytometry to study drug tolerant (persisters) mycobacterial populations.

6.3 References

1. **Davies AP, Billington OJ, Bannister BA, Weir WR, McHugh TD, Gillespie SH.** 2000. Comparison of fitness of two isolates of *Mycobacterium tuberculosis*, one of which had developed multi-drug resistance during the course of treatment. J Infect. **241**:184–7.

2. **Sander P, Springer B, Prammananan T, Sturmfels A, Kappler M, Pletschette M, *et al.*** 2002. Fitness Cost of Chromosomal Drug Resistance-Conferring Mutations. Antimicrob Agents Chemother. **46**:1204–11.

3. **Loots DT.** 2014. An Altered *Mycobacterium tuberculosis* Metabolome induced by *katG* mutations resulting in isoniazid resistance. Antimicrob Agents Chemother **58**:2144–9.

4. **Zhang M, Yue J, Yang Y, Zhang H, Lei J, Jin R, *et al.*** 2005. Detection of mutations associated with isoniazid resistance in *Mycobacterium tuberculosis* isolates from China. J Clin Microbiol. **43:**5477–82.

5. C**olangeli R, Helb D, Sridharan S, Sun J, Varma-Basil M, Hazbón MH, *et al.*** 2005. The *Mycobacterium tuberculosis iniA* gene is essential for activity of an efflux pump that confers drug tolerance to both isoniazid and ethambutol. Mol Microbiol. **55:**1829–40.

6. **Brauner A, Fridman O, Gefen O, Balaban NQ. 2016.** Distinguishing between resistance, tolerance and persistence to antibiotic treatment. Nat Rev Microbiol. **14**:320–30.

7. **Denkinger CM, Pai M, Dowdy DW**. 2014. Do We Need to Detect Isoniazid Resistance in Addition to Rifampicin Resistance in Diagnostic Tests for Tuberculosis? PLoS ONE.

8. **Bergval I, Kwok B, Schuitema A, Kremer K, van Soolingen D, Klatser P, *et al.*** 2012. Pre-existing isoniazid resistance, but not the genotype of *Mycobacterium tuberculosis* drives rifampicin resistance codon preference in vitro. PloS One. **7**:29108.

9. **Keren I, Kaldalu N, Spoering A, Wang Y, Lewis K.** 2004. Persister cells and tolerance to antimicrobials. FEMS Microbiol Lett. **230**:13–8.

APPENDICES

APPENDIX A: (i) Blood agar plates and ZN staining

The blood agar and ZN staining were done to monitor possible contamination. These included plating *M. tuberculosis* cultures (10 µl) onto blood agar (Sigma-Aldrich, St Louis, Missouri, USA) for period of two days as *M. tuberculosis* does not grow on blood agar for that period. The composition of blood agar includes, a protein source (e.g. Tryptones), soybean protein digest, sodium chloride (NaCl), agar and 5% sheep blood. Secondly, ZN staining was done as follows. The smear cultures were prepared and heat fixed at 100°C for 2 hours. They were then stained with carbol-fuchsin (Becton, Dickinson and Company, Maryland, USA) for 5 min, followed by 3 min with acid alcohol and finally counterstaining them with methylene blue (BD, Bioscience, New Jersey, USA) for 5 min. The counterstained smears were visualized at 100x (oil immersion) magnification under the microscope for acid-fast bacilli. As *M. tuberculosis* is an acid-fast bacilli which retains dyes when handled and heated with acid containing compounds, the bacilli were expected to appear pink.

APPENDIX A: (ii) Generating RIF resistant M. tuberculosis *in vitro* mutant

RIF-resistant mutant (generated by *in vitro* selection) with *rpoB* Ser531Leu mutation (denoted as $K636^{RIF}$) derived from the pan- susceptible K636 progenitor a by growing/ inoculating a 100 µl of the filtered culture of (pan- susceptible K636) onto a number of Middlebrook 7H10 agar plates (Becton Dickinson) either with or without 2 µg/ml rifampicin, 100 µg/ml 150 µg/ml or 200 µg/ml and supplemented with 0.5% (v/v) glycerol (Merck Laboratories), 10% (v/v) OADC. The plates were incubated for 21 days at 37°C after which CFU was determined to calculate mutation frequency and colonies were randomly picked from each plate. Picked colonies were mixed with the ddH_2O by pipetting up and down to resuspend. Following this, crude DNA was obtained by incubating 200 µl aliquots of the colonies at 100^0C for 30 min. The extracted crude DNA concentration was measured using NanoDrop™ 2000 (Thermo Fisher Scientific) and the DNA was stored at 4^0C for subsequent analysis. The extracted crude DNA with concentrations ≥ 100 ng/µl for RIF-resistant mutant K636 was PCR amplified for the *rpoB* Ser531Leu gene. To confirm the presence or absence of the RIF resistance-conferring Ser531Leu mutation in the *rpoB* gene, the PCR products were submitted for PCR clean-up and sequencing at the Central Analytic Facility (CAF) at Stellenbosch University The sequencing was done using the ABI 3730xl DNA Sequencer (Thermo Fisher Scientific). To detect genetic variants, gene sequences obtained from CAF were aligned to the gene sequence of *M. tuberculosis* H37Rv reference strain (http://genolist.pasteur.fr/Tuberculist) using DNA MAN Version 4.1.

APPENDIX A: (iii) genomic DNA extraction (As per reference 23, the method used)

The *M. tuberculosis* clinical isolate of *M. tuberculosis* was inoculated under biosafety level 3 conditions onto 7H10 Middlebrook agar plates and incubated at 37°C with for 21 days. Confluent growth was observed. Thereafter, the outer surface of each agar plate was sterilized by swabbing with 5% Hycolin (William Pearson Chemicals, United Kingdom) and then placed in a stainless steel rack within an unsealed biosafety autoclave bag (305 by 660 mm; Sterilin, United Kingdom) and transferred to a prewarmed circulating fan oven (580 by 540 by 510 mm) at 80°C for 1h to ensure heat killing. Three milliliters of extraction buffer (5% sodium glutamate, 50 mM Tris-HCl [pH 7.4], and 25 mM EDTA) was added to each slant in a biosafety class 2 laminar flow hood, and the colonies were gently scraped from the solid medium with a disposable 10 µl loop. The suspension from both agar plates was then transferred to a sterile 50 ml polypropylene Falcon tube containing approximately 20 glass beads (diameter, 4 mm) and vigorously vortexed to disrupt all colonies. Lysozyme (25 mg; Roche, Germany) and RNase A (50 µg; Roche, Germany) (preheated to remove DNases) were added, and the suspension was incubated after gentle mixing for 2h at 37°C. Thereafter, 600 µl of 10× proteinase K buffer (5% sodium dodecyl sulfate, 100 mM Tris-HCl [pH 7.8], 50 mM EDTA) and 1.5 mg of proteinase K (Roche, Germany) were added and the suspension was incubated at 45°C for 16 h. An equal volume of phenol-chloroform-isoamyl alcohol (25/24/1) was then added (standard fume cabinet) and intermittently mixed over a period of 2h at room temperature. Following centrifugation at 3,000 × g for 20 min, the resultant aqueous phase was reextracted with an equal volume of chloroform-isoamyl alcohol (24/1) and centrifuged as described above. The resultant DNA was then precipitated with the addition of 3 M sodium acetate (pH 5.2) (600 µl) and an equal volume of isopropanol and immediately collected on a fine glass rod. The DNA was washed in 70% ethanol and allowed to air dry at room temperature. The purified DNA was redissolved in 300 µl TE (10 mM Tris-HCl [pH 8.0], 1 mM EDTA) (23).

APPENDIX B: Chapter 3: RNA-Seq bioinformatics analysis:

Removal of adapters from reads: Trimmomatic software and TrueSeq-PE.fa code

The "Trimmomatic software and TruSeq3-PE.fa" in R programming language (free software platform for statistical computing): bioconductor: java -jar Trimmomatic-0.36/trimmomatic-0.36.jar "PE -phred33 -threads12 Forward_1.fastq reverse_2.fastq forward_1_paired.fastq forward_1_unpaired.fastq reverse_2_paired.fastq reverse_2_unpaired.fastq ILLUMINACLIP:TruSeq3-PE.fa :2:30:10 LEADING:3 TRAILING:3 SLIDINGWINDOW :4:15 MINLEN:36" was used to remove adapters and low quality reads from FASTQ files of the all Illumina RNA sequencing data [from chapter 3 methods (section 3.2.7**)].**

APPENDIX C: Chapters results supplementary data

Chapter 3: Results supplementary data

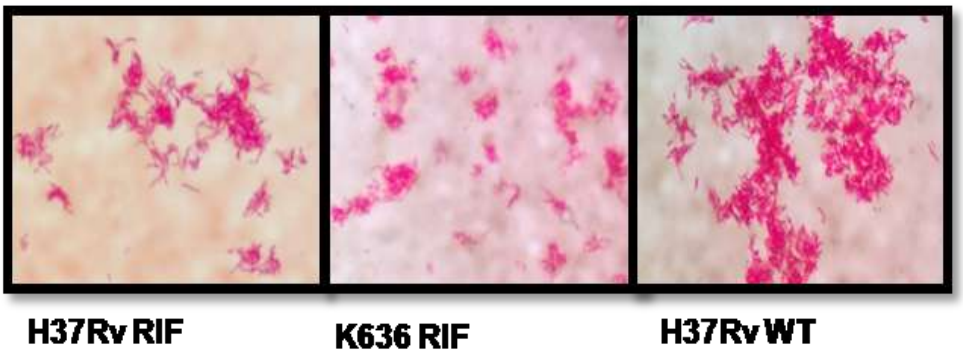

Figure S3.1 ZN straining of *M. tuberculosis* stains. All *M. tuberculosis* strains stained acid-fast and confirmed to be mycobacteria. WT = wildtype

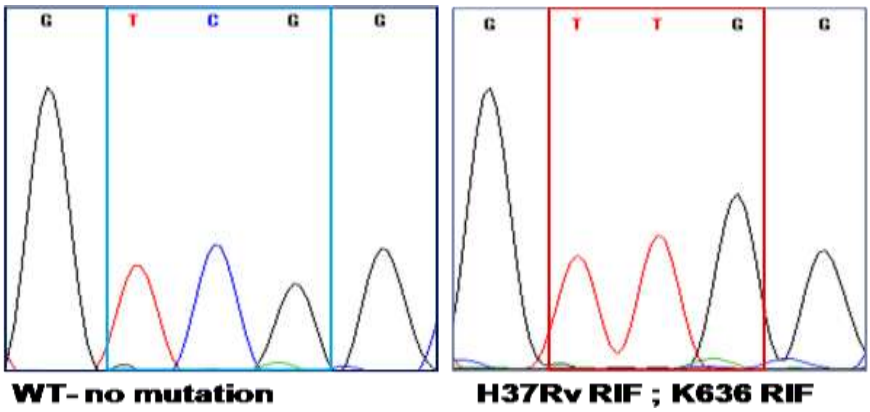

Figure S3.2 Sequence chromatograms of *M. tuberculosis* strains. PCR and DNA sequencing confirmed the expected genotypes in the RIF resistant *in vitro* mutants, $K636^{RIF}$ and $H37Rv^{RIF}$ (with *rpoB* Ser531Leu mutation).

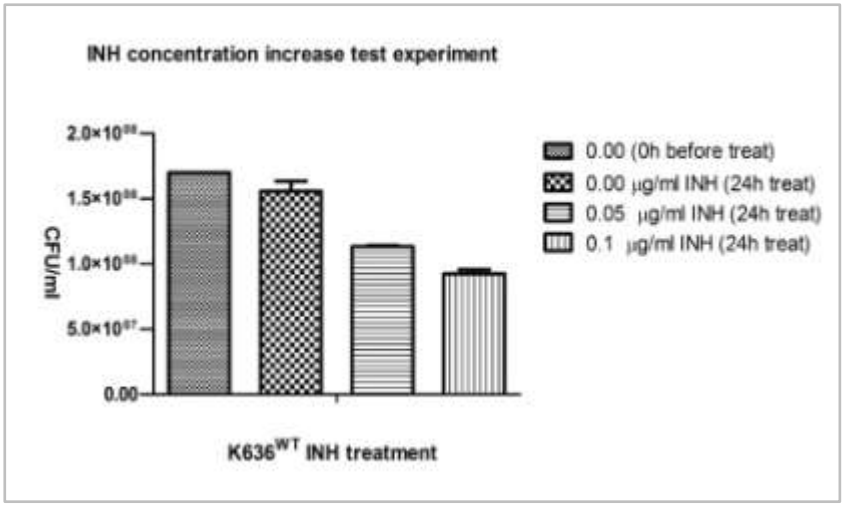

Figure S3.3 Increased INH Concentration for RNA-Seq cultures treatment Preliminary experiment to increase INH concentration was performed by plating out a mid-log phase *M. tuberculosis* culture ($K636^{WT}$) exposed/unexposed to sub-lethal concentration of INH (0.05 µg/ml and 0.1 µg/ml) on 7H10 Middlebrook agar. The 0.05 µg/ml and 0.1 µg/ml INH showed a drop in CFUs (2-fold) when compared to untreated controls in $K636^{WT}$. Therefore, 0.05 µg/ml INH concentration was found to be the ideal concentration and it was validated and used to treat *M. tuberculosis* RNA extracted for RNA-Seq. The plot is the demonstration of the mean values and standard deviation (SD) of the biological replicates.

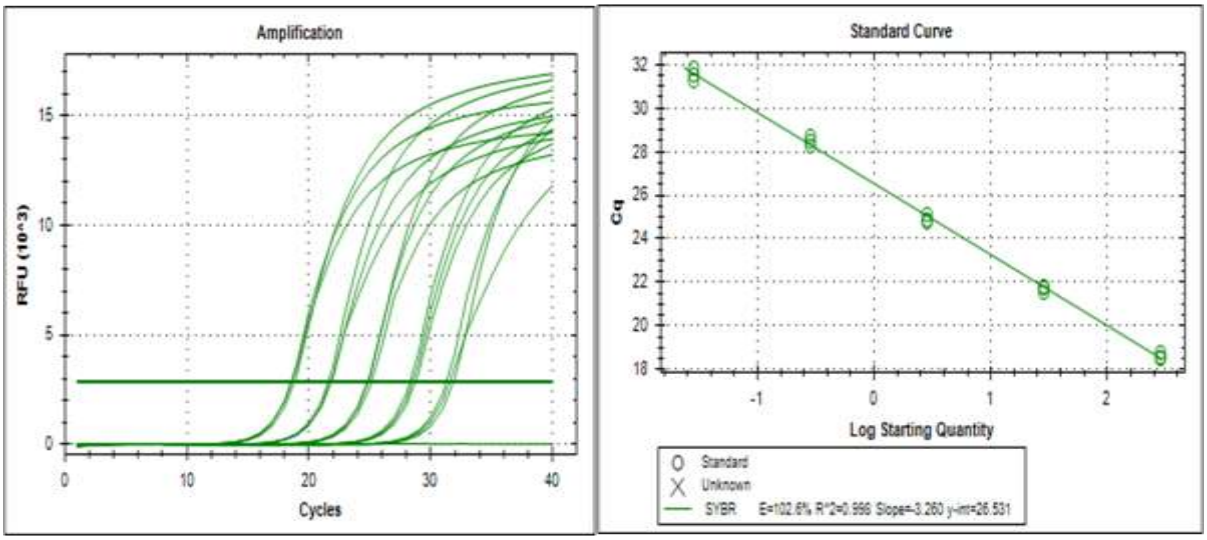

Figure S3.4An example of generated *kasA* standard curve illustrating determined % efficiency and cq values. Previously determined T_m (60.4 – 61.8 °C) by gradient PCR was used to construct gDNA standard curves of optimized primers, for RT-qPCR experiment to assess gene expression. The generated standard curves cq values were found to be between cycles 15 -30 cq at 60.4 – 61.8 °C, with efficiency values between 90 – 110 % as per requirements.

Chapter 4: supplementary data

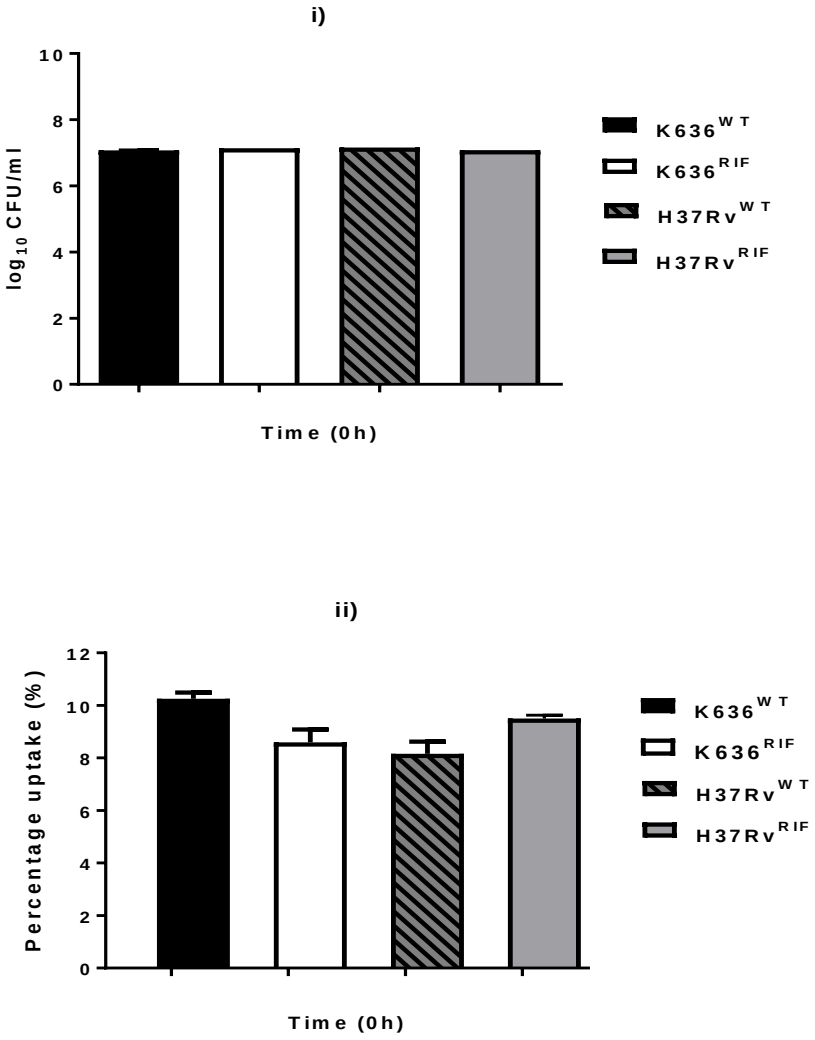

Figure S4.1 Inoculum size and percentage uptake of *M. tuberculosis* strains in RAW264.7 macrophages (i) Represents the inoculum sizes (1.2 x10^7 CFU/100 ul $K636^{WT}$; 1.3 x10^7 CFU/100 µl $K636^{RIF}$**;** 1.4 x10^7 CFU/100 µl $H37Rv^{WT}$ and 1.2 x10^7 CFU/100 µl $H37Rv^{RIF}$) per well for each bacterial strain (ii) Represents the percentage (%) uptake of *M. tuberculosis* strains by RAW264.7. Results expressed as mean with standard deviation (SD) (analysis done in GraphPad Prism 8 software) and a representation of 3 biological replicates, (each with three technical replicates).

i) IL-6 ($p \leq 0.00004$)

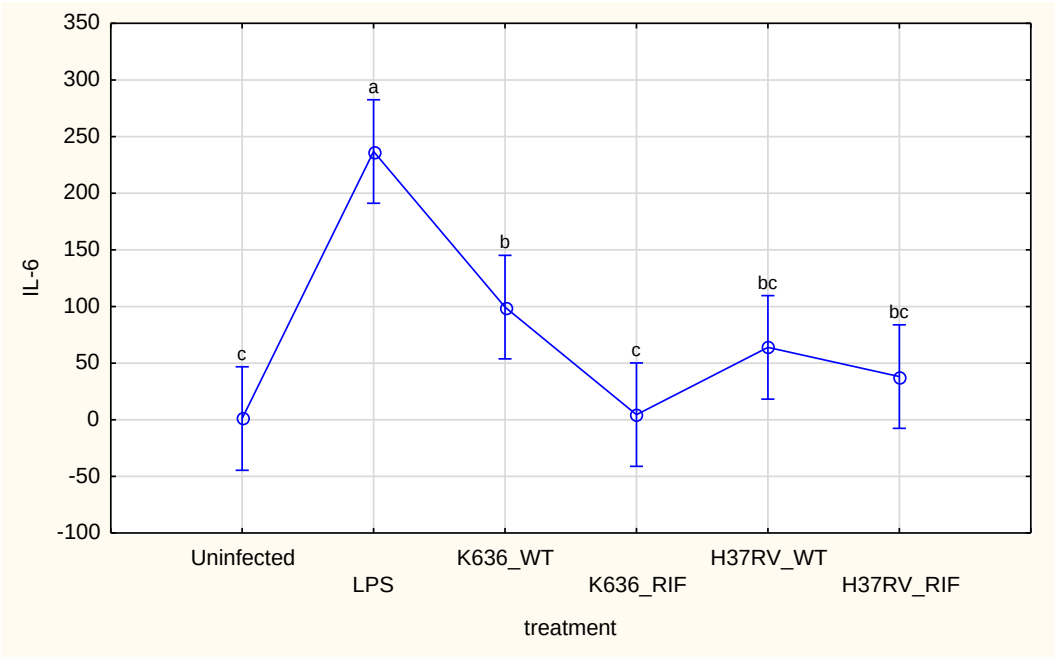

ii) IL-12p40 ($p \leq 0.00045$)

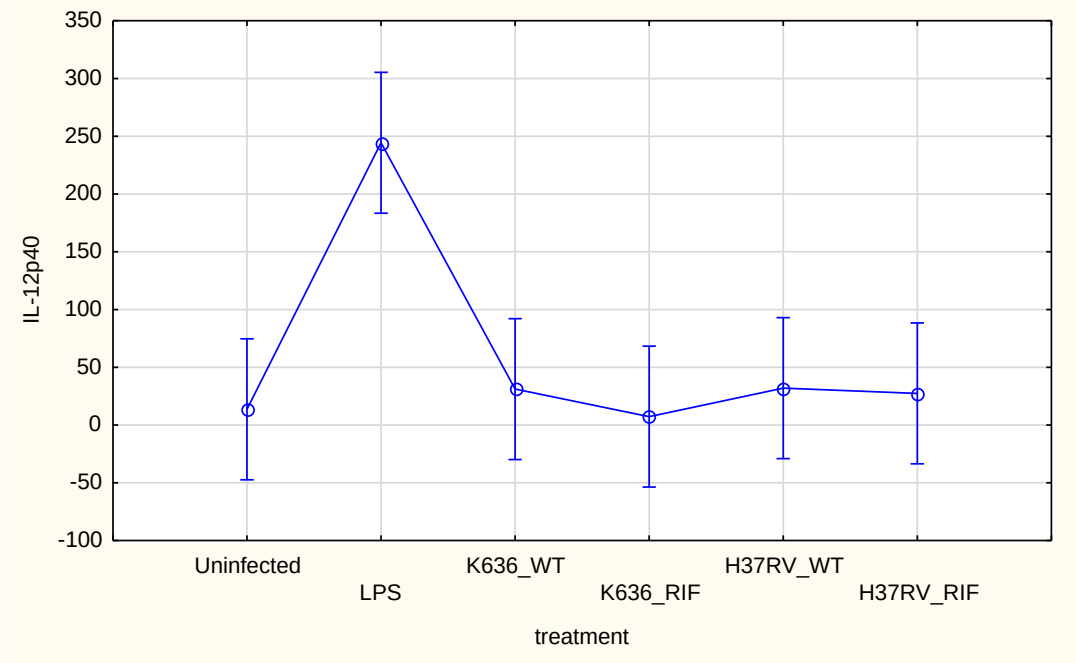

iii) RANTES ($p \leq 0.000001$)

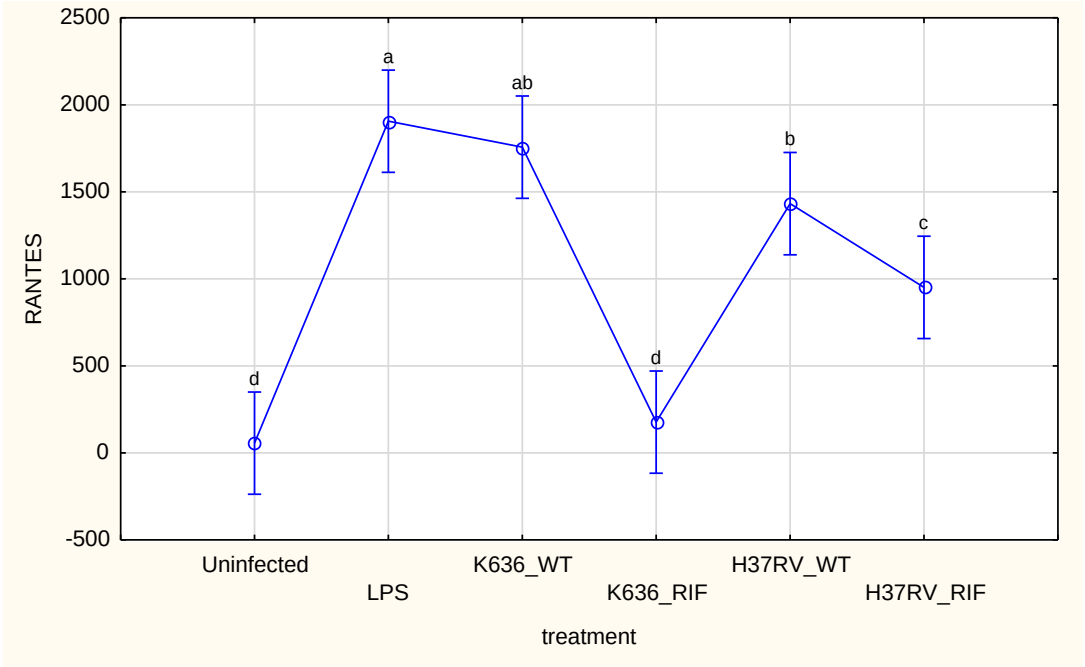

iv (a)) MCP-1 ($p \leq 0.06$)

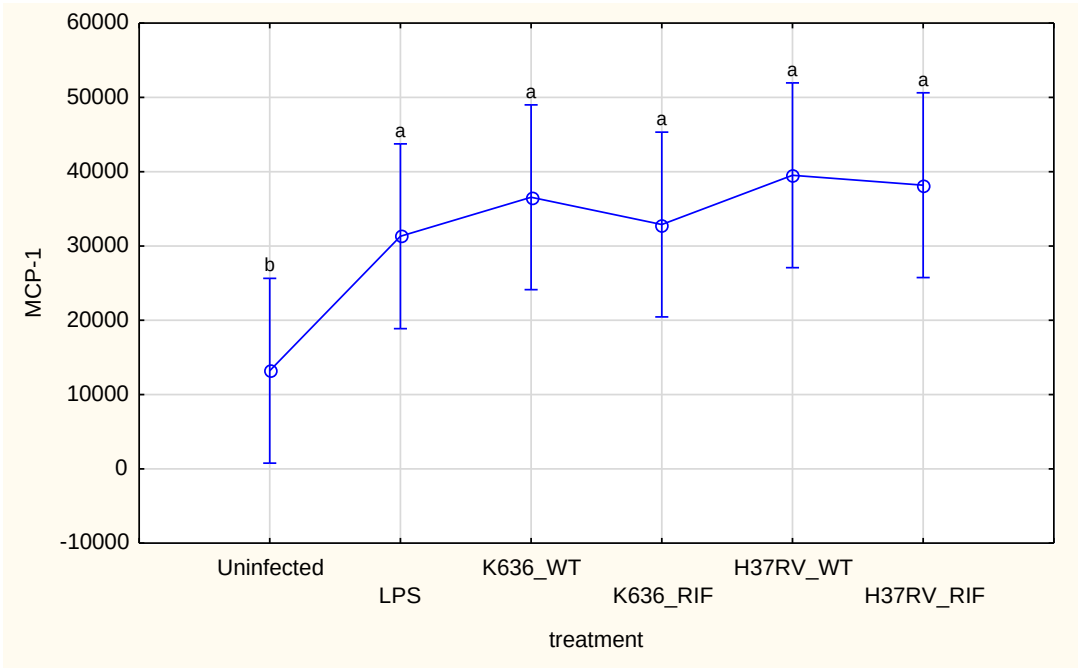

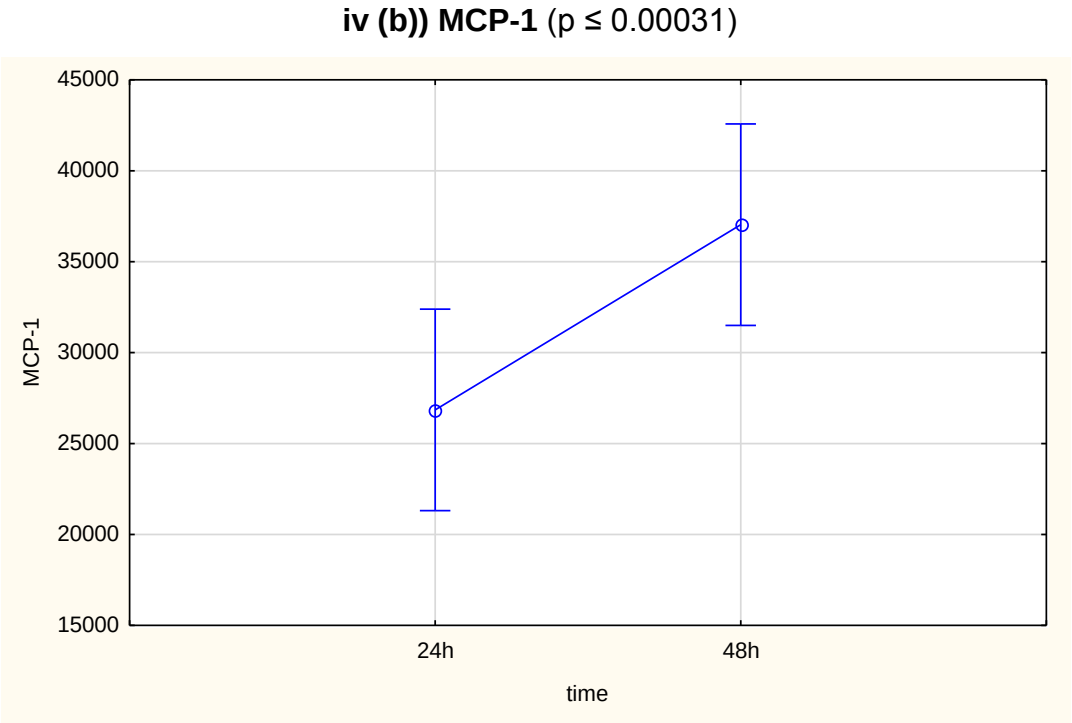

Figure S4.2 (i-v) The statistical significance differences of the secreted cytokines and chemokines Three of the differentially secreted cytokines indicated on graph plots above include (i) IL-6 ($p \leq 0.00004$), ii) IL-12p40 ($p \leq 0.00045$) and a chemokine iii) RANTES ($p \leq 0.000001$) were found to be significantly secreted when compared to the uninfected and LPS treated RAW264.7 macrophages after infection with various susceptible and resistant *M. tuberculosis* strains, at both 24h and 48h post-infection. Additionally, for the chemokine MCP-1 graphs, it was significantly increased iv (b)) MCP-1 ($p \leq 0.00031$) from 24h to 48h but the increase did not significantly depend on the specific strain genotypes iv (a)) MCP-1 ($p \leq 0.06$). One-way ANOVA descriptive statistics was performed and vertical bars denote 0.95 confidence intervals. The letters a, ab, cd, etc. on the plots indicate the significant difference and insignificance between the stains. When letters are similar = no significant difference and when different = significant difference.

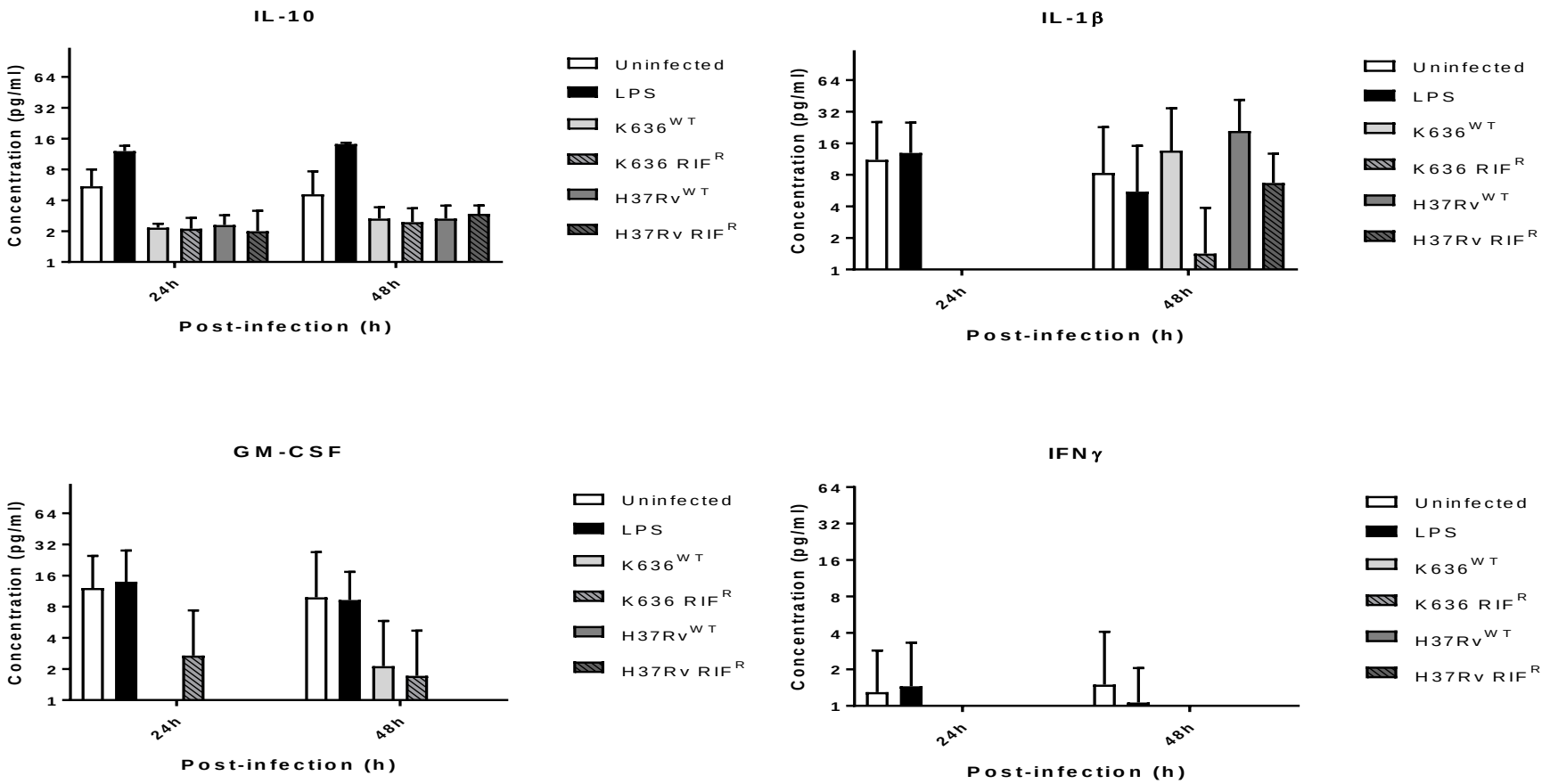

Figure S4.3 Illustrations of the normalized fluorescent intensities of the secreted cytokines and chemokines analyte above is the graphs plots of the 4 the cytokines and chemokines that were secreted at extremely low or non-detectable concentrations in the supernatants of RAW264.7 macrophages infected with various *M. tuberculosis* strains ($K636^{WT}$, $K636^{RIF}$, $H37Rv^{WT}$ and $H37Rv^{RIF}$) when compared to LPS induced and uninfected macrophages, over a period of 24h and 48h. Namely, IL-10 (14.16 pg/ml), IL-1β (20.98 pg/ml), GM-CSF (13.92 pg/ml) and IFN-γ (1.50 pg/ml).Data is depicted in mean with standard deviation (SD) of 3 independent biological replicates.

Appendix C: S4.3 Supplementary raw data: Luminex assay

BioPlex Mouse Chemokine Group
Reader Serial Number:
LX10006153404
Assay Lot: bioplexchemokine
Plate ID: 1
RP1 PMT (Volts): 521.61
RP1 Target: 3684

			Mo IL-1b (19)	Mo IL-4 (39)	Mo IL-6 (38)	Mo IL-10 (56)	Mo IL-12(p40) (76)	
Type	**Well**	**Description**	**Obs Conc**	**Obs Conc**	**Obs Conc**	**Obs Conc**	**Obs Conc**	**Dilution**
X1	A4,B4	**KWT_24h**	0	0.33	44.22	0	17.51	**N**
X2	C4,D4	**KRIF_24h**	15.42	0.47	14.36	2.85	6.13	**N**
X3	E4,F4	**HWT_24h**	0	0.32	46.7	0.48	14.99	**N**
X4	G4,H4	**HRIF_24h**	0	0.33	20.58	0.62	10.06	**N**
X5	A5,B5	**KWT_48h**	24.26	0.27	177.24	0	49.42	**N**
X6	C5,D5	**KRIF_48h**	0	0.29	14.09	0	22.47	**N**
X7	E5,F5	**HWT_48h**	27.78	0.27	144.66	0.55	62.13	**N**
X8	G5,H5	**HRIF_48h**	0	0.31	32.02	1.01	51.9	**N**
X9	A6,B6	**KWT_24h**	0	0.32	10.75	0	6.13	**1_5**
X10	C6,D6	**KRIF_24h**	18.03	0.53	4.34	3.61	3.28	**1_5**
X11	E6,F6	**HWT_24h**	0	0.37	10.82	0	4.21	**1_5**
X12	G6,H6	**HRIF_24h**	0	0.40	4.86	0.04	3.55	**1_5**
X13	A7,B7	**KWT_48h**	1.57	0.35	42.5	0	13.51	**1_5**
X14	C7,D7	**KRIF_48h**	0	0.33	3.04	0	4.95	**1_5**
X15	E7,F7	**HWT_48h**	0	0.34	29.96	0	13.23	**1_5**
X16	G7,H7	**HRIF_48h**	0	0.32	6.43	0.48	11.35	**1_5**
X17	A8,B8	**KWT_24h**	0	3.28	6.96	0.88	4.29	**1_10**
X18	C8,D8	**KRIF_24h**	10.49	0.47	2.26	2.73	1.66	**1_10**
X19	E8,F8	**HWT_24h**	0	0.37	6.08	0.48	2.59	**1_10**
X20	G8,H8	**HRIF_24h**	0	0.38	2.74	0	2.09	**1_10**
X21	A9,B9	**KWT_48h**	0	0.35	21.26	0	6.53	**1_10**
X22	C9,D9	**KRIF_48h**	0	0.38	1.92	0	2.74	**1_10**
X23	E9,F9	**HWT_48h**	0	0.37	16.46	0	7.38	**1_10**
X24	G9,H9	**HRIF_48h**	0	0.36	3.39	0.27	6.31	**1_10**

X25	A10,B10	**Uninf_24h**	0	0.35	0.64	1.52	4.52	**N**
X26	C10,D10	**Uninf_48h**	0	0.37	0.94	0.88	6.9	**N**
X27	E10,F10	**LPS_24h**	0	0.41	340.77	7.25	264.41	**N**
X28	G10,H10	**LPS_48h**	0	0.37	283.09	9.2	418.4	**N**
X29	A11,B11	**Uninf_24h**	0	0.44	0.42	0.34	14.21	**1_5**
X30	C11,D11	**Uninf_48h**	0	0.34	0.50	0	0.13	**1_5**
X31	E11,F11	**LPS_24h**	0	0.37	77.26	2.43	96.19	**1_5**
X32	G11,H11	**LPS_48h**	0	0.38	56.64	3.26	120.2	**1_5**
X33	A12,B12	**Uninf_24h**	0	0.38	0.64	0.04	0.17	**1_10**
X34	C12,D12	**Uninf_48h**	0	0.37	0.54	0	0.24	**1_10**
X35	E12,F12	**LPS_24h**	0	0.37	41.51	1.33	48.33	**1_10**
X36	G12,H12	**LPS_48h**	0	0.42	33.09	2.37	58.49	**1_10**

			Mo GM-CSF (73)	**Mo IFN-g (34)**	**Mo MCP-1 (51)**	**Mo RANTES (55)**	**Mo TNF-a (21)**	
Type	**Well**	**Description**	**Obs Conc**	**Obs Conc**	**Obs Conc**	**Obs Conc**	**Obs Conc**	**Dilution**
X1	A4,B4	**KWT_24h**	0	0	21123.15	1333.44	0	**N**
X2	C4,D4	**KRIF_24h**	17.95	4.29	25119.11	215.23	87.99	**N**
X3	E4,F4	**HWT_24h**	0	0.07	28832.55	1344.84	13.18	**N**
X4	G4,H4	**HRIF_24h**	0	0.26	26276.95	560.66	21.41	**N**
X5	A5,B5	**KWT_48h**	0	0.11	26436.59	1664.73	0	**N**
X6	C5,D5	**KRIF_48h**	0	0.23	26884.7	264.84	0	**N**
X7	E5,F5	**HWT_48h**	0	0	29533.72	1408.4	0	**N**
X8	G5,H5	**HRIF_48h**	0	0.26	30404.41	497.35	7.16	**N**
X9	A6,B6	**KWT_24h**	0	0.36	20541.4	252.88	0	**1_5**
X10	C6,D6	**KRIF_24h**	15.02	3.99	12639.54	35.64	3.18	**1_5**
X11	E6,F6	**HWT_24h**	0	0.46	20874.32	252	0	**1_5**

X12	G6,H6	**HRIF_24h**	0	0.67	19375.13	107.83	21.71	**1_5**
X13	A7,B7	**KWT_48h**	0	0.31	33531.55	794.17	0	**1_5**
X14	C7,D7	**KRIF_48h**	0	0.36	26224.08	74.92	0	**1_5**
X15	E7,F7	**HWT_48h**	0	0.51	27623.67	432.88	0	**1_5**
X16	G7,H7	**HRIF_48h**	0	0.51	26919.66	146.7	0	**1_5**
X17	A8,B8	**KWT_24h**	0	1.38	16064.15	133.4	0	**1_10**
X18	C8,D8	**KRIF_24h**	12.53	3.13	7606.35	17.92	0	**1_10**
X19	E8,F8	**HWT_24h**	0	0.56	15486.73	120.61	9.64	**1_10**
X20	G8,H8	**HRIF_24h**	0	0.64	12754.76	64.22	19.02	**1_10**
X21	A9,B9	**KWT_48h**	0	0.31	29667.3	384.98	0	**1_10**
X22	C9,D9	**KRIF_48h**	0	0.43	20343.38	39.71	0	**1_10**
X23	E9,F9	**HWT_48h**	0	0.26	23750.74	212.85	0	**1_10**
X24	G9,H9	**HRIF_48h**	0	0.70	21675.34	83.36	1.28	**1_10**
X25	A10,B10	**Uninf_24h**	1.62	0.78	14388.77	71.23	0	**N**
X26	C10,D10	**Uninf_48h**	0	1.10	16006.54	64.23	9.64	**N**
X27	E10,F10	**LPS_24h**	0	0.41	25940.89	1946.07	5.41	**N**
X28	G10,H10	**LPS_48h**	4.46	0.41	35547.88	1933.61	9.50	**N**
X29	A11,B11	**Uninf_24h**	1.62	0.72	6004.1	15.4	0	**1_5**
X30	C11,D11	**Uninf_48h**	0	0.64	8650.82	18.27	0	**1_5**
X31	E11,F11	**LPS_24h**	0	0.62	20911.8	1926.40	9.92	**1_5**
X32	G11,H11	**LPS_48h**	0	0.62	23480.95	1767.92	0	**1_5**
X33	A12,B12	**Uninf_24h**	0	0.78	4598.63	9.16	8.26	**1_10**
X34	C12,D12	**Uninf_48h**	0	0.94	5506.18	10.02	0	**1_10**
X35	E12,F12	**LPS_24h**	0	0.51	16143.37	1774.75	18.58	**1_10**
X36	G12,H12	**LPS_48h**	0	1.05	15027.76	1413.69	28.14	**1_10**

Exp Conc = Expected Concentration**;** **Obs Conc** = Observed Concentration

Chapter 5: Supplementary data

Table S5.1 DNA concentrations of screened of VBNR and AR single colonies *in M. smegmatis*

Colony no.	VBNR		Colony no.	AR	
	DNA conc (ng/µl)	PCR (+/-)		DNA conc (ng/µl)	PCR (+/-)
1	795,3	+	**1**	317,5	+
2	158,4	+	**2**	263,9	+
3	174,8	+	**3**	217,9	+
4	936,4	+	**4**	587,8	+
5	245	+	**5**	572,9	+
6	479,3	+	**6**	358,3	+
7	495,2	+	**7**	522,4	+
8	411,2	+	**8**	347,5	+
9	441,3	+	**9**	121,4	+
10	374,2	+	**10**	497,7	+
11	459,9	+	**11**	614,7	+
12	192,1	+	**12**	660,7	+
13	283,1	+	**13**	683,4	+
14	686,5	+	**14**	682,6	+
15	742,1	+	**15**	679,6	+
16	642,6	+	**16**	472,1	+
17	533,4	+	**17**	617,9	+
18	688,8	+	**18**	677,1	+
19	358,5	+	**19**	762,2	+
20	480,0	+	**20**	972,6	+
21	401,3	+	**21**	842,7	+
22	651,2	+	**22**	531,4	+
23	888,2	+	**23**	426,7	+
24	402,3	+	**24**	503,1	+
25	879,6	+	**25**	469,2	+

i)

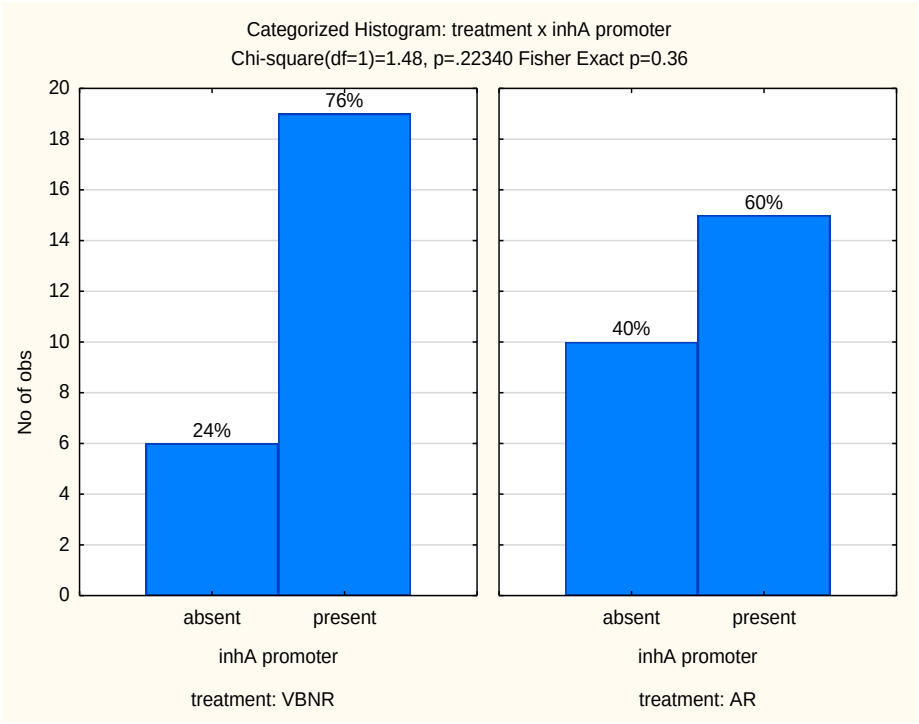

ii)

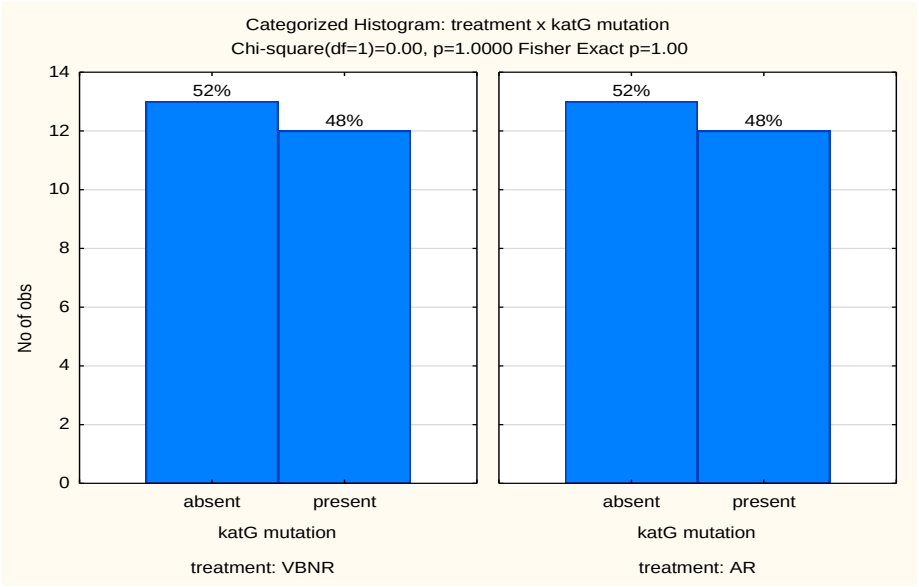

Figure S5.1 Statistical analysis of *inh*A promoter and *katG* resistant causing mutation frequencies differences. The graphs above depicts the calculated 95% Poisson confidence intervals using a Pearson's Chi-Squared-test (X^2) estimation to determine the statistical significant differences in the proportion of identified *katG* and *inhA* promoter mutations between VBNR and AR colonies. This showed no statistical significant difference in the proportion of the identified mutaions (i) *inh*A promoter and ii) *katG* regions between VBNR and AR colonies in *M.smegmatis* ($p > 0.1$).

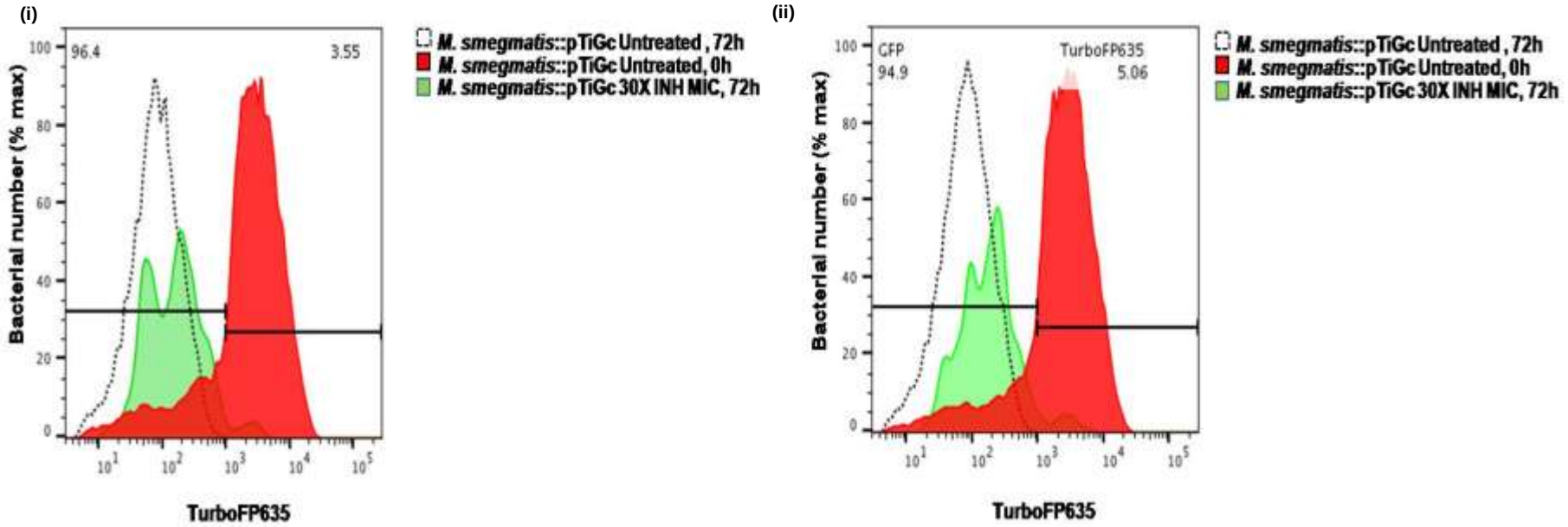

Figure S5.2 (i-ii) The detection of VBNR from AR bacterial population in *M. smegmatis*::*pTiGc* treated with high INH concentrations. Above in the figure is the representation of the two technical replicates of the flocytometry histogram plot shown in Figure 5.1 (ii). The FD reporter system in combination with flow cytometry was exploited to detect and quantify the VBNR in *M. smegmatis*::pTiGc. *M. smegmatis*::pTiGc cultures were grown in 7H9-OGT in the presence of 2 mM theophylline for 24h. After 24h samples were prepared and treated with 150 µg/ml INH (30x MIC) for 72h, with theophylline being retained for another 24h before being withdrawn. Samples were then analyzed by flow cytometry. The histogram plots (i-ii) depicts the detected VBNR persisters from AR (green) bacterial population when comparing the population growth dynamics of INH treated and untreated *M. smegmatis*::pTiGc at 0h and 72h. The VBNR persisters is confirmed by the observed overlap gated (based on high TurboFP635 (TurboFP635++++) signal) between green and red populations.